Predicting the impact of climate change on vernalization for *Arabidopsis thaliana*

Susan Duncan

A thesis submitted for the degree of Doctor of Philosophy

May 2015

Department of Cell and Developmental Biology, John Innes Centre

School of Environmental Science, University of East Anglia

© This copy of the thesis has been supplied on condition that anyone who consults it is understood to recognize that its copyright rests with the author and that use of any information derived there from must be in accordance with current UK Copyright Law. In addition, any quotation or extract must include full attribution.

Abstract

Winter annual *Arabidopsis thaliana* plants require a prolonged period of cold, known as vernalization, to ensure prompt floral transition occurs in spring. This thesis addresses the question of whether partial saturation of cold requirements might delay flowering under future climate scenarios. Laboratory experiments set up to parameterize a predictive model revealed a surprising optimal vernalizing temperature for the Swedish accession Lov-1. Field experiments in Northern Sweden support the theory that this optimum likely reflects adaptation to autumn, rather than winter temperatures.

A chilling unit model incorporating empirically derived parameters forecast an overall increase in effective vernalizing days for *A. thaliana* in northern Sweden. This increase is the result of an overall reduction in sub-zero temperatures that are predicted for northerly latitudes by the end of the century. Reductions in the number of effective vernalizing days were predicted for England and Spain, however these are unlikely to counteract the forcing effects of increased spring temperatures at these locations.

This thesis also presents a novel method that enables single RNA molecules to be visualized for the first time in plants. This method was used to determine cell-to-cell variation and sub-cellular distribution of key vernalization gene transcripts before, during and after cold exposure. These results provide a unique insight into how plants perceive and integrate long-term temperature cues at the cellular level.

In summary, this thesis predicts the potential impact of climate change on *A. thaliana* vernalization across its species' range. It also dissects transcriptional mechanisms that underlie long-term temperature integration. Modulation of these mechanisms is likely to be key for survival of some wild species and for maximizing crop yields under future climate scenarios.

Acknowledgements

I am sincerely grateful to my supervisor Caroline Dean. She has been a true inspiration to me throughout my PhD. I am also grateful to the other members of my supervisory panel, Alastair Grant and Judith Irwin, for all their support and encouragement. I also wish to thank Svante Holm for sharing his infectious passion for ecology with me and for his hospitality during my visits to Sweden.

All members of the Dean lab have helped to make my PhD an enjoyable and fulfilling experience. I am grateful to Mathew Box and Clare Lister for helping me at the start of my project. I am also thankful for all the support and encouragement I have received from Stefanie Rosa, Julia Questa, Jie Song and Ryo Ishikawa.

I am grateful for the permission to include Julia Questa's ChIP analysis and Arthur Korte's (GMI, Vienna) flowering time data in this thesis. I also appreciate all the help that I have received during my project from the horticultural staff at JIC and from the students: Man Yu, Kate Dzubinska and Barley Collier. Thanks also to Matthew Hartley and Tjelvar Olsson for saving me from the pain of counting thousands of dots.

I am especially grateful to my UEA lecturer Andy Johnston for pointing me in the direction of JIC and for having faith in me from the beginning. Last, but certainly not least, I want to express my heartfelt thanks to my family for all their love, support and patience.

Table of Contents

Abstract 2

Acknowledgements 3

Table of Contents 4

Table of Figures 8

List of Abbreviations 11

Chapter 1 – Introduction 13
- **1.1 Biogeography of *Arabidopsis thaliana*** 13
- **1.2 Life history strategies in *A. thaliana*.** 14
- **1.3 Multiple Pathways Control Flowering Time** 16
- **1.4 Activators of *FLC* Expression** 17
  - 1.4.1 PAF1 Complex 17
  - 1.4.2 RAD-BRE1 17
  - 1.4.3 FACT Complex 18
  - 1.4.4 COMPASS-LIKE Complex 18
  - 1.4.5 SWR1 Complex 19
  - 1.4.6 FRIGIDA Complex 19
- **1.5 Autonomous Repression of *FLC*** 20
- **1.6 Three stages of vernalization provide a memory of cold** 20
  - 1.6.1 Cold-induced transcriptional repression of *FLC*. 22
  - 1.6.2 Nucleation of PHD-PRC2 at an intragenic site within *FLC* 23
  - 1.6.3 Spreading of PHD-PRC2 across the whole *FLC* locus 24
- **1.7 Molecular basis of natural variation in vernalization response** 24
- **1.8 *FLC* haplotype groups account for the majority of variation in vernalization response** 26
- **1.9 Vernalization and fitness** 29
- **1.10 Phenotypic plasticity in a changing climate change** 29
- **1.11 Thesis outline** 30

Chapter 2 - Consequences of varying vernalization temperature for flowering time and seed yield 33
- **2.1 Introduction** 33
- **2.2 Temperatures between 0°C and 14°C accelerate Col*FRI*^{Sf2} flowering** 35
- **2.3 *FLC*, *FRI* and *VIN3* synergistically contribute to Col*FRI*^{Sf2} vernalization plasticity.** 36
- **2.4 *VIN3* mediated *FLC* repression and subsequent *FT* up-regulation accelerates flowering across the effective temperature range** 36
- **2.5 Natural variation in vernalization thermal sensitivity** 39
- **2.6 Vernalization temperatures impact seed yield** 40
- **2.7 *FLC* contributes to Lov-1 vernalization temperature sensitivity and fecundity.** 42
- **2.8 Determining the impact of vernalization temperature on fecundity and dormancy** 44
- **2.10 Materials and Methods** 51
  - 2.10.1 Plant growth conditions. 51

2.10.2 RNA Extraction 51
2.10.3 Reverse Transcription 52
2.10.4 Quantitative Polymerase Chain Reaction (qPCR) 53
2.10.5 Seed Yield 54
2.10.6 Seed Germination Assay 54

Chapter 3 - Seasonal shift in timing of vernalization as an adaptation to extreme winter 55
3.1 Introduction 55
3.2. Flowering Time 55
3.2 Gene Expression 56
3.4 Chromatin Immunoprecipitation Analysis 58
3.5 Lov-1 life history and climate analysis 61
3.6 Testing the hypothesis of a seasonal shift in vernalization timing 64
3.8 Natural variation observed in field vernalization and subsequent seed yield 65
3.9 Contribution of the Lov-1 *FLC* allele to flowering time and seed yield ... 65
3.2.7 Differential thermal sensitivity observed under field conditions 69
3.10 Discussion 70
3.4 Materials and Methods 73
3.4.1 Plant growth conditions. 73
3.4.2 Sweden Field Experiments 73
3.4.3 Climate Analysis 73
3.4.4 RNA extraction 73
3.4.5 Reverse Transcription 73
3.4.6 Quantitative Polymerase Chain Reaction (qPCR) 74
3.4.7 ChIP and RT-qPCR Analysis. 74

Chapter 4 - Predicting the impact of climate change on vernalization .. 75
4.1 Introduction 75
4.2 Determining vernalization temperature parameters 75
4.2.1 Predictions based on the summation of hours within effective temperature ranges 77
4.2.2 Predictions made using accession-specific chilling-unit models 79
4.2.3 Predictions based the summation of average daily temperatures within effective temperature ranges 80
4.2.4 Predictions based on the effectiveness of cumulative average temperature 80
4.3 Testing daily temperature integration 81
4.4 Temperature integration is not dependent on declining temperatures or photoperiod 84
4.4 Vernalization threshold temperatures predict diverse outcomes under a changing climate. 87
4.5 Discussion 91
4.6 Material and Methods 96
4.6.1 Plant material and growth conditions. 96
4.6.2 Sweden Field Experiments 96
4.6.3 Hourly chilling unit accumulation calculations 96
4.6.4 Accession specific model 97
4.6.5 Accumulation of effective daily average temperatures 99
4.6.6 Using cumulative average temperatures to predict vernalization responses under field conditions 99
4.6.7 Norwich Field Experiment 101

4.6.8 RNA extraction 101
4.6.9 Reverse Transcription 101
4.6.10 Quantitative Polymerase Chain Reaction (qPCR) 101
4.6.11 Modelling present and future effective vernalizing days 102

Chapter 5 - Detecting RNA molecules *in planta* 103
5.1 Introduction 103
5.2 Gene Selection 104
5.2 Tissue selection 104
5.3 Sample Preparation 104
5.4 Detection of *PP2A* mRNA 105
5.5 Detecting sites of *PP2A* transcription 107
5.5 Image analysis and quantification of RNA 108
5.6 Discussion 113
5.7 Materials and Methods 115
5.7.1 Plant Growth Conditions 115
5.7.2 smFISH Protocol 115
5.7.3 Reagent preparation 116
4% Paraformaldehyde (50mL) 116
2X Saline-Sodium Citrate (SSC) (20mL) 116
Hybridization Buffer (10mL) 116
Wash Buffer (50mL) 116
Nuclear stain: 4',6-diaidino-2-phenylindole (DAPI) (20mL) 116
Anti-fade GLOX buffer minus enzymes (1mL) 116
Anti-fade GLOX buffer plus enzymes (100µL) 117
5.7.4 Imaging 117
5.7.4 smFISH Image analysis 117
Splitting the confocal image into channels 117
Finding seeds from nuclei 117
Cell Segmentation 117
Locating probe molecules 118
Generating an annotated image 118

Chapter 6 – Using smFISH to analyse transcriptional regulation during vernalization 119
6.1 Introduction 119
6.3 Determining cell-to-cell variation of *FLC* mRNA during vernalization 120
Co-ordinated sense and antisense *FLC* transcription is a rare event 122
6.5 *VIN3* induction occurs in a graded manner during vernalization 126
6.6 Post-cold reactivation of Lov-1 *FLC* occurs in a digital manner 127
6.7 Discussion 131
6.8 Materials and Methods 134
6.8.1 Plant growth conditions 134
6.8.2 RNA extraction 134
6.8.3 Reverse Transcription (RT) 134
6.8.4 Quantitative Polymerase Chain Reaction (qPCR) 134
6.8.5 smFISH protocol 135
6.8.6 smFISH image analysis 135

Chapter 7 - Discussion 136
6.1 Introduction 136
6.2 The potential ecological significance of effective vernalizing temperatures 136

6.3 Exploring the molecular basis of vernalizing temperature effectiveness 138
6.4 The predicted impact of climate change on *A. thaliana* vernalization... 139
6.5 Concluding Remarks 141

Appendices 142
Appendix Figure 1 143
Appendix Figure 2 144
Appendix Table 1 - Markers used to map the introgressed regions on Chromosome 5 145
Appendix Table 2 – Primers used for ChIP analysis 146
Appendix Table 3 – smFISH probe set used to detect *PP2A* mRNA 147
Appendix Table 4 – smFISH probes used to detect nascent *PP2A* RNA..... 148
Appendix Table 6 – smFISH probes used to detect nascent *FLC* RNA 149
Appendix Table 5 – smFISH probe set used to detect *FLC* mRNA..... 150
Appendix Table 7 – smFISH probe set: nascent antisense *FLC* RNA 151
Appendix Table 8 – smFISH probe set: spliced antisense *FLC* RNA 152
Appendix Table 9 – smFISH probe set used to detect *VIN3* RNA 153

References 154

Table of Figures

Chapter 1

Figure 1.1-	Area of geographic distribution of *Arabidopsis thaliana*	14
Figure 1.2 -	A simplified diagram showing how *FLC* regulation contributes to pathways controlling flowering time	15
Figure 1.3 -	Vernalization provides a quantitative memory of cold	25
Figure 1.4 -	Collection sites of representative accessions of major *FLC* haplotype groups	28
Figure 1.5 -	Published predictions of effective vernalization temperature for crop and ornamental species	30

Chapter 2

Figure 2.1 -	Testing the effectiveness of Col*FRI*^{Sf2} vernalization temperatures	34
Figure 2.2 -	Determining the relative contributions of *FLC*, *FRI* and *VIN3* to Col*FRI*^{Sf2} vernalization plasticity	35
Figure 2.3 -	Opposing trends of *VIN3*, *FT* and *FLC* expression observed during and after vernalization	37
Figure 2.4 -	*FLC* expression determined after vernalization	38
Figure 2.5 -	Flowering time and seed yield recorded following a range of vernalization of treatments	41
Figure 2.6 -	Contribution of vernalization period on Var2-6 inflorescence architecture	42
Figure 2.7 -	*FLC* plus an additional Lov-1 locus are required for an enhanced vernalization response at 8^{o}C	43
Figure 2.8 -	Flowering time and seed yield recorded for NILs	45
Figure 2.9 -	Determining fecundity for vernalized Col*FRI*^{Sf2}, NIL1^{Lov-1} and Lov-1 plants	46
Figure 2.10 -	Variable germination observed for Col*FRI*^{Sf2} and NIL1^{Lov-1} seeds originating from plants vernalized at a range of temperatures	47

Chapter 3

Figure 3.1 -	Vernalization responses at a range of constant temperatures	57
Figure 3.2 -	Co*FRI*^{Sf2} vernalization responses after two weeks	

	of cold	58
Figure 3.3 -	*FLC* expression determined before and after 4 weeks vernalization	59
Figure 3.4 -	Changes in gene expression and accumulation of repressive chromatin modifications determined for Col*FRI*^{Sf2} and Lov-1	60
Figure 3.5 -	The Lov-1 natural population flowers rapidly after snow-melt in spring	61
Figure 3.6 -	Snow consistently covers plants during winter in northern Sweden	62
Figure 3.7 -	Subzero winter temperatures are preceded by optimal vernalizing conditions	63
Figure 3.8 -	An empirically derived temperature range predicts that Lov-1 vernalization occurs before winter	64
Figure 3.9 -	Data collection locations and field sites in Sweden	65
Figure 3.10 -	Field experiments reveal vernalization occurs in autumn in northern Sweden	66
Figure 3.11 -	2012 field experiments confirm vernalization occurs during autumn in northern Sweden	67
Figure 3.12 -	Plants flowered synchronously with natural populations after 5 months of continuous snow cover	68
Figure 3.13 -	An enhanced initial vernalization response recorded for Lov-1 coincided with higher field temperatures	69
Figure 3.14 -	Lov-1 vernalization completes by the end of autumn in northern Sweden	70

Chapter 4

Figure 4.1 -	IPCC global annual average temperature increases predicted over the coming century	76
Figure 4.2 -	The accumulation of effective vernalizing hours during Swedish field experiments	77
Figure 4.3 -	Accession specific predictions of vernalization progress	78
Figure 4.4 -	Predictions of vernalization progress in the field based on accumulation of effective average daily temperatures	82
Figure 4.5 -	Predictions of vernalization progress based on cumulative average temperatures	83
Figure 4.6 -	Testing daily temperature integration	84
Figure 4.7 -	Vernalization in a field setting occurs independently of photoperiod and decreasing temperature trends	86

Figure 4.8 - Annual temperature rises predicted by the end of the century 88
Figure 4.9 - Upper temperature thresholds for vernalization predict diverse impacts of climate change 89
Figure 4.10 - Predicted changes in effective vernalizing days for *A. thaliana* during the 21st century 91

Chapter 5

Figure 5.1 - *A. thaliana* root meristem cells are suitable for smFISH analysis 105
Figure 5.2 - Detecting *PP2A* RNA using multiplexed single molecule fluorescence In situ hybridization 106
Figure 5.3 - *PP2A* mRNA observed in root meristem cells 107
Figure 5.4 - Evidence of transcriptional bursting 108
Figure 5.5 - Multiplexed probe sets enable simultaneous detection of spliced and unspliced *PP2A* RNA 109
Figure 5.6 - An absence of transcription during mitosis 110
Figure 5.7 - Image analysis pipeline used to detect probe signals and generate counts of probes per cell 111
Figure 5.8 - Quantification of *PP2A* RNA 112
Figure 5.9 - Simultaneous *PP2A* transcription by sister chromatids 112

Chapter 6

Figure 6.1 - Visualizing *FLC* mRNA 120
Figure 6.2 - *FLC* mRNA levels decrease in a graded manner during vernalization 121
Figure 6.3 - *PP2A* expression after three weeks cold exposure 122
Figure 6.4 - *FLC* mRNA detected after three weeks cold exposure 123
Figure 6.5 - Multiplexed smFISH probe sets used to simultaneously detect sense and antisense *FLC* RNA 123
Figure 6.6 - *FLC* Sense and Antisense transcription occurs rarely in the same cell 124
Figure 6.7 - *COOLAIR* associates *in cis* with *FLC* chromatin 126
Figure 6.8 - Induction of *VIN3* mRNA can be equally explained by graded or digital increases 127
Figure 6.9 - Graded induction of *VIN3* mRNA 128
Figure 6.10 - Reactivation of *FLC* transcription in Lov-1 can be equally explained by graded or digital increases 129

List of Abbreviations

AZT	Above zero threshold
CCD	Charge coupled device
CER	Controlled environment room
ChIP	Chromatin immuno-precipitation
DAPI	4',6-diamidino-2-phenylindole
DNA	Deoxyribonucleic acid
EDTA	Ethylenediaminetetraacetic acid
EM-CCD	Electron multiplying charge coupled device
FISH	Fluorescence in situ hybridization
GLOX	Glucose Oxidase
GWA	Genome wide association
HCl	Hydrogen chloride
iceFISH	Intron chromosomal fluorescence in situ hybridization
IPCC	The Intergovernmental Panel on Climate Change
LD	Long day
LiCl	Lithium chloride
me3	Trimethylation
MPTU	Modified photothermal units
mRNA	Messenger ribonucleic acid
MS	Murashige and Skoog media
NaCl	Sodium chloride
NaOH	Sodium hydroxide
NIL	Near isogenic line
NOAA	National Oceanic and Atmospheric Administration
NS	Not significant
NV	Non-vernalized
PBS	Phosphate buffered saline
PFA	Paraformaldehyde
QTL	Quantitative trait locus
RCP	Representative concentration pathway
RH	Relative humidity
RNA	Ribonucleic acid
RNAi	RNA interference

RT-qPCR	Reverse transcription quantitative polymerase chain reaction
SCC	Saline-sodium citrate
SD	Standard deviation
SDS	Sodium dodecyl sulfate
SEM	Standard error of the mean
smFISH	Single molecule fluorescence in situ hybridization
SNP	Single nucleotide polymorphism
snpFISH	Single nuleotide polymorphism fluorescence in situ hybridization
T	Days of post cold growth
Tris	Tris(hydroxymethyl)aminomethane
UPL	Universal probe library
W	Weeks

Chapter 1 – Introduction

1.1 Biogeography of *Arabidopsis thaliana*

Arabidopsis thaliana (L.) Heyhn is a spring ephemeral weed commonly known as mouse ear cress or thale cress. The *Arabidopsis* genus belongs to the Brassicaceae family and comprises of nine species and eight sub-species (Al-Shehbaz and O'Kane 2002). Of all these species *A. thaliana* has the widest observed geographical distribution. It can be found growing in a variety of disturbed habitats and at a wide range of altitudes (Al-Shehbaz and O'Kane 2002).

A. thaliana is thought to have originated from Central Asia and survived the last ice age by retreating to two refugia at the southern limit of its range. Following de-glaciation it rapidly re-populated varied climatic regions across the Northern Hemisphere from near the equator to the Arctic Circle (see Figure 1.1) (Sharbel et al., 2000; Hoffmann 2002; Schmid et al., 2006; Nordborg et al., 2005; Françoiset al., 2008). This rapid re-colonization, combined with the diverse range of niches now inhabited by this species demonstrates its ability to adapt to a variety of different biotic and abiotic conditions (Shindo et al., 2007).

Although there is evidence of local adaptation to climate across *A. thaliana* genome (Hancock et al., 2011) the ease with which animals or humans can transport seeds make it unlikely that all catalogued lines have persisted long enough at a single location for local adaptation to have occurred. For this reason natural lines of *A. thaliana* are now referred to by the neutral word 'accession' rather than 'ecotype' as this removes the automatic implication of adaptation to conditions at the native collection site (Weigel, 2012).

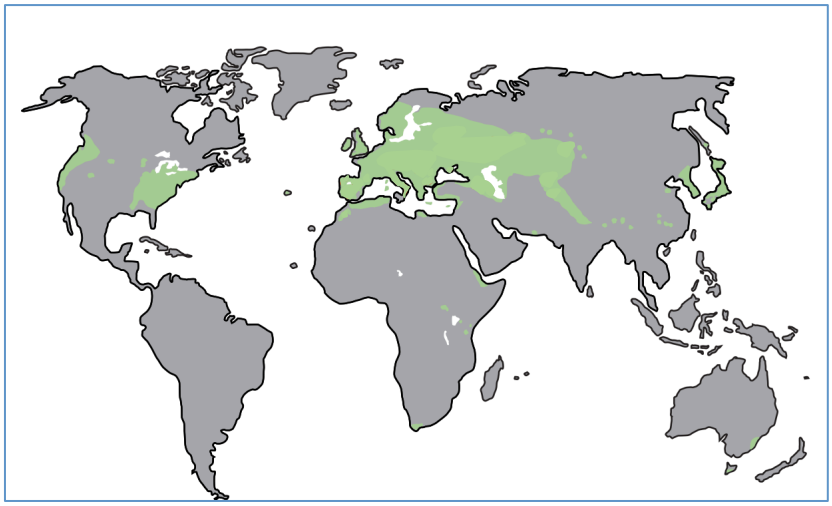

Figure 1.1- Area of geographic distribution of *Arabidopsis thaliana*. (Adapted from Weigel and Mott 2009)

1.2 Life history strategies in *A. thaliana*.

Selective pressures created by unstable environmental conditions promote a range of traits that include high fecundity, small body size and short generation time (Promislow and Harvey, 1990). The monocarpic life history observed for natural *A. thaliana* populations suggests that this strategy maximizes fitness in areas characterized by harsh winters and/or dry summers.

A. thaliana accessions can be classified as being either winter or summer annuals. Winter annual accessions germinate during wet conditions in autumn, persist through the winter in a vegetative state and then enter a final reproductive phase in spring. This strategy minimizes nutrient competition between seedlings and maximizes chances of reproductive success by aligning plant senescence, silique desiccation and seed maturation with warm, dry conditions (Boss et al., 2004; Henderson and Dean 2004). Many natural accessions of *A. thaliana* adapted to temperate climates have a summer annual/rapid-cycling habit (Nordborg et al., 2005; Shindo et al., 2005). Without the need to over-winter, rapid-cycling accessions can often achieve multiple generations per year compared to winter annuals and this provides them with a significant fitness advantage in some locations.

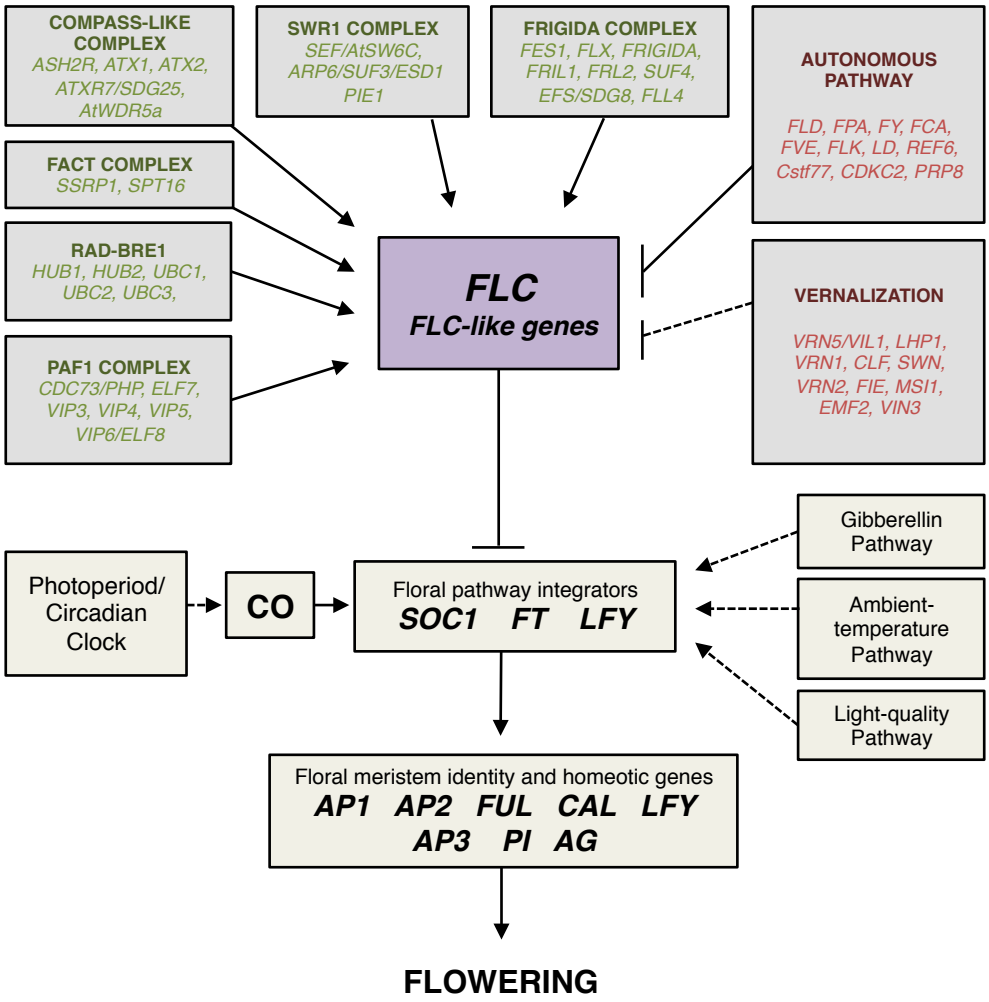

Figure 1.2 – A simplified diagram showing how *FLC* regulation contributes to pathways controlling flowering time.

1.3 Multiple Pathways Control Flowering Time

Flowering time studies in *A. thaliana* date back over seventy years (Laibach 1943, 1951) and experiments over the intervening years have revealed more than 100 genes to be involved in the control of this key developmental transition (Skikanth and Schmid 2011). These results have shown that environmental and endogenous cues are continually integrated within *Arabidopsis* plants via the pathways outlined in Figure 1.2 to control the timing of flowering. The essence of this network is that multiple input pathways converge on a common set of target genes (floral pathway integrator genes) that are quantitatively activated and switch the meristem to a floral fate once a threshold level has been reached. The gibberellin, light quality, photoperiod (involving *CONSTANS* (*CO*) and the circadian clock) and ambient temperature pathways activate expression of floral pathway integrators under long-day photoperiod conditions. This activation is antagonized by a number of floral repressors including *FLOWERING LOCUS C* (*FLC*) (shown in purple in Figure 1.2). Many repressors have been found to act via an upregulation of *FLC* whilst many floral activators mediate a reduction of *FLC* (red and green in Figure 1.2, respectively). Several floral repressors also work independently of FLC to repress expression of floral pathway integrators. Examples not shown in Figure 1.2 include, *TERMINAL* FLOWER1 (*TFL1*), *SHORT VEGETATIVE PHASE* (*SVP*), *TARGET OF EAT1, TARGET OF EAT2* (*TOE1/2*), *EMBRYONIC FLOWER 1* (*EMF1*), *SCHNARCHZAPFEN* (*SNZ*) and *SCHLAFMUTZE* (*SMZ*) (Bradley et al., 1997; Hartmann et al., 2000; Aukerman and Sakai 2003; Yoshida et al 2001; Bradley et al. 2007).

Downstream of the floral pathway integrator genes *SOC1*, *FT* and *LFY* (*LEAFY*) are the floral meristem identity and homeotic genes *APETALA1/2/3* (*AP1/2/3*), *FRUITFUL* (*FUL*), CAULIFLOWER (*CAL*), *PISTILLATA* (*PI*) and *AGAMOUS* (*AG*) that commit the shoot apical meristem progenitor cells to switch from a vegetative to a floral fate. Together this complex gene network ensures that plants switch to a reproductive phase of development when conditions are permissive for flower production and seed set (Boss et al., 2004, Henderson and Dean, 2004).

My work has focused on the regulation of the major floral repressor gene *FLC.* This encodes a MADS box transcription factor that effectively prevents floral transition

through direct transcriptional repression of floral pathway integrator genes in response to prolonged cold (Deng et al., 2011). This response differs from cold acclimation where a short cold exposure (days rather than weeks), results in transcriptional changes that enable plants to survive freezing conditions (reviewed by Thomashow 1999).

1.4 Activators of *FLC* Expression

Extensive studies in yeast and mammals have revealed transcription elongation to be a complex process where many aspects of the chromatin environment determine whether an RNA polymerase binding event results in mRNA production. Many homologous genes involved in chromatin-modifying activities have been found to promote *FLC* expression, and thus delay floral transition (Crevillen and Dean 2011). These activating protein complexes are described below.

1.4.1 PAF1 Complex

The highly conserved RNA polymerase associated factor 1 complex (PAF1C) contributes to multiple aspects of RNA polymerase II (PolII) transcriptional regulation. The role of this complex remains unclear, but it is required for effective elongation, various histone modifications, chromatin remodeling and for recruiting 3' end mRNA processing factors (Selth et al., 2010).

High levels of tri-methylation (me3) of histone 3 lysine 4 residues (H3K4me3) across a gene are associated with transcriptional activity in eukaryotes (Schneider et al., 2004). In Arabidopsis *paf1c* mutants displayed decreased H3K4me3 across *FLC*, lower levels of transcription and an early flowering phenotype. Consistent with diverse regulatory roles identified for PAF1C in other systems, many of these mutants also exhibited a range of other developmental defects in plants. (Zhang et al., 2002; Oh et al., 2004; Zhang et al., 2003; He et al., 2004; Yu and Michaels 2010; Park et al., 2010; Oh et al., 2008).

1.4.2 RAD-BRE1

Studies in yeast have shown that the RAD-BRE1 complex mono-ubiquitinates histone 2B (H2B). The PAF1 complex is required for this ubiquitination and this modification is required for H3K4me3 deposition (Wozniak and Strahl 2014). Arabidopsis has two genes homologous to the E3 ubiquitin ligase BRE1 (HUB1 and HUB2) and three homologues of the E2 carrier protein RAD (UBC1, UBC2 and

UBC3). Lesions in either HUB1 or HUB2 result in loss of H2B ubiquitination and reduced H3K4me3 in addition to reduced levels of another active chromatin mark H3K36me3. These chromatin changes have been associated with reduced *FLC* transcription and early flowering in addition to a range of other developmental defects. Similar phenotypes were also been reported for *ubc1ubc2* double mutants (Cao et al., 2008; Xu et al., 2009; Gu et al., 2009; Lolas et al., 2010). The sensitivity of *FLC* expression to the ubiquitination status of H2B was further highlighted by the *FLC* misregulation and early flowering phenotype of *ubp26* mutants that are unable to catalyze the H2Bub1 deubiquitination reaction (Schmitz et al., 2009).

1.4.3 FACT Complex

Mono-ubiquitination of H2B by the RAD-BRE1 complex is required for activating the removal of H2A/H2B dimers by the FAcilitates Chromatin Transcription (FACT) complex and is thought to enhance PolII transit through nucleosomes. Inhibited PolII transcription is considered the likely cause of *FLC* misregulation and the late flowering phenotype reported for FACT subunit mutants *ssrp1* and *spt16*. Furthermore, the range of severe developmental phenotypes observed is indicative of global transcriptional disruption in these mutants (Lolas et al., 2010).

1.4.4 COMPASS-LIKE Complex

Histone methylation reactions are typically catalyzed by proteins that contain conserved SET domains originally identified in *Drosophila*: Su(var)3-9, 'Enhancer of zeste' and Trithorax proteins. The *A. thaliana* genome contains at least 29 genes that contain SET domains. In yeast SET1 is part of the multi-protein complex COMPASS (Complex proteins associated with SET) that physically associates with PAF1C to catalyse the methylation of H3K4 residues (Betz et al., 2002; Krogan et al., 2003). Consistent with this role, the late flowering Arabidopsis mutant of a homologous SET1 protein *atxr7/sdg25* showed decreased H3K4me3 across *FLC* and associated up-regulated levels of expression. Similarly, late flowering was also observed in addition to reduced levels of H3K4me3 and H3K4me2 for *atx1* and *atx2* mutants respectively (Pien et al., 2008; Saleh et al., 2008; Tamada et al., 2009; Berr et al., 2011). Further COMPASS-LIKE components identified in Arabidopsis include the methyltransferase AtWDR5a that is also required for H3K4me3 deposition at *FLC* and the SET2 homologue EFS/SDG8 that catalyzes H3K36me3 reactions that are also associated with active transcription (Zhao et al., 2005; Jiang et al., 2009).

1.4.5 SWR1 Complex

The SWR1 chromatin-modelling complex incorporates the histone variant H2AZ into nucleosomes. This affects chromatin stability and alters the ability of PolII to transit through associated nucleosomes. Mutations of genes within the SWR1 complex (*ARP6*, *PIE1*, *ESD1*/*SEF*/*AtSW6C*) result in the loss of H2AZ occupancy, reduced levels of *FLC* transcription and a late flowering phenotype. (Noh and Amasino 2003; Deal et al., 2005; Choi et al., 2005; Choi et al., 2007; Martin-Trillo et al., 2006; March-Diaz et al., 2007; Lazaro et al., 2008; Deal et al., 2007)

1.4.6 FRIGIDA Complex

Components of the FRIGIDA complex (FRIC) have been shown to mediate *FLC* transcriptional activation (Choi et al., 2011). These include *FRIGIDA* (*FRI*), *FRIGIDA ESSENTIAL 1* (*FES1*), *FRI-LIKE 1* (*FRL1*), *FRI-LIKE 2* (*FRL2*), *SUPPRESSOR OF FRIGIDA 4* (*SUF4*), *FLC EXPRESSOR* (*FLX*), *FLOWERING LOCUS C EXPRESSOR-LIKE 4* (*FLL4*) (Schmitz et al., 2009; Michaels et al., 2004; Kim et al., 2006; Andersson et al., 2008; Ding et al., 2013; Lee and Amasino 2013). The mechanism by which FRI exerts its effects is unclear, but biochemical assays suggest it is a scaffolding protein that facilitates close association of FRIC components with the chromatin remodeling complex SWR1 (Choi et al., 2011). There is also evidence of FRI promoting the accumulation of *FLC* mRNA by interacting with nuclear cap-binding complexes (Geraldo et al., 2009).

FRI is the most ecologically significant activator of *FLC* (Johansen et al., 2000), since a combination of dominant *FLC* and *FRI* alleles confers a requirement for vernalization, necessitating the plants to over-winter before flowering. Prior to cold exposure, high *FLC* levels prevent the floral transition in the presence of other reproductive cues (Michaels and Amasino 1999; Sheldon et al., 1999). During vernalization levels of *FLC* are quantitatively reduced in response to prolonged exposure to cold. Once *FLC* levels are low enough to no longer pose a barrier to the expression of downstream floral integrators, increased daylength and temperature can rapidly activate reproductive growth.

Many rapid-cycling accessions of Arabidopsis carry *FRI* alleles with loss-of-function mutations (Johanson et al 2000; Shindo et al., 2005). These *FRI* null plants have evolved as the result of at least 20 independent mutational events from winter annual

ancestors that had a vernalization requirement (Shindo et al., 2005; Johanson et al., 2000). This implies strong selection for loss of *FRI* function in some environmental contexts. Although *FRI* has been found to play a predominant role in determining the winter annual phenotype, other loci have also been shown to contribute to natural variation in flowering time (Salome et al., 2011, Srikanth and Schmid, 2011). These are discussed in more detail later in this chapter.

1.5 Autonomous Repression of *FLC*

The autonomous pathway functions to antagonize *FLC* expression (see Figure 1.2) and involves the following genes: *LUMINIDEPENDENS* (*LD*), *FCA*, *FPA*, *FY*, *FLOWERING LOCUS D* (*FLD*), *FVE*, *FLOWERING LOCUS K* (*FLK*), *RELATIVE OF EARLY FLOWERING 6* (*REF6*)*, CstF77, CstF64, DICER-LIKE 4 (DCL4), CDKC2 and PRP8* (Koornneef et al., 1991; Macknight et al., 1997; Schomburg et al., 2001; Lim et al., 2004; Noh et al., 2004; Simpson et al., 2003; Jiang et al., 2007, Wang et al., 2014; Liu et al., 2010; Marquardt et al., 2014; Liu et al., 2012) Together these components promote flowering via *FLC* down-regulation through a mechanism that links 3' mRNA processing to chromatin modifications where a specific *FLC* antisense mRNA isoform represses H3K4me3 deposition across the gene and effectively dampens *FLC* transcriptional activity (Hornyik et al., 2010; Liu et al., 2007; Liu et al., 2010).

Functioning in parallel to the autonomous pathway is vernalization, the cold-induced repression of *FLC*. Key genes involved in this process include the cold inducible *VERNALIZATION INSENSTIVE 3* (*VIN3*) in addition to *VERNALIZATION 5* (*VRN5*)*, VERNALIZATION 1* (*VRN1*), *LIKE-HETEROCHROMATIN PROTEIN 1* (*LHP1*) and *VERNALIZATION 2* (*VRN2*). The distinctive roles these genes play in the cold induced reduction of *FLC* transcription are described in more detail below.

1.6 Three stages of vernalization provide a memory of cold

Vernalization is a classic epigenetic process that provides the plant with a molecular memory of cold through a cell-autonomous mechanism involving stable transcriptional silencing of *FLC* (Angel et al., 2011). Epigenetic regulation often involves heritable chromatin modifications that bring about a change in gene expression not determined by the underlying gene sequence. Winter annual

Arabidopsis plants are fully vernalized after experiencing a saturating period of cold exposure, during which *FLC* chromatin switches from an epigenetically active to an epigenetically silent state in the majority of cells of the plant (see Figure 1.3). Chromatin marks associated with the epigenetically silent state are propagated to daughter cells through cell division ensuring *FLC* silencing is mitotically stable.

Exposure to low temperatures induces a quantitative reduction of *FLC* mRNA levels and this reduction has been shown to correlate with flowering time (Michaels and Amasino, 1999, Sheldon et al., 1999). However vernalization can still accelerate flowering in *FLC* null plants, so despite this gene playing a major role in permitting floral transition, *FLC* cannot be the only downstream target of vernalization (Michaels and Amasino 2001; Moon et al., 2005).

In addition to activating *FLC*, many of the activating protein complexes described previously also activate expression of five *FLC* related MADS-Box proteins named *MAF1* to *5* that share 53-87% identity (de Bodt et al., 2003; Ratcliffe et al., 2003). It has also been shown that the cold induced protein *VIN3* is required to silence these *FLC-like* genes and ensure maximum acceleration of the flowering response (Kim and Sung 2013; Scortecci et al., 2003; Michaels and Amasino, 2001). There is also evidence to suggest that FLC-mediated floral repression requires direct interaction of these clade members (Gu et al., 2013).

An additional role has been identified for *MAF1* (also known as *FLOWERING LOCUS M*) in controlling flowering under ambient temperature growth conditions. Two isoforms FLMβ and FLMδ compete to bind SVP. In cool temperatures an increase in FLMβ production results in increased levels of FLMβ-SVP complex that actively repress flowering, whereas at higher temperatures FLMδ-SVP complexes predominate and activate a flowering response (Pose et al., 2014; Lee et al., 2013)

Two further genes, *AGAMOUS-LIKE 24* (*AGL24*) and *AGAMOUS-LIKE 19* (*AGL19*), have also been found to contribute toward the acceleration of flowering in an *FLC* independent manner following exposure to prolonged cold. VIN3 is required for the induction of these transcription factors that promote expression of floral identity genes (Schonrock et al 2006; Yu et al., 2002; Michaels et al., 2003; Alexandre and Hennig 2008).

Vernalization can be viewed as occurring in three steps. These are described below.

1.6.1 Cold-induced transcriptional repression of *FLC*.

FLC transcription decreases rapidly upon exposure to cold (Helliwell et al., 2015) and this decrease is associated with a significant increase in *FLC* anti-sense transcription (Swiezewski et al., 2007). Loss of this antisense transcription results in a slower decrease in *FLC* transcription during cold exposure (Csorba et al., 2014). The antisense transcription generates long non-coding transcripts, known as *COOLAIR*, which undergo alternative splicing and polyadenylation events to create two major sets of splice variants that have each been linked to altered chromatin states at *FLC* (Csorba et al., 2014, Ietswaart et al., 2012, Marquardt et al., 2014). When plants are growing in warm conditions *COOLAIR* transcription is inhibited by an R-loop located at the 3' region of *FLC* in the *COOLAIR* promoter region. The R-loop is stabilized by a single stranded DNA binding protein *AtNDX* (Sun et al., 2013). How *COOLAIR* transcription/transcripts cause *FLC* transcriptional repression is unclear at present, but they stay associated with *FLC* chromatin (Csorba et al., 2014) and emerging evidence from RNA SHAPE (Selective 2'-hydroxyl acylation analyzed by primer extension) analysis suggests that *COOLAIR* secondary structure is an important aspect of this regulation (Sanbonmatsu, Hawkins et al., in prep).

Induction of another non-coding *FLC* transcript called *COLDAIR* has also been reported that originates from within intron 1 of the sense sequence of *FLC*. *COLDAIR* expression peaks after 3 weeks of cold and transcripts have been reported to recruit the repressive PHD-PRC2 to the locus (Heo and Sung 2010). Analysis in *Arabidopsis alpina* (a cold requiring *A. thaliana* perennial relative) confirmed conservation of *COOLAIR*, but not *COLDAIR* induction during cold (Castaings et al., 2014).

The cold-induced reduction in *FLC* transcription and increase of *COOLAIR* transcription coincides with altered higher order chromatin structure at *FLC*. Chromosome Conformation Capture (3C) experiments showed the existence of a 5' to 3' loop at *FLC* when the gene is expressed (Crevillen et al., 2013). A recent study has also shown that BAF60 (a component of the SWI/SNF chromatin-modifying complex) is required for maintenance of this loop in the warm (Jegu et al., 2014). The

loss of this loop is not dependent on factors known to regulate *FLC* transcription in the warm. In addition, recovery of *FLC* expression levels observed when *vin3* mutants are returned to warm conditions was not associated with loop reformation (Crevillen et al., 2013).

1.6.2 Nucleation of PHD-PRC2 at an intragenic site within *FLC*

The second step of vernalization involves formation and nucleation of a modified Polycomb complex. This modified Polycomb complex is composed of the well-conserved PRC2 with two homologous PHD domain-containing proteins, VRN5 (also known as VIL1 in the literature – Sung & Amasino 2006) and VIN3 (Greb et al., 2007, De Lucia et al., 2008). *VIN3* expression is cold-dependent with maximal levels found after 40 days of cold. VIN3 heterodimerises with the constitutively expressed VRN5 and these associate with the Polycomb Repressor Complex 2 (PRC2) complex already positioned across the *FLC* locus (De Lucia et al., 2008, Kim et al., 2010). The PHD proteins somehow 'superactivate' PRC2 activity and homologous complexes have been described in Drosophila (Nekrasov et al., 2007) and humans (Sarma et al., 2008).

Polycomb-group proteins were first shown to play an important role in maintaining the repressed state of homeotic (*Hox*) genes in *Drosophila melanogaster* and they have since been implicated in imprinting, stell cell specification, cancer initiation and inactivation of X chromosomes in a range of organisms (Schuettengruber et al., 2007; Schwartz and Pirrotta, 2008). In plants, a core conserved PRC2 consisting of *VRN2* (a Su(z)12 homologue), SWINGER (an E(Z) histone methyl transferase homologue, FIE (an ESC homologue) and MSI1 (a p55 homologue) associates across the *FLC* locus in ambient temperatures. Exposure to cold allows the PHD proteins VIN3 and VRN5 to associate with PRC2 at a specific region in the first intron of *FLC* termed the nucleation region (De Lucia et al., 2008). This PHD-PRC2 generates a peak of tri-methylated lysine 27 residues on histone 3 (H3K27me3) in this localized region, concomitant with reduction in the antagonizing activating histone mark H3K36me3 (Angel et al., 2010; Yang et al., 2014).

The nucleation event at *FLC* is correlated with a change in nuclear reorganization of the *FLC* locus. Cold exposure quantitatively increases the frequency of physical

clustering of *FLC* alleles and is maintained once plants are returned to warm conditions. This clustering response was shown to be dependent on the presence of Polycomb proteins (Rosa et al., 2013).

1.6.3 Spreading of PHD-PRC2 across the whole *FLC* locus

The last step in vernalization occurs when plants are returned to warm temperatures. The PHD-PRC2 complex spreads along the length of *FLC* resulting in high levels of H3K27me3 across the whole gene body (Angel et al., 2011; Yang et al 2014). The maintenance of this epigenetic mark requires the stabilizing activity of LHP1 (Mylne et al., 2006, Sung et al., 2006). A H3K27 demethylase *ELF6* then resets *FLC* expression during embryogenesis to ensure that the next generation inherits a vernalization requirement (Crevillen et al., 2014).

There are two explanations that can equally explain the changes in *FLC* H3K27me3 observed during vernalization. The rising peak can either be the result of gradually increasing levels of chromatin modifications in every cell, or an increasing proportion of cells being flipped from a low to a high H3K27me3 nucleated state. Modelling and lab experiments support the second hypothesis and suggest that stochastic digital switching provides the plant with a quantitative biological measure of cold exposure (Figure 1.3) (Yang et al., 2014; Angel et al., 2010; Satake 2012; Angel et al., 2015).

1.7 Molecular basis of natural variation in vernalization response

Consistent with *FLC* acting as a major floral repressor, several Quantitative Trait Loci (QTL) studies have linked *FLC* and *FRI* variation to flowering time control (Kover et al., 2009, Shindo et al., 2005, Shindo et al., 2006, Strange et al 2011; Li et al., 2014). Other genes identified through this type of analysis include *FT*, *FLM, FRI* homologues *FRL1* and *FRL2* and *FLC* homologues *FLM/MAF1* and *MAF2* (Werner et al., 2005; Schlappi et al., 2006; Caciendo et al., 2009; Roslostski et al., 2006; Schwartz et al., 2009; Li et al., 2010; Huang et al., 2011; Salome et al., 2011; Strange et al., 2011).

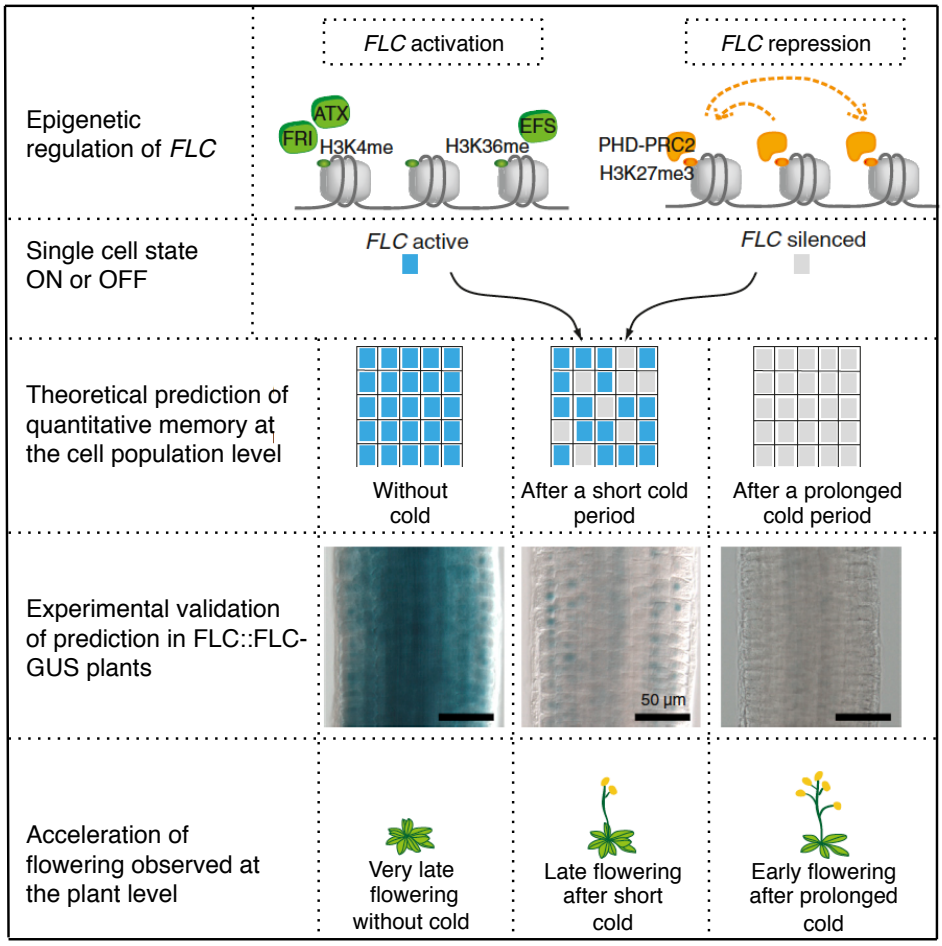

Figure 1.3 – Vernalization provides a quantitative memory of cold
Antagonistic chromatin marks either maintain the *FLC* allele in an active or silenced state. An increase in population of cells that have been silenced provides a quantitative memory of cold. (Figure adapted from Song et al., 2014)

Genome Wide Association (GWA) mapping is a powerful tool that allows single nucleotide polymorphisms (SNPs) to be associated with specific phenotypes without the need to generate a mapping population (Weigel et al., 2012). Unfortunately, population structure can create spurious associations in GWA studies and this can hamper identification of true associations when investigating complex adaptive traits in *A. thaliana*. Although statistical methods have been developed to remove false positives, these methods can create false negative results by reducing positive signals to a level below the significance threshold (Atwell et al., 2010). Despite these limitations this approach has associated genetic variation around *FLC* both with variation of flowering time observed under constant temperature treatments (Atwell et al., 2010) and semi-natural conditions where CERs were programmed to mimic natural temperatures and photoperiods (Li et al. 2010; Li et al., 2014).

Surprisingly, despite partial vernalizing conditions being predicted by a model of *A. thaliana* field development (Wilzcek et al., 2009), genes associated with *FLC* regulation were not associated with variation in flowering time in a study that combined QTL with GWA analyses of plants grown under natural field conditions. Instead an *FT* homologue called *TWIN SISTER OF FT* (*TSF*) and a number of genes important to the regulation of the circadian clock including *TOC1* and *COL1* were identified (Brachi et al., 2010). Considering that laboratory growth conditions are significantly warmer and wetter compared to typical natural settings, these and other field studies results (e.g. Weinig et al., 2002) have led to some to question of the ecological significance of laboratory-derived phenotype data (Hoffman 2002; Weigel 2012; Shindo et al., 2007).

1.8 *FLC* haplotype groups account for the majority of variation in vernalization response

Haplotype group refers to a group of individuals that share a set of single nucleotide polymorphisms (SNPs) within a defined chromosomal region. Analysis of SNP data across 1307 accessions identified 5 major *FLC* haplotype groups (Li et al., 2014). Strikingly, high quality sequencing of this region revealed no polymorphisms within the coding regions of *FLC*; all SNPs were identified within non-coding sequence. Further genetic and transgenic experiments confirmed these haplotypes to be functionally distinct with each exhibiting divergent *FLC* silencing dynamics. Collection

sites of four accessions (Ull2-5, Var2-6, Lov-1, Edi-0) that represent four of the haplotype groups are shown in Figure 1.4.

Three of the major *FLC* haplotype groups contain representative accessions from Sweden (Li et al., 2014). Var2-6 and Ull2-5 have an obligate requirement for cold exposure before the reproductive transition can occur under inductive conditions. They originate from areas in the Skåne region in south of Sweden and were taken from coastal and field habitats, respectively. Ull2-5 has emerged as a representative member of a slow vernalizing *FLC* haplotype group with many members originating from southern Sweden. Fine mapping in F_2 lines from a cross between Col-0 and Ull2-5 revealed QTL over *FLC*, *FRI* and *FT* (Shindo et al., 2006; Strange et al., 2011). Despite Var2-6 being another slow vernalizing accession collected in south Sweden, sequence analysis indicates that it shares *FLC* sequence homology with many accessions collected from northern Sweden. Recent work has revealed that the slow vernalization phenotype of this haplotype is determined by a single intronic SNP that alters the splicing pattern of *COOLAIR* (Li et al., 2015).

The Lov-1 accession originates from the Swedish High Coast, a world heritage site that is located around 300Km north of Stockholm. It is reported as one of two members of a rare slow vernalizing *FLC* haplotype group that also have an obligate cold requirement (Coustham et al., 2012). The significance of specific regions of *FLC* were tested in the Lov-1 accession through the generation of a set of transgenic lines that contained different sections of Lov-1 *FLC* substituted into the Col genome. Analysis of vernalization response in these plants indicate that sequence variation, specifically within the nucleation region of *FLC,* contributes most toward variation in the stability of *FLC* silencing between the two alleles (Coustham et al., 2012).

An accession originating from the Botanical Gardens in Edinburgh called Edi-0 is a representative member of the fourth *FLC* haplotype group. It becomes resistant to *FLC* reactivation after only a short period of cold exposure and is therefore considered to be a rapidly responding accession (Li et al., 2014, Shindo et al., 2006, Strange et al., 2011). Edi-0 only requires six weeks of cold to fully saturate its vernalization requirement; this is in contrast to the relatively cold insensitive accessions Var-2-6, Ull-2-5 and Lov-1 that all require around twelve weeks of cold treatment to achieve similar acceleration of floral transition.

Col-0 is a representative of the fifth major *FLC* haplotype group. Since this accession lacks a functional *FRI* allele, an introgressed line that contains the *FRI* allele from the Spanish San Feliu 2 (Sf2) accession is commonly used in vernalization studies (Michaels and Amasino, 1999). Like Edi-0, this genotype also exhibits a rapidly responding phenotype. Extensive knowledge of rapid-cycling Columbia genetics allows it to be used effectively as a "control" when comparing the vernalization response of accessions that belong to different *FLC* haplotype groups.

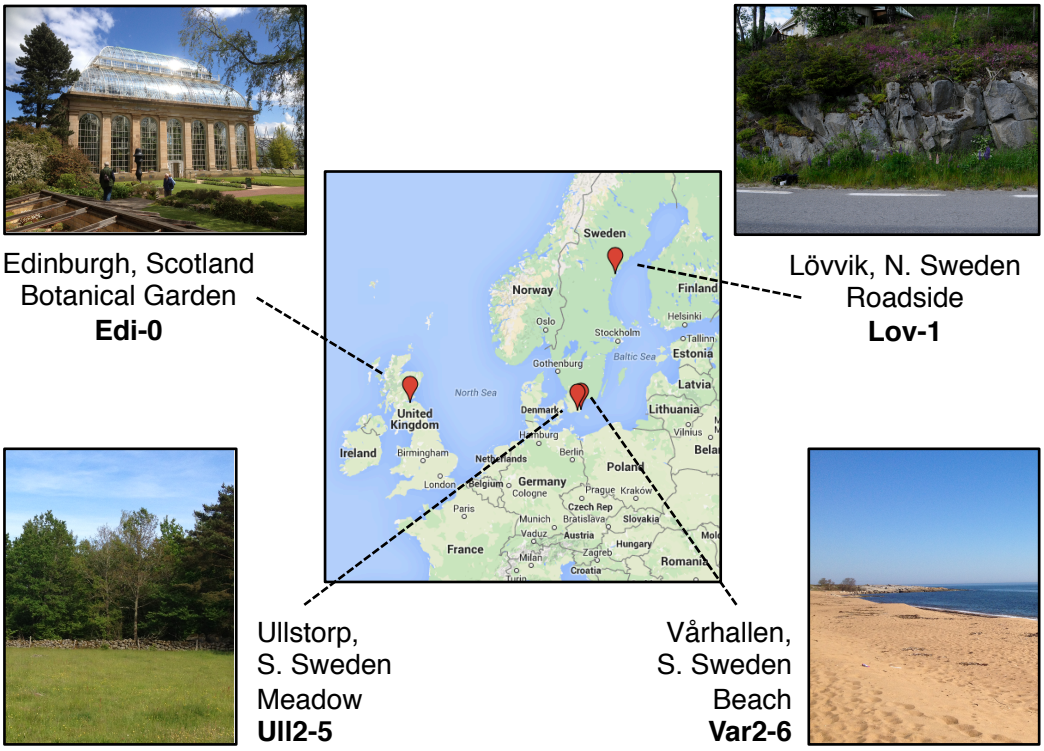

Figure 1.4 – Collection sites of representative accessions of major *FLC* haplotype groups

1.9 Vernalization and fitness

Apart from delaying the flowering response, partial vernalization also impacts crop yield and quality (Campoli and von Korff 2014; Ami et al., 2013). This has provided an incentive for research to determine minimum, optimum and maximum vernalizing temperatures in economically important plant species (Byrne and Bacon 1992). Figure 1.5 presents examples of effective vernalizing temperatures where upper and lower thresholds have either been estimated from field data or by extrapolation of data beyond the temperature range tested. These ranges broadly reflect the conclusions of an early review of empirical data suggesting that vernalization typically occurs between 0^{o}C and 14^{o}C (Chouard, 1960). However notable exceptions exist in the literature such as the optimal response of blackcurrent (*Ribes nigrum*) at -5^{o}C (Jones et al., 2014) and the effective (-3^{o}C, 27^{o}C) range reported for winter wheat (Craigon 1995). Reports of ornamental perennials similarly suggest that many species vernalize efficiently between Chouard's general range of between 0^{o}C and 14^{o}C (Padhye and Cameron 2009, Padhye and Cameron 2008), although -2.5^{o}C was found to activate an optimal response for *Veronica spicata* 'Red Fox' (Fausey and Cameron 2007).

1.10 Phenotypic plasticity in a changing climate change

Phenotypic plasticity can be described as the range of phenotypes a single genotype can express as a function of its environment (Nicotra et al., 2010). This phenotypic range is important in enabling plants to vary their phenotypes and is fundamental to survival under fluctuating environmental conditions. There is evidence that climate change has already caused a shift in the flowering time of annual plants (Franks and Weis, 2008) through a combination of rapid evolution and phenotypic plasticity (Nicotra et al., 2010). There is a general consensus that plasticity will be vital for plant populations over the coming century. This could determine whether populations persist long enough for rapid evolution to provide the novel genotypes required for long-term survival (Nicotra et al., 2010, Visser, 2008).

Climate change has advanced flowering phenology for many plants (Fitter and Fitter, 2002; Menzel et al., 2006; Willis et al., 2008). But a smaller group of non- responding and later flowering species have also been identified where warmer winters have

been suggested to be the result of insufficient vernalization (Cook et al., 2012). It has been speculated that as temperatures rise over the coming century, there will be an increase in both the number of affected species in this group and the extent of the phenological delay (Cook et al., 2012). At present these impacts are difficult to predict as little is known about either the effective vernalization temperature ranges of natural plant species and/or the phenotypic plasticity of this trait.

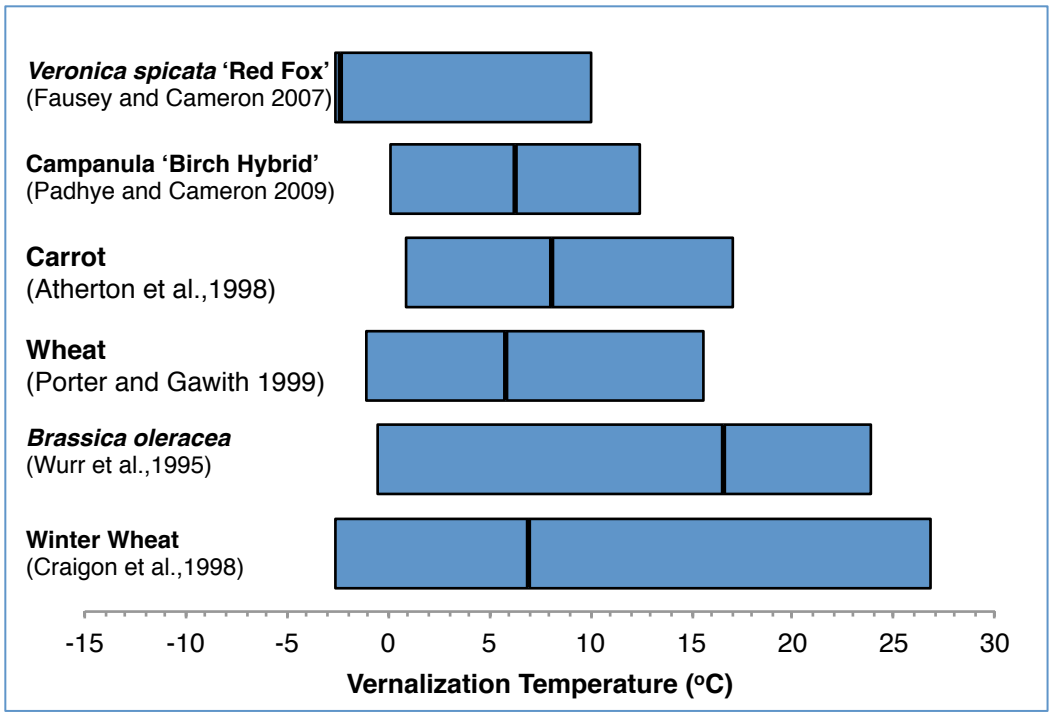

Figure 1.5 – Published predictions of effective vernalization temperature for crop and ornamental species
Upper and lower threshold temperatures are indicated by the ends of the blue boxes and predicted optimum temperatures are indicated by black bars.

1.11 Thesis outline

The aim of work presented in this thesis was to gain an insight into how climate change might affect vernalization over the coming century. Extensive molecular and ecological knowledge, in addition to the wide geographical and vernalization range, makes *Arabidopsis thaliana* an ideal plant in which to address this issue.

The majority of published *Arabidopsis* vernalization research reports response of plants that have been exposed to constant 4 or 5°C treatments for varying periods of time. This temperature preference dates back to early work published by Prof. Klaus Napp-Zinn that showed a late flowering Swedish accession called Stockholm vernalized efficiently between 2 and 4°C, but less well at lower temperatures (Napp-Zinn 1957). So I decided to determine the extent of plasticity in the vernalization response in natural *Arabidopsis* accessions as a starting point to understand how this model plant might be affected by climate change.

Chapter 2 reports results of laboratory experiments that were set up to determine the effective vernalization temperature range for representative accessions from the five major *FLC* haplotype groups. These revealed a surprising optimal response for Lov-1, at a temperature that exceeds the assumed effective vernalizing range for *A. thaliana* (Wilzcek et al., 2009; Chew et al., 2012). In addition the effect of vernalizing temperature was found to extend beyond enhanced acceleration of flowering to seed yield and dormancy.

The genetic basis and potential adaptive significance of the Lov-1 temperature optimum is explored further in **Chapter 3** where population life history and climate analyses led to a hypothesis that was tested during field experiments in northern Sweden.

Vernalization responses activated under constant conditions were then used to validate parameter selection for the chilling unit model presented in **Chapter 4**. Predictions of temperature integration were then interrogated for all accessions by comparing expected with observed results from field experiments. The vernalization model was then used to predict the potential impact of future climate scenarios at locations that span the species' latitudinal range.

Results presented in chapters 2-4 highlighted that complex temperature integration is a key aspect of vernalization that is still poorly understood. Determining the molecular basis of the integration of long-term temperature trends still presents a major challenge. Complex molecular circuitry has evolved to effectively modulate *FLC* transcription rather than protein metabolism to control flowering. This makes experimental approaches that determine expression levels invaluable for

vernalization research. Reverse transcription quantitative polymerase chain reaction (RT-qPCR) is commonly used to achieve this aim, however this method lacks cellular resolution and potentially important information about cellular localization of mRNA. In **Chapter 5** I report results of experiments that validate a novel single molecule fluorescent *in situ* hybridization (smFISH) method that enables mRNA to be quantified at the single cell level for the first time in plants.

Results of smFISH experiments are then presented in **Chapter 6** that address outstanding questions relating to memory of cold during vernalization. These results advance our current understanding of cold perception and could help inform future modelling efforts aiming to simulate complex temperature integration at the cellular level.

In **Chapter 7** the findings presented in each chapter are summarised and discussed in the context of related research. Finally, areas of development and future work are proposed.

Chapter 2 - Consequences of varying vernalization temperature for flowering time and seed yield

Division of work – Kate Dziubinska and Man Yu helped with seed collection, Clare Lister and Amy Strange generated the near isogenic lines (John Innes Centre). Arthur Korte collected 0°C flowering time data at Gregor Mendel Institute, Vienna.

2.1 Introduction

The climate envelope for the population range of *Arabidopsis thaliana* is extensive (Hoffmann et al., 2002) so it is perhaps unsurprising that variation exists in the length of vernalization required by winter annual accessions. Much of the variation in flowering time measured after vernalization at ~4°C has been shown to be attributable to non-coding polymorphisms within *FLC* (Coustham et al., 2012; Li et al., 2014; Li et al., 2015), but less is known about vernalization at other temperatures. In addition to knowledge of temporal requirements for cold, it was clear that exploring the effective temperature range would be important for predicting future impacts of climate change on the vernalization process.

Standard conditions traditionally used to study the vernalization process in *A. thaliana* date back to work published in 1957 that showed 4°C effectively accelerated flowering of a late flowering accession originating from Sweden (Napp-Zinn, 1957). I have continued the analysis of northern *A. thaliana* accessions and here I report that vernalization is effective at temperatures significantly higher than 4°C. I also found that the temperature effects extended beyond flowering time to impact fecundity and seed germination. This work has been corroborated by studies on *A. thaliana* accessions collected in Spain (Wollenburg and Amasino, 2011). Together these findings have implications for modelling the life history impacts of vernalization temperature under future climate scenarios.

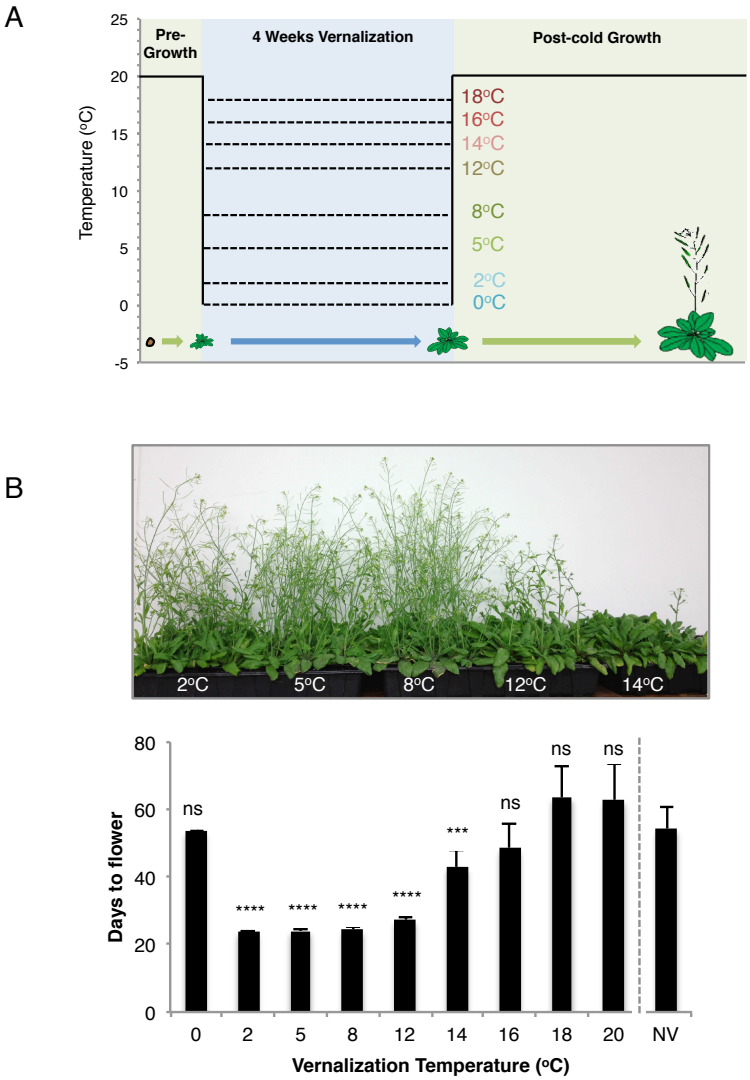

Figure 2.1–Testing the effectiveness of Col*FRI*^{Sf2} vernalization temperatures
(A) The range of temperatures used to test the vernalization response for Col*FRI*^{Sf2}. The flowering times observed for these experiments are shown in **(B)**. NV = Non-vernalized. *n*=12. Results shown are +SD. Student's *t*-test results are reported for each treatment compared to NV. ****p≤0.0005, *** ≤ p<0.001, p>0.05 = ns, not significant.

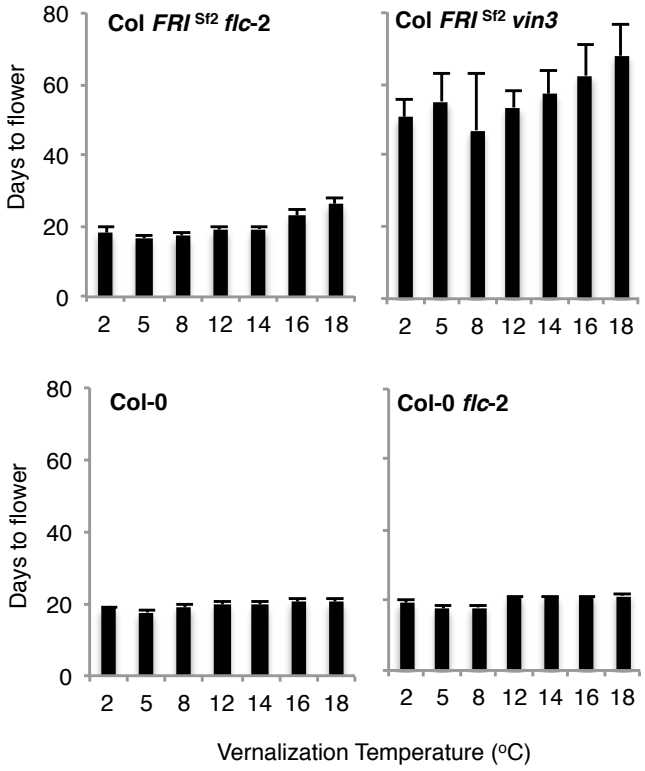

Figure 2.2 – Determining the relative contributions of *FLC*, *FRI* and *VIN3* to Col*FRI*^{Sf2} vernalization plasticity
Days to flower recorded after 4 weeks vernalization at a range of temperatures. Results are presented +SD. *n*=12.

2.2 Temperatures between 0°C and 14°C accelerate Col*FRI*^{Sf2} flowering

The effective vernalization temperature range was first determined in the reference genotype Col*FRI*^{Sf2}. A schematic of the experimental approach taken is shown in Figure 2.1A. Briefly, plants were pre-grown for one week before being transferred into short-day temperatures ranging between 0°C and 20°C. Flowering time was scored as the number of days from transfer back to inductive conditions until floral buds were first visible. Results from this experiment revealed that Col*FRI*^{Sf2} flowered significantly earlier than non-vernalized plants following treatments ranging between 2°C and 14°C (Figure 2.2B). Furthermore, 12°C was found to be a significantly more effective than either 14°C or 16°C (Student's *t*-test, $p<0.0001$).

2.3 *FLC*, *FRI* and *VIN3* synergistically contribute to Col*FRI*^{Sf2} vernalization plasticity.

Accelerated flowering following a 14°C treatment was unexpected since in flowering research this is generally considered an ambient rather than a chilling temperature. This finding prompted further experiments to explore the genetic basis of the phenotypic plasticity observed for Col*FRI*^{Sf2}. Results from a flowering time experiment in a Col*FRI*^{Sf2} line lacking *FLC* (Col*FRI*^{Sf2} *flc-2*) showed a similar trend, but dampened response across the temperature range. In the absence of *FLC*, *FRI* delayed flowering times following treatments above 14°C. This was perhaps due to FRI mediated up regulation of *FLC* related *MAF* genes (Ratcliffe et al., 2003). Consistent with this hypothesis, the delay observed for treatments above 14°C was abolished in Col*FRI*^{Sf2} genotypes that lacked *FRI* (Col-0) or both *FLC* and *FRI* (Col-0 *flc-2*) (Figure 2.2).

The lack of response observed for the Col*FRI*^{Sf2} *vin3* genotype confirms that VIN3 is a necessary component for vernalization, potentially as an early thermo-sensitive step (Figure 2.2). Together these results indicate that *FLC*, *FRI* and *VIN3* are all required for the phenotypic plasticity of flowering time observed for Col*FRI*^{Sf2}.

2.4 *VIN3* mediated *FLC* repression and subsequent *FT* up-regulation accelerates flowering across the effective temperature range

Despite the confirmation that both *FLC* and *FRI* are necessary for the observed delay in flowering across the effective temperature range, it was still unclear whether the flowering plasticity could be attributed to variation in vernalization efficiency. To address this question both *FLC* and *VIN3* expression levels were determined before, during and after cold treatments.

These experiments revealed an opposing trend of expression where lower levels of *FLC* were generally associated with both higher *VIN3* and subsequent *FT* levels. This relationship was less clear for *FT* expression after 12 week treatments. Although 5 and 8°C treatments resulted in the highest levels of *VIN3* induction and *FLC* repression, 8 and 12°C treatments resulted in higher levels of *FT* expression

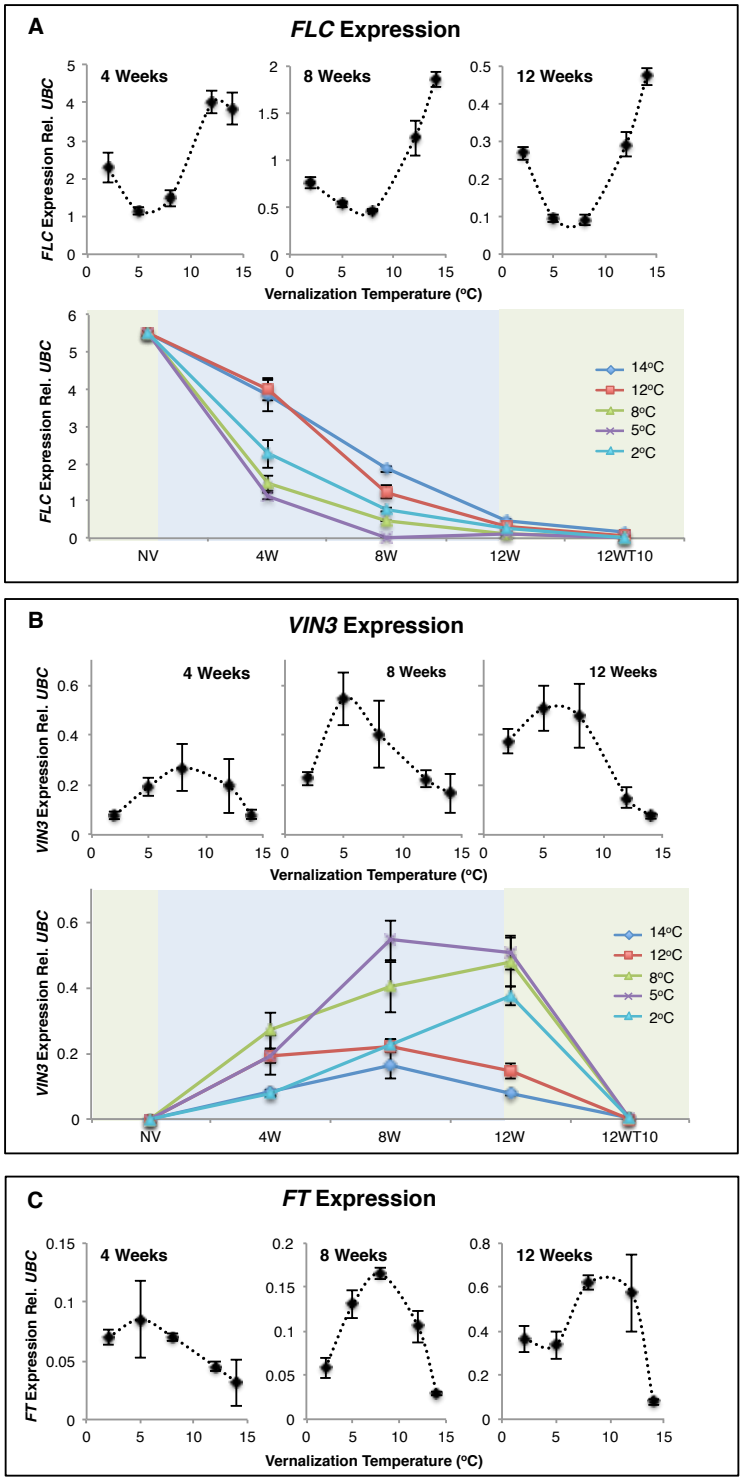

Figure 2.3 – Opposing trends of *VIN3*, *FT* and *FLC* expression observed for Col*FRI*^{Sf2} during and after vernalization

Quantitative PCR results for *FLC* (A) and *VIN3* (B) before, during and after cold. *FT* expression levels shown in (C) were determined 10 days after transfer to warm conditions, when induction of this gene first became apparent (FT expression was not detected for the other T0 timepoints shown, data not shown). Error bars = SD. NV = Non-vernalized, W = weeks, T10 = 10 days post-cold growth, *n*=3.

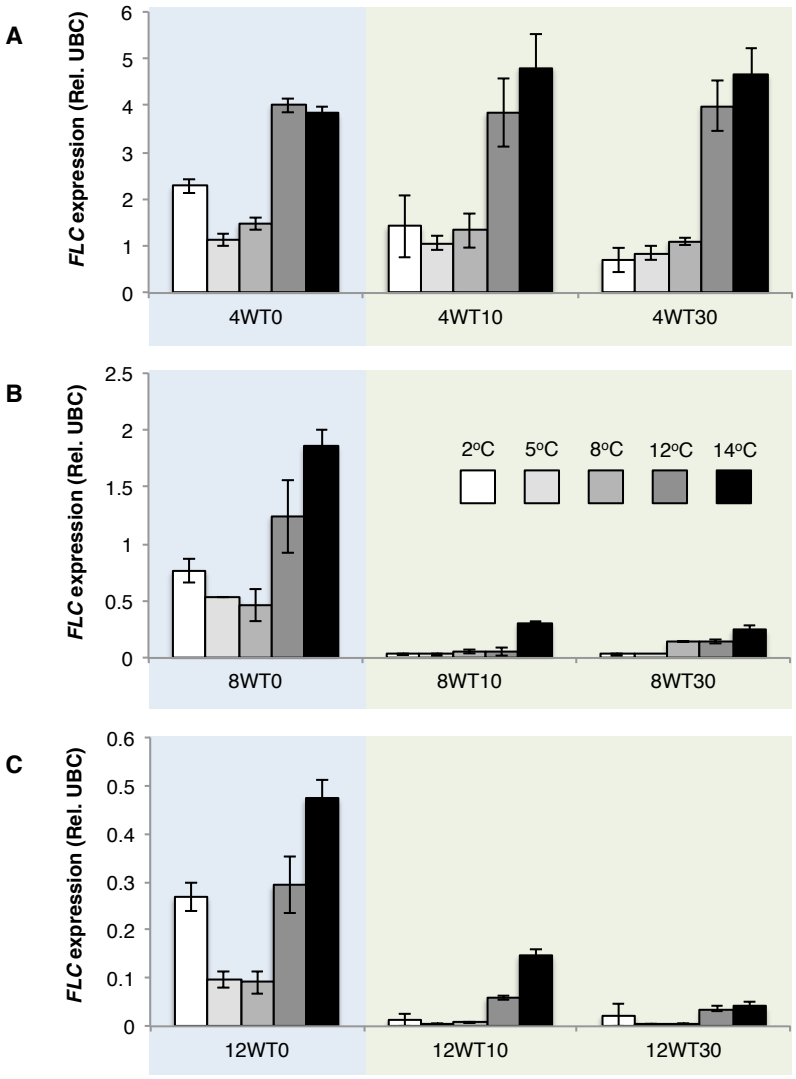

Figure 2.4 – *FLC* expression determined for Col*FRI*^{Sf2} after vernalization
Quantitative PCR results for *FLC* expression for **(A)** 4 week, **(B)** 8 week and **(C)** 12 week vernalization experiments carried out at a range of temperatures. Samples were collected at three time points: immediately after vernalization (T0), and following 10 days (T10) and 30 days (T30) post-cold growth. W = weeks. *n*=3.

post-cold (Figure 2.3). This may reflect saturation of the Col*FRI*^{Sf2} cold requirement with *FT* levels determined 10 days after 12 week treatments not accurately informing the effectiveness of preceding temperature (Figure 2.3C).

In the Swedish accession Lov-1, reactivation of *FLC* expression occurs following exposure to standard vernalizing conditions. This reactivation is associated with reduced levels of the silencing chromatin modification H3K27me3 and a late flowering phenotype (Coustham et al., 2012). For Col*FRI*^{Sf2} a slight increase in *FLC* expression was observed following growth for four weeks at 14^{o}C, but reactivation was not observed following 4, 8 or 12 weeks treatments for any other temperature (Figure 2.4). Together these results indicate that all temperatures achieved variable levels of stable epigenetic silencing at *FLC* and this variability mainly determined the flowering times observed across the effective temperature range.

2.5 Natural variation in vernalization thermal sensitivity

The impact of global temperature rises on plant chilling periods prompted us to investigate natural variation of vernalization thermal sensitivity (Cook et al., 2012). Although this variation had previously been explored in Spanish accessions (Wollenburg and Amasino, 2011) we decided to systematically test this trait in representative lines from 5 major *FLC* haplotype groups (Li et al., 2014) and include potentially vulnerable populations from northerly regions (see Chapter 1, Figure 1.4).

Strikingly, all genotypes responded to the same effective temperature range identified for Col*FRI*^{Sf2} (2-14^{o}C) with differing levels of plasticity. Both Edi-0 and Ull2-5 flowered at similar times following treatments between 2-12^{o}C, whereas Lov-1 and Var2-6 exhibited much more plasticity across this temperature range (Figure 2.5). The enhanced effect identified between 5-8^{o}C for these lines was unexpected given that Lov-1 was collected from a location close to the northerly limit of the *A. thaliana* range and Var2-6 shares *FLC* sequence homology with the majority of northern Swedish accessions (Li et al., 2014.) This was surprising given that enhanced effects at *lower* temperatures are generally associated with adaptation to colder climates. Results from experiments that explore the ecological significance of enhanced effectiveness of higher vernalization temperatures are presented in Chapter 3.

2.6 Vernalization temperatures impact seed yield

Incomplete vernalization of crops delays the harvest dates and reduces crop yield (Rollins et al., 2013, Campoli and von Korff, 2014, Ami 2013), but little is known about the impact of vernalization on the fitness of natural plant species. To address this question seeds were collected from plants following vernalizing treatments between 2°C and 14°C and weighed to explore the potential impact of suboptimal vernalization on fitness.

Consistent with agricultural data, vernalization mostly increased seed yield for facultative cold-requiring genotypes Col*FRI*^{Sf2} and Edi-0; only 12-week 2°C treatments failed to produce higher yield than non-vernalized plants for these genotypes (Figure 2.5). Rather than just being advantageous, vernalization is vital for the fitness of Var2-6, Ull2-5 and Lov-1 because these accessions do not flower without cold exposure. Interestingly, a negative correlation was observed for both Var2-6 and Ull2-5 across the temperature range indicating that increasing vernalizing temperatures progressively reduce fitness. Furthermore, a predominant impact of time, rather than temperature was clear for the fitness of Var2-6. Late flowering (~80 days) was found to result in stunted inflorescence development, whereas faster flowering (~20 days) following 12 weeks vernalization visibly alleviated the dwarf phenotype (Figure 2.6).

A striking inverse relationship was revealed between days to flower and seed yield for Lov-1 (Figure 2.5). But unlike for Var2-6 and Ull2-5 the small difference observed in flowering time between 8°C, and both 2°C and 14°C treatments, consistently resulted in significantly less seed production.

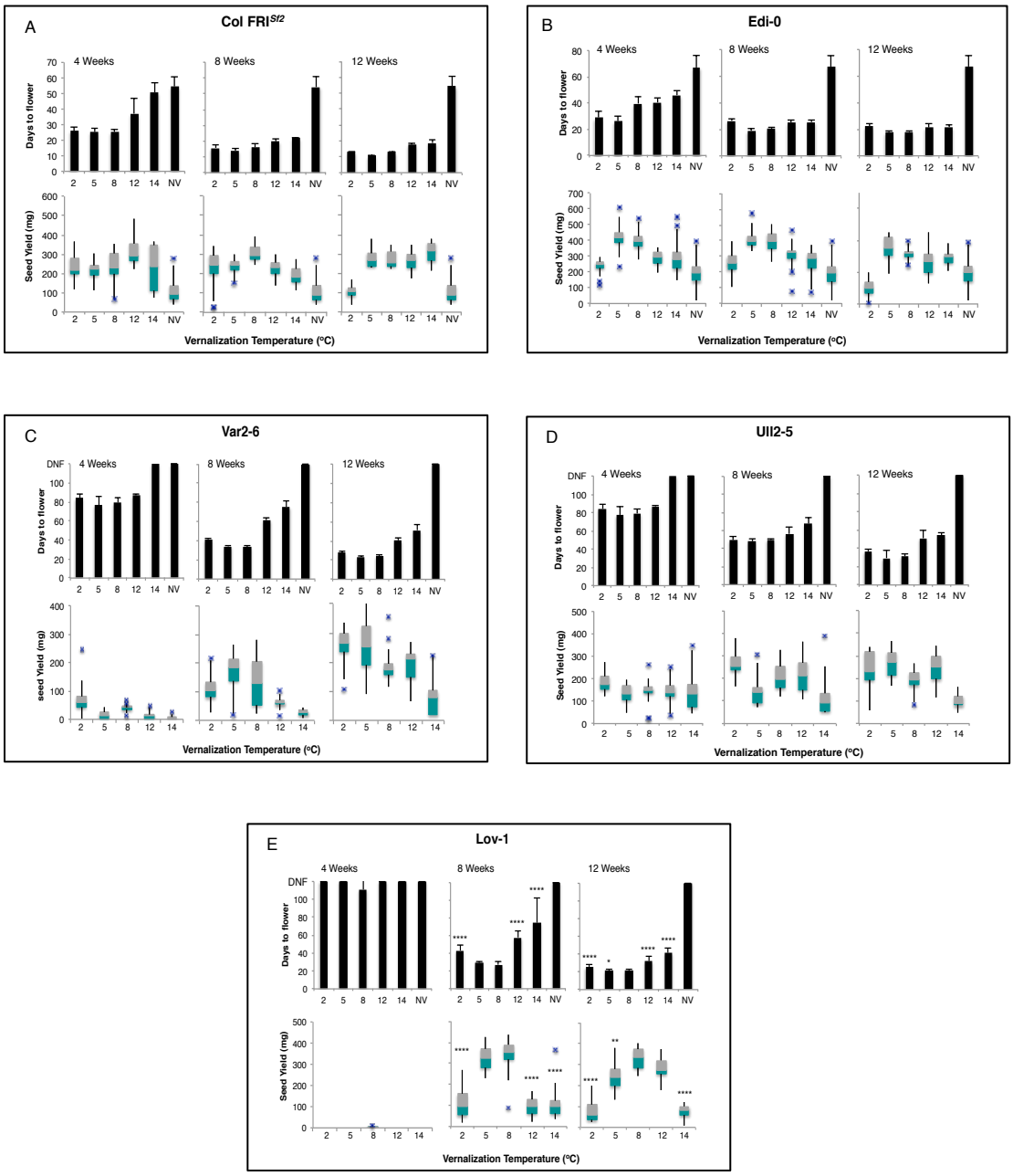

Figure 2.5 – Flowering time and seed yield recorded following a range of vernalization of treatments

Days to flower are presented ±SD**.** Seed yield data are presented as box plots where green and grey boxes = median to 1st and 3rd quartiles, respectively. Upper and lower whiskers represent 1.5* Inter Quartile Range (IQR) or highest / lowest values. Blue crosses = outlier values greater than 1.5*IQR. Mann-Whitney *U* tests were carried for Lov-1 to determine the significance of each 8°C treatment.

* $p \leq 0.05$, ** $p \leq 0.01$, *** $p \leq 0.001$, **** $p \leq 0.0001$.

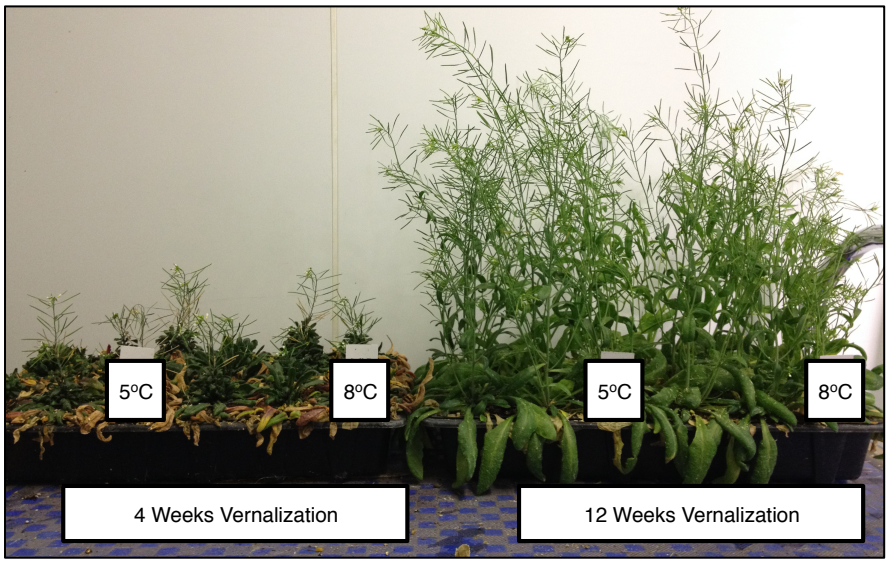

Figure 2.6 – Contribution of vernalization period on Var2-6 inflorescence architecture
Photos were taken after 4 and 12 weeks vernalization at 5°C and 8°C.

2.7 *FLC* contributes to Lov-1 vernalization temperature sensitivity and fecundity.

Natural variation in vernalization temperature sensitivity was apparent from the flowering times observed (Figure 2.5) and Lov-1 was found to display the greatest degree of plasticity. In this accession 8°C treatments resulted in faster flowering than 2°C, 5°C, 12°c and 14°C. Also vernalization at 5°C - 8°C resulted in higher levels of seed yield than 2°C, 12°C and 14°C. Four SNPs located within intron 1 were found previously to destabilize repression of Lov-1 *FLC* under standard vernalizing conditions (Coustham et al., 2012) so we considered whether these SNPs might also contribute to Lov-1 thermal sensitivity. The molecular basis of the observed differential flowering response was explored further with near isogenic lines (NILs). Replacement of the Lov-1 *FLC* loci in a Col*FRI*^{Sf2} background allowed genetic contributions to be tested (Figure 2.7A). As reported previously (Coustham et al., 2012), NILs that contain Lov-1 *FLC* are very late flowering (Figure 2.7B and C), but vernalization at 5°C and 8°C revealed that the presence of a second locus on chromosome 5 was necessary, in addition to Lov-1 *FLC*, to recreate an enhanced flowering response at 8°C. (Figure 2.7C).

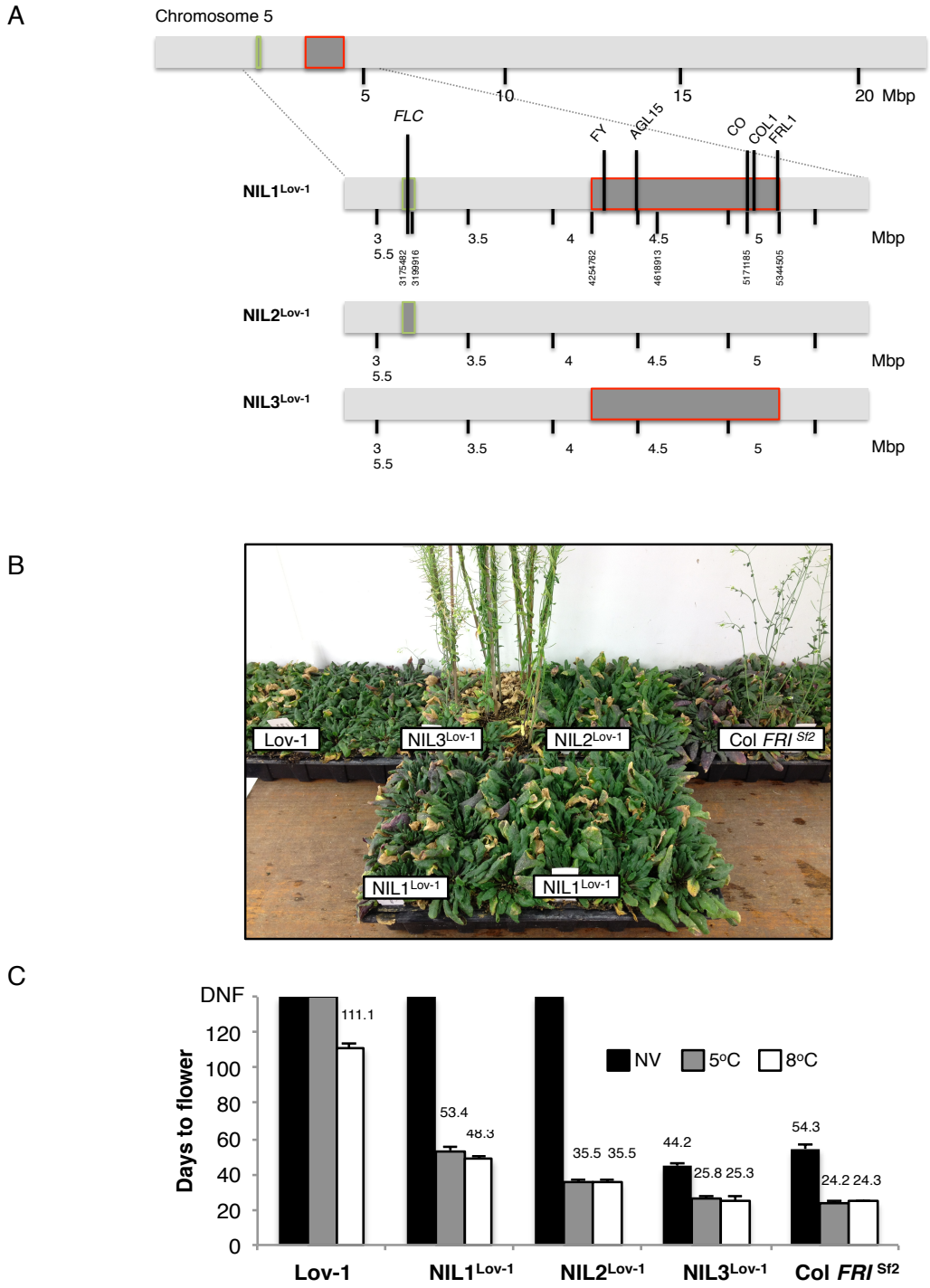

Figure 2.7 – *FLC* plus an additional Lov-1 locus are required for an enhanced vernalization response at 8°C

(A) A genetic map showing two Lov-1 regions in three Col*FRI*^{Sf2} Near Isogenic Lines (NILs). One region containing *FLC* is outlined in green and an additional downstream region that contributes to vernalization temperature senstitivity is outlined in red. **(B)** Photograph showing NIL flowering phentypes. **(C)** Flowering times recorded for parent plants and NILs after 4 weeks vernalziation at two temperatures. Error bars = SD. NV = Non-vernalized. Genetic markers used to generate this map listed in Appendix Table 1.

Further experiments were then carried out to determine the impact of constant vernalization temperature on seed yield for NIL1$^{Lov\text{-}1}$ and NIL2$^{Lov\text{-}1}$. The results obtained after 4 and 8 week treatments indicate a general negative correlation between temperature and seed yield. However 12 week treatments resulted in a differential effect between 2-14^{o}C (Figure 2.8) that differed from the homogeneous response of Col *FRI* ^{Sf2}. This response appeared more similar to the results obtained for Lov-1 (Figure 2.5). Despite a smaller impact of temperature on flowering time, seed yield data for both NILs after 12 weeks vernalization suggest that the Lov-1 *FLC* allele contributes to the levels of seed yield observed for this accession.

2.8 Determining the impact of vernalization temperature on fecundity and dormancy

The potential impact of vernalization temperature on fitness cannot be inferred from total seed yield alone since this measurement represents contributions from both seed size and number and overlooks potential impacts on viability. With this in mind, variations in seed yield were investigated further in Col*FRI*^{Sf2}, Lov-1 and NIL1$^{Lov\text{-}1}$.

One thousand seed weight (i.e. the weight of 1000 seeds) is a seed size measurement that is commonly used to compare crop yields e.g. (Belle et al., 2014). To dissect whether differences observed in total seed weight for each accession were primarily due to differences in seed number or seed size one thousand seeds from each treatment group were weighed and these measurements were used to calculate approximate seed numbers. This resulted in a trend of seed yield across the temperature range that appeared similar to the seed number inferred by this calculation for each genotype. These results suggest that vernalization temperature has little impact on seed mass and indicates that higher fecundity underlies the increased seed yield observed for Lov-1 and NIL1$^{Lov\text{-}1}$ plants vernalized at 8^{o}C (Figure 2.9).

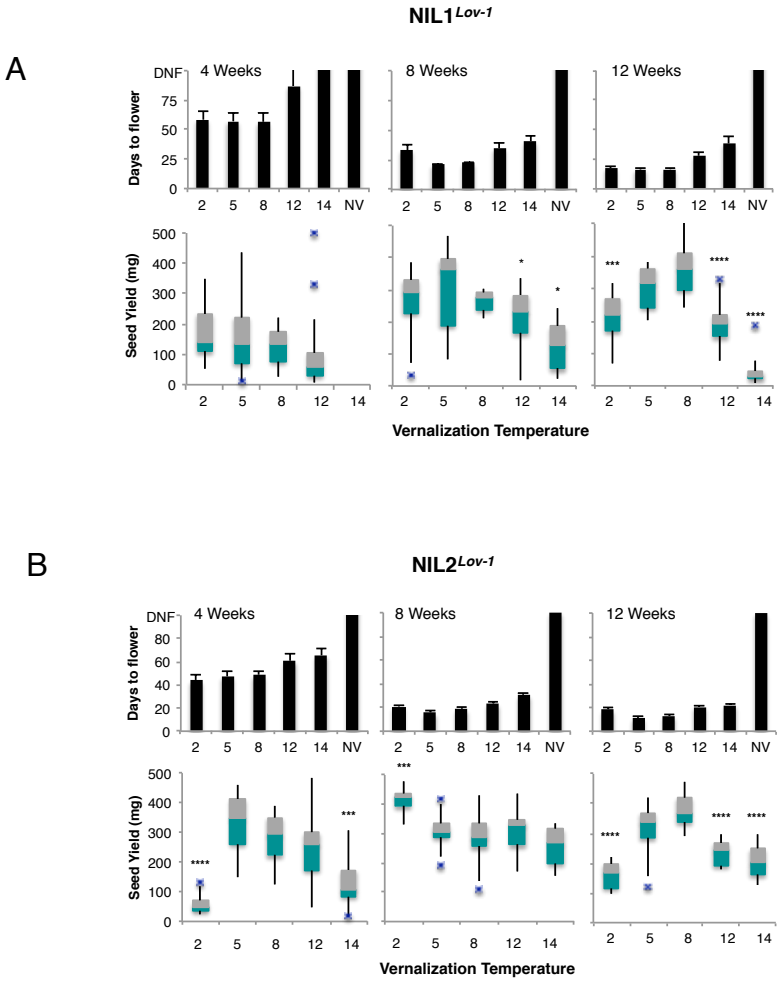

Figure 2.8 – Flowering time and seed yield recorded for NILs
Days to flower and seed yield were determined for (A) NIL1^{Lov-1} and (B) NIL2^{Lov-1} plants that had been vernalized at a range of temperatures. Seed yield data are presented as box plots where green and grey boxes = median to 1st and 3rd quartiles, respectively. Upper and lower whiskers represent 1.5* Inter Quartile Range (IQR) or highest / lowest values. Blue crosses = outlier values greater than 1.5*IQR. Mann-Whitney *U* tests were carried to determine the significance of each 8^{o}C treatment. * p≤0.05, ** p≤0.01, *** $p \leq 0.001$, **** $p \leq 0.0001$. Error bars = ± SD. NV = Non-vernalized.

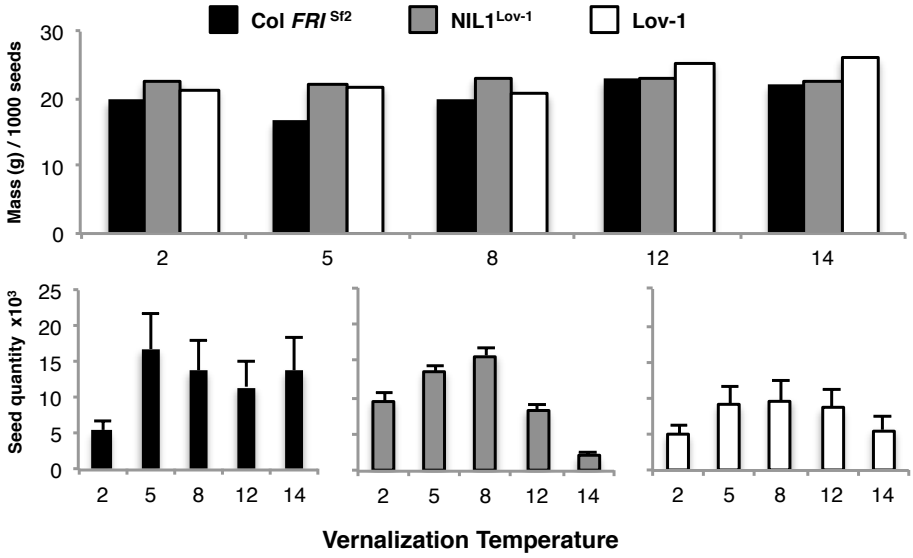

Figure 2.9 – Determining fecundity for vernalized Col*FRI*^{Sf2}, NIL1^{Lov-1} and Lov-1 plants
The seeds were collected from plants that had been vernalized for 12 weeks at a range of temperatures.

Germination was then tested for the Col *FRI* ^{SF2}, Lov-1 and NIL1^{Lov-1} seeds that were collected from plants exposed to a range of vernalizing treatments. Despite a three day stratification treatment at 5^{o}C to break dormancy, seeds produced by Col *FRI* ^{SF2} and NIL1^{Lov-1}plants vernalized for 4 weeks at 8^{o}C still exhibited an early delay of germination, however all seeds from the 4 week temperature treatments germinated successfully following exposure to 9 days of inductive conditions (Figure 2.10). All seeds from Lov-1 plants vernalized for either 8 or 12 weeks germinated after 9 days, regardless of treatment, although a similar early delay was observed for seeds originating from plants vernalized for 12 weeks at 8 and 5^{o}C. Surprising results were obtained for seeds originating from plants that had been vernalized at higher temperatures for 12 weeks. Delayed germination followed by 100% seedling emergence was observed for NIL1^{Lov-1} seeds originating from 12 week 12^{o}C treated plants, but 45% of similar Col *FRI* ^{Sf2} seeds failed to germinate at all. Furthermore, less than 75% of Col *FRI* ^{Sf2} and NIL1^{Lov-1} seeds also failed to germinate if the mother plant had been vernalized for 12 weeks at 14^{o}C (Figure 2.10).

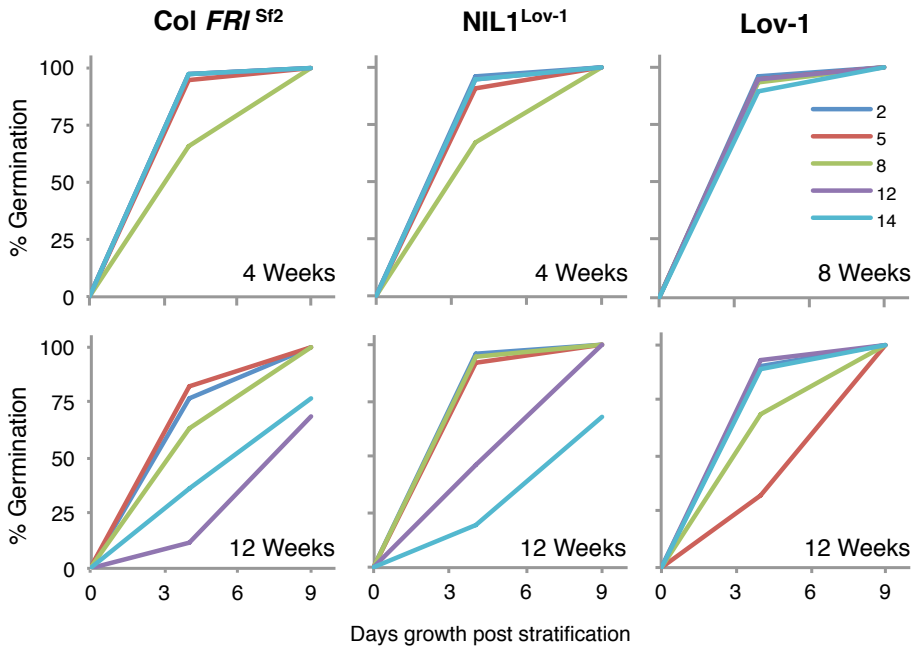

Figure 2.10 – Variable germination observed for Col*FRI*^{Sf2} and NIL1^{Lov-1} seeds originating from plants vernalized at a range of temperatures
The number of weeks vernalization is indicated on each graph. The numbers in the legend refer to different temperature treatments (^{o}C).

2.9 Discussion

The flowering response observed for all accessions was consistent with an effective 0^{o}C to 14^{o}C vernalization range reported in an early review that summarized empirical data for a range of crops (Chouard, 1960). These findings are also consistent with a more recent study that reported effective acceleration of Col*FRI*^{Sf2} flowering following vernalization at 13^{o}C, but not 16^{o}C. Although the authors concluded that 13^{o}C represents the upper vernalization temperature threshold (Wollenberg and Amasino 2012), we suggest extending this upper limit to reflect the significant acceleration of flowering observed at 14^{o}C (Figure 2.1).

It was surprising to observe effective vernalization at 14^{o}C since this is typically assumed to be an ambient, rather than a chilling temperature (Wigge 2013). However significant *VIN3* induction associated with stable repression of *FLC* transcription and limited *FT* induction (Figure 2.3) are consistent with the hypothesis

that 14°C accelerates flowering via a limited vernalization response. In addition, the observation that the flowering time trend observed for Col*FRI*^{Sf2} (Figure 2.1) was abolished in lines lacking the key vernalization genes *FLC*, *FRI* or *VIN3* (Figure 2.2) indicates that elevated *FLC* levels before cold are required for the efficacy of higher temperatures to become evident. It is therefore likely that the effectiveness of higher vernalization temperatures may have gone unnoticed because ambient temperature researchers typically assess effects in genotypes that lack functional *FRI* alleles. Natural variation studies of flowering time that typically include *FRI*+ and *FRI*- genotypes, have also been carried out under ambient, long day conditions. This mix of winter annual and rapid cycling accessions combined with long photoperiod conditions effectively masks not only the effectiveness of higher vernalizing temperatures, but also its genetic basis. However, consistent with our results, a genome-wide association study found SNPs around *FLC* to be most highly associated with flowering time of plants grown at 10°C (Atwell et al., 2010).

Although the effective vernalizing range between 2-14°C identified for Col*FRI*^{Sf2} was shared by the other accessions tested, natural variation in temperature sensitivity was evident (Figure 2.4). Similar flowering times were recorded following vernalization of Edi-0 and Ull2-5 between 2-8°C, but increased plasticity was observed for the northern Swedish accession Lov-1 and the representative northern *FLC* haplotype accession Var2-6.

A low optimal temperature response had been anticipated for Lov-1 as it had been collected from close to the northerly limit of the species range. But contrary to these expectations we found these plants consistently vernalized efficiently at 8°C (Figure 2.4). Furthermore, an inverse relationship was observed between flowering and seed yield. Although it is necessary to exercise caution when inferring ecological significance from phenotypic data generated under laboratory conditions (Weigel, 2012; Hoffman et al., 2002, Brachi et al., 2010, Weinig et al., 2002) this suggests fitness benefits are associated with vernalization temperatures that extend beyond the timing of floral initiation (Figure 2.4).

In accordance with findings in crop species (Rollins et al., 2013, Campoli and von Korff, 2014), our seed yield data indicates that vernalization generally increases yield for cold requiring accessions. In general, a negative correlation was observed

between temperature and yield for treatments between 5°C and 14°C. Inconsistent results for yield observed after 2°C treatments may be the result of a positive vernalization effect being counteracted by a progressively negative impact on biomass accumulation during cold exposure.

In addition to enabling an assessment of the impact of temperature on seed yield, our experiments allowed us to independently assess the impact of vernalization time on this trait. Longer treatments did not appear to significantly increase the seed yield of the faster flowering lines Col*FRI*^{Sf2} and Edi-0 (Figure 2.4), however significantly higher seed yield was observed after 12 week compared to after 4 week treatments for all the later flowering Swedish accessions (Wilcoxon Sum Rank Test: $p < 0.005$). The increase in yield over time was most apparent for Var2-6 and examination of inflorescence architecture indicate that this was due to incomplete vernalization inhibiting stem development, rather than the result of suboptimal growing conditions preventing the plants from achieving their reproductive potential (Figure 2.6).

Variation in climate has contributed to the selection of divergent *FLC* haplotype groups that exhibit variation in temporal requirements for cold (Li et al., 2014). Detailed functional analyses have shown that two haplotype groups have independently evolved long vernalization requirements via subtle changes in non-coding *FLC* sequence (Coustham et al., 2012; Li et al., 2015.) Results in Figure 2.7 suggest that in addition to eliciting a temporal effect, Lov-1 *FLC* also contributes to a synergistic effect with another Lov-1 locus located downstream on chromosome 5 to further delay flowering. The anti-correlation observed between seed yield and flowering time for Lov-1 (Figure 2.4) was also evident for two near isogenic *FLC*$^{Lov-1}$ lines after 12 week treatments (Figure 2.8) indicating that seed yield can be added to the growing list of life history traits affected by genetic variation at *FLC* (Chiang et al., 2009).

Recent work in *FRI* null genotypes has demonstrated that maternal growth temperature contributes to variation in seed dormancy (Chen et al., 2014). As in our experiment, they found that the preceding temperature exposure of the parent affected germination of the offspring, despite seed development and maturation occurring under standard inductive conditions. They showed that this variation was due to FT levels within the maternal silique tissue that affected biochemical

composition of the seed coat. This suggests that the variation observed in our germination assays might also reflect different levels of FT induction that occur following different temperature treatments (Figure 2.3). However, unless FT levels within the silique vasculature are different to those observed for homogenised plant samples, this does not sufficiently explain the delay in germination observed for seeds originating from Col*FRI*^{Sf2} plants vernalized for 12 weeks at 12^{o}C and 14^{o}C (Figure 2.9).

The results presented in this chapter show that variation in vernalization time and temperature significantly effects flowering and seed yield for a range of natural accessions. Several of these intriguing findings have been followed up in this thesis. The molecular mechanisms that underlie the distinct Lov-1 vernalization temperature response and potential selecting environmental cues are discussed in Chapter 3. Chapter 4 explores how constant temperature responses relate to natural fluctuating field conditions and determines how informative threshold temperatures are for predicting responses in the real world. Together these results form the foundation for predictions about the future impact of climate change on *A. thaliana* vernalization.

2.10 Materials and Methods

2.10.1 Plant growth conditions.

For the daily averaging experiment seeds from each accession were sown onto Arabidopsis compost mix and stratified for 3 days at 5°C. Seedlings were pre-grown for 7 days (16 hours light, 100µmol m^{-2} s^{-1}, 22°C) and vernalized for 4 weeks at 14°C, 12°C, 10°C, 8°C (8 hours light) in cabinets (Sanyo MLR-351H), 5°C (walk-in vernalization room), 2°C (modified Liebherr KP3120) or 0°C (Johnson Controls). All temperatures were recorded ± ≤1.5°C, 70% ± ≤10% RH. Low light (~30µmol m^{-2} s^{-1}). Plants were then transferred to random locations in a controlled environment room (16 hours light, 100µmol m^{-2} s^{-1}, 22°C ± 2°C) and flowering time was scored as the number of days of growth until floral buds became visible.

2.10.2 RNA Extraction

The RNA extraction was carried out using a similar protocol to that reported by Box and colleagues in 2011. ~200mg of above soil tissue was collected into 1.5mL micro-centrifuge tubes (Eppendorf, Hamburg, Germany) and immediately frozen by immersion into liquid nitrogen. Samples were then placed into pre-cooled blocks and ground to a fine powder by 3mm tungsten-carbide beads (Qiagen, Venlo, Netherlands) using a 30 second 1200 rpm setting on a Geno/Grinder® 2010 bead mill (SpexSamplePrep, New Jersey, USA). The samples were then stored at -80°C.

RNA extraction buffer (0.1M Tris pH8.0, 5nM EDTA pH 8.0, 0.1M NaCl, 0.5% SDS) was heated to 60°C and 300µL was added to each sample and mixed briefly before addition of 300µL 1:1 acidified phenol pH 4.3±0.2: Chloroform (Sigma-Aldrich, Missouri, USA). The tubes were mixed vigorously for 10 minutes and then spun down in a centrifuge at room temperature for 15 minutes at top speed. The supernatant was then carefully removed to fresh 1.5mL micro-centrifuge tubes containing 240µL of isopropanol (2-propanol) and 30µL of 3M sodium acetate (pH 5.2). Nucleic-acids were left to precipitate at -80°C for a minimum of 15 minutes. The samples were then spun down again for 30 minutes in a centrifuge at 4°C. The supernatant was pipetted off and the pellets were then washed twice with 750µL of 70% ethanol with a 5 minute maximum speed centrifugation step after each wash. Residual ethanol was then carefully removed and all pellets were left to dry for 15 minutes before being fully re-suspended in 500µL RNase free water (Qiagen). 500µL 4M LiCl was then added to each sample before being left overnight at 4°C. Samples

were then centrifuged at full speed for 30 minutes at 4°C to pellet the RNA. Genomic DNA was then removed along with the supernatant and the pellet was washed again twice with 750µL of 70% ethanol with a 5 minute maximum speed centrifugation step after each wash. Residual ethanol was then carefully removed and the pellets were left to dry for 15 minutes before being re-suspended in 50µL RNase free water.

Concentration and quality was determined for each RNA sample using a NanoDrop ND-1000 Spectrophotometer (NanoDrop Technologies Inc., Denver USA) and each sample was then diluted to 200ng/µL using RNase free water.

2.10.3 Reverse Transcription

Reverse transcription was carried out using reagents from Primerdesign (Southampton, UK)

Reaction 1	
8µL	RNase free water
1µL	Oligo (d)T primer
5µL (1µg)	Total RNA
Samples were incubated for 5 minutes at 65°C then transferred onto ice before addition of the following:	
2µL	10X buffer
1µL	dNTP mix
2µL	DTT
4µL	PCR grade water
1µL	Reverse transcription enzyme
Reaction 2	
55°C	20 minutes
5°C	15 minutes
Sample Dilution	
180µL	PCR grade water

2.10.4 Quantitative Polymerase Chain Reaction (qPCR)

A LightCycler 480 II instrument (Roche Life Science, Penzberg, Germany) was used in conjunction with probes from the LightCycler 480 Universal Probes Library (UPL) range to determine expression levels. An EpiMotion (Eppendorf) robot was used to pipette triplicates of the following reaction mixes into in 384 well plates (Roche):

6.5µL Reaction	
5µL	Universal Probes Library master mix
0.1µL	Forward primer (200mM)
0.1µL	Reverse primer (200mM)
0.4 µL	Universal Probe Library Probe
0.9µL	PCR grade water

Thermo-cycler program used to amplify the cDNA		
Step	**Temperature**	**Time**
1	95°C	10 minutes
2	95°C	10 seconds
3	60°C	20 seconds
4	72°C	1 second
45 cycles repeating steps 2-4		
Cooling	40°C	10 seconds

All mRNA levels were assayed using Roche Universal Probe Library (UPL) Probes using the primers shown below.

***FLC* (At5g10140)**	
sFLC_UPL_#65_F	5'-gtgggatcaaatgtcaaaaatg-3'
sFLC_UPL_#65_R	5'-ggagagggcagtctcaaggt-3'
UPL #65	5'-ctggagga-3'

***VIN3* (At5g57380)**	
VIN3_UPL_#67_F	5'-cgcgtattgcggtaaagataa-3'
VIN3_UPL_#67_R	5'–tctctttcgccaccttcact-3'
UPL #67	5'-ctccagca-3'

***FT* (At1g65480)**	
FT_UPL_#138_F	5'-ggtggagaagacctcaggaa-3'
FT_UPL_#138_R	5'-ggttgctaggacttggaacatc-3'
UPL #138	5'-tggtggat-3'

***UBC* (At5g25760)**	
UBC_UPL_#9_F	5'-tcctcttaactgcgactcagg-3'
UBC_UPL_#9_R	5'-gcgaggcgtgtatacatttg-3'
UPL#9	5'-tggtgatg-3'

Relative levels of gene expression were calculated using the comparative Ct method (also known as the 2-[delta][delta]Ct method) (Schmittgen and Livak 2008) and statistical analysis of was performed using GraphPad Prism version 6 software for Mac (La Jolla, California, USA).

2.10.5 Seed Yield

Once plant dessication was evident, glassine bags (Global Polythene, Preston, UK) were placed over the plants and secured around the stem using tape. Watering was then continued until senescence was considered complete. Plants were then left at 22^{o}C, 18 hour daylength, until completely dry. Seeds were collected from each plant and weighed.

2.10.6 Seed Germination Assay

100 seeds from each genotype were sown onto MS (minus glucose) 3cm media plates (Sterilin, Cheshire, UK) and stratified at 5^{o}C for 3 days before being transferred to 22^{o}C (18 hour light, 100µmol m^{-2} s^{-1}, 70% humidity). Germination was scored on day 3 and day 9 of inductive growth. The experiment had to stopped on day 9 due to fungal growth around un-germinated seeds.

Chapter 3 - Seasonal shift in timing of vernalization as an adaptation to extreme winter

Division of work: Svante Holm (Mid-Sweden University) collected field temperature data and set up the field experiments in Sweden. Arthur Korte (Gregor Mendel Institute, Vienna) scored flowering time after vernalizing plants at 0°C. Julia Questa (John Innes Centre) completed the ChIP experiments. Clare Lister and Amy Strange generated the near isogenic lines.

3.1 Introduction

Results in the previous chapter revealed that Lov-1, an accession that originates from close to northerly limit of the species range, vernalizes most effectively at 8°C and exhibits a significant vernalization response at temperatures as high as 14°C. In this chapter the underlying genetic cause of the differential temperature sensitivity and the potential adaptive significance of this 8°C optimum are explored further.

3.2. Flowering Time

A direct comparison of flowering time recorded following vernalization at a range of temperatures revealed natural variation in temperature sensitivity (Figure 3.1, also Chapter 2, Figure 2.5). Consistent with results obtained for the reference genotype Col*FRI*^{SF2}, all lines tested (Edi-0, Var2-6, Ull2-5 and Lov-1) showed limited vernalization after 4 and 6 weeks exposure to 0°C and vernalized more efficiently at all other temperatures. In contrast to the other three accessions however, Lov-1 plants showed a differential response to temperature with 2 and 12°C consistently less effective than 5 and 8°C. The only temperature that resulted in flowering after 4 weeks exposure was 8°C and, although this enhanced effect diminished over time, 8°C treatments consistently resulted in the fastest flowering times (Figure 3.1). Results from further analyses also revealed that in addition to flowering time effects, vernalization temperature also impacts fecundity (Chapter 2, Figure 2.5).

Initial assessments of the temperature sensitivity trends observed for Col*FRI*^{Sf2} and Lov-1 were complicated by the large phenotypic variation in flowering time observed between the two lines. However, results from Ull2-5 vernalization experiments confirm that the enhanced temperature sensitivity across the 2-8^{o}C range observed for Lov-1 is distinguishable from a later flowering phenotype (Figure 3.1). Conversely, results presented in Figure 3.2 confirm that this enhanced sensitivity had not been masked by a saturating cold treatment for the early flowering line Col*FRI*^{Sf2}.

3.2 Gene Expression

The requirement for a longer period of cold for effective vernalization of Lov-1 has previously been shown to involve quantitative variation in epigenetic silencing of *FLC* (Coustham et al., 2012). Quantitative variation in the silencing of Col *FRI*^{Sf2} and Lov-1 *FLC* alleles was determined after 4 weeks cold exposure at temperatures between 2 and 14^{o}C. In contrast to Col *FRI*^{Sf2}, the Lov-1 allele re-activated 30 days later in the warm after vernalization at all the tested temperatures. However, the degree of re-activation was significantly lower (p=0.0299) after vernalization at 8^{o}C than at 5^{o}C, consistent with the view of vernalization being most effective at this temperature (Figure 3.3). Further analysis after a 6 week treatment also revealed a similar pattern for *FLC* expression, with significantly higher reactivation observed for 5^{o}C versus 8^{o}C treated plants both 10 and 30 days after return to warm conditions (p=0.0262 and p=0.0216 respectively, unpaired Student's t-tests, Figure 3.4A).

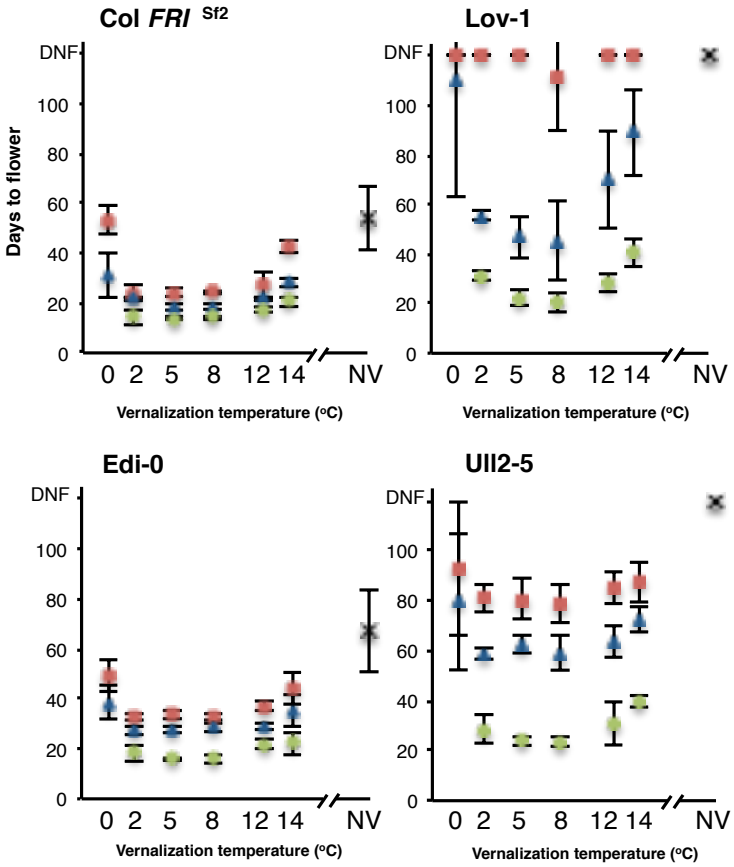

Figure 3.1 - Vernalization responses at a range of constant temperatures (Graphs represent re-plotted data previously shown in Figure 2.5) Days to flower were recorded after 4 weeks (red squares), 6 weeks (blue triangles) and 12 weeks (green circles) of vernalization at a range of temperatures. Error bars = ± SD. *n* ≥10.

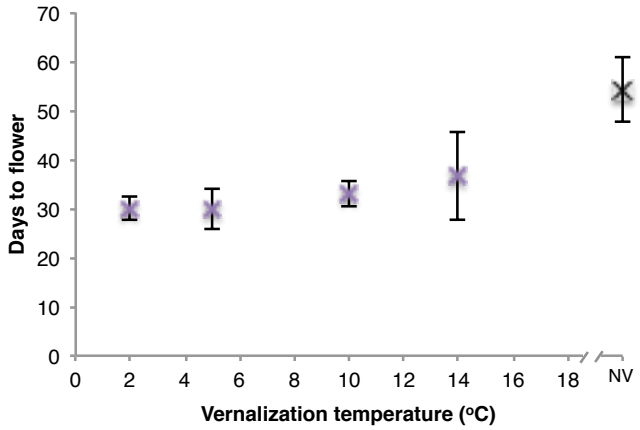

Figure 3.2 - Co*FRI*^{Sf2} vernalization responses after two weeks of cold
Days to flower were recorded after 2 week treatments (purple crosses). A black cross indicates the non-vernalized (NV) flowering time. Error bars = ± SD. *n* =12.

For both genotypes, similar levels of *VIN3* expression were observed following 5°C and 8°C treatments, but significantly lower levels were observed for 14°C treated plants (Figure 3.4B). The differences in flowering time made it more informative to compare *FT* expression for Lov-1 after 30 days post-cold growth with Col *FRI* ^{Sf2} following 10 days post-cold growth. Consistent with 8°C treatments being observed as most effective for accelerating Lov-1 flowering, this treatment also resulted in the highest level of *FT* induction (p=0.001 unpaired Student's *t*-test, Figure 3.4C).

3.4 Chromatin Immunoprecipitation Analysis

Epigenetic silencing of *FLC* is associated with Polycomb silencing and accumulation of H3K27me3 over the gene body (Angel et al., 2011; Yang et al. 2014). In Lov-1 it takes longer to accumulate the H3K27me3, mainly due to lower starting levels (Coustham et al., 2012). Similar accumulation of gene body H3K27me3 was found across the Col *FRI*^{Sf2} *FLC* allele at 5, 8 or 14°C after six weeks treatment, but differential H3K27me3 accumulation across the Lov-1 allele. Vernalization at 8°C resulted in higher levels of H3K27me3 compared to 5 or 14°C (p <0.0001 Wilcoxon matched-pairs signed rank test, Figure 3.4D), suggesting that the Polycomb silencing is most effective at 8°C for the Lov-1 *FLC* allele.

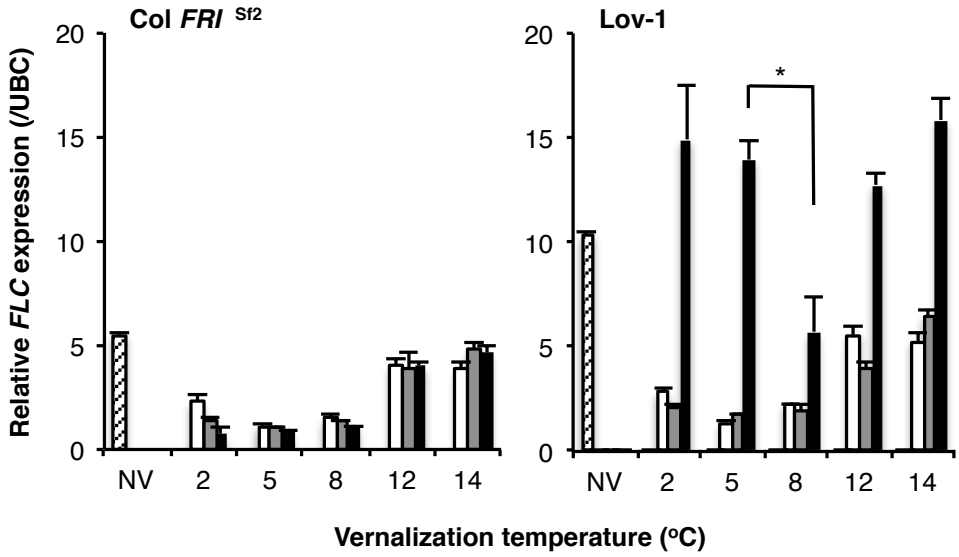

Figure 3.3 - *FLC* expression determined before and after 4 weeks vernalization
Quantitative PCR analysis showing non-vernalized (NV) *FLC* expression levels (hatched), after 4 weeks of cold (white) and after 10 days (grey) and 30 days (black) subsequent growth at 20°C. * $p < 0.05$, two-tailed Student's *t*-test. Error bars = SD. n=3.

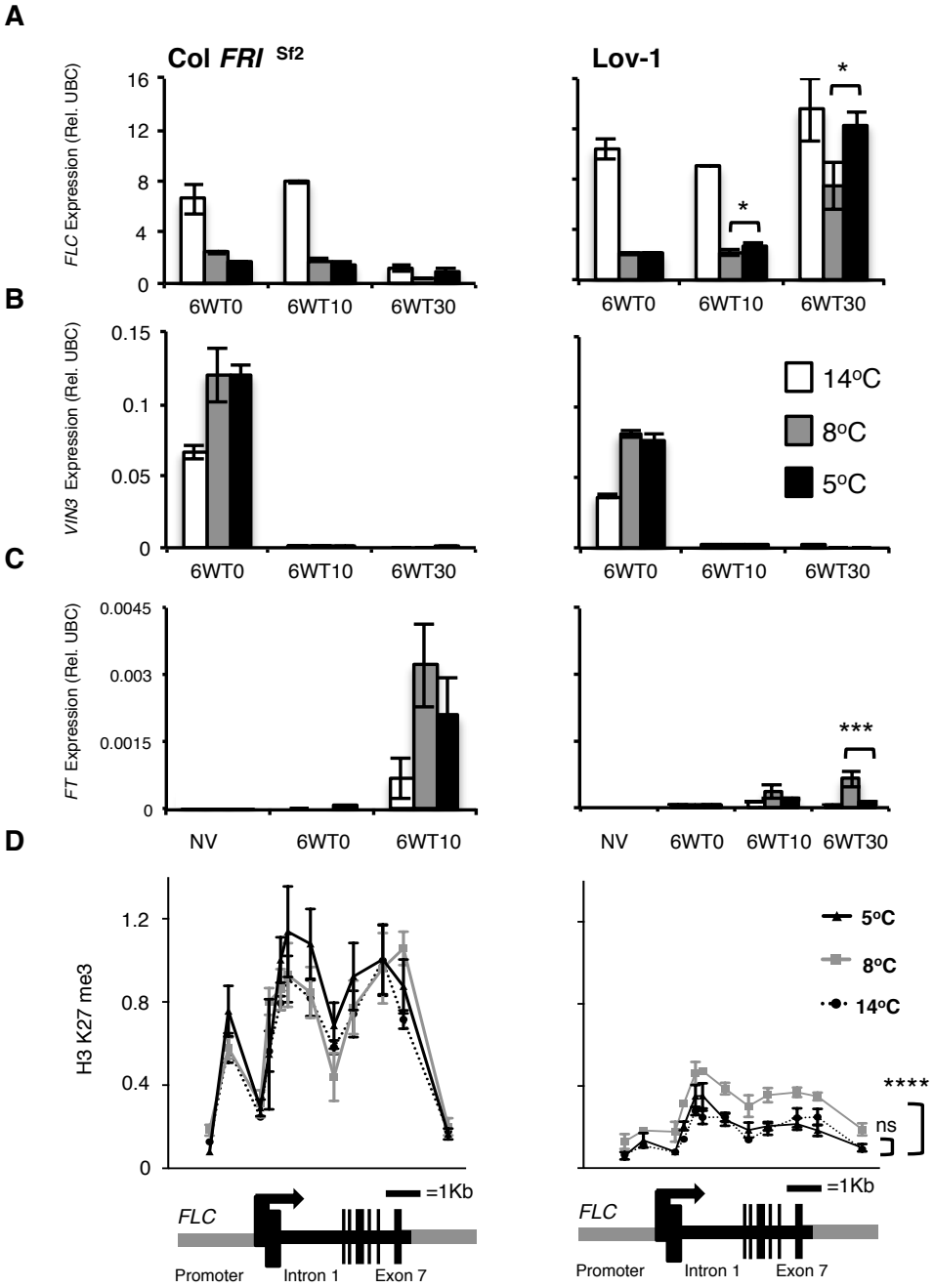

Figure 3.4 - Changes in gene expression and accumulation of repressive chromatin modifications determined for Col*FRI*^{Sf2} and Lov-1

Quantitative PCR analysis revealed changes in *FLC* (A), *VIN3* (B) and (C) *FT* expression in samples collected immediately after 6 weeks of cold (T0) and again following 10 (T10) and 30 days (T30) subsequent growth at 20°C. * $p < 0.05$, ***$p < 0.005$ n=3, two-tailed Student's t-test (D) H3K27me3 levels over the *FLC* locus were significantly higher for Lov-1 after 6 weeks vernalization at 8°C than 14°C or 5°C (samples were harvested 30 days post cold.) Wilcoxon matched-pairs signed rank test, **** $p \leq 0.0001$, n=4. Error bars represent ± SD in (A), (B), (C) and ± SEM in (D). NV = Non-vernalized, and ns = not significant.

3.5 Lov-1 life history and climate analysis

The relatively high effective temperature range identified for this northern Swedish accession was surprising given that flower buds appear within two weeks of snowmelt in April at its native Swedish site in Lövvik (Figure 3.5). It is likely that flowering this early limits herbivory and helps in the competition for nutrients, whilst maximizing the relatively short growing season dictated by recurrent annual snow cover (Akiyama and Agren, 2012, Kawagoe and Kudoh, 2010) (Figure 3.6).

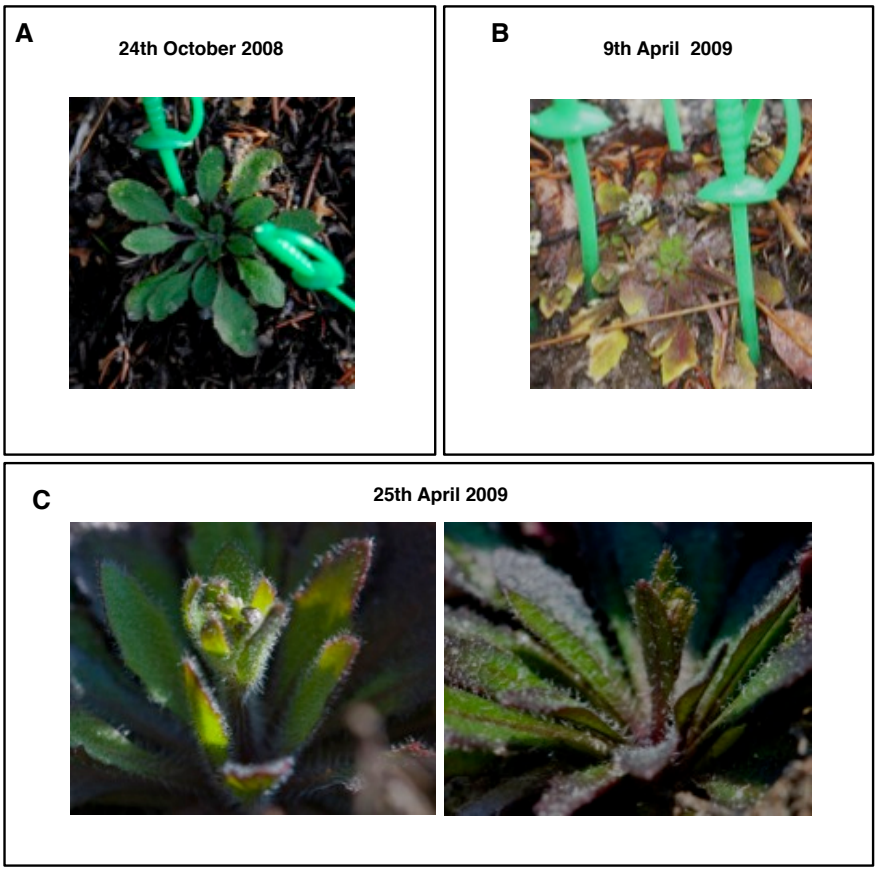

.

Figure 3.5 - The Lov-1 natural population flowers rapidly after snow melt in spring
(A) Photographs of representative Lov-1 rosettes taken before snow cover and **(B)** immediately after snow melt (green markers indicate rosette size). **(C)** Evidence of stem elongation apparent 16 days post snowmelt. These images and dates are representative of Lov-1 phenology over the last five years. (Images courtesy of Svante Holm).

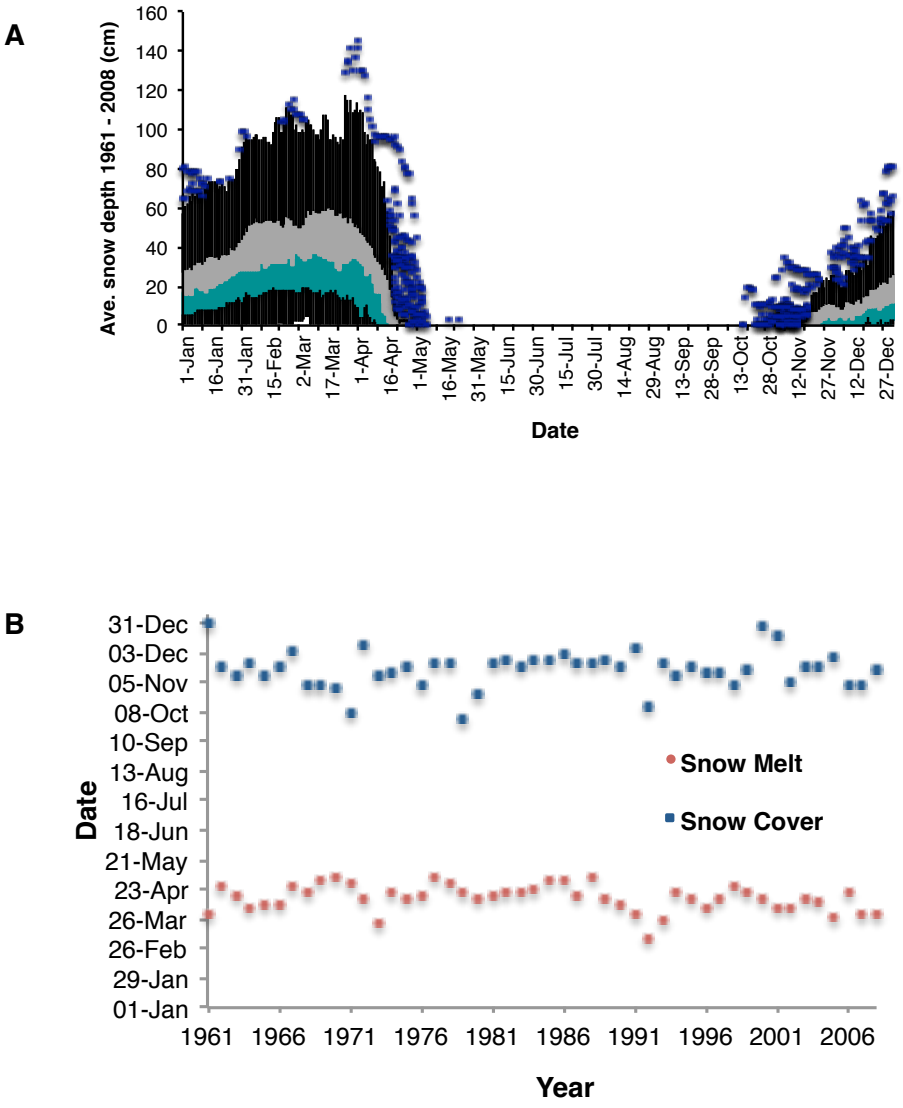

Figure 3.6 - Snow consistently covers plants during winter in northern Sweden **(A)** Snow depth and **(B)** snow cover period recorded near Lövvik over 47 years.

Such early flowering predicts that vernalization must have occurred before the end of November given the very low temperatures at the Lövvik site over the winter months (Figure 3.7A). Analysis of both hourly (Figure 3.C) and national (Figure 3.6B) data between the date of germination (1st August) until snow cover (~30th November) revealed average autumn temperatures around 8^{o}C. An overall average of 8.86^{o}C was calculated for average daily temperatures between 1961 and 2008 (S.D.=0.63) with over 86% of days falling within the range identified as being effective for Lov-1 vernalization, >0^{o}C - 14^{o}C. The agreement of average autumn temperatures with the effective vernalization temperatures identified for Lov-1 reinforced the view that epigenetic silencing of *FLC* must occur before snowfall

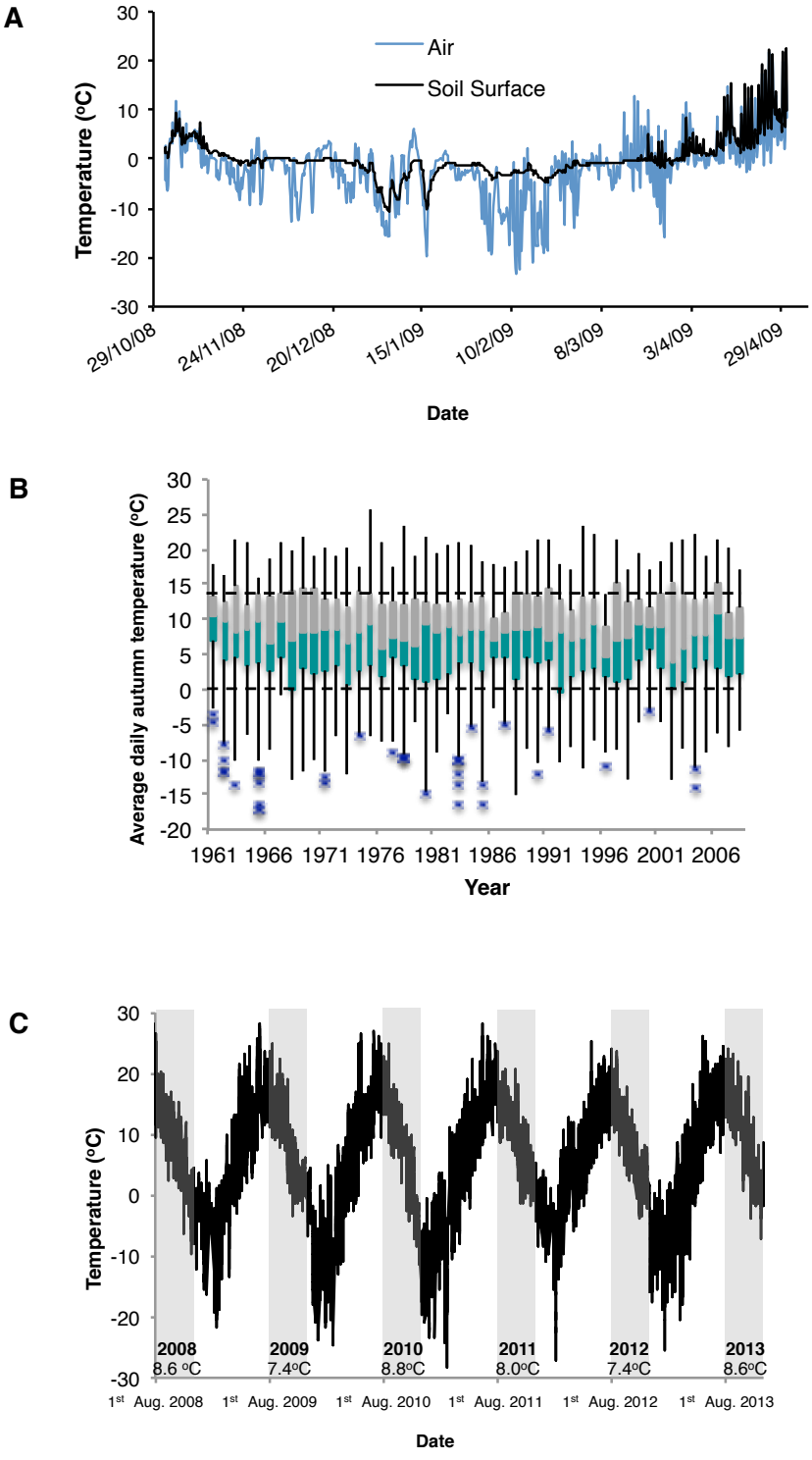

Figure 3.7 - Subzero winter temperatures are preceded by optimal vernalizing conditions

(A) Air and soil temperatures collected hourly over winter. **(B)** Average autumn daily temperatures over 47 years and **(C)** hourly air temperatures collected over 6 years. Upper and lower dashed lines in (B) indicate upper and lower thresholds identified for Lov-1 vernalization. Shaded areas in (C) indicate the period between germination and snow cover. Green and grey boxes = median to 1st and 3rd quartiles, respectively. Upper and lower whiskers represent 1.5* Inter Quartile Range (IQR) or highest / lowest values. Blue crosses = outlier values greater than 1.5*IQR.

3.6 Testing the hypothesis of a seasonal shift in vernalization timing

In addition to indirect evidence of the optimal vernalizing response matching average autumn temperatures, the effective temperature range identified for Lov-1 contradicted the seasonal timing of vernalization predicted by model threshold parameters suggested for *A. thaliana* (Wilzcek et al., 2009; Chew et al., 2012; Chew 2014). To test the hypothesis of a seasonal shift in the timing of vernalization in northern Sweden directly, field experiments were set up close to the Lövvik site in autumn 2011 and 2012 (locations are shown in Figure 3.9).

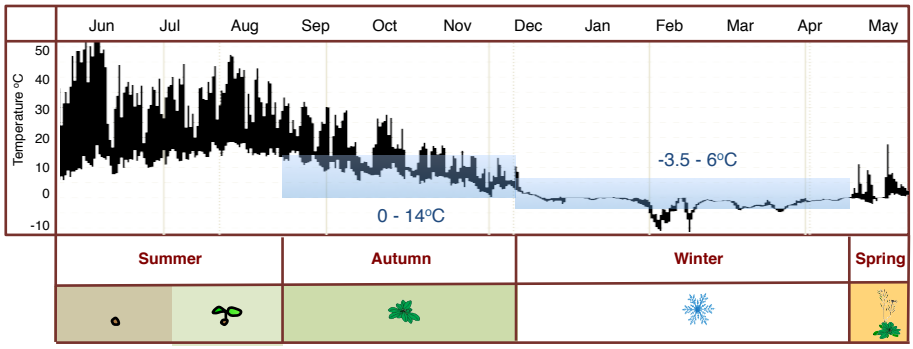

Figure 3.8 - An empirically derived temperature range predicts that Lov-1 vernalization occurs before winter
Hourly temperatures recorded throughout a Lov-1 life cycle. Shading indicates autumn or winter vernalization predicted by the 0-14°C or -3.5-6°C effective temperature ranges respectively.

Seedlings were transplanted into the field at the beginning of September and then transferred to a warmed greenhouse at three time points during autumn (Figure 3.10A and 3.11A). Although plants were sown later than observed flushes of germination of local populations, this enabled us to explicitly test whether twelve weeks of growth preceding winter would be sufficient to fully vernalize Lov-1. Flowering time of the different cohorts showed that vernalization was complete by the end of November in both 2011 (Figure 3.10B) and 2012 (Figure 3.11B). Furthermore, plants left to overwinter in the field flowered immediately at snowmelt, at the same time as native *A. thaliana* populations (Figure 3.12).

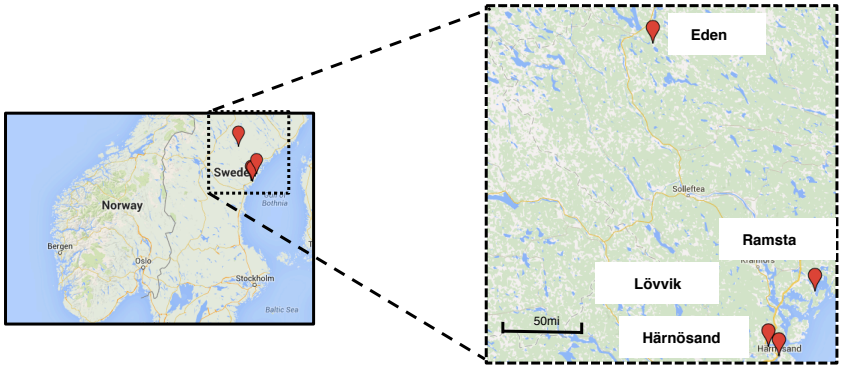

Figure 3.9 - Data collection locations and field sites in Sweden
Map (Google, Geobasics) showing geographical locations: Lövvik – the collection site of Lov-1. Hourly temperature data presented Figures 3.7 and 3.8 were collected in Eden. Swedish climate data were calculated from Swedish Hydrological and Meteorological Institute weather stations located in Härnösand. 2011 and 2012 field experiments were carried out at Ramsta.

3.8 Natural variation observed in field vernalization and subsequent seed yield

The order in which the natural accessions flowered following vernalization in the field was broadly similar to the order observed under laboratory conditions (Figure 3.1, 3.10B, 3.11B). And again, later flowering was associated with poor seed yield with increasing vernalization periods resulting in moderate increases (see Chapter 2 Figure 2.4, Figure 3.10C).

3.9 Contribution of the Lov-1 *FLC* allele to flowering time and seed yield

In order to link the flowering time changes with the changed epigenetic silencing at *FLC* we included a near isogenic line carrying the Lov-1 *FLC* allele (NIL1$^{Lov\text{-}1}$) in the genetic background of Col *FRI* ^{Sf2} in the field experiments. This line was generated through six generations of introgression and had been genotyped with markers to define the introgressed segment (see Chapter 2, Figure 2.7).

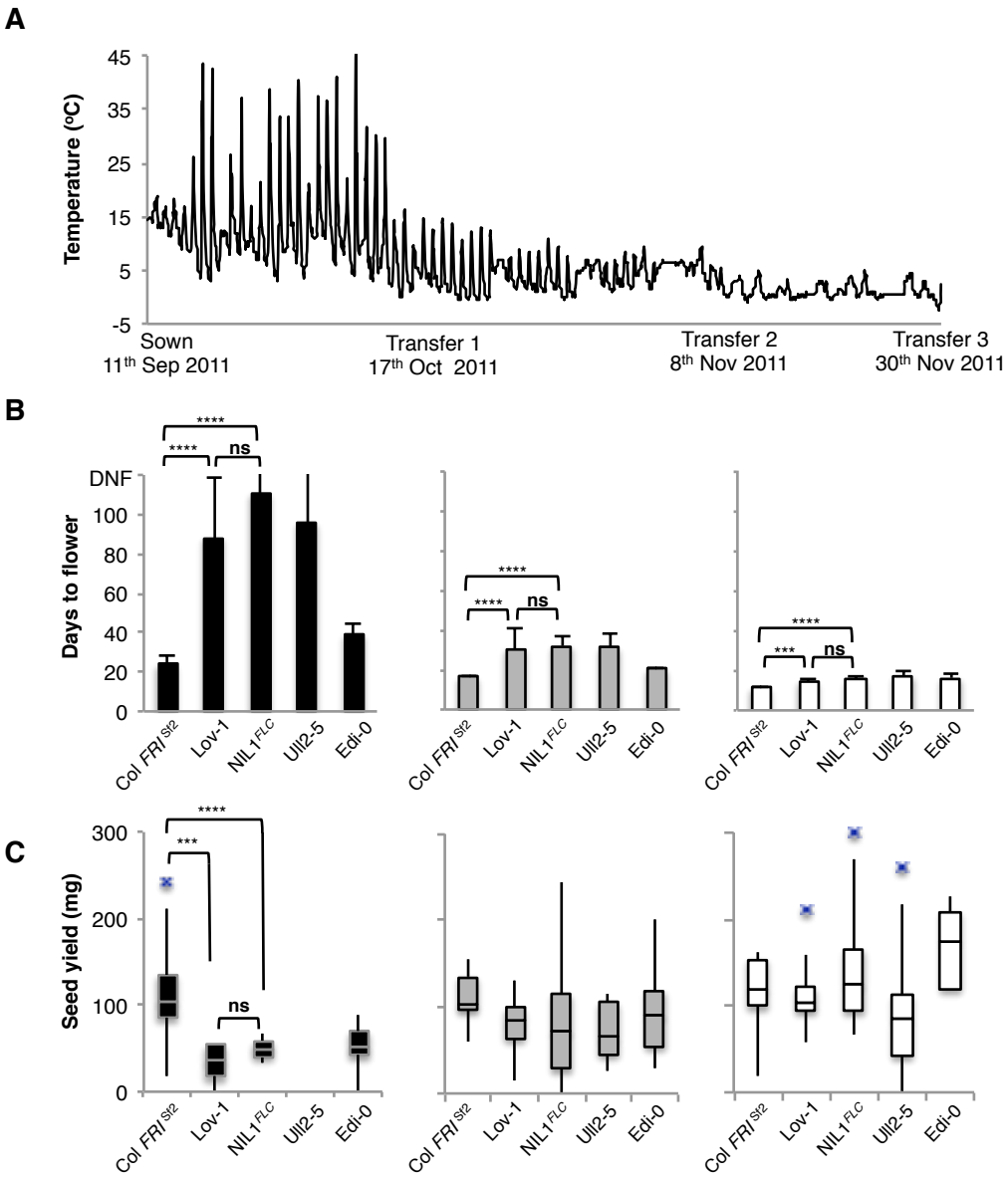

Figure 3.10 - Field experiments reveal vernalization occurs in autumn in northern Sweden

(A) The dates of sowing and of plant transfers to the greenhouse are shown with hourly soil surface temperatures recorded during autumn 2011. **(B)** Days to flower recorded after transfer to a warmed greenhouse, black bars = Transfer 1, grey bars = Transfer 2 and white bars = Transfer 3. $n \geq 10$. Error bars represent ± SD. **(C)** Seed yield data are presented as box plots where boxes = 1st, median and 3rd quartiles. Upper and lower whiskers represent 1.5* Inter Quartile Range (IQR) or highest / lowest values. Blue crosses = outlier values greater than 1.5*IQR. Mann-Whitney *U* tests results: *** $p \leq 0.001$, **** $p \leq 0.0001$. ns= not significant ($p > 0.05$).

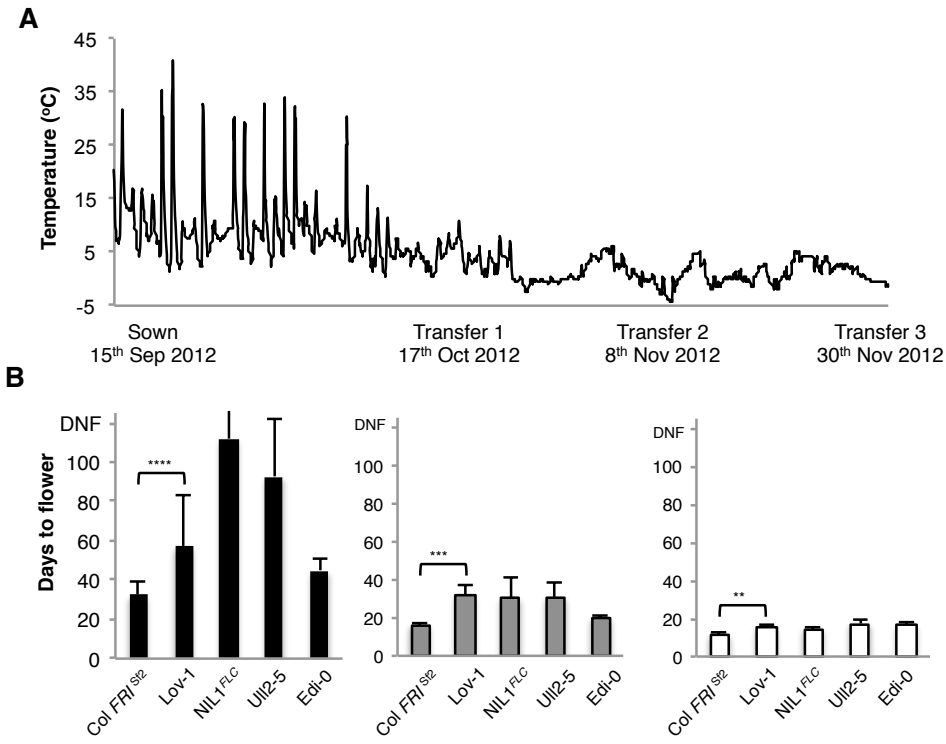

Figure 3.11 - 2012 field experiments confirm vernalization occurs during autumn in northern Sweden
(A) The dates of sowing and plant transfers to the greenhouse are shown with hourly soil surface temperatures recorded during autumn 2012. **(B)** Days to flower recorded after transfer to a warmed greenhouse, black bars = Transfer 1, grey bars = Transfer 2 and white bars = Transfer 3. $n \geq 10$. Error bars represent ± SD. *** $p \leq 0.001$, **** $p \leq 0.0001$ ***, ns = not significant ($p > 0.05$), Mann-Whitney *U* test.

Both Lov-1 and NIL1$^{Lov\text{-}1}$ took longer to flower than Col*FRI*^{Sf2} after all three transfers in both 2011 and 2012 (Figure 3-10B and 3-11B). The Lov-1 *FLC* allele also contributed to differences in seed yield. Faster flowering of Col*FRI*^{Sf2} after transfer 1 resulted in significantly higher seed yield than for Lov-1 and NIL1$^{Lov\text{-}1}$ (Figure 3.11C). These results indicate a clear contribution of the Lov-1 *FLC* allele to differential vernalization response under field conditions in addition to potential fitness consequences.

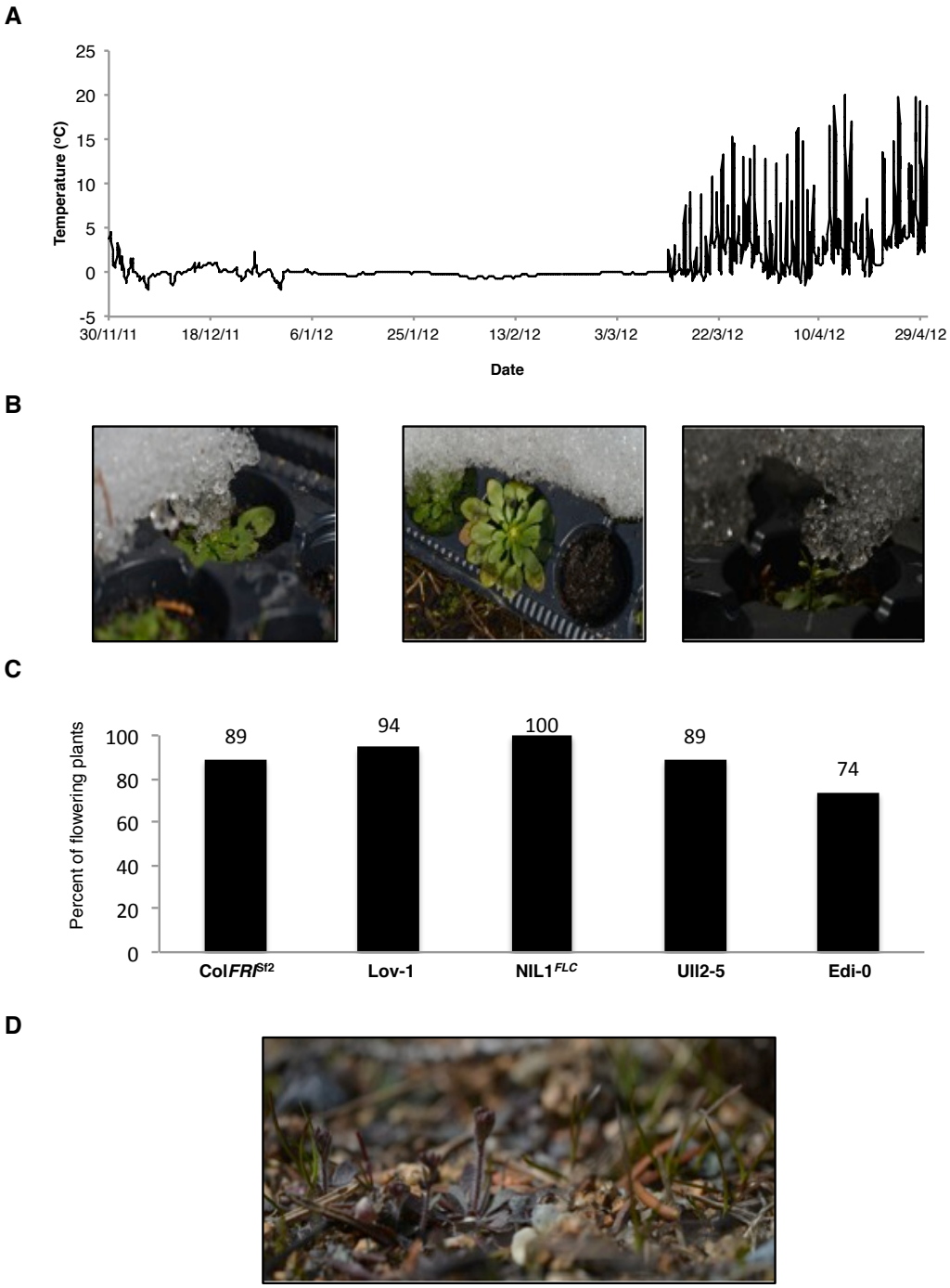

Figure 3.12 - Plants flowered synchronously with natural populations after 5 months of continuous snow cover

(A) Surface temperature recorded at Ramsta indicating that over wintered plants were continuously covered by snow during winter 2012. **(B)** Representative images of the overwintered cohort with floral buds visible. **(C)** Percentages of plants with visible buds on 26th April 2013, 5 days after snow melt and **(D)** Image of natural population taken 26th April 2013 (courtesy of Svante Holm).

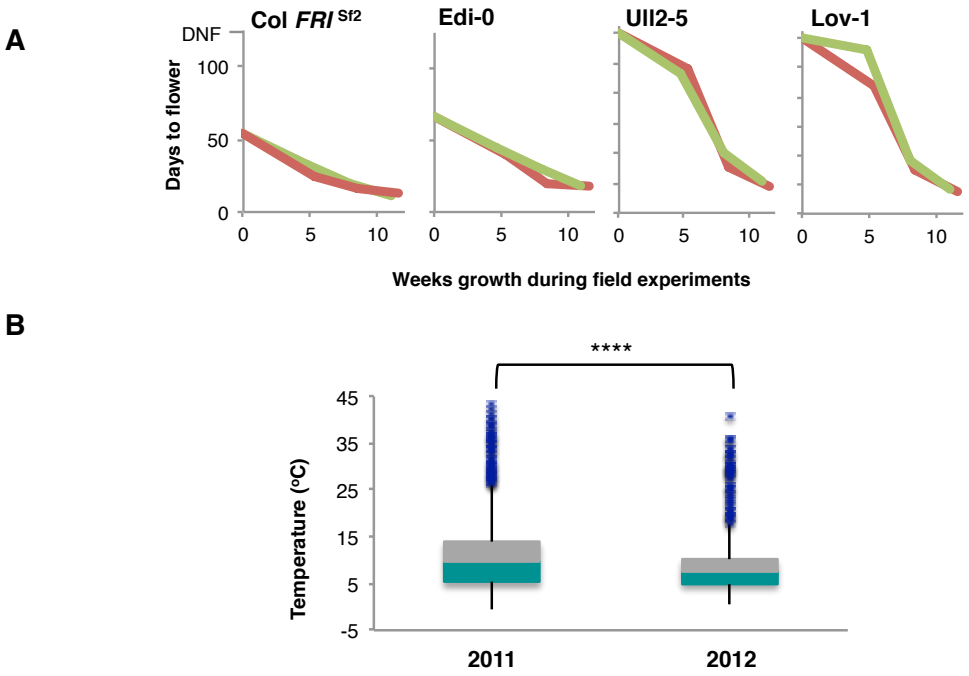

Figure 3.13 - An enhanced initial vernalization response recorded for Lov-1 coincided with higher field temperatures
(A) A comparison of averaged vernalization responses recorded during field experiments carried out in 2011(red) and 2012 (green). **(B)** Box plots of hourly temperature data recorded between the sowing date and Transfer 1. Green and grey boxes = median to 1st and 3rd quartiles, respectively. Upper and lower whiskers represent 1.5* Inter Quartile Range (IQR) or highest / lowest values. Blue crosses = outlier values greater than 1.5*IQR. **** $p < 0.0001$, Mann-Whitney *U* test.

3.2.7 Differential thermal sensitivity observed under field conditions

An increased level of plasticity was observed for Lov-1 vernalization responses between 2°C-5°C compared to the other genotypes (Figure 3.1). We directly compared the flowering results over both years to see whether this plasticity had led to differential responses under field conditions. Lov-1 flowered later at transfer 1 in autumn 2012 compared to 2011, whereas Col *FRI*^{Sf2}, Ull2-5 and Edi-0 plants flowered similarly both years (Figure 3.13A, p=0.0120 Mann Whitney Test, U=54). It was significantly colder between the sowing date and transfer 1 in 2012 compared to the previous year (Figure 3.13B) and plants were exposed a larger proportion of hours below 8°C in 2012 (55%) than in 2011 (38%). This suggests that reduced efficiency of vernalization in Lov-1 at lower constant temperatures had translated to a similar phenotype under natural field conditions.

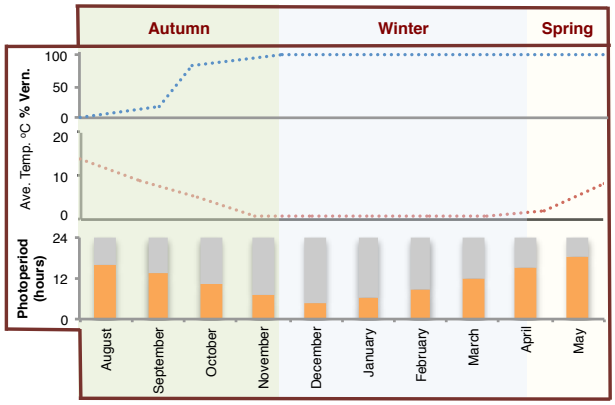

Figure 3.14 - Lov-1 vernalization completes by the end of autumn in northern Sweden
Comparison of the Lov-1 vernalization with daylength and temperatures throughout the growth season shows that vernalization saturates after the critical photoperiod has passed. This ensures that plants are prevented from flowering in autumn and must wait for permissive temperatures and daylength in the spring to flower.

3.10 Discussion

Extensive variation has been shown to exist in thermal sensitivities of many biological processes (Huey and Kingsolver 2011; Dell et al., 2011). Differences in thermal sensitivity and optimal temperature responses typically reflect adaptation to specific environmental conditions and are thought to be key determinants of survival and Darwinian fitness (Angiletta, 2009). Quantitative assessment of thermal sensitivity for vernalization across a range of *A. thaliana* accessions revealed variation in temperature responses within a shared effective range (Figure 3.1).

The molecular basis of an unexpected flowering response observed for Lov-1 after four-weeks vernalization at 8°C was explored further in this chapter. Consistent with enhanced stability of epigenetic repression being achieved by 8°C vernalization, the lowest level of *FLC* reactivation was also observed following 4 and 6 week treatments that resulted in a significantly higher level of *FT* induction (Figures 3.3, 3.4A). Furthermore, significantly higher H3K27me3 levels were also observed for 8°C versus 5°C treated plants 30 days after transfer to the warm. However the similar levels of *VIN3* induction observed for 5°C and 8°C treatments suggest that an increased opportunity for PHD-PRC2 complex formation does not underlie this response (Figure 3.4B).

Four non-coding polymorphisms in *FLC* close to the nucleation site of the PHD-PRC2 complex were previously defined as underpinning the molecular variation in *FLC* epigenetic silencing between Lov-1 and Col FRI^{Sf2} (Coustham et al., 2012). Genotyping of $NIL1^{Lov\text{-}1}$ revealed that in addition to carrying the Lov-1 *FLC* allele it also carried an additional short segment of Lov-1 chromosome 5 (Chapter 2, Figure 2.7). Under controlled conditions this segment provided maximal delay of flowering in addition to an enhanced 8°C response in the presence of a Lov-1 *FLC* allele, but did not delay flowering after vernalization in the presence of a Col *FLC* allele (Figure 2.7C). The vernalization response of $NIL1^{Lov\text{-}1}$ was also found to be more similar to Lov-1 following growth in the field than under comparable constant conditions (Figures 3.10B, 3.11B, 2.6C). Thus, it is likely that the changed vernalization temperature response of Lov-1 involves a complex interaction between *FLC* and gene products at linked loci that synergistically repress flowering in natural fluctuating temperatures.

A combination of molecular and ecological approaches have been employed to demonstrate that adaptation to extreme winters at the northern limit of the *A. thaliana* species range has involved a seasonal shift in the timing of vernalization. Perhaps as a response to selection in these extreme conditions one northern Swedish accession, Lov-1, responds to temperatures within the range observed between August and November in that geographical region (Figure 3.7). Early germination enables vernalization to complete before snowfall and allows flowering to occur directly after snowmelt when the photoperiod and ambient temperatures increase (Figure 3.14). Although genotypes with a wide range of cold requirements were also found to vernalize effectively during autumn (Figure 3.10B, Figure 3.11B), the low seed dormancy reported for Lov-1 (Atwell et al., 2010; Debieau et al., 2013) is consistent with this hypothesis. Furthermore, a reduced effectiveness identified for temperatures below 5°C (Figure 1A) was found to effectively buffer cool periods during early autumn (Figure 3.13). This perhaps is an extra mechanism that has evolved to ensure that unseasonal cooler periods at the end of summer do not leave plants susceptible to flowering in response to subsequent warm autumn temperatures and permissive day lengths.

Together the results presented in this chapter challenge the current dogma that plants vernalize during winter. We demonstrate that Lov-1 effectively integrates and remembers temperatures during autumn.

3.4 Materials and Methods

3.4.1 Plant growth conditions.

For the daily averaging experiment seeds were sown onto Arabidopsis mix compost and stratified for 3 days at 5°C. Seedlings were pre-grown for 7 days (16h light: 8h dark, 22°C) and vernalized for 4 weeks at either 14°C, 12°C, 10°C, 8°C (8h light: 16h dark) in cabinets (Sanyo MLR-351H), 5°C (walk-in vernalization room), 2°C (modified Liebherr KP3120) or 0°C (Johnson Controls). All temperatures were recorded as ± ≤1.5°C, 70% ± ≤10% RH. Low light (~30µmol m^{-2} s^{-1}). Plants were then transferred to random locations in a controlled environment room (16h light: 8h dark 16, 22°C ± 2°C) and flowering time was scored as the number of days of growth until floral buds became visible.

3.4.2 Sweden Field Experiments

Seeds were stratified for 4 days at ~5°C, sown into trays using a randomized block design and placed outside (62° 23.463´N, 17° 18.272´E). Seedlings were thinned to one plant per cell after seven days and then transferred to Ramsta (62° 50.988´N, 18° 11.570´E) one week later. At each transfer date, plants were returned to a greenhouse in Mid-Sweden University, Sundsvall (16 hours light, 22°C ± 2°C) where flowering time was determined as the number of days growth until floral buds became visible.

3.4.3 Climate Analysis

Hourly temperatures were recorded using Tinytag data-loggers (Chichester, UK). Historical climate data were obtained from Swedish Meteorological and Hydrological Institute. Three temperature and snow-depth readings taken at 0600hr, 1200hr and 1800hr were used to calculate daily means. Boxplots graphs were created using QI Macros add-ins for Excel (Denver, Colorado, USA). Statistical analyses of climate data were performed using GraphPad Prism version 6 software (La Jolla, California, USA).

3.4.4 RNA extraction

See Chapter 2 Materials and Methods section 2.10.2.

3.4.5 Reverse Transcription

See Chapter 3 section Materials and Methods section 2.10.3.

3.4.6 Quantitative Polymerase Chain Reaction (qPCR)

See Chapter 3 section Materials and Methods section 2.10.4 Expression levels were determined using Roche Universal Probe Library (UPL) Probes and the primers shown below.

***FLC* (At5g10140)**	
sFLC_UPL_#65_F	5'-gtgggatcaaatgtcaaaaatg-3'
sFLC_UPL_#65_R	5'-ggagagggcagtctcaaggt-3'
UPL #65	5'-ctggagga-3'

***VIN3* (At5g57380)**	
VIN3_UPL_#67_F	5'-cgcgtattgcggtaaagataa-3'
VIN3_UPL_#67_R	5'–tctctttcgccaccttcact-3'
UPL #67	5'-ctccagca-3'

***UBC* (At5g25760)**	
UBC_UPL_#9_F	5'-tcctcttaactgcgactcagg-3'
UBC_UPL_#9_R	5'-gcgaggcgtgtatacatttg-3'
UPL#9	5'-tggtgatg-3'

Gene expression was calculated relative to *UBC* levels using the comparative Ct method (Schmittgen and Livak 2008) and statistical analysis of was performed using GraphPad Prism version 6 software for Mac (La Jolla, California, USA).

3.4.7 ChIP and RT-qPCR Analysis.

The ChIP assays were performed by Julia Questa. The protocol uses H3K27me3 and H3 antibodies (Abcam, Cambridge, UK) and was previously described by Sun et al., 2013. Primers used in this analysis are shown in Appendix Table 2.

SHOOT MERISTEMLESS (*STM*) was used as the internal control and data are represented as the ratio of H3K27me3*FLC*/H3 *FLC* to H3K27me3 *STM*/H3 *STM*. Statistical analysis of ChIP data was performed using GraphPad Prism version 6 software for Mac (La Jolla, California, USA.)

Chapter 4 - Predicting the impact of climate change on vernalization

Division of work: Prof. Alastair Grant created the vernalization threshold models used in this chapter.

4.1 Introduction

The most recent Intergovernmental Panel on Climate Change (IPCC) report forecasts that average global temperatures will rise by 3°C by the end of the century, with greater increases anticipated if concerted efforts are not made to reduce greenhouse gas emissions (IPCC 2014, Figure 4.1). There is evidence that warmer winters have already contributed to delayed flowering in a subset of species but it is unknown how future temperature increases will affect vernalization over the coming century (Cook et al., 2012). This chapter reports results from a model that uses empirically derived upper and lower threshold temperatures for *A. thaliana* to predict the future impact of climate change on vernalization across the species' range.

4.2 Determining vernalization temperature parameters

Significant progress has been made to model *A. thaliana* development under field conditions. A modified photothermal unit (MPTU) model incorporates parameters for major drivers of development: growth rate, vernalization and photoperiod to effectively predict flowering times at various European locations (Wilzcek et al., 2009). The vernalization component of this model uses a lower threshold (T_{min}) of 0°C and an extrapolated upper threshold (T_{max}) of 6°C to specify the effective vernalization temperature range (Wilzcek et al., 2009). As for classic agricultural chilling-unit models, the MPTU model uses these thresholds to calculate the summation of effective temperatures within this range over time. Based on laboratory data obtained for Col*FRI*^{Sf2} (Michaels and Amasino 1999), this model predicts vernalization to be saturated following the accumulation of 960 effective chilling hours i.e. 40 vernalizing days (Wilzcek et al., 2009). These parameters were maintained through subsequent iterations of the model since alterations did not significantly improve flowering time predictions for the genotypes tested (Wilzcek et al., 2009; Chew et al. 2012, Chew at al., 2014).

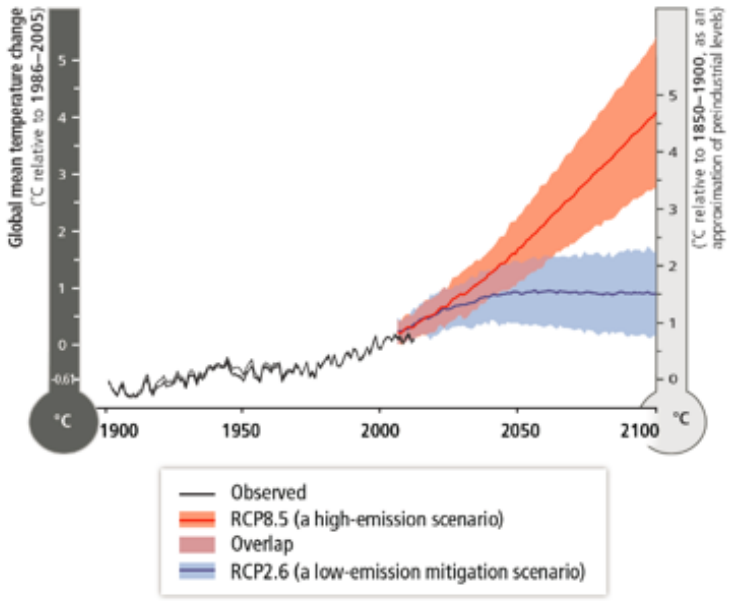

Figure 4.1 - IPCC global annual average temperature increases predicted over the coming century
Figure taken from the most recent IPCC report (IPCC 2014).

There is now evidence to suggest that existing MPTU parameters would be unsuitable for predicting the vernalization responses of later flowering accessions. The 960 hour (5.7 week) saturation threshold was based on the response of the reference genotype Col*FRI*^{Sf2} (Wilczek et al., 2009; Micheals and Amasino 1999), however there are many reported examples of natural accessions that exceed this requirement (Shindo et al., 2005; Li et al., 2014; Méndez-Vigo et al., 2011). Moreover, there is now clear evidence of the effectiveness of temperatures higher than 6^{o}C in many accessions (Chapter 2, Figure 2.5) (Wollenberg and Amasino 2012). The laboratory results presented in Chapter 3 and the field experiments presented in Chapter 4 enabled us to explicitly test threshold parameters in accessions that span the natural range of vernalization requirement.

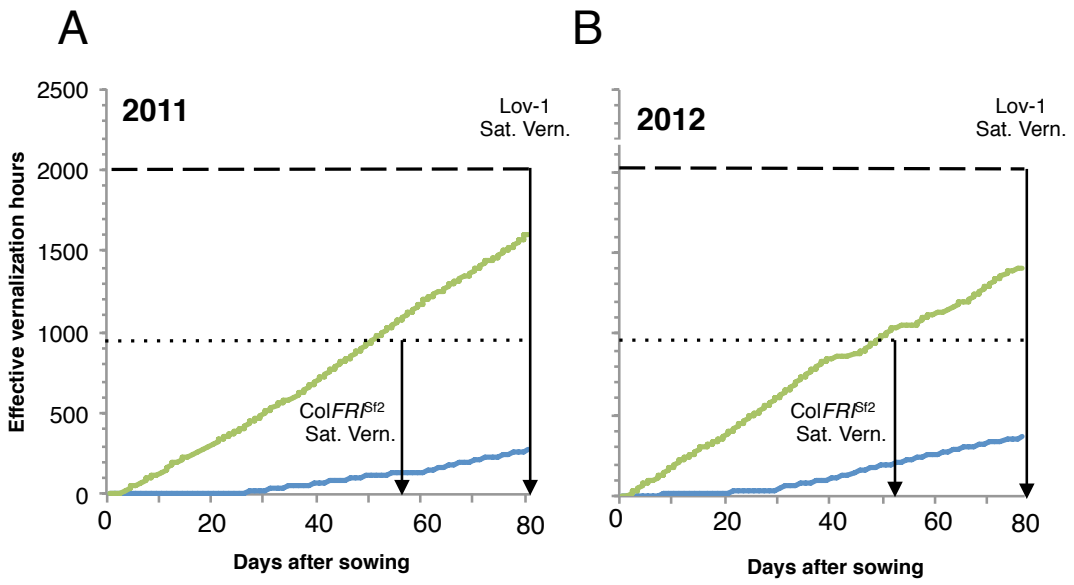

Figure 4.2 - The accumulation of effective vernalizing hours during Swedish field experiments
Temperatures recorded during Swedish field experiments carried out during **(A)** 2011 and **(B)** 2012 were used to calculate the accumulation of hours within two ranges. The accumulation of daytime hours within the 0-6°C range are shown in blue and hours between 0-15°C calculated from both day *and* night temperatures are shown in green. The dotted lines and dashed lines represent Col *FRI* ^{Sf2} and Lov-1 vernalization accumulation requirements (960 and 2016 hours), respectively. Flowering time results presented in Chapter 3, Figure 3.1 were used to predict saturated vernalization (Sat. Vern.) responses for Col*FRI*^{Sf2} and Lov-1.

4.2.1 Predictions based on the summation of hours within effective temperature ranges

Flowering times recorded after vernalization at a range of constant temperatures validated the decision to maintain a T_{min} of 0°C since prolonged periods at freezing point do not activate a significant response (Napp-Zinn 1957; Chapter 3, Figure 3.1). Extension of the range up to a T_{max} of 15°C was suggested by the significant acceleration of flowering observed following vernalization at 14°C, but not at 16°C (Chapter 2, Figure 2.1).

To test the (0°C, 6oC) and (0°C, 15°C) temperature ranges, hourly accumulations were calculated from temperature data collected during the Swedish field experiments in 2011 and 2012 (shown in Chapter 3, Figures 3.10 and 3.11). Accumulated time within both ranges was then used to predict the progress of vernalization observed under natural conditions.

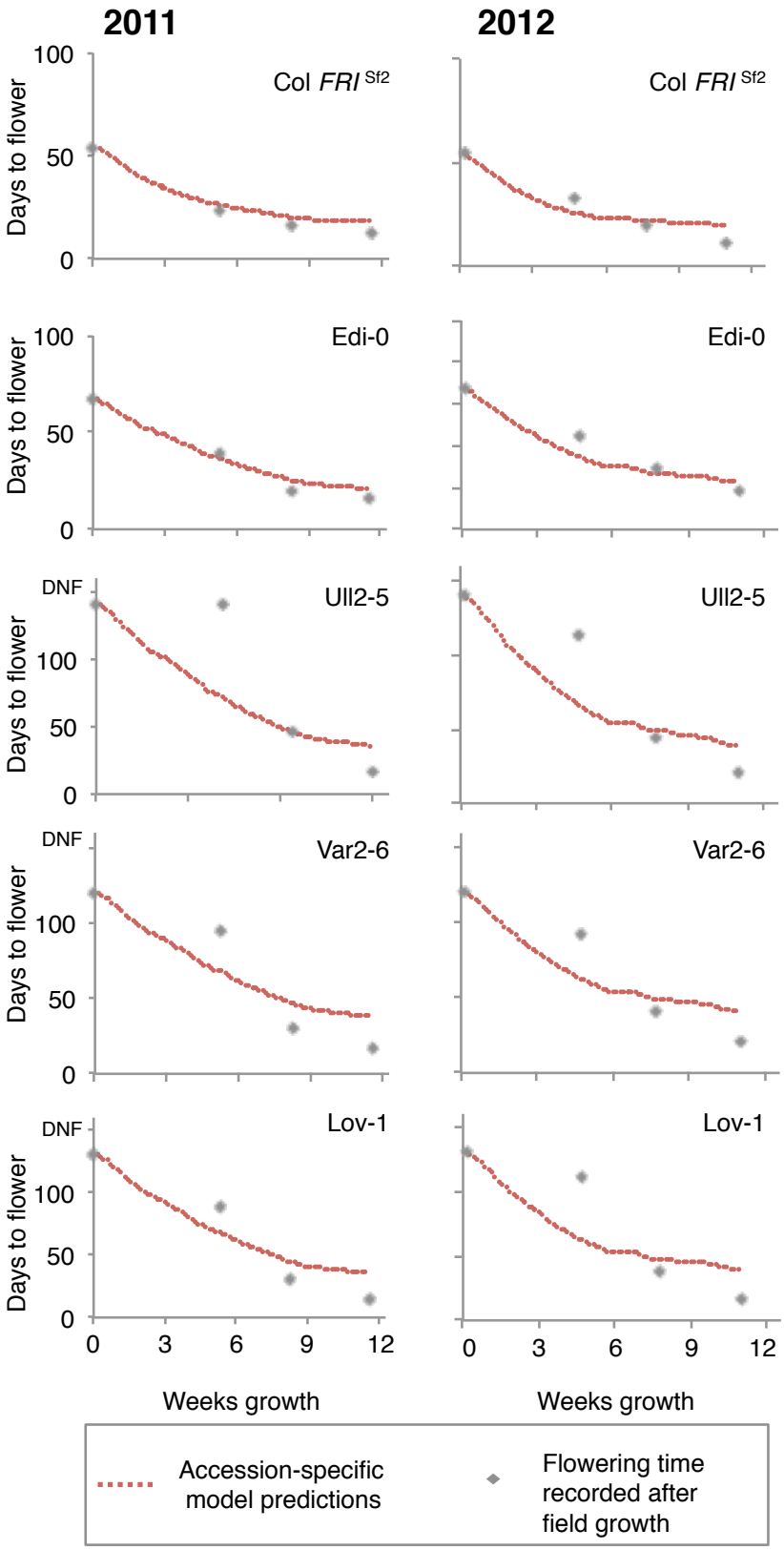

Figure 4.3 –Accession specific predictions of vernalization progress
Days to flower recorded after growth under field conditions in Sweden in 2011 and 2012 (grey diamonds) are shown together with vernalization responses predicted by accession specific models (red dashed line). See text for details.

The MPTU model predicts that effective vernalization only occurs during daytime hours when the temperature is between 0 and 6°C (Wilzcek et al., 2009). But these conditions only predicted the equivalent of ~1.5 and ~2 weeks of effective cold accumulation by the end of the 2011 and 2012 field experiments, respectively (Figure 4.2). This contradicts Col*FRI*^{Sf2} and Lov-1 flowering time responses recorded after plants were transferred from the field to inductive conditions that show the vernalization requirements of both genotypes were saturated by the end of autumn (Chapter 3, Figure 3.10 and 3.11).

Predictions were improved when both day *and* night hourly temperatures were taken into account, however vernalization was still under-estimated for both genotypes using the (0°C, 6°C) range (data not shown). Next, all hourly temperatures were considered effective between 0°C and 15°C. This extension of the effective temperature range correctly predicted that the number of vernalizing hours would exceed the Col*FRI*^{Sf2} threshold requirement during 2011 and 2012, however it underestimated the response observed for Lov-1 by 22% and 30% in the 2011 and 2012 experiments, respectively (Figure 4.2).

4.2.2 Predictions made using accession-specific chilling-unit models

So far, the chilling-unit predictions presented in this chapter have used two temperature ranges to determine whether each hour (Figure 4.2) generates a maximal vernalization response. But this is inconsistent with results from constant temperature experiments that suggest a graded effect exists across the effective temperature range. It also ignores the variation in relative temperature responsiveness observed for different accessions (Chapter 2, Figure 2.5, Chapter 3, Figure 3.1).

Peach producers identified a similar variation in chilling responsiveness and developed a model to take this into account. The Utah chilling-unit model predicts vernalization progress under field conditions through the summation of chilling units that reflect the relative effectiveness of each temperature. It also subtracts high temperature periods when de-vernalization is thought to occur (Byrne and Bacon 1992). We took a similar approach for *A. thaliana* by calculating relative temperature response profiles for each accession (based on responses observed for constant temperature treatments) and used these to predict vernalization progress during the

2011 and 2012 Swedish field experiments (see Materials and Methods at the end of this chapter for details). Overall, these accession-specific models provided good predictions of Col*FRI*^{Sf2} and Edi-0 vernalization, but they over-estimated responses at earlier time points and under-estimated later responses for the Swedish lines (Figure 4.3).

4.2.3 Predictions based the summation of average daily temperatures within effective temperature ranges

Moderate chilling conditions were suggested by the 48% and 35% of hourly temperatures observed as higher than 5^{o}C during the 2011 and 2012 field experiments respectively. Since average daily temperatures can provide better estimates of vernalization progress than hourly data in moderate chilling areas (Byrne and Bacon 1992) accumulations were repeated for both the (0^{o}C, 6^{o}C) and (0^{o}C, 15^{o}C) ranges using daily average temperatures. The (0^{o}C, 6^{o}C) range provided reasonable forecasts for vernalization saturation for Col*FRI*^{Sf2}, but it did not accurately predict vernalization progress made by later flowering accessions (Figure 4.4). Predictions were observed when the upper threshold of effective daily temperature range was raised from 6^{o}C to 15^{o}C. Apart from over-estimated responses at some early time points, this wider temperature range provided a good match between observed versus expected responses – especially for later flowering accessions. Strikingly, vernalization saturation was accurately predicted for all genotypes by the end of both the 2011 and 2012 field experiments (Figure 4.4).

4.2.4 Predictions based on the effectiveness of cumulative average temperature

Temperatures were then considered over time-scales longer than a day on the basis that monthly and seasonal mean temperatures are used by some commercial growers to estimate the suitability of low to moderate chilling locations for cold-requiring cultivars (Byrne and Bacon 1992). Also, a maximal vernalization response was observed for Lov-1 at a constant temperature that matched the autumn seasonal average (Chapter 3, Figure 3.7). Furthermore, natural fluctuating temperatures within a proceeding six-week period were found to best predict *FLC* expression levels, and therefore vernalization progress, for the *A. thaliana* relative *A. halleri* (Aikawa et al., 2010).

So cumulative average temperature datasets were calculated for field temperatures where each value represented the average of all the hourly temperatures that preceded it. Predictions of flowering responses were then made by selecting results from constant laboratory experiments where the conditions most closely matched average temperature values (see Appendix Figure 1 for data selected). This approach provided remarkably accurate flowering time predictions for all accessions (Figure 4.5) suggesting that constant temperatures generate equivalent responses to temperatures that match the long-term average.

4.3 Testing daily temperature integration

The results presented in Figure 4.5 prompted a growth chamber experiment that aimed to determine whether day and night temperatures have an equal chilling effect over a four week period. All plants were exposed to 12 hours light and 12 hours dark each day and reciprocal regimes were set up: 14°C day and 8°C night; 8°C day and 14°C night in addition to constant treatments of 14°C, 8°C and 11°C. This enabled the flowering response observed for both alternating regimes to be directly compared to the flowering responses following the 11°C treatment - a temperature that matched the average.

As expected, 14°C and 8°C constant temperature treatments resulted in the latest and earliest flowering times respectively. 8°C day, 14°C night treated plants were also found to respond similarly to plants vernalized at 11°C, a constant temperature that matched the mean. However the plants grown at 14°C during the day and 8°C at night flowered later than expected, i.e. later than plants vernalized at 11°C. It was noticeable that these plants had grown larger than plants in the other alternating temperature treatment, however this difference was negligible after around seven days growth in warm conditions (Figure 4.6).

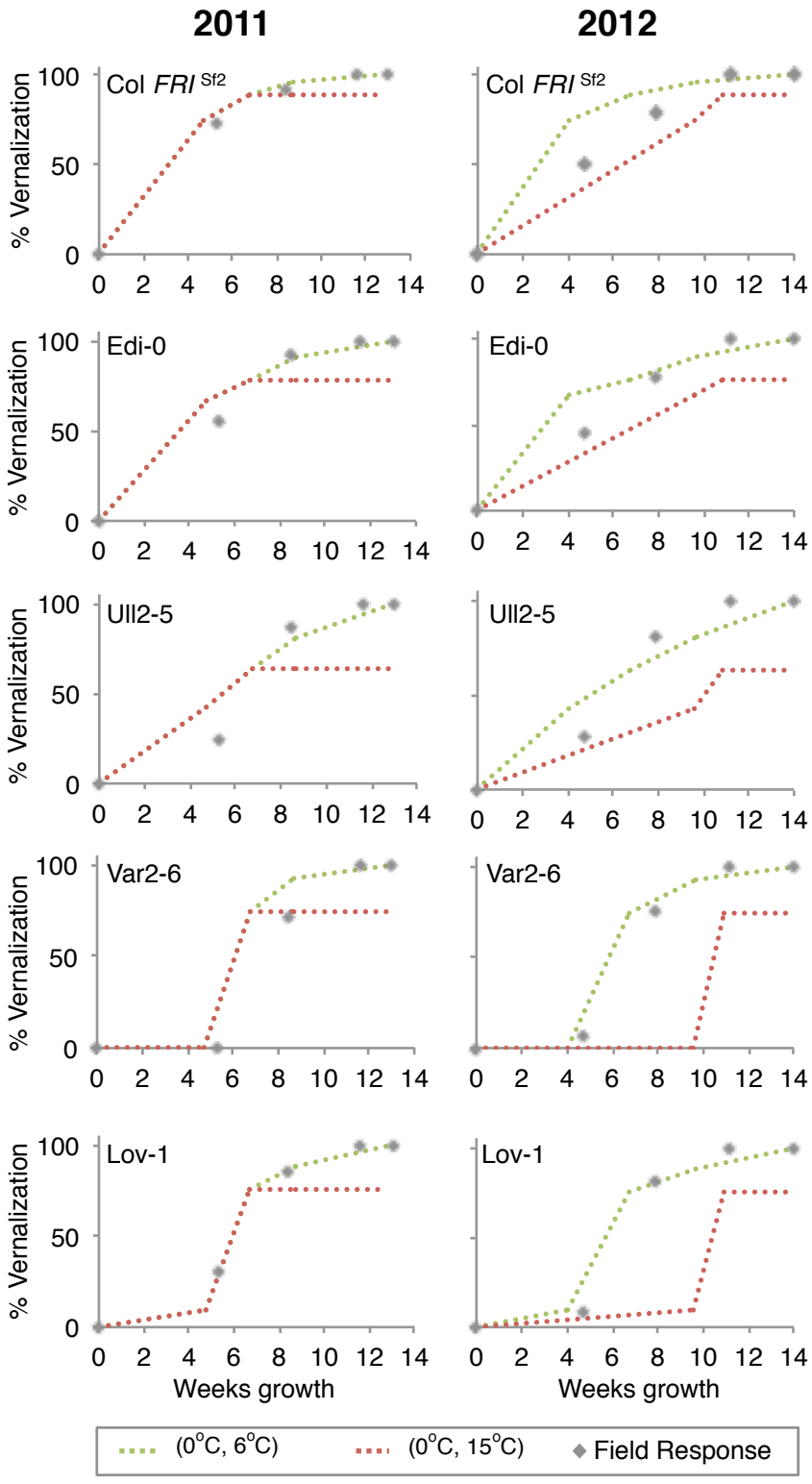

Figure 4.4 – Predictions of vernalization progress in the field based on accumulation of effective average daily temperatures
Vernalization responses calculated from Swedish field experiments carried out in 2011 and 2012 (grey diamonds) are shown along with responses predicted by (0°C, 6°C) (red dashed line) and (0°C, 15°C) (green dashed line) effective temperature ranges. See text for details.

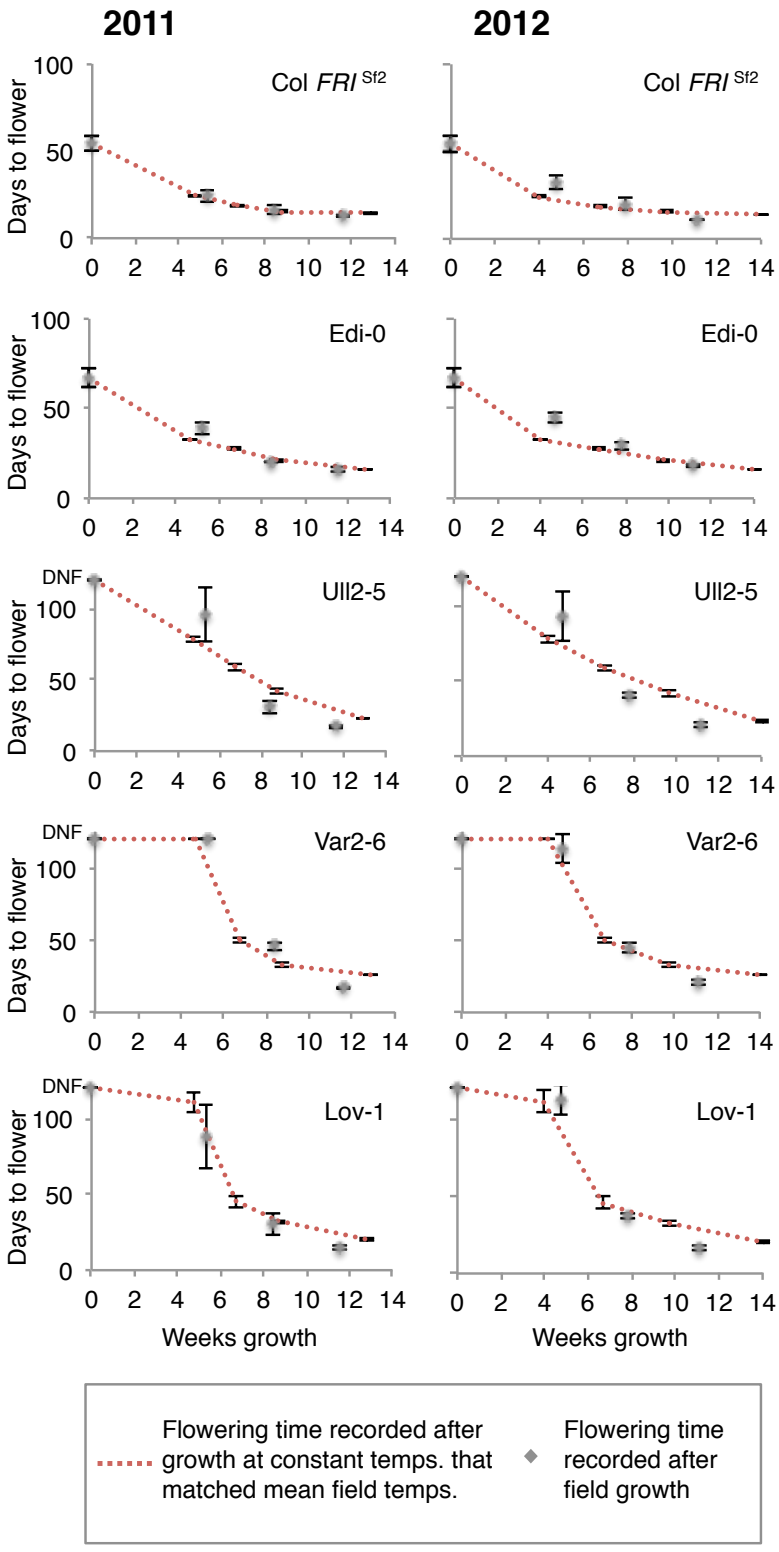

Figure 4.5 – Predictions of vernalization progress based on cumulative average temperatures.
Days to flower recorded after growth under field conditions in Sweden in 2011 and 2012 (grey diamonds). Days to flower were predicted by experiments where constant temperature conditions closely matched cumulative average field temperature (see Appendix Table 3 for data selection).

The similarity of flowering times observed following the 8°C day/14°C night and 11°C constant treatments suggest that it is possible for twelve hour periods of temperature to be evenly integrated. However the later flowering observed for plants vernalized at 14°C during the day and 8°C at night (compared with 11°C treated plants) suggest that higher daytime temperatures might disproportionately dampen the vernalization response.

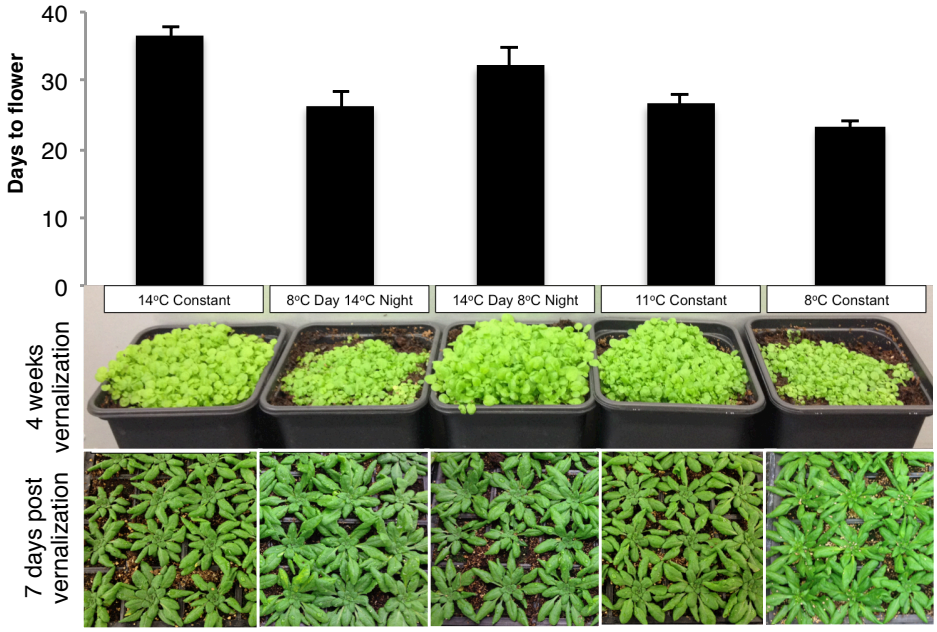

Figure 4.6 - Testing daily temperature integration
Plants were vernalized by two alternating 14°C and 8°C day / night regimes, or at 14°C, 11°C or 8°C constantly with a 12 hour photoperiod. Flowering time was then scored following transfer to constant 16hr 22°C LD conditions (*n*=12).

4.4 Temperature integration is not dependent on declining temperatures or photoperiod

Field experiments confirmed that twelve weeks of Swedish autumn temperatures fully vernalize a range of later flowering accessions (Chapter 3, Figures 3.10 and 3.11). Although the temperatures differed between the two years, these experiments were repeated during the same season, so they do not inform on whether effective vernalization under natural conditions requires declining trends of temperature and/or photoperiod. So a common garden experiment was set up in Norwich to test the

importance of these environmental cues and also provide a more stringent test for the two effective vernalizing temperature ranges.

Un-stratified seeds from all genotypes were sown directly onto bare soil during mid February in Norwich and left to germinate naturally. Over the subsequent weeks the seedlings were exposed to increases of both temperature and photoperiod, as opposed to the decreasing trends that naturally drive their growth during autumn. Edi-0 seeds did not germinate so vernalization progress could only be estimated for the remaining four genotypes, each of which had around 50 seedlings survive through to flowering (Figure 4.4A).

A total of 88 days elapsed between the Col*FRI*^{Sf2} sowing date and observation of the first inflorescence. The average temperature over this period was 9.35^{o}C and the summation of days with average daily temperatures between 0-6^{o}C and 0-15^{o}C ranges predicts totals of 11 and 77 days respectively. Col*FRI*^{Sf2} has a facultative requirement for cold so it is impossible to confirm whether this genotype had been forced to flower by strong environmental cues that overrode an outstanding ~30 day cold requirement or if flowering had been delayed until a permissive 15 hour photoperiod had been reached. But *FLC* expression levels determined 60 days after sowing supports the second hypothesis since the 57 effective vernalizing days predicted by the 0-15^{o}C temperature range resulted in a similar ~95% reduction that was observed after 56 days of growth at 5^{o}C (Figure 4.7, Chapter 2, Figure 2.3). Phenology of the Swedish accessions also provided evidence supporting an effective (0^{o}C, 15^{o}C) temperature range.

A total of 82 days elapsed between sowing and flowering of Var2-6, Ull2-5 and Lov-1 plants. An overall average temperature of 9.57^{o}C was recorded over this period and only 11 days were recorded with an average temperature between 0-6^{o}C. For these obligate cold-requiring accessions it is unlikely that 11 effective days had permitted reproductive transition. These plants had however been exposed to a total of 72 days within the 0-15^{o}C range during this period - 12 days less than the 84 days required for vernalization saturation (Shindo et al., 2006).

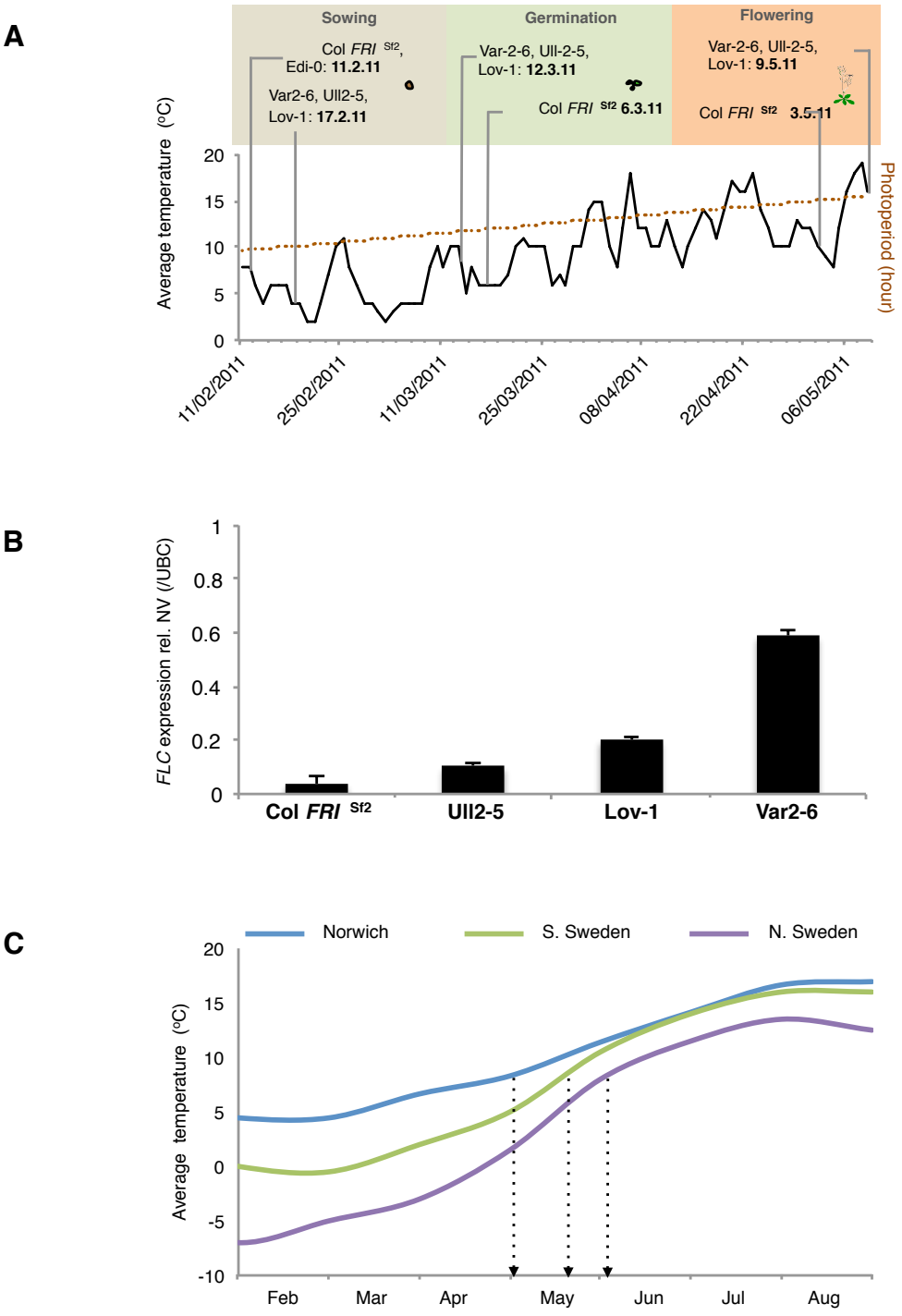

Figure 4.7 - Vernalization in a field setting occurs independently of photoperiod and decreasing temperature trends

(A) Sowing, germination and flowering dates are indicated along with average daily temperatures and daylength. **(B)** Reductions in *FLC* expression (relative to NV levels) were determined 60 days after the Col*FRI*^{Sf2} sowing date. **(C)** Average daily temperatures recorded during spring in Norwich, S. Sweden and N. Sweden. NV=Non-vernalized.

The synchronous flowering observed during this field experiment has hampered interpretation of the results. Relative differences in flowering enable comparisons to be made of vernalization progress, however the synchronous flowering observed could equally be explained by sufficient vernalization or conserved stress-related flowering pathways overriding any residual cold requirements. At the time of flowering the daylength matched that experienced during native flowering times in Sweden (~15.5 hours, see Chapter 3, Figure 3.14) and north and south Sweden would not have experienced similar temperatures until early June and mid May respectively (Figure 4.7). So it is likely that the environmental conditions in Norwich would have exerted forcing effects that could have overridden the 12 day cold discrepancy predicted by the daily average (0^{o}C, 15^{o}C) range for the Swedish accessions. Tracking changes in stress-related and floral pathway genes during this experiment may have helped to resolve this uncertainty.

Together the results from the Norwich and Swedish field experiments support the assumption that average daily temperatures between 0 and 15^{o}C provide reasonable estimates of vernalization progress, even in the absence of decreasing temperature and photoperiod cues.

4.4 Vernalization threshold temperatures predict diverse outcomes under a changing climate.

The extent to which winter annual *A. thaliana* accessions risk having their phenology disrupted by future climate change remains an open question. In order to address this, vernalization periods were predicted for the current climate and for the end of the century at three locations that cover the latitudinal extent of the species' range: Sundsvall (Northern Sweden), Oxford (Central England) and Barcelona (Spain) (Figure 4.8A).

Predicted future global temperature increases (Figure 4.1) reflect extensive geographical variation. Generally higher rises are predicted over landmasses versus the ocean and greatest increases are predicted for the Arctic region (IPCC, 2014). The most recent IPCC assessment report includes predictions for four possible

climate futures* in different regions (IPCC, 2014). They forecast 2-6°C and 1-5°C increases in annual average temperature by the end of the century for Northern and Southern Europe, respectively (Figure 4.5B and C). So a 3°C rise was considered appropriate for predicting changes in effective vernalization periods at all locations. The use of a uniform temperature rise ensured that model outputs would reflect current distributions, rather than different magnitudes of temperature increase.

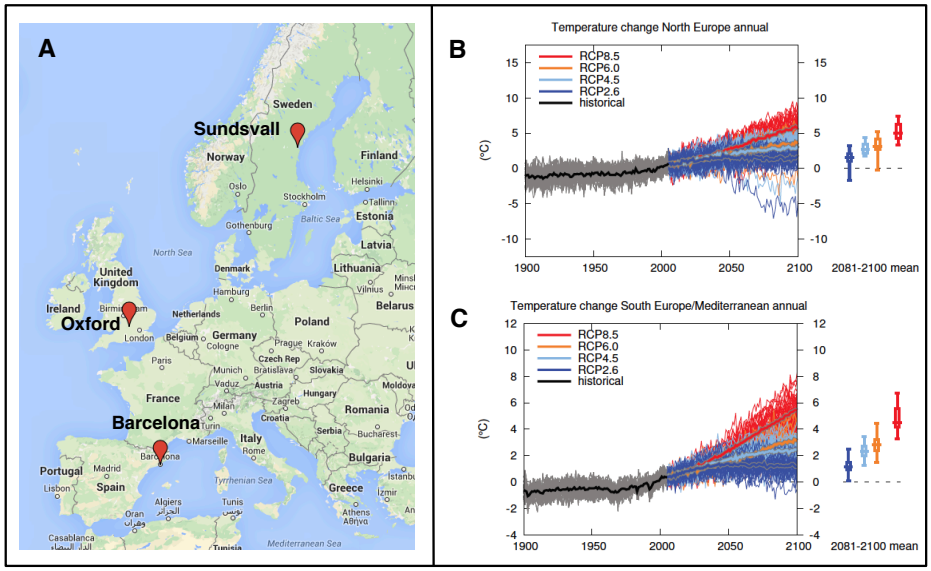

Figure 4.8 - Annual temperature rises predicted by the end of the century
(A) A map (Google, INEGI) showing locations selected to predict the impact of vernalization. Ranges of increases in annual temperature predicted under different representative concentration pathway scenarios for Northern (B) and Southern (C) regions of Europe. See footnote for explanation of scenarios (IPCC, 2014).

Climate change literature often assumes equal effectiveness of all temperatures below a given threshold, including those below 0°C (Prentice 1992). Although freezing temperatures may be perceived and accumulated by certain species (Jones et al., 2013), direct evidence from laboratory experiments together with indirect ecological evidence identified for Lov-1 (Chapter 3, Figure 3.14) suggests that sub-zero temperatures are ineffective for *A. thaliana* accessions. Therefore an Above

* Four Representative Concentration Pathway (RCP) trajectories RCP2.6, RCP4.5, RCP6 and RCP8.5 relate to potential radiative forcing values in 2100 relative to pre-industrial levels: +2.6, +4.5, +6.0, and +8.5 W/m^2 respectively.

Zero Threshold (AZT) model was used to predict the number of effective vernalizing days in each location from the germination date through to flowering (see methods section for details). In accordance with improved Swedish field predictions, average daily, rather than hourly temperatures were considered at each location.

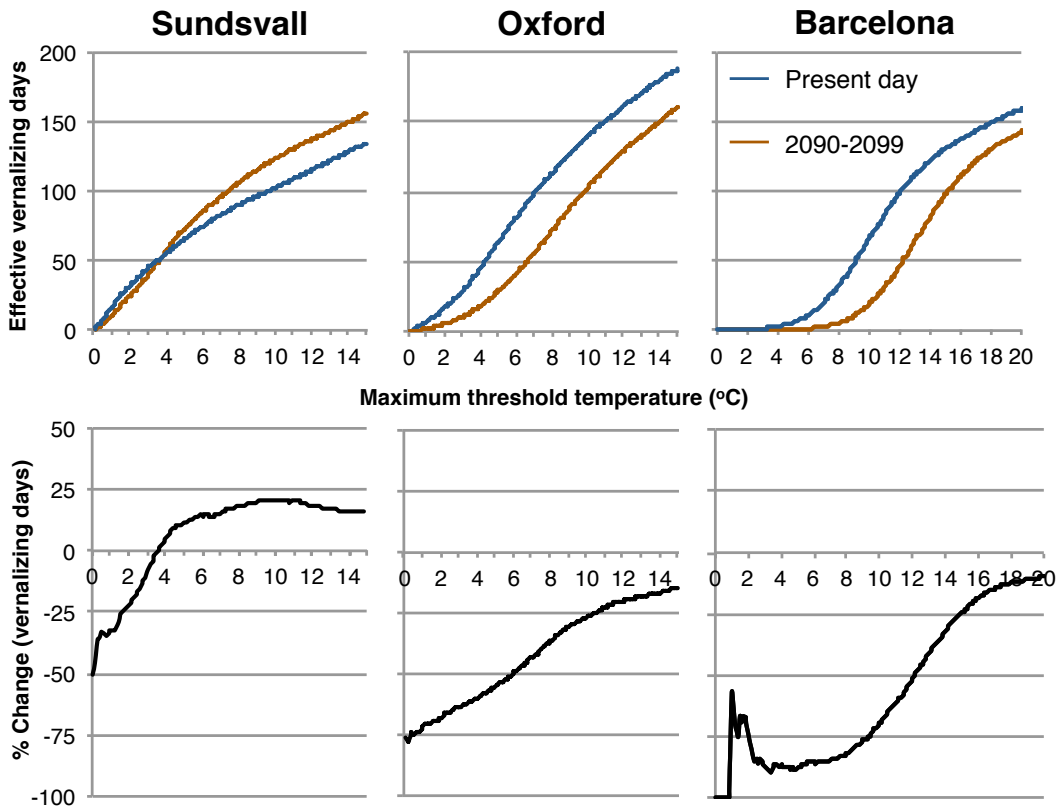

Figure 4.9 - Upper temperature thresholds for vernalization predict diverse impacts of climate change
The minimum vernalizing threshold temperature was set to 0°C and the effective vernalizing days per growing season were calculated for maximum threshold levels up to 15°C for Sundsvall and Oxford and 20°C for Barcelona. The upper panel shows present day results in blue and projected 2090-2099 climate results in red. The lower panel shows the percentage change expected in the quantity of vernalization by the end of the century at each location.

Data from the AZT model enabled impacts to be determined across a range of T_{max} threshold temperatures (Figure 4.9). In addition to providing predictions for *A. thaliana* vernalization, this also allows the impact to be determined for many species that also require minimum average daily temperatures above 0°C to vernalize effectively (see Chapter 1, Figure 1.4).

The maximum threshold temperature (T_{max}) of a species was found to make a significant difference to the predicted impact of climate change on vernalization (Figure 4.9). An overall reduction in vernalizing days was predicted in both Oxford and Barcelona for the majority of maximum threshold temperatures. Although little change is predicted in Sundsvall for plants with a T_{max} below 4°C, a striking increase in vernalizing days is predicted for plants with thresholds above this temperature (Figure 4.9). Although initially counterintuitive, this prediction reflects a loss of days above these thresholds being exceeded by the number of days above 0°C moving into the effective temperature window.

Next upper thresholds were applied to forecast the changes in the number of vernalizing days in these locations for *A. thaliana* over the coming century. The 15°C threshold was applied to both Sundsvall and Oxford data to reflect the accuracy of a 0-15°C range in predicting field responses of British and Swedish accessions (Figure 4.4). A threshold of 20°C was applied to the Barcelona data as 19°C was reported to mildly accelerate flowering in a significant number of Spanish accessions (Wollenburg and Amasino 2012). A reduction in the number of vernalizing days was predicted for both Oxford (26 days) and Barcelona (15 days). Despite these results representing a ~12% decrease in the effective vernalizing period at both these locations, this is unlikely to impact flowering time because the remaining 20 weeks of effective cold exceeds any reported vernalization requirement for *A. thaliana* (Shindo et al., 2005; Mendez-Vigo et al., 2011).

The impact of climate change was next considered for Sundsvall. As suggested in Figure 4.9 an increase in effective vernalizing days was forecast near the northerly limit of the range for *A. thaliana* plants with a T_{max} of 15°C. Early germinating plants are currently exposed to a total of 19 weeks of cold, but this period is predicted to

rise by ~10% at a rate of 0.23 days year^{-1} to reach a total of 22.2 weeks by the end of the century (Figure 4.10).

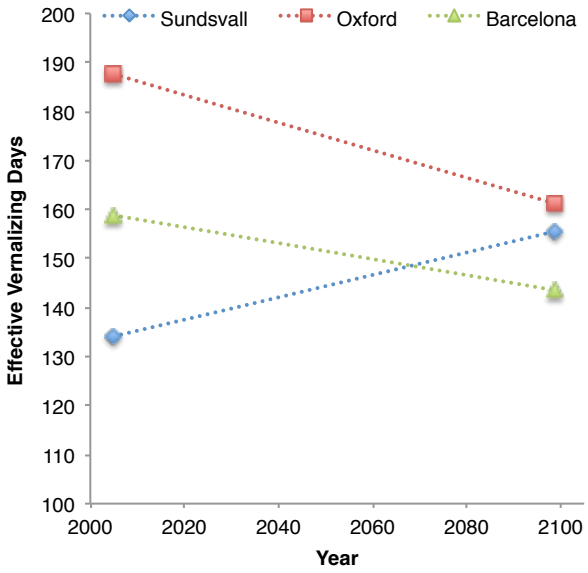

Figure 4.10 - Predicted changes in effective vernalizing days for *A. thaliana* during the 21st century
Effective days were calculated as the number of days between 0^{o}C and the maximum threshold temperature identified for accessions at each location to predict the impact on *A. thaliana* vernalization over the coming century.

4.5 Discussion

With very few exceptions (Aikawa et al., 2010), studies on vernalization responses are typically undertaken under standard, non-fluctuating laboratory conditions. Although these experiments have greatly improved our understanding of the molecular basis of chilling accumulation during exposure to constant temperature, much less is known about how these responses compare to those generated under natural conditions where daily temperatures can vary by ~1^{o}C hour^{-1*} (Chapter 3, Figure 3.7C).

* Calculated from Swedish temperature data, see Materials and Methods section.

Determining an appropriate period of vernalization temperature integration was the first step toward accurate predictions being made about the impact of climate change on vernalization. To achieve this, iterative comparisons were made between laboratory results with those obtained under natural field conditions. These revealed that accumulation of hourly temperatures significantly underestimated vernalization responses for all temperature thresholds (Figure 4.2 and other data not shown). A model that simulated different vernalization responses each day reflecting the effectiveness observed under constant temperature conditions also underestimated field responses for the Swedish accessions (Figure 4.3). But extension of the integration period significantly improved vernalization response estimates, perhaps because this disregards the minority of ineffective hours around midday and effectively extends the period of chilling perception. When maximum responses were considered for all average daily temperatures above 0°C, but below 6°C, reasonable predictions were made for Col*FRI*^{Sf2} and Edi-0 vernalization responses. But increasing the T_{max} to 15°C significantly improved predictions for all accessions (Figure 4.4). Also averaging temperatures over progressively longer periods accurately predicted responses of all lines (Figure 4.5). The similarity of constant and long-term average temperature responses provides a potential explanation for how Lov-1 can exhibit an optimal vernalizing response at a constant temperature that matches the autumn seasonal average (Chapter 3, Figure 3.7).

Results from an experiment designed to test for differential weighting of day and night temperatures suggested that warmer daytime temperatures might dampen an averaged vernalization response (Figure 4.4). From an ecological perspective, consistent higher daytime temperature cues may be indicative of late summer, therefore a tempered response may have evolved under these conditions to ensure vernalization does not complete until the critical photoperiod has passed. Consistent with this theory, daytime temperatures have also been shown to control the timing of orchid flowering (Blanchard and Runckle 2006). Differences observed in plant size suggest a potential mechanism for this inhibited response. At the end of the vernalization treatment plants grown at 14°C constantly and under 14°C day / 8°C night conditions were visibly larger than plants grown at 11°C or 8°C constantly or at 8°C day/14°C night (Figure 4.6). Previous studies suggest that this may be due to the activity of *SPATULA*, a transcription factor that represses vegetative growth when plants are grown under cool daytime temperatures (Thingnaes et al. 2003;

Sideaway-Lee et al., 2013). Although mitosis is thought to be required for stable epigenetic silencing of *FLC* (Finnegan et al., 2007) every DNA replication event risks the loss of histone based memory of preceding environmental exposure (Dodd et al., 2007, Angel et al., 2011, Angel et al., 2015). Therefore an increased rate of cell division achieved through relief of *SPATULA* repression during warm days, might have increased the probability of H3K27me3 nucleation loss at *FLC* compared to the plants grown at 11^{o}C constantly or at 8^{o}C during the day and 14^{o}C at night.

Increasing the maximum temperature threshold from 6^{o}C to 15^{o}C improved predictions of vernalization progress for later flowering accessions during the field experiment in Sweden, but this improvement was less obvious for Col*FRI*^{Sf2} (Figure 4.4). An experiment carried out during spring in Norwich provided a more stringent test for these two thresholds because the plants where exposed to a much larger proportion of warmer temperatures and this increased the disparity between the estimates (Figure 4.7A). Although vernalization was assessed in the same way as during the Sweden experiment, observed flowering times and *FLC* expression validated the decision to extend the effective temperature range for *A. thaliana* from 0-6^{o}C to 0^{o}C-15^{o}C (Figure 4.7A, B). Additionally, the accuracy of responses predicted by constant temperature responses in CERs of responses under complex natural environments suggested vernalization temperatures are integrated on a daily basis, regardless of overall trends of temperature or photoperiod.

Multiple climate models now predict that most locations across the globe will get hotter and experience fewer extreme cold temperatures by the end of the century. In addition, a retreat in permafrost and a reduction in snow cover in the northern hemisphere of between 7-25% is expected (IPCC, 2014). The extent to which both warmer autumn and winters will disrupt plant development and counteract the direct effects of warming has been identified as a key gap in our knowledge (Chuine et al., 2010; Cook et al., 2012; Laube et al., 2013). In order to address this question an optimal combination of effective temperatures and time period of assessment needed to be identified. Long-term temperature averaging was found to provide good approximations of both early and late vernalization responses for all genotypes (Figure 4.5). But the long-term averaging method requires flowering time responses to be known for a range of constant temperature treatments to enable field responses to be estimated for each accession. This makes it ideal to address

questions relating to a limited number of accessions in specific locations, but limits its suitability for making species-wide predictions. An AZT (Above Zero Threshold) model was also used to sum effective daily average temperatures between 0 and 15^{o}C to successfully predict vernalization saturation under natural field conditions (Figures 4.4). This more general model was selected as it only requires existing knowledge of T_{max} and vernalization requirements at 5^{o}C to predict the impact of climate change for the vernalization of *A. thaliana*.

The most striking AZT prediction was the increase in vernalization period at northerly latitudes by the end of the century. This increase is likely to be applicable to many species that do not vernalize below 0^{o}C and have maximum threshold temperatures above 4^{o}C (Chouard, 1960). An opposite effect would be predicted for this region by climate change models that apply only a maximum threshold value (Prentice et al., 2010) because unlike AZT, they accumulate *all* temperatures below a threshold in present and future datasets and disregard the fact that sub-zero temperatures are ineffective for many species (Chouard, 1960). For thresholds between 1^{o}C and 15^{o}C more intuitive reductions in effective days of 75% to 15% in Oxford and 85% to 10% in Barcelona are predicted.

AZT predictions suggest that vernalization requirements of many *A. thaliana* accessions are likely to be met following a 3^{o}C increase in average temperature across the species range (Figure 4.10). This in turn suggests that warmer spring temperatures will advance the phenology of this species over the coming century. This prediction is consistent with a recent report by Li and colleagues that showed three simulated future climates in Sweden and Spain all advanced flowering times for a global panel of accessions (Li et al., 2014). Although an assessment of relative accession fitness in field experiments revealed a lag in the adaptation of *A. thaliana* to warmer climates (Wilczek et al., 2014), the ability to advance flowering in response to warming bodes well for this species as this is associated with increased chance of survival under climate change (Willis et al., 2008).

Results in this chapter suggest that climate change will not result in a delay of *A. thaliana* flowering over the next 85 years. However significant reductions in effective temperatures were predicted for plants in southern Europe that have lower vernalization thresholds (Figure 4.9). The manner in which impaired vernalization

affects the flowering, seed production and dormancy of these species will determine their chances of survival as average temperatures continue to increase over the coming century.

4.6 Material and Methods

4.6.1 Plant material and growth conditions.

For the daily averaging experiment seeds were sown in a randomized design in Arabidopsis mix and stratified for 3 days at 4°C. Seedlings were pre-grown for 7 days (16h light: 8h dark) at 22°C and then vernalized for 4 weeks (12h light: 12h dark) in cabinets (Sanyo MLR-351H) at constant 8°C, 11°C or 14°C settings or 14°C day/8°C night or 14°C night/ 8°C day, All temperatures were recorded as ± ≤1.5°C, 70% ± ≤10% RH. Low light (~30µmol m^{-2} s^{-1}). Plants were then transferred to random locations in a controlled environment room (16h light: 8h dark, 22°C ± 2°C) and flowering time was scored as the number of days of growth until floral buds became visible.

4.6.2 Sweden Field Experiments

See Chapter 3 Material and Methods section 3.4.2.

4.6.3 Hourly chilling unit accumulation calculations

In this model, effective vernalizing hours accumulate when the recorded temperature is above a minimum effective temperature, T_{MIN}; but below the maximum effective temperature, $T_{MAX.}$ The rate of vernalization is zero or negligible for periods where the temperature is either above or below this specified effective temperature range and maximal during periods where the temperature is between T_{MIN} and T_{MAX}. Plant responses therefore depend on upon both the temperature and the treatment duration. (Craigon et al., 1995; Streck 2002; Streck and Schuh 2005).

Data presented in Figure 4.2 uses two ranges to predict vernalization progress during the 2011 and 2012 field experiments

Range 1: T_{MIN} = 0°C, T_{MAX} = 6°C
Range 2: T_{MIN} = 0°C, T_{MAX} = 15°C

The vernalization response was considered saturated (V_{SAT}) when accumulated vernalizing hours reached the number of hours required to saturate the response under an optimal constant temperature treatment:

Col*FRI*^{SF2} V_{SAT} = 960 hours

Lov-1 V_{SAT} = 2016 hours

4.6.4 Accession specific model

Vernalization functions were determined by flowering time results recorded for constant temperature treatments (0°C, 2°C, 5°C, 8°C, 12°C and 14°C, see Chapter 2 for details). Smooth curves were fitted to the temperature dependent rates using cubic splines in MATLAB (MathWorks Inc., Massachusetts, UK) constrained to zero at 0°C and 16°C. These splines were used to generate predicted rates between these extremes.

The models were fitted as follows:

$$\text{Log}_{10}(\text{mean days to flower-factor*fastest time to flower})$$
$$=\text{Log}_{10}(\text{NV} - \text{factor*fastest time to flower}) - b * \text{weeks}$$

Where the values of b are the temperature dependent vernalization rates.
r^2 values exclude 0°C data.

Taking antilogs and rearranging gives:
Mean days to flower = (NV- factor * fastest) $*10^{-b\ \text{weeks}}$ + factor * fastest

$$b_{\text{temperature}} \times \text{duration}$$

Where b is the value of the rate for the temperature in that time period, and the duration is measured in weeks (so one day = 1/7 of a week). All values were then added together and to calculate:

Mean days to flower = (NV- factor * fastest) $*10^{-(\text{sum of b x duration calculated above})}$ + factor * fastest

Col*FRI*^{Sf2}

r^2 = 0.978

Non vernalized (NV) flowering time = 54.27

Fastest time to flower = 13.9

Factor = 0.97

Edi-0

r^2 = 0.973

NV flowering time = 67.08

Fastest time to flower = 16.08

Factor = 0.85

Ull2-5

r^2 = 0.845

NV flowering time = 120

Fastest time to flower = 23.25

Factor = 0.85

Var2-6

r^2 = 0.83

NV flowering time = 140

Fastest time to flower = 25.25

Factor = 0.817

Lov-1

r^2 = 0.848

NV flowering time = 130

Fastest time to flower = 20.27

Factor = 0.85

4.6.5 Accumulation of effective daily average temperatures

Rather than accumulating temperatures recorded every hour in the field (as described in 4.6.3), accumulations of average daily temperatures were made based on the following ranges:

Range 1: T_{MIN} = 0°C, T_{MAX} = 6°C
Range 2: T_{MIN} = 0°C, T_{MAX} = 15°C

The following equation was used to calculate %Vernalization values shown in Figure 4.4:

% Vernalization = (OBS_{DTF} – MIN_{DTF}) / (NV_{DTF} - MIN_{DTF})*100 = % un-vernalized

100 - % un-vernalized = % vernalized

Where:
OBS_{DTF} = Observed number of days to flower
NV_{DTF} = Days to flower recorded / assigned for non-vernalized plants
MIN_{DTF} = Minimum number of days to flower observed

4.6.6 Using cumulative average temperatures to predict vernalization responses under field conditions

Field temperature data was assessed to determine dates in the field when 4, 6, 8 and 12 weeks of effective average daily temperatures were accumulated based on Range 2 thresholds (T_{MIN} = 0°C, T_{MAX} = 15°C).

For each of these dates cumulative average temperatures (T_{CA}) were calculated where T_{CA} = the mean of all preceding hourly temperatures since the sowing date. Flowering time data was then selected for each date that most closely matched the T_{CA}. The selected data used to predict vernalization responses for all accessions during autumn 2011 and 2012 is shown on the next page.

2011					
Field Temperatures					
Weeks after sowing	4	5	6	8	12
T_{CA}	12.48°C	10.82°C	9.72°C	8.40°C	6.42°C
Selected Cabinet Data					
Weeks vernalization	4	5	6	8	12
Constant temperature	12°C	10°C	8°C	8°C	5°C

2012				
Field Temperatures				
Weeks after sowing	4	6	8	12
T_{CA}	9.49°C	7.34°C	5.61°C	4.55°C
Selected Cabinet Data				
Weeks vernalization	4	6	8	12
Constant temperature	8°C	8°C	5°C	5°C

4.6.7 Norwich Field Experiment

Seeds were sown liberally onto moist, weed-free soil (52° 62.83'N 1 ° 29.67'E) and left to germinate naturally without prior stratification. The area was cordoned off with barrier tape to limit herbivory. Some weeding was carried out during the experiment to minimize competition from endogenous plants, but no watering. Growth was monitored a minimum of three times each week. Day length and daily average temperature data were taken from http://www.timeanddate.com and http://www.wunderground.com, respectively.

4.6.8 RNA extraction

See Chapter 2 Materials and Methods section 2.10.2.

4.6.9 Reverse Transcription

See Chapter 3 section Materials and Methods section 2.10.3.

4.6.10 Quantitative Polymerase Chain Reaction (qPCR)

See Chapter 3 section Materials and Methods section 2.10.4 Expression levels were determined using Roche Universal Probe Library (UPL) Probes and the primers shown on the next page.

***FLC* (At5g10140)**	
sFLC_UPL_#65_F	5'-gtgggatcaaatgtcaaaaatg-3'
sFLC_UPL_#65_R	5'-ggagagggcagtctcaaggt-3'
UPL #65	5'-ctggagga-3'

***UBC* (At5g25760)**	
UBC_UPL_#9_F	5'-tcctcttaactgcgactcagg-3'
UBC_UPL_#9_R	5'-gcgaggcgtgtatacatttg-3'
UPL#9	5'-tggtgatg-3'

FLC gene expression was calculated relative to *UBC* levels using the comparative Ct method (also known as the 2-[delta][delta]Ct method) (Schmittgen and Livak 2008) and statistical analysis of was performed using GraphPad Prism version 6 software for Mac (La Jolla, California, USA).

4.6.11 Modelling present and future effective vernalizing days

To examine changes in vernalization in Oxford we obtained simulated hourly temperature data for the current climate and for the 2090-2099 climate predicted for Oxford (51.8 °N 1.3 °W) from United Kingdom Climate Impacts Programme (UKCIP-www.metoffice.gov.uk/climatechange/science/monitoring/ukcp09/). The magnitude of the predicted change in temperatures in the UKCIP data was assessed by fitting a linear regression to the relationship between hourly temperatures under the current climate sorted into ascending order and predicted future temperatures sorted in the same way. For current temperatures of 0^{o}C, the predicted increase in Oxford is 2.9^{o}C. To examine impacts for Spanish and Swedish accessions we obtained temperature data collected between 1973 to 2012 at Barcelona airport in Spain (41.4 °N, 2.2 °E) from NOAA (www1.ncdc.noaa.gov) and between 1961 to 2011 at Sundsvall airport in Sweden (62.4 °N 17.2 °E) from the Swedish Meteorological and Hydrological Institute (www.smhi.se). Some data gaps of one or two hours in the Barcelona time series were filled by linear interpolation, and gaps of one day were filled by substituting the previous day's data. To predict likely impacts of future climate change at Barcelona and Sundsvall, an increment of 3°C was added to all temperatures. For each chilling model, the total number of effective days was calculated between the predicted germination and flowering at each location. This corresponds approximately to 1st August until 1st May in Sundsvall, 1st September until 31st March in Oxford and 1st October to 15th March in Barcelona (Montesinos et al., 2009, Pico 2012). We used a range of threshold temperatures from 0 to 15 °C for UKCIP and Sundsvall projections and from 0 to 20 °C for Barcelona. The number of effective days in the warmer climate was expressed as a percentage of the value for the current climate. All calculations were carried out using Mathematica 5.2 (Wolfram Research Inc, Champaign, IL)

Chapter 5 - Detecting RNA molecules *in planta*

Division of work: Tjevlar Olsson and Matthew Hartley created the image analysis programme used to quantify mRNA levels. Stefanie Rosa helped to optimize tissue preparation.

5.1 Introduction

Understanding how vernalizing temperatures are perceived and remembered by plants at the molecular level has proved challenging (Song et al., 2013). Modelling approaches have fundamentally advanced this knowledge and correctly predicted that cold-induced cell autonomous switching of epigenetic states lies at the heart of vernalization (Angel et al., 2011; Angel et al., 2015; Satake 2012). Addressing the questions raised by these models is likely to be important to progress understanding of how fluctuating temperatures are integrated over time, but progress has been hampered by the lack of techniques that provide cellular resolution.

Calculating relative changes in gene transcription by qRT-PCR overlooks potentially important information relating to cell-to-cell variation and sub-cellular localization of RNA molecules. Single molecule RNA fluorescence in situ hybridization (smFISH) was developed to achieve these aims (Femino et al., 1998). This technique uses multiple, single-labeled oligonucleotide probes to bind target RNA and generate diffraction-limited signals that can be detected using a standard wide-field fluorescence microscope (Raj et al., 2008). Despite advances in many model systems (Castelnuovo et al., 2013, Neuert et al., 2013, Yang et al., 2014, Ji et al., 2013), this method has yet to be adapted for use in plants. We decided this would be an important technique for *FLC* analysis so I embarked on establishing it for *A. thaliana*. This chapter describes optimization and validation of this technique by determining mRNA levels of a housekeeping gene in the common Arabidopsis lab strain Columbia (Col-0).

5.2 Gene Selection

At1G13320 is the A2 scaffolding A subunit of *Protein Phosphatase2A* (*PP2A*) (Lillo et al., 2014). This gene was selected for study using smFISH because, unlike several environmentally regulated phosphatase subunits, it exhibits mRNA levels that are relatively unperturbed by a range of abiotic and biotic stresses. Furthermore, this gene is transcribed evenly across many tissue types throughout development. These robust properties led to At1G13320 being identified as a superior gene for RT-qPCR normalization (Czechowski et al., 2005).

5.2 Tissue selection

Autofluorescence is inherent in many plant tissues so it occurs at higher levels in *A. thaliana* than normally observed for many other organisms. This autofluorescence has proved to be a significant barrier to the development of fluorescence microscopy techniques in plants (Frost, 1995). It was therefore essential to carry out an assessment of naturally occurring spectral emissions across all areas of the plant to determine the most suitable tissue for smFISH. Although significant levels of autofluorescence were detected everywhere, the root tip appeared to be the best tissue in which to attempt the smFISH technique. Closer observation of root cells prior to the application of probes revealed punctate autofluorescence signals in endoreduplicated nuclei in the transition zone and further up the root. This finding restricted analysis to the relatively undifferentiated diploid cell population in the root apical meristem (Figure 5.1).

5.3 Sample Preparation

Standard epi-fluorescence microscopy using a CCD camera has been recommended for smFISH rather than confocal microscopy (Raj et al., 2008). Since multi-layered plant tissue cannot be resolved using standard fluorescence microscopy, this meant that samples needed to be prepared in single cell layers.

Researchers have traditionally used wax embedding and sectioning to produce thin layer tissue sections, but this process left samples with fluorescence levels that exceeded probe signals (data not shown). Cryosectioning was also attempted, but residual mounting media also inhibited signal detection (data not shown). It became

apparent that a novel method of sample preparation was required that would both preserve cellular architecture and minimize background fluorescence.

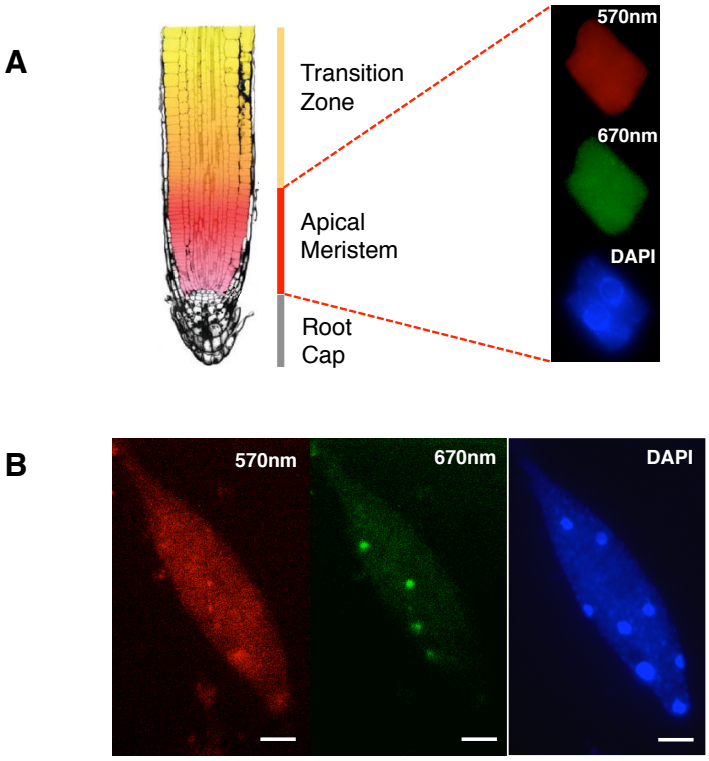

Figure 5.1 – Arabidopsis root meristem cells are suitable for smFISH analysis Regions of growth are indicated along a longitudinal section of root (A). Cells from the apical meristem labeled with the nuclear stain DAPI (blue) exhibited low levels of autofluorescence at wavelengths that match probe emission maxima (A). Punctate signals observed in differentiated nuclei precluded them from further analysis. Details of probe excitation and emission spectra tested are included in Appendix Figure 1. Root image was adapted from Verbelen et al., 2006.

5.4 Detection of *PP2A* mRNA

Unlike other *in situ* techniques smFISH does not rely on signal amplification for detection. Instead each 20nt probe is conjugated to a single fluorophore and a set of probes hybridizing to a single RNA molecule generates a diffraction-limited spot that is detectable by a wide-field fluorescence microscope. A probe set of 48 probes (see Appendix Table 3) was labeled with Quasar©670 dye and designed to be complimentary to *PP2A* exons to enable detection of *PP2A* mRNA (Figure 5.2A).

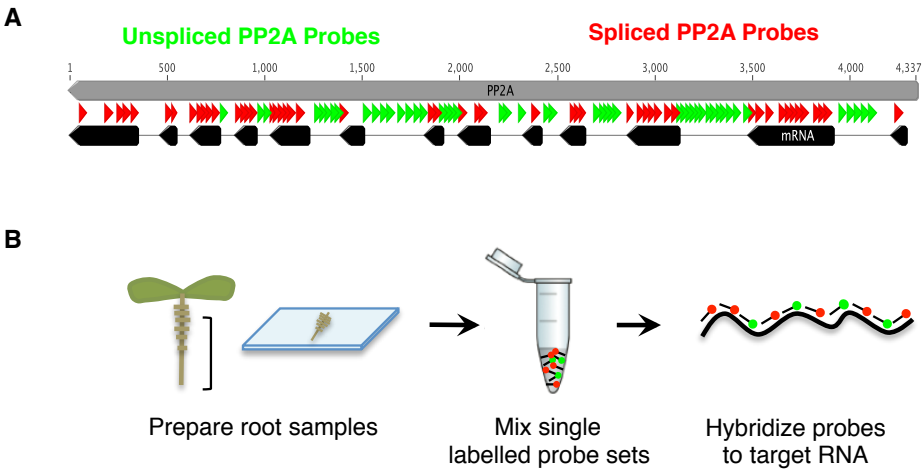

Figure 5.2 - Detecting *PP2A* RNA using multiplexed single molecule fluorescence In Situ hybridization
(A) Unspliced and spliced *PP2A* probes sets designed to target intronic and exonic RNA sequences respectively. (B) Schematic representation of smFISH.

After considerable optimization, a process was developed to produce meristematic root tissue samples suitable for smFISH analysis. Details of the sample preparation are included in the Materials and Methods section at the end of this chapter. Briefly roots were fixed with paraformaldehyde and squashed onto slides before undergoing a freeze-thaw procedure to ensure tissue adherance. Ethanol was used to permeabilize the tissue before probes were left to hybridize to the target RNA overnight (Figure 5.2B). DAPI was added to each sample to label the nuclei before imaging.

This method of sample preparation was found to yield several single cell-layers from each root in addition to many isolated cells that were also suitable for analysis (Figure 5.3 A-D). Weak probe signals were observed when the samples were imaged using a standard CCD camera (data not shown) however the enhanced sensitivity of an EMCCD camera greatly improved the signal-to-noise ratio. Consistent with other reports, smFISH probes enabled RNA molecules to be visualised as punctate signals approximately 0.5µm in diameter, homogeneously dispersed throughout the cell (Raj et al., 2008; Raj and Tyagi 2010) (Figure 5.3). These signals were no longer visible following RNase treatment (Appendix Figure 2).

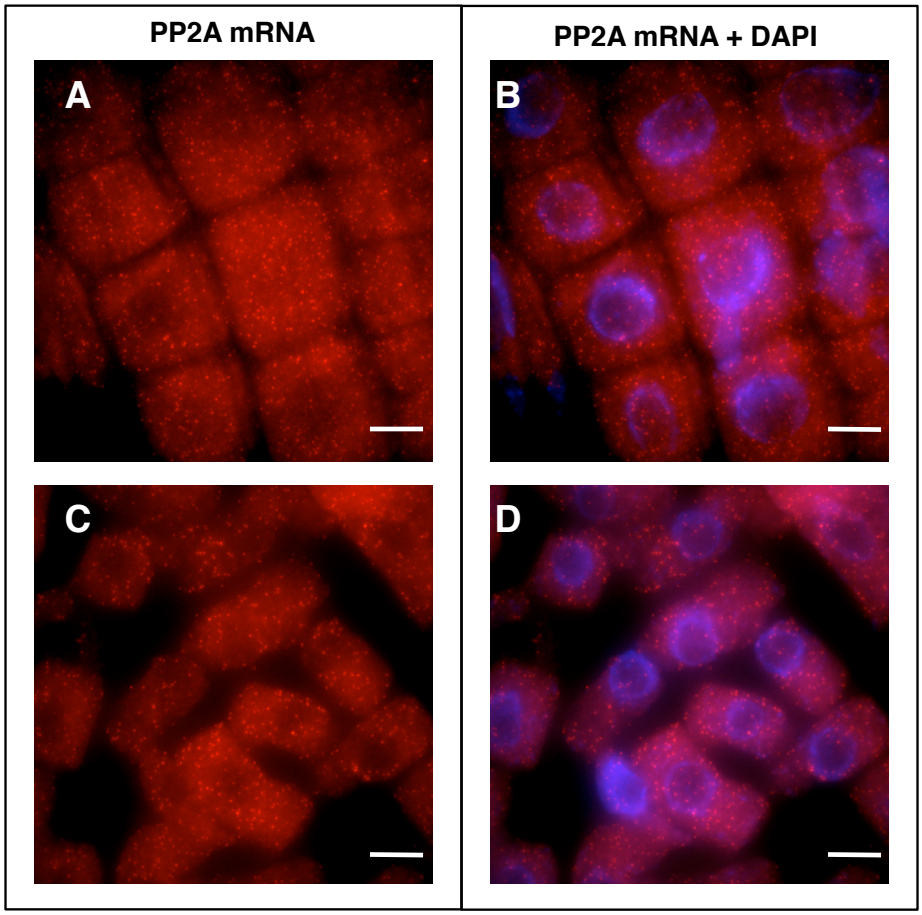

Fig 5.3 - *PP2A* mRNA observed in Col-0 root meristem cells
Maximum projection images of cell files (A and B) and isolated cells (C and D). *PP2A* mRNA Quasar©570 probe signals are shown in red and nuclear stain DAPI in blue. Scale bar = 10µm.

5.5 Detecting sites of *PP2A* transcription

Advances in single molecule RNA labeling have revealed that transcription is not a smooth, continuous process; for some genes quiescent periods of gene inactivity are interspersed by bursts of transcriptional initiation (Golding et al., 2005; Chubb et al., 2006; Raj et al., 2008). Nuclear signals observed in *A. thaliana* samples were indicative of the bursts identified in other organisms, with transcriptional events producing foci that were both larger and of higher intensity than mRNA observed in

the cytoplasm (Figure 5.4). They are likely the result of probes binding to RNA associated with multiple polymerases simultaneously transcribing *PP2A*.

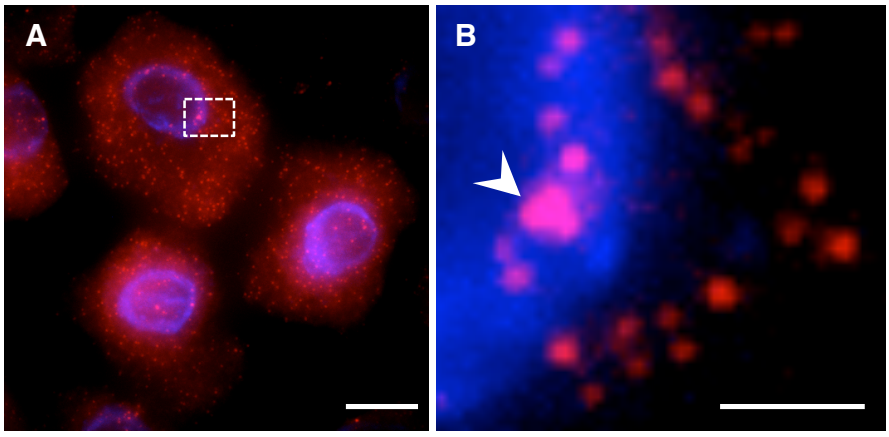

Figure 5.4 – Evidence of transcriptional bursting in Col-0 meristematic cells
Red *PP2A* exon probe signals are observed both in nuclei (DAPI, blue) and in the cytoplasm (A). Magnification of the region outlined in (A) is shown in (B). The arrowhead indicates a burst of *PP2A* transcription. This signal is larger than the others in this image that are likely represent single mRNA molecules. Scale bar = 10µm in (A), 2.5µm in (B).

Intron chromosomal expression FISH (iceFISH) is a direct method to visualize sites of transcription by using probes complementary to intronic gene sequences (Levesque and Raj 2013). We designed a second set of 48 probes complimentary only to *PP2A* introns and labeled them with Quasar©670 dye to allow iceFISH to be combined with standard smFISH (Figure 5.2A). As expected, putative sites of transcription were restricted to the nucleus and invariably co-localized with exonic probe signals (Figure 5.5). Consistent with transcription being halted during mitosis, no unspliced signals were observed at this stage of the cell cycle (Figure 5.6). mRNA observed in the cytoplasm of these cells was therefore likely to have been synthesized prior to chromosome condensation.

5.5 Image analysis and quantification of RNA

Quantification of RNA from smFISH images is typically achieved through automated image analysis. Two stages of processing were required for analyzing our images, cell segmentation and spot counting (Figure 5.7). Determining cell boundaries proved to be the most challenging aspect of the analysis, so annotated results were

checked manually to ensure accurate segmentation. Details of the image analysis are provided in the Material and Methods section at the end of this chapter.

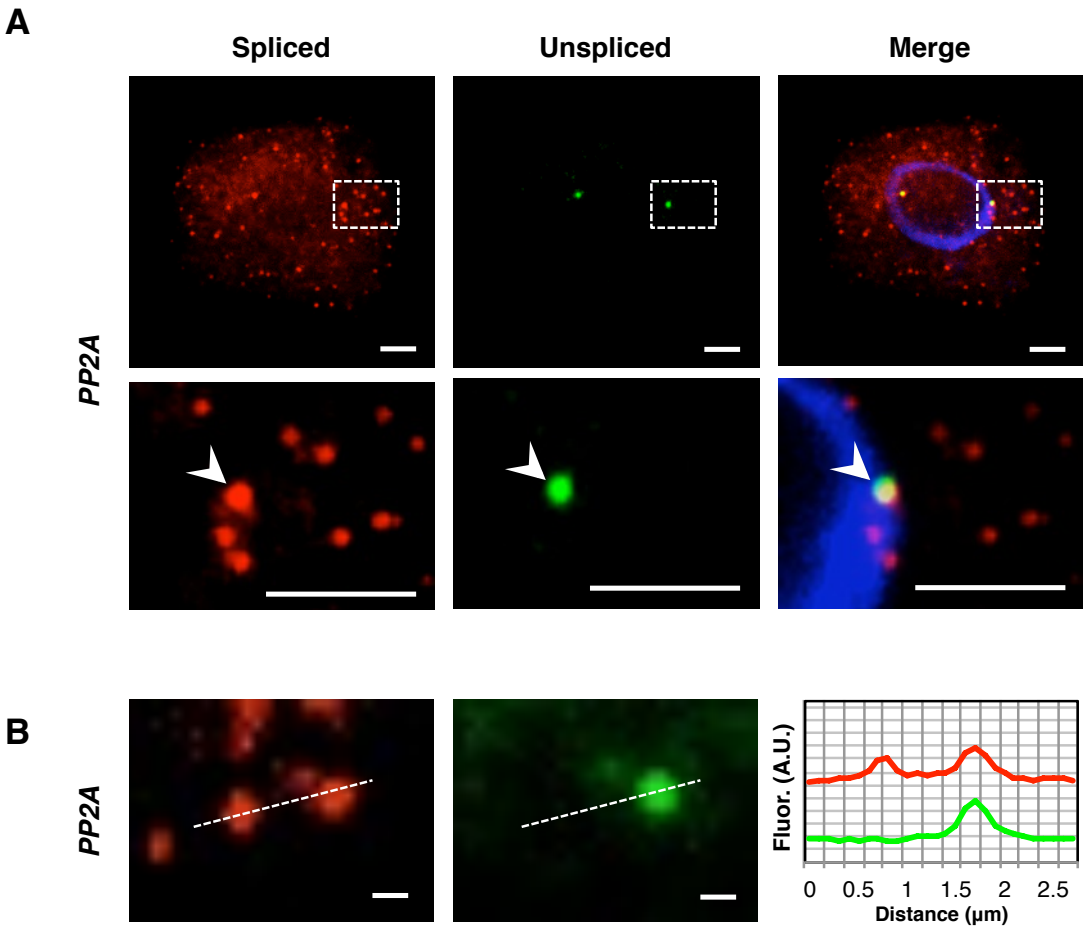

Figure 5.5 – Multiplexed probe sets enable simultaneous detection of spliced and unspliced *PP2A* RNA in Col-0 meristematic cells
A representative image of isolated meristem cell showing two sites of active transcription located within the nucleus that are both co-localized with *PP2A* mRNA signals. (A). (B) Magnified image of two mRNA signals, one co-localized with an unspliced *PP2A*. (C) Fluorescence intensity of these signals have been plotted against length (µm). Scale bars = 5µm in A and 0.5µm in B.

Image analysis results indicated that the numbers of PP2A mRNA per cell were not normally distributed. 71% of cells contained between 20 and 60 mRNA whilst the remaining 29% contained between 70 and 220 molecules (Figure 5.8A). It was notable that every cell analysed contained *PP2A* RNA with a minimum of 15 transcripts observed (Figure 5.8A). An average of 74 mRNA were detected in each

cell (Figure 5.8B). Consistent with *PP2A* being considered a superior normalization gene (Czeweski et al., 2010) the signal from intronic probes showed the gene is expressed in over 80% of cells (Figure 5.8C). The cells being analysed were assessed to be diploid as two PP2A transcription foci were generally detected. 4% of cells had three foci and 10% had four, consistent with the proportion of cells that would have likely undergone DNA synthesis but had yet to divide. This suggests that expression occurs from alleles located on two sets of sister chromatids (Figure 5.9).

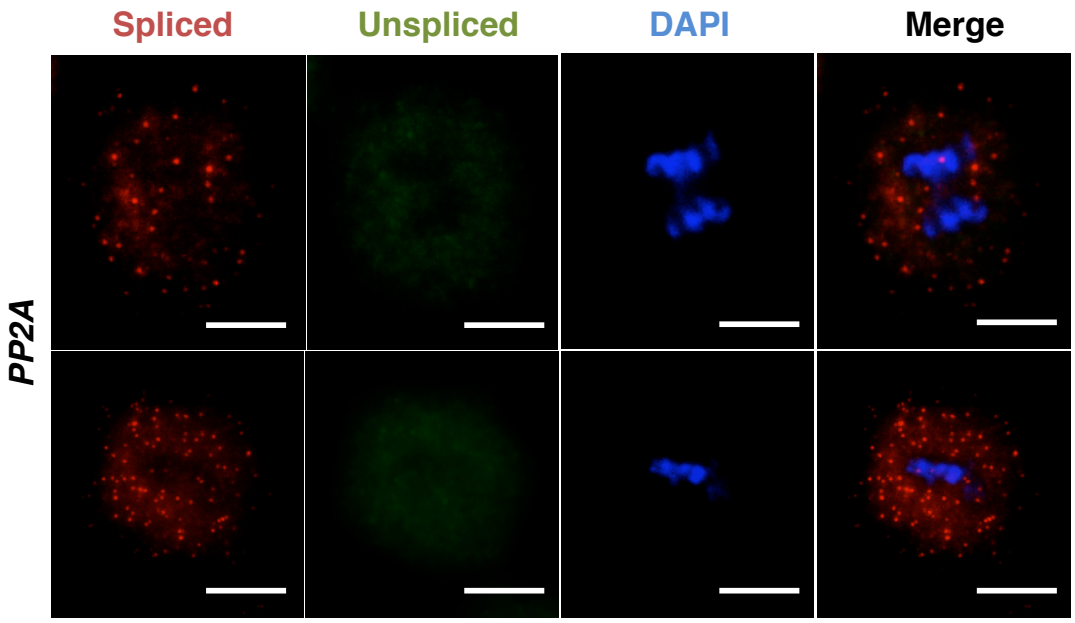

Figure 5.6 – An absence of transcription during mitosis in Col-0 meristematic cells. Representative images of cells undergoing mitosis. Condensed DNA are labeled with DAPI (Blue), spliced *PP2A* RNA, Red and unspliced *PP2A* RNA, Green. Scale Bar =10 µm.

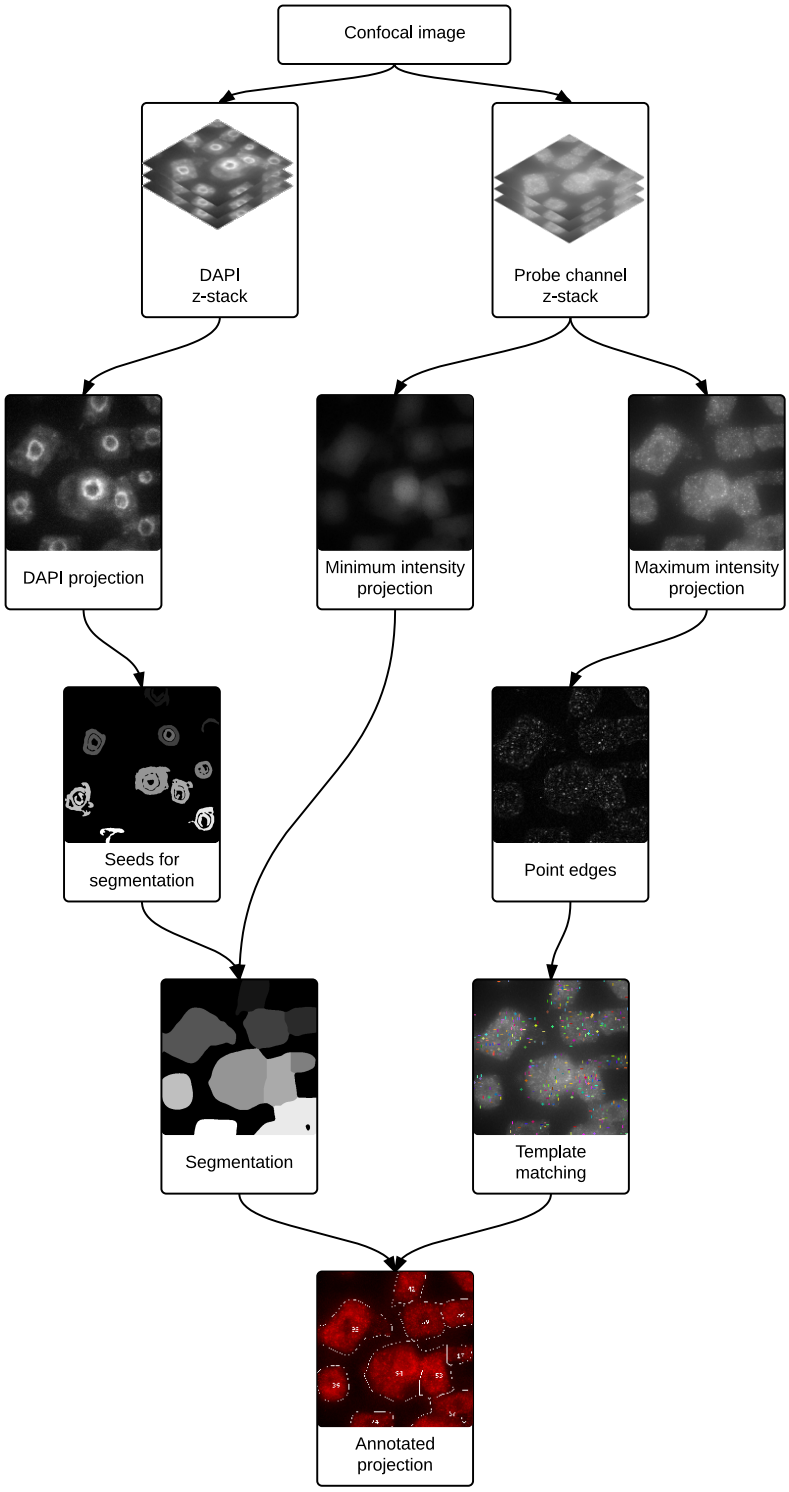

Figure 5.7 – Image analysis pipeline used to detect probe signals and generate counts of probes per cell A maximum intensity projection of the nuclear DAPI signal was used to determine cell boundaries and segment the image. Find edges and template matching commands identified the probe signals that were used generate annotated projected images. Details of image analysis can be found in the materials and methods section at the end of the chapter. Figure courtesy of Dr Matthew Hartely.

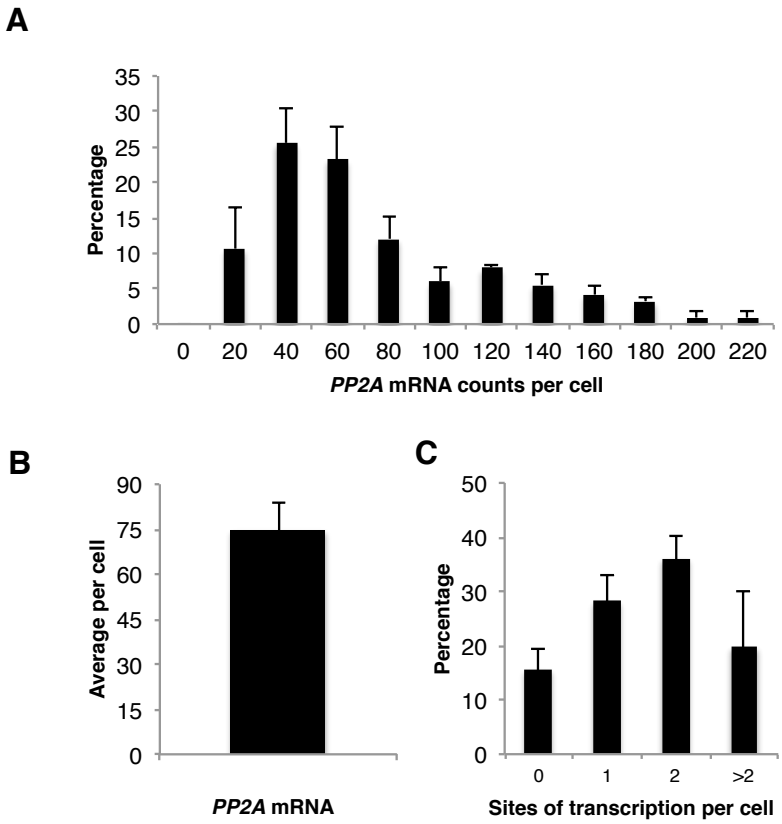

Figure 5.8 - Quantification of *PP2A* RNA in Col-0 meristematic cells
Frequency distribution of RNA molecules per cell is shown in (A). The overall average RNA number per cell is shown in B and active sites of *PP2A* transcription are presented in (C). All error bars are +SEM, *n*=3.

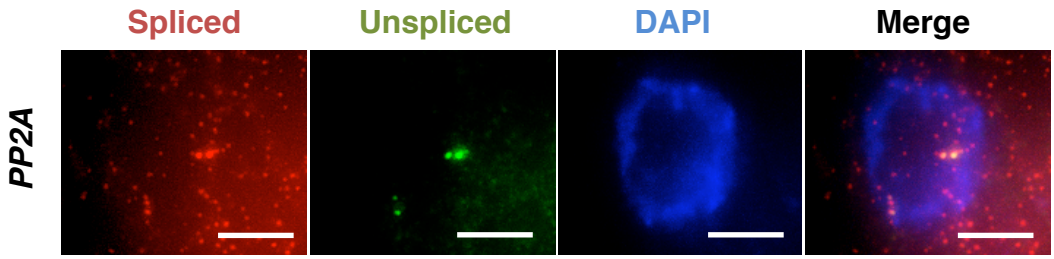

Figure 5.9 - Simultaneous *PP2A* transcription by sister chromatids
A representative maximum projected image showing 4 sites of *PP2A* transcription. The nucleus is labeled with DAPI (Blue), spliced *PP2A* mRNA is red and unspliced *PP2A* RNA is shown in green. Scale Bar =10 µm.

5.6 Discussion

The ability to quantify RNA at the cellular level has led to a greater understanding of transcriptional regulation in many organisms (Castelnuovo et al., 2013, Neuert et al., 2013, Yang et al., 2014, Ji et al., 2013). The results presented in this chapter confirm that smFISH can now also be used to analyse transcript behaviour in *A. thaliana*. Analysis of the housekeeping gene *PP2A* revealed significant cell-to-cell variability with the number of transcripts per cell found to span one order of magnitude. There was also evidence that steady state mRNA levels are maintained by high levels of transcription (Figure 5.8).

There are many advantages associated with using this single cell approach to quantify RNA. Not only does smFISH greatly improve the resolution offered compared to standard plant RNA *in situs*, it is also much faster than the traditional wax embedding and sectioning process (Drea et al., 2009). Report of a shorter version of this method, termed turboFISH, indicates that five minutes of hybridization followed by a three minute wash can be sufficient to produce images suitable for RNA quantification (Shaffer et al., 2013). It is likely that this protocol could also be shortened considerably; indeed reducing the hybridization step to 3 hours did not compromise *PP2A* signal intensity (data not shown). But a typical experiment requires 5 hours to image ~400 cells, so it was more convenient to split the protocol over two days.

Indication of gene activity at a cellular resolution is typically achieved in plants by generating transgenic lines that contain protein-fusion constructs. However smFISH provides an insight into gene transcription from an endogenous locus and avoids misleading results that could be caused by random gene insertions in transgenic lines (Levesque and Raj 2013). Furthermore, sequence conservation between accessions means that one probe set can be used to determine natural variation in endogenous expression, although introns and exon lengths ultimately determine the suitability of genes for ice or smFISH respectively.

In addition to quantifying mRNA and visualizing active sites of transcription at the single cell level, adapted probe sets have also been shown to successfully identify RNA derived from maternal and paternal gene copies that differ in as little as 12

base pairs (Hansen et al., 2013). Furthermore, combining targeted probe sets with masking oligonucleotides make it possible to detect RNA transcripts that differ by only a single nucleotide (Levesque et al., 2013). In addition to these applications, smFISH has also been used to detect and analyze the regulatory role of long non-coding RNA (Maamar et al., 2013). Adaptation of smFISH for use in *A. thaliana* now opens up these exciting possibilities to members of the plant research community.

5.7 Materials and Methods

5.7.1 Plant Growth Conditions

Columbia (Col-0) seeds were sown onto MS media minus glucose in 10cm square plates (Sterilin Ltd, Cheshire, UK) and stratified for 3 days at 5°C. They were then transferred to a growth cabinet (Sanyo MLR-351) with the following settings: 16h light: 8h dark, 100µmol m^{-2} s^{-1}, 22°C ± 1°C.

5.7.2 smFISH Protocol

N.B. Details of reagents highlighted in bold are listed at the end of the protocol.

Seedlings were removed from the media and the root tips were cut using a razor blade and placed into glass wells containing **4% paraformaldehyde** and fixed for 15 minutes. They were then removed and washed twice with nuclease free 1X PBS (Thermo Scientific, Lutterworth, UK). Three roots were then arranged on each Poly-L-Lysine slide (Thermo Scientific, Lutterworth, UK) and covered by 22mm x 22mm No.1 glass coverslips (Slaughter, Uppminster, UK). The meristems were then squashed before each slide was submerged (together with the coverslip) for 10 seconds in liquid nitrogen. The coverslips were then flipped off the slides using a razor blade and the roots left to dry at room temperature for 30 minutes.

Tissue permeabilization was achieved by immersing the samples in 70% ethanol for one hour. The ethanol was then left to evaporate away at room temperature for 5 minutes before two washes were carried out with **wash buffer**, each wash was left on for 2 minutes.100µl of **hybridization buffer** containing probes at a final concentration of 250nM was then added to each slide. Coverslips (Slaughter, Uppminster, UK) were carefully laid over the samples to prevent the evaporation of the buffer and the probes were left to hybridize at 37°C overnight in the dark.

Unbound probes were pipetted off in the morning. Each sample was washed twice with **wash buffer** with the second wash left to incubate for 30 minutes at 37°C. 100µL of the nuclear stain **DAPI** was then added to each slide and left to incubate at 37°C for 30 minutes. The **DAPI** was removed and 100µl **2xSSC** was added and then removed. 100µL **GLOX buffer minus enzymes** was added to the samples and left to equilibrate for 2 minutes. This was removed and replaced with 100µL of **GLOX buffer containing enzymes**. The samples were then covered by 22mm x 22mm

No.1 coverslips (Slaughter, Uppminster, UK), sealed with nail varnish and immediately imaged.

5.7.3 Reagent preparation

4% Paraformaldehyde (50mL)

150µL 1M NaOH was dissolved in 25mL H_2O in a 100ml glass beaker before the addition of 2g prilled paraformaldehyde pellets. The solution was heated to 60°C and stirred continuously until the pellets fully dissolved. The beaker was then removed from the heat before 25mL 2 x PBS was added. ~50µl 1M H_2SO_4 was then also added to bring the pH up to pH7. The final solution was immediately chilled on ice until before being aliquoted and stored at -20°C.

2X Saline-Sodium Citrate (SSC) (20mL)

2mL nuclease free 20 X SSC (Thermo Fisher Scientific, Paisley, UK) diluted up to final volume of 20mL with nuclease free water (Qiagen, Manchester, UK).

Hybridization Buffer (10mL)

Final composition: 100mg/mL dextran sulfate and 10% formamide in 2X SSC

1g dextran sulfate (Sigma-Aldrich, St Louis, USA) was dissolved in 1mL nuclease free 20X SCC, 1mL deionized formamide (Thermo Fisher Scientific, Paisley, UK) and nuclease free water up to 10mL final volume.

Wash Buffer (50mL)

Final composition: 10% formamide in 2X SSC

5mL nuclease free 20X SSC mixed with 5mL nuclease free deionized formamide and nuclease free water up to 50mL final volume.

Nuclear stain: 4',6-diaidino-2-phenylindole (DAPI) (20mL)

Final composition 50ng/µL of 10% formamide in 2X SSC

1mg DAPI dissolved in 20mL wash buffer

Anti-fade GLOX buffer minus enzymes (1mL)

Final composition: 0.4%glucose in 10nM Tris, 2X SCC

40µL 10% glucose in nuclease-free water, 10µL 1M Tris-HCl, pH 8.0 (Thermo Fisher Scientific, Paisley, UK) and 100µL 20X SCC was mixed with 850µL nuclease-free water.

Anti-fade GLOX buffer plus enzymes (100µL)

1µL glucose oxidase stock (3.7mg/mL in 50nM sodium acetate, pH5 (Sigma-Aldrich, St Louis, USA) and 1µL mildy vortexed catalase suspension added to 100µL GLOX minus enzyme solution.

5.7.4 Imaging

A Zeiss Elyra PS1 inverted super-resolution microscope was used for imaging. A 100x oil-immersion objective (1.46NA) and cooled EM-CCD Andor ixon 897 camera (512 x 512 QE >90%) was used to obtain all images in the standard, rather than super-resolution mode. A 561nm laser was used to excite Quasar 570 probes and emission signals were detected between 570-640nm. A 642nm laser was used to excite Quasar 670 probes and emission signals were detected between 655-710nm. A 405nm laser was used to excite the DAPI and signals were detected between 420-480nm. A series of ~ 30 of 0.2µm z-steps were collected for each sample.

5.7.4 smFISH Image analysis

The image analysis pipeline was created by Dr Matthew Hartley and Dr Tjelvar Olsson to find probe locations and generate counts on detected probes per cell. The pipeline uses code written specifically for the task of using the numerical Python libraries (van der Walt et al., 2011) and the Python image processing library scikit-image (van der Walt et al., 2014).

Splitting the confocal image into channels

Bioformats (Linkert et al., 2010) was used to separate the confocal images and generate a z-stack for each channel.

Finding seeds from nuclei

From the DAPI channel z-stack the image intensity was normalized for each image in the stack before generating a maximum intensity projection. Contrast Limited Adaptive Histogram Equalization (CLAHE) (Pizer et al., 1987) was then used to adjust intensities across the image. A Sorbel filter was used to find edges in the image, and Otsu's thresholding was used to find positions of the nuclei. The centroid of each detected nucleus was then used as a seed for segmentation.

Cell Segmentation

A minimum intensity projection of the probe channel was used to capture the cell's autofluorescence and CLAHE was used to adjust the intensity across the image. A Gaussian filter was used for smoothing and a Watershed algorithm was used with the seeds derived from the nuclear positions to segment the image.

Locating probe molecules

To locate the probe signals each image was normalized in the probe channel z-stack then a maximum intensity projection was taken and a Sobel filter used to find edges within the projection. A small disk shaped element (of a size appropriate to the diffraction radius of the confocal microscope used to take the image) was then used to apply fast, normalized cross-correlation based template matching. The best match located at this stage is then used as a template to repeat the matching process and determine probe locations within the image.

Generating an annotated image

Cell segmentation is then combined with the probe locations to generate an annotated image showing outlined cells, a label for each cell centroid and a count to number of probes detected within each cell.

Chapter 6 – Using smFISH to analyse transcriptional regulation during vernalization

Division of work: Tjevlar Olsson and Matthew Hartley created the image analysis programme used to quantify mRNA (see Chapter 5 materials and methods) and Stefanie Rosa helped with sample preparation.

6.1 Introduction

The natural variation observed in the length of cold requirement among Arabidopsis accessions suggests that variability exists in how plants measure cold duration. This type of measurement requires a quantitative memory system that can withstand high rates of histone turnover and multiple rounds of cell division (Dodd et al 2007; Angel et al., 2011; Angel et al., 2015; Satake 2012). A combination of modeling and experimental validation have shown that memory of vernalization is achieved by stochastic digital switching of epigenetic states at *FLC* with the proportion of stably silenced cells provides a biological measure of cold exposure (Yang et al., 2014; Angel et al., 2010; Satake 2012; Angel et al., 2015).

Single molecule RNA FISH (smFISH) is an ideal method to complement other experimental strategies for analysis of the cell-autonomous epigenetic switching at *FLC* (Angel et al., 2011; Angel et al., 2015, Berry et al., 2015). My aim was to use smFISH to improve our understanding of cold perception and epigenetic memory and obtain data for modelling the integration of complex temperature cues.

The questions addressed in this chapter using smFISH are:

- How do *FLC* transcription and mRNA levels change during cold?
- Can sense and antisense *FLC* transcription occur in the same cell?
- Does cold-induced *VIN3* expression reflect high transcription in a small population of cells or low transcription in all cells?
- Does transcriptional reactivation of Lov-1 *FLC* alleles occur in a small population of cells or in all cells after a partial cold treatment?

6.3 Determining cell-to-cell variation of *FLC* mRNA during vernalization

FLC mRNA molecules were visualized using at set of 38 probes designed to be complementary to RNA derived from exonic sequences (Figure 6.1A, Appendix Table 5). An automated image analysis pipeline was then used to quantify the number of transcripts within each cell (see Chapter 5, Figure 5.7 and Chapter 5 Materials and Methods section).

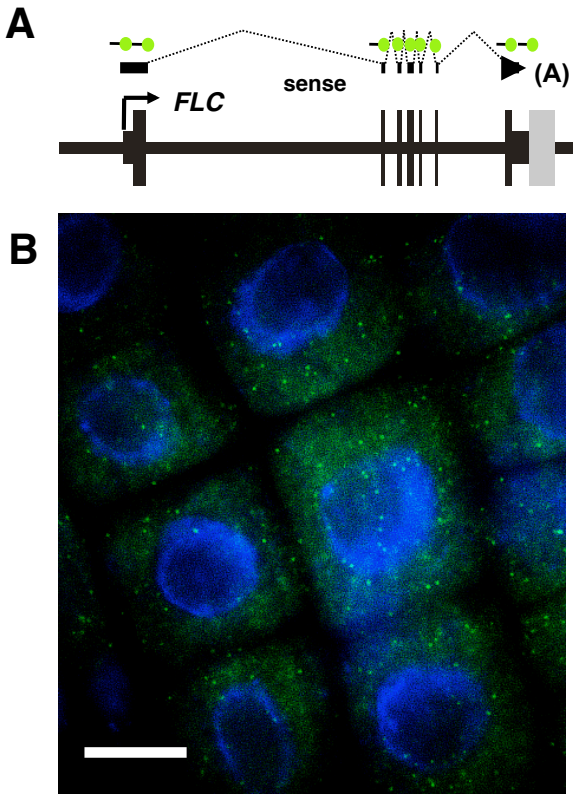

Figure 6.1 - Visualizing *FLC* mRNA in Col*FRI*^{Sf2} meristematic cells
(A) A diagrammatic representation showing probe binding sites within *FLC* exons. **(B)** Representative maximum projected image showing *FLC* mRNA detected in non-vernalized Col*FRI*^{Sf2} cells using a Quasar 670 probes. Scale bar = 10μm.

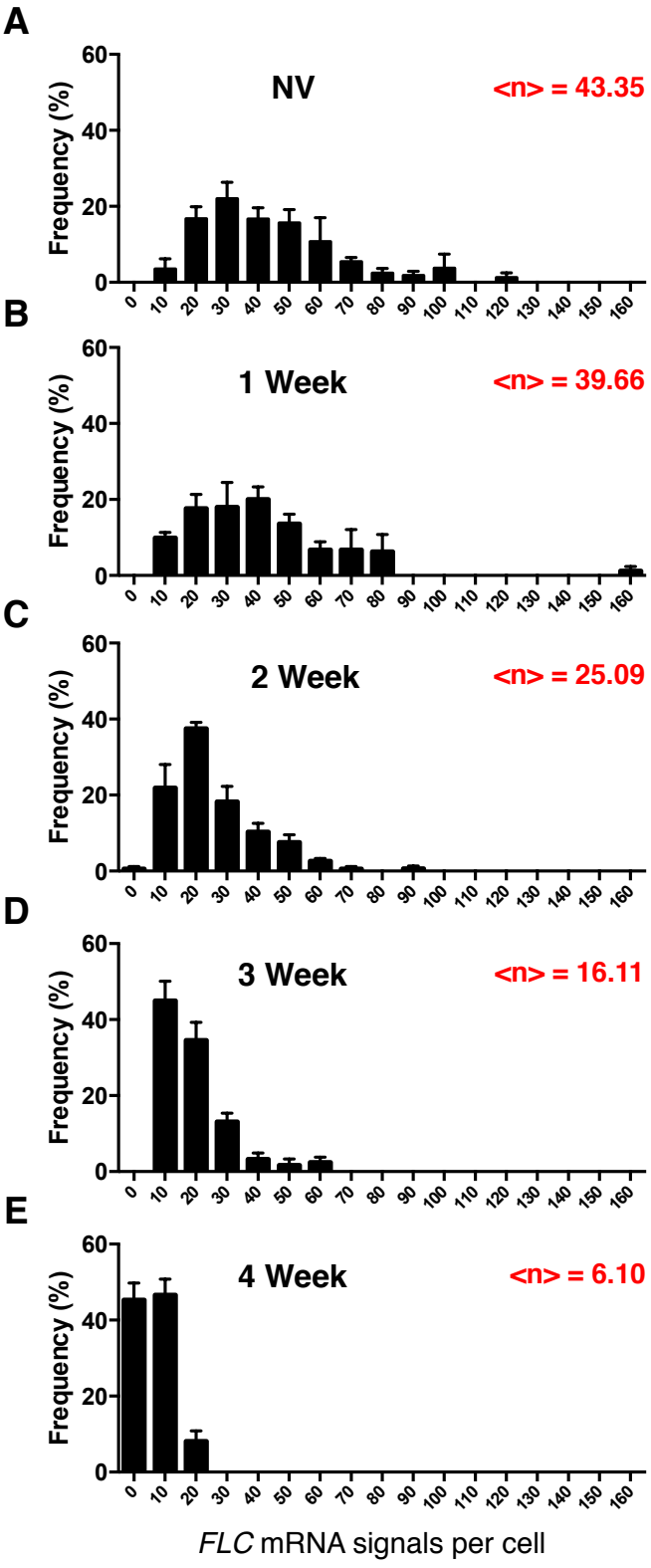

Figure 6.2 - *FLC* mRNA levels decrease in a graded manner during vernalization in Col*FRI*^{Sf2} meristematic cells

(A) Frequency of *FLC* mRNA per cell determined in non-vernalized plants before cold then after 1 **(B)**, 2 **(C)**, 3 **(D)**, and 4 **(E)** weeks of cold exposure. NV = non-vernalized. <n> = mean mRNA signals per cell. Error bars = SEM, *n*=3.

Cell-to-cell variation was revealed in non-vernalized samples with an average of 43 *FLC* mRNAs per cell calculated from a range that extended from 6 to 125 molecules per cell (Figure 6.2A). Both the mean and the dynamic range of *FLC* mRNA reduced during 4 weeks cold exposure (Figure 6.2B-E), but there was clear evidence of *PP2A* transcription and abundant *PP2A* mRNA even after eight weeks vernalization (Figure 6.3).

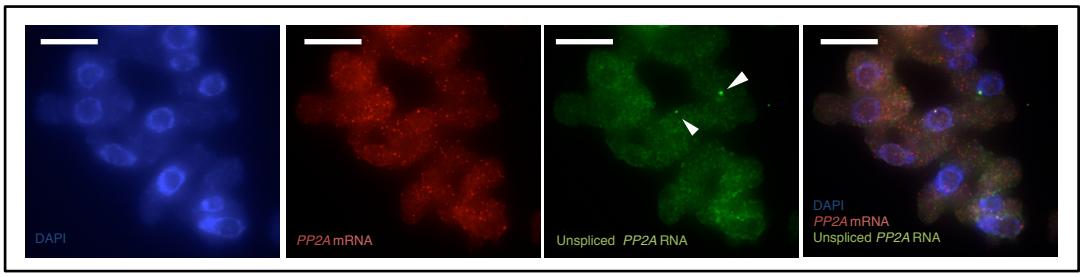

Figure 6.3 – *PP2A* mRNA detected after eight weeks cold exposure
Representative maximum projection image of cells hybridized with probe sets complimentary to *PP2A* mRNA (Quasar 570) and *PP2A* unspliced RNA (Quasar 670). White arrows indicate putative sites of *PP2A* transcription. Scale bars = 10µm.

Previous experiments had suggested that *FLC* transcripts have a long-half life in the cold (Csorba et al., 2014). There is evidence that environmental stress can result in certain transcripts being protected from RNA decay pathways and stored for future translation in processing bodies (P-bodies) (Brengues et al., 2005). We considered smFISH to be an ideal technique to monitor changes in cell-to-cell variation of *FLC* mRNA and determine whether *FLC* transcripts are found within specific particles/compartments during vernalization. However, contrary to this hypothesis, no evidence was found of *FLC* mRNA localization either before or during vernalization (Figure 6.1 and Figure 6.4).

Co-ordinated sense and antisense *FLC* transcription is a rare event

COOLAIR transcription peaks after ~2 weeks of cold exposure (Swiezewski et al., 2010). Loss of *COOLAIR* attenuates the cold-induced transcriptional repression of *FLC* (Csorba et al., 2014). This raises the question of whether *COOLAIR* transcription is the cause of the reduction in *FLC* transcription, potentially either through transcriptional interference or an RNAi-type mechanism. Both mechanisms would require sense and antisense transcription from the same locus. With this question in mind smFISH probes were designed to enable sense and antisense

transcripts to be visualized in both nascent and spliced forms (Figure 6.5, Appendix Tables 6-8).

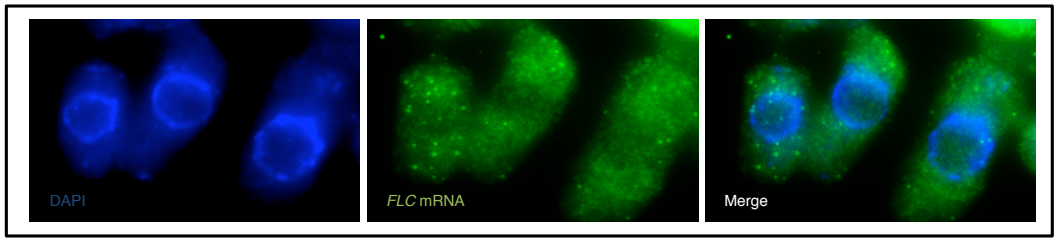

Figure 6.4 – *FLC* mRNA detected after three weeks cold exposure
Representative maximum projection image showing cells labeled with Quasar 670 probes complimentary to *FLC* mRNA

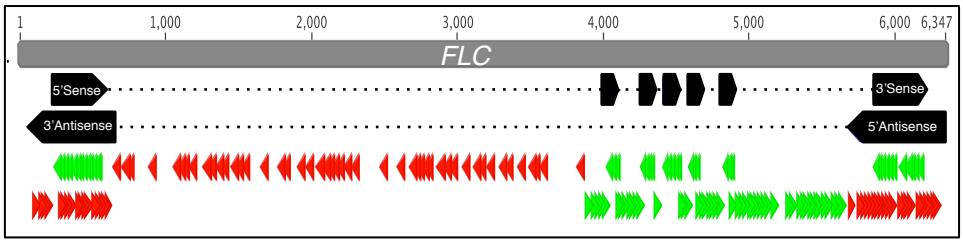

Figure 6.5 - Multiplexed smFISH probe sets used to simultaneously detect sense and antisense *FLC* RNA
Binding sites are shown for four probe sets. Together they enable spliced and unspliced sense *FLC*, spliced and unspliced antisense *FLC* transcripts to be visualized.

Analysis of nascent RNA FISH showed that >70% of cells express *FLC* before cold (Figure 6.6D). This drops to around 1 in 5 cells after one week of cold exposure and to around 1 in 10 after three weeks. In agreement with role of antisense *FLC* transcripts modulating sense transcription in the autonomous pathway (Ietswaart et al., 2012) low levels of nascent *COOLAIR* RNA were detected before vernalization (Figure 6.6A, D). As anticipated, an increase in the frequency of cells expressing antisense transcription was observed during cold exposure with a peak of ~25% occurring at the two week time point (Figure 6.6D).

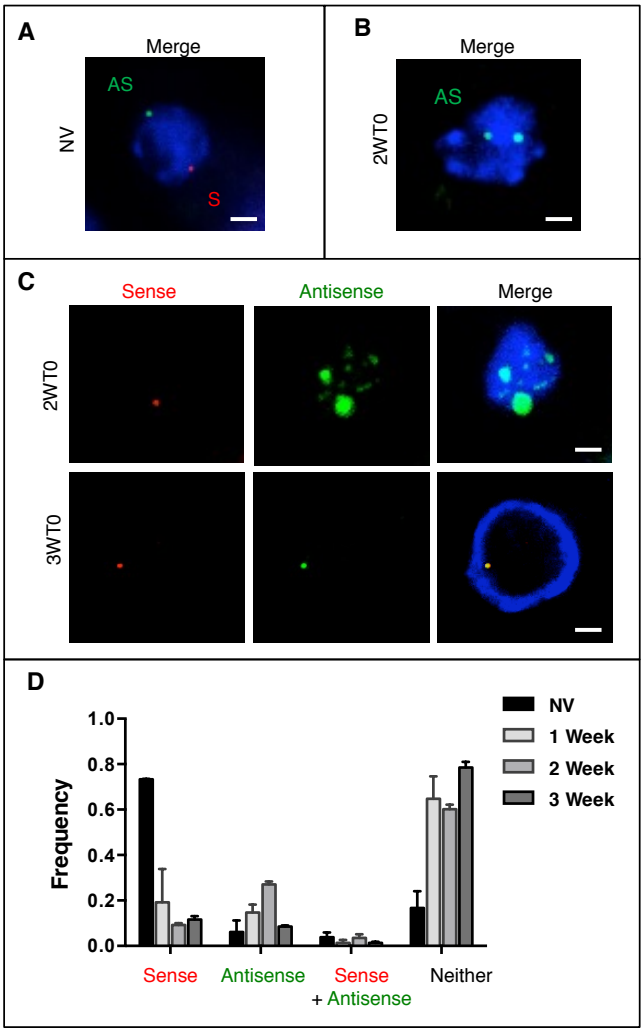

Figure 6.6 - *FLC* Sense and Antisense transcription occurs rarely in the same cell

(A) Unspliced sense (S, red) and antisense (AS, green) transcripts detected in non-vernalized samples. **(B)** Antisense transcripts detected using a spliced antisense probe set (green). **(C)** Representative maximum projected images of unspliced sense and antisense transcript signals detected after 2 weeks (2WT0) and 3 weeks (3WT0) cold. **(D)** Quantification of transcriptionally active cells from data obtained using multiplexed nascent sense and antisense *FLC* probe sets. Blue = DAPI, nuclear stain. NV = non-vernalized. Scale bars = 10μm. Error bars = SEM. *n*=3.

A low probability of simultaneous sense and antisense *FLC* transcription was evident both before cold and this probability did not increase during vernalization (Figure 6.6D). This finding does not support an RNAi-type mechanism and reinforces custom tiling array data that suggested antisense transcriptional interference is unlikely to be the primary mechanism reducing sense transcription because complimentary RNA transcripts are rarely exist in the same cell (Swiezewski et al., 2010; Csorba et al., 2014).

In addition to the probes used to detect nascent antisense transcripts, another set was designed to detect spliced antisense mRNA. A set consisting of 48 probes is recommended for optimal detection of target RNA, but the length of the different spliced *COOLAIR* isoforms prevented each of them being targeted specifically.

To maximise probe occupancy on each transcript, a set containing 37 probes was designed to be complimentary to all *COOLAIR* exons. It is unlikely that 20 probes would be produce sufficient signal for detection of the shorter proximal isoform, so essentially distal transcripts were being targeted that include all exons. (Figure 6.5). Cell fractionation assays have previously suggested that antisense transcripts are efficiently transported into the cytoplasm (Csorba et al., 2014), however signals from this spliced probe set were only ever detected in the nucleus (Figure 6.4B). The number, size and intensity of these signals suggested that these probes were binding nascent transcripts still attached to the locus.

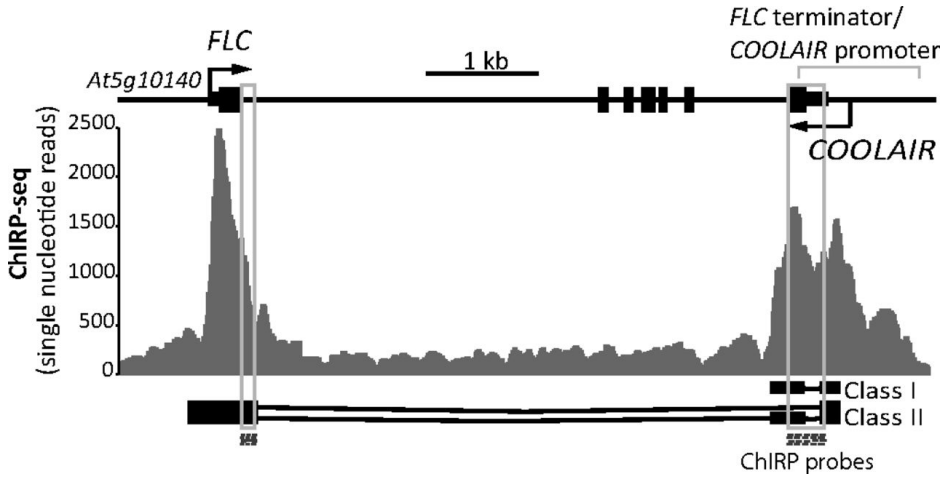

Figure 6.7 - *COOLAIR* associates *in cis* with *FLC* chromatin.
ChIRP deep sequencing analysis data shows *COOLAIR* associates with *FLC* chromatin in two distinct regions. Locations of biotinylated DNA probes used for *COOLAIR* ChIRP are shown (dashed boxes). A schematic of the *FLC* locus is shown with the structure of the class I and class II *COOLAIR* transcripts. This figure was reproduced from Csorba et al., 2014.

During the peak of *COOLAIR* transcription, multiple foci with increased signal size were observed in many cells (Figure 6.6C). They were found to accumulate transiently and were only ever observed after two weeks of cold exposure. These are likely to include sites of high antisense transcriptional activity; consistent with this at least one of the foci co-localized with a nascent sense *FLC* transcript signal (Figure 6.6C), but two foci could also represent the nuclear loci identified by Chromatin Isolation by RNA Purification (ChIRP), where antisense *FLC* transcripts were shown to physically associate with specific chromatin at *FLC* (Csorba et al., 2014, see Figure 6.7). A more intriguing explanation is that these foci represent nuclear paraspeckles. These are RNA/protein nuclear bodies that have been shown to sequestrate specific regulatory proteins to regulate gene expression in other organisms (Kawagutchi et al., 2015; Hirose et al., 2014).

6.5 *VIN3* induction occurs in a graded manner during vernalization

VIN3 induction is an important cold-dependent step central to the vernalization mechanism (De Lucia et al., 2008). We were interested in the dynamics of the cold-induction of *VIN3.* RT-qPCR assays show *VIN3* transcription gradually increases during vernalization (Sung and Amasino 2004, Figure 6.8A, also see Chapter 2, Figure 2.3). This pattern could arise from two alternatives (see Figure 6.8B): Graded Induction, a homogeneous rise of the transcription level in all cells or Digital Induction, a population of cells that express *VIN3* at high levels, whose fraction increases over time.

Signals from transgenic plants carrying a *VIN3*::*GFP* transgene after 8 weeks of cold suggest that highest levels of expression occur in the root apical meristem and lateral roots (data not shown). These results were also confirmed by immunocytochemistry using anti-GFP and secondary antibodies conjugated to fluorophores (data not shown), but autofluorescence levels inhibited both direct and indirect methods of protein detection after shorter cold periods. We therefore used smFISH to provide the molecular resolution required to establish whether *VIN3* up-regulation was graded or digital.

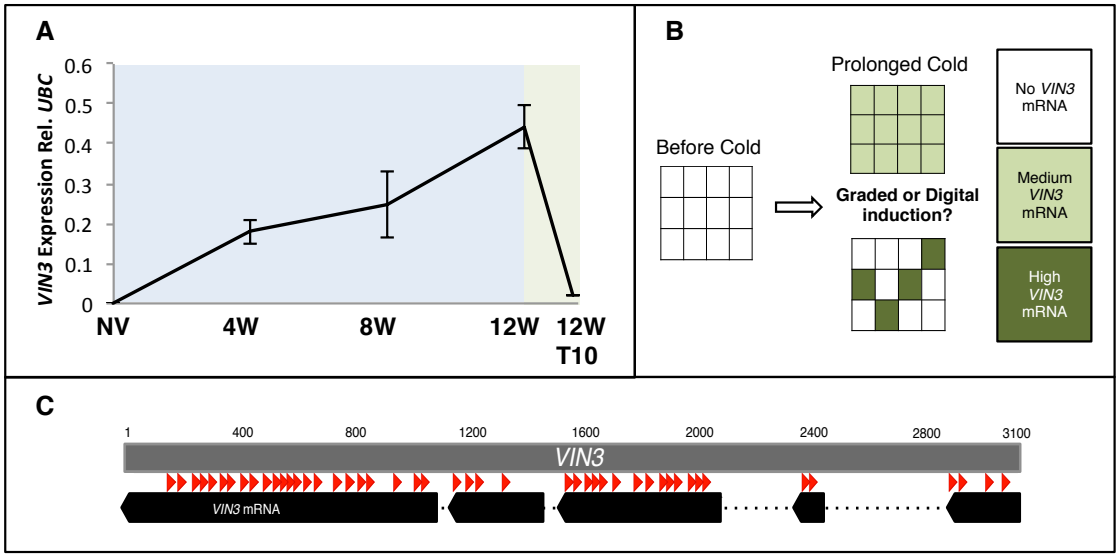

Figure 6.8 – Induction of *VIN3* mRNA can be equally explained by graded or digital increases
(A) Quantitative PCR results for *VIN3* expression determined before, during and after cold. **(B)** A diagram presenting two hypotheses to explain *VIN3* induction. **(C)** Binding sites of smFISH probes used to visualize *VIN3* mRNA. Error bars = ±SEM. *n*=3.

Consistent with RT-qPCR assays, FISH signals from a set of 48 *VIN3* mRNA probes (Figure 6.8C and Appendix Table 9) were first detected after two weeks of cold (Figure 6.9B and C). The average number of transcripts per cell increased over time (Figure 6.9A and B), supporting a graded induction during cold exposure. This was further supported by the presence of *VIN3* mRNA in 93%, 95% and 97% of cells after 2, 5, and 8 weeks of vernalization (Figure 6.9C).

6.6 Post-cold reactivation of Lov-1 *FLC* occurs in a digital manner

Previous work had shown that after non-saturating vernalization *FLC* re-activated in a proportion of cells after transfer of plants back to warm conditions (Angel et al., 2010). This result helped to demonstrate that memory of cold is achieved through the cell-autonomous silencing of *FLC* (Angel et al., 2010). This experiment used the Col *FLC* allele, which is classified as a rapid-vernalizing *FLC* haplotype (Li et al., 2015). I wanted to analyse the pattern of *FLC* re-activation in a slow-vernalizing haplotype and selected the Lov-1 allele. Four SNPs at the 5' end of the gene distinguish the Lov-1 and Col *FLC* alleles with respect to how much cold is required for full

epigenetic silencing (Coustham et al., 2012). RT-qPCR data shows Lov-1 *FLC* transcription is reduced to a similar level to Col *FLC* after 4 weeks cold (Figure 6.10A), however, the Lov-1 *FLC* allele reactivates to pre-vernalized levels after a further 30d growth in the warm (Figure 6.10A, also see Shindo et al., 2006 and Coustham et al., 2012). This re-activation is associated with a drop in H3K27me3 and an increase in H3K36me3 over the *FLC* gene body (J. Questa pers. comm.).

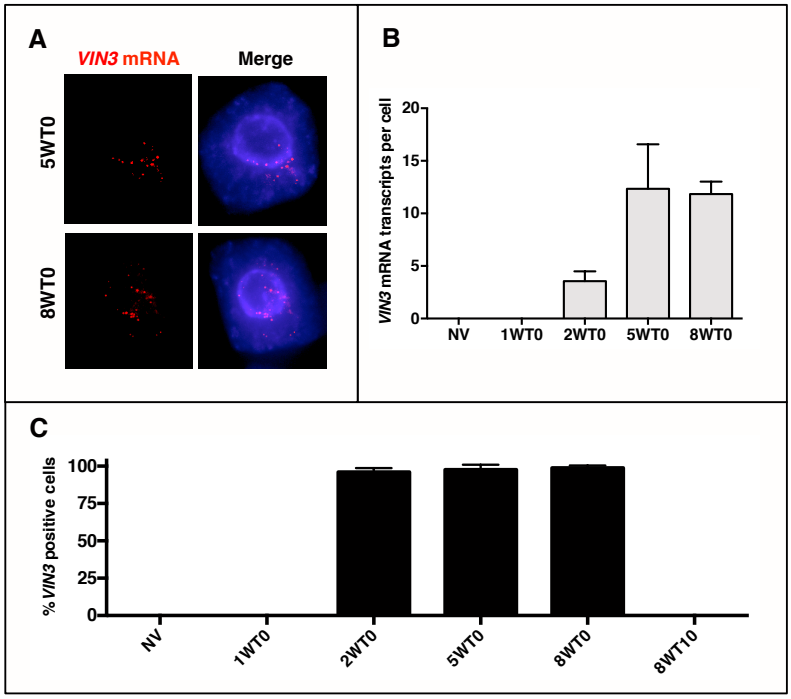

Figure 6.9 – Graded induction of *VIN3* mRNA
(A) Representative images of *VIN3* mRNA cellular distribution. **(B)** Quantification of *VIN3* mRNA per cell and **(C)** frequency of *VIN3* mRNA positive cells. NV = Non-Vernalized, W = weeks cold exposure and T= days post-cold growth. Error bars = SD, *n*=3.

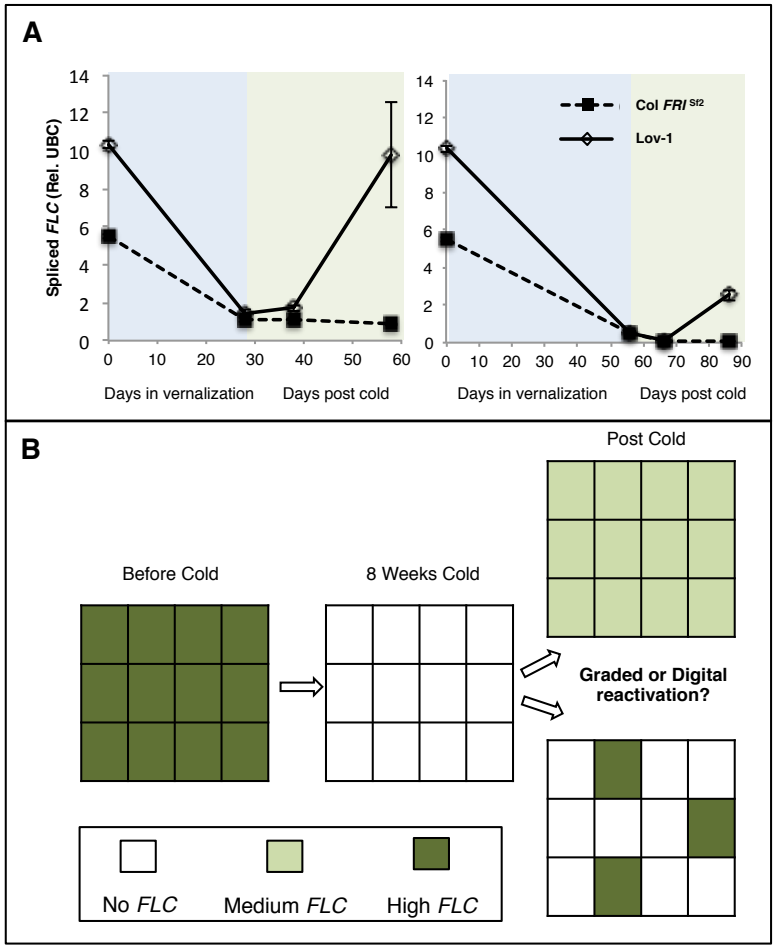

Figure 6.10 – Reactivation of *FLC* transcription in Lov-1 can be equally explained by graded or digital increases
(A) Quantitative PCR data showing *FLC* expression of Col*FRI*^{Sf2} and Lov-1 after four and eight weeks cold treatment. **(B)** Schematic diagram showing potential hypotheses that explain the basis of Lov-1 *FLC* reactivation. Error bars = SEM, *n*=3.

The extent of reactivation observed for Lov-1 after four weeks cold suggests that memory loss occurs for almost all cells across the population. But the lower reactivation apparent for Lov-1 after 8 weeks cold (Figure 6.10A) allows two hypotheses to be tested using smFISH. Graded reactivation of *FLC* would produce images with low numbers of mRNA observed in a high proportion of cells and digital reactivation would produce images with high transcript numbers occurring in a small subset of cells (see Figure 6.10B). Results shown in Figure 6.11 support the second hypothesis of digital reactivation since only a small number of cells were found to contain *FLC* mRNA molecules following eight weeks vernalization. “On” cells were

found to either exist alone or in small patches that were consistent with ongoing propagation of the “on” state through division of a founder cell (Figure 6.11A).

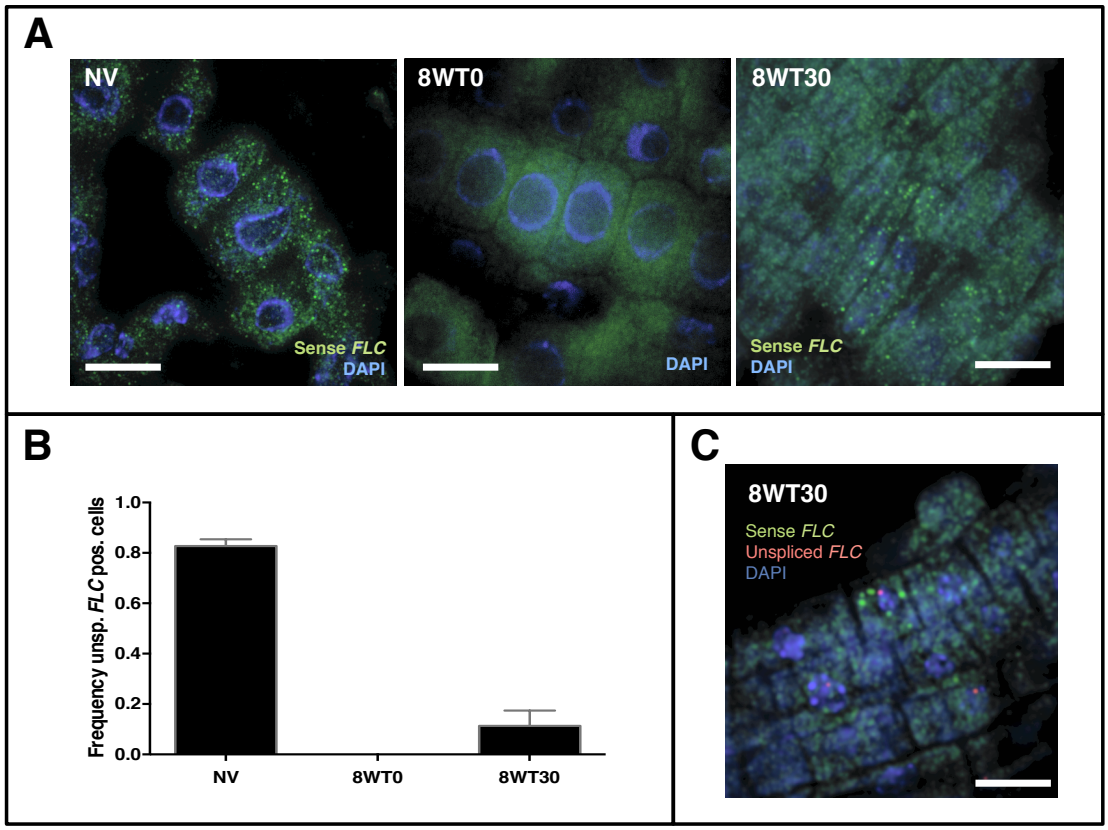

6.11 – Digital reactivation of Lov-1 *FLC*
(A) Representative maximum projected images showing *FLC* mRNA before cold, after 8 weeks vernalization and after 30 days growth in warm conditions. **(B)** Quantification of cells containing unspliced *FLC* signals before, after 8 weeks vernalization and 30 days after return to warm conditions. **(C)** Representative maximum *Z*-projected image showing Lov-1 *FLC* reactivation. Scale bar = 10μm. NV = Non-Vernalized, W = weeks cold exposure and T = days of post-cold growth. Error bars = SEM, *n*=3.

6.7 Discussion

Results of techniques such as RT-qPCR and ChIP average across large populations of cells so fail to reveal specific spatial regulation important for vernalization, or whether quantitative changes in expression are through a graded or digital mechanism. These issues are important in order to dissect how genetic variation can change perception and memory of cold exposure.

During the first two weeks of vernalization, in addition to an upregulation of *COOLAIR*, cold temperatures may induce thermodynamic re-organization of the DNA polymer that favours shutdown of *FLC* transcription (Helliwell 2015). Consistent with the theory, smFISH analysis found no evidence of *VIN3* induction but confirmed a significant reduction in *FLC* transcription after only two weeks of cold exposure (Figure 6.2). This reduction, in combination with the relatively long half-life observed for *FLC* mRNA, (Figure 6.2D; Csorba et al., 2014) effectively ensures that a reserve supply of mRNA is maintained whilst permitting the transcriptional shutdown required for effective epigenetic silencing. In a natural context, this mechanism might have evolved to help prevent precocious flowering in the event of a temperature rise after exposure to a short period of cold.

Alternative spliced forms of antisense *FLC* RNA contribute to the starting level of *FLC* transcription in non-vernalized plants (Li et al., 2015; Ietswaart et al., 2013). In addition, antisense upregulation during the early stages of cold facilitates a reduction in sense transcription and mediates the switching of active to repressive chromatin marks (Csorba et al., 2014). The question of whether sense and antisense *FLC* transcripts exist in the same cell is fundamental to gaining mechanistic understanding of these diverse functions. A transcriptional interference mechanism was not supported by either smFISH or customtiled-array data (Figure 6.6; Swiezewski et al., 2009). Instead it suggests a system analogous to that reported for the *PHO84* locus in yeast where sense and antisense transcripts are rarely found in the same cell (Castelnuovo et al., 2013).

Csorba and colleagues reported results from ChIRP assays that showed antisense *FLC* RNA located at both the sense and antisense promoter regions of the *FLC* locus after two weeks of cold (see Figure 6.7 taken from Csorba et al., 2014). The observation of several antisense nuclear foci after two weeks cold, some of which co-localized with nascent sense *FLC* transcripts (Figure 6.6) is consistent with an "ON" chromatin role predicted for *COOLAIR*. The idea that the other large foci might represent paraspeckles is an intriguing possibility. Recent data has shown that both the long non-coding RNA *NEAT1* and the SWI/SNF chromatin-remodelling complex are required for formation of ribonucleoprotein subnuclear complexes known as paraspeckles (Kawaguchi et al., 2015). These bodies have previously been shown to regulate the expression of genes within developmental and stress related pathways via the sequestration of specific protein(s) and RNAs (Prasanth et al., 2005; Hirose et al., 2014; Imamura et al., 2014). Consistent with my observations for *COOLAIR*, it is the nascent *NEAT1_2* RNA transcript, rather than the spliced and polyadenylated *NEAT1_1* isoform that is incorporated within these foci. A recent report has also shown that the *A. thaliana* SWI/SNF subunit BAF60 is required for the maintenance of a 5'-3' gene loop that exists at *FLC* before cold (Jegu et al., 2014). This loop is lost after around two weeks of cold exposure and is thought to be an early step in the switch from an expressed to an epigenetically silenced state (Crevillen et al., 2013; Zhu et al., 2014). The coincidence of *COOLAIR* foci with maximal loop disruption suggests a potential mechanism where *COOLAIR* acts to sequester BAF60 into paraspeckles to relieve loop maintenance. Experiments to determine co-localization of the observed *COOLAIR* foci with BAF60 and conserved paraspeckle proteins would be the first step to test this intriguing hypothesis.

VIN3 induction is vital to the vernalization process as this protein is required for deposition of silencing chromatin marks at *FLC* during cold (De Lucia et al., 2008). smFISH images showed that *VIN3* transcription is initiated at a low level in almost all cells and that transcript levels increase over time (Figure 6.9). The finding that *VIN3* transcription occurs in this graded manner rules it out as a digital signal that could contribute to quantitative changes in cell-autonomous silencing. However, the unusual predominance of *VIN3* mRNA within the nucleus perhaps reflects a barrier to export that might act as a rate-limiting step during vernalization. This might also explain the difficulties associated with detecting GFP signals in VIN3 reporter lines.

Consistent with the theory that it is the cell-autonomous silencing of *FLC* expression that is central to the quantitative nature of vernalization, smFISH results confirmed digital post-cold reactivation of the Lov-1 *FLC* allele (Figure 6.11). Furthermore, evidence of transcriptional activity (intronic probe signals) in the absence of spliced *FLC* mRNA suggested that unproductive transcription may precede full reactivation (Figure 6.11C). These results are likely to direct future experiments aiming to dissect the complex interplay between non-coding gene sequence and epigenetic stability.

In this chapter, smFISH has been demonstrated as a powerful approach to determine transcriptional changes of key vernalization genes during cold. Together, these data provide a unique insight into the molecular basis of cold perception and epigenetic memory at the cellular level.

6.8 Materials and Methods

6.8.1 Plant growth conditions

Col*FRI*^{Sf2} seeds were sown on MS media (minus glucose) in 10cm square plates (Sterilin Ltd, Cheshire, UK) and stratified for 3 days at 5°C before being transferred to a growth cabinet (Sanyo MLR-351, 16h light: 8h dark, 100µmol m^{-2} s^{-1}, 22°C ± 1°C) for seven days pre-growth. They were then transferred to a walk-in vernalization chamber set at 5°C, 70% ± ≤10% RH, 8h light: 16h dark, 30µmol m^{-2} s^{-1}. For post-cold assays plants were returned to a growth cabinet (Sanyo MLR-351, 16h light: 8h dark, 100µmol m^{-2} s^{-1}, 22°C ± 1°C, 100µmol m^{-2} s^{-1}, 22°C ± 2°C) before sampling.

6.8.2 RNA extraction

See Chapter 2 Materials and Methods section 2.10.2.

6.8.3 Reverse Transcription (RT)

See Chapter 3 section Materials and Methods section 2.10.3.

6.8.4 Quantitative Polymerase Chain Reaction (qPCR)

See Chapter 3 section Materials and Methods section 2.10.4 Expression levels were determined using Roche Universal Probe Library (UPL) Probes and the primers shown below.

***FLC* (At5g10140)**	
sFLC_UPL_#65_F	5'-gtgggatcaaatgtcaaaaatg-3'
sFLC_UPL_#65_R	5'-ggagagggcagtctcaaggt-3'
UPL #65	5'-ctggagga-3'

***VIN3* (At5g57380)**	
VIN3_UPL_#67_F	5'-cgcgtattgcggtaaagataa-3'
VIN3_UPL_#67_R	5'–tctctttcgccaccttcact-3'
UPL #67	5'-ctccagca-3'

***UBC* (At5g25760)**	
UBC_UPL_#9_F	5'-tcctcttaactgcgactcagg-3'
UBC_UPL_#9_R	5'-gcgaggcgtgtatacatttg-3'
UPL#9	5'-tggtgatg-3'

Gene expression was calculated relative to *UBC* levels using the comparative Ct method (also known as the 2-[delta][delta]Ct method) (Schmittgen and Livak 2008) and statistical analysis of was performed using GraphPad Prism version 6 software for Mac (La Jolla, California, USA).

6.8.5 smFISH protocol

See Chapter 5 Material and Methods sections 5.7.2 and 5.7.3.

6.8.6 smFISH image analysis

See Chapter 5 Material and Methods sections 5.7.4.

Chapter 7 - Discussion

6.1 Introduction

The ability of plants to align reproduction with favourable environmental conditions is key for survival as this is thought to maximise fitness potential. The impact of recent climate change on plant phenology has been well documented (e.g. Menzel et al., 2006; Cleland et al., 2007; Miller-Rushing et al., 2008). Although earlier flowering has been reported for most species (Dech and Nosko 2004; Bertin 2008; Gordo and Sanz 2009), there is also evidence that some species have either maintained their flowering dates or have flowered progressively later over the last century (Cook et al. 2010; Fitter and Fitter 2002). Unaltered and late flowering responses have been associated with phylogenetic patterns of species loss. This not only suggests that the ability to shift reproductive timing is shared between related species, but also indicates that advancing phenology is likely to be important for plant survival in the future (Willis et al., 2008).

Winter annual *A. thaliana* populations typically flower early in spring. This is a strategy common in annual herbs that grow at northerly latitudes. Early flowering may be required for a bet-hedging germination strategy where exposure of the mother plant to a specific range of temperatures during seed set ensures that progeny develop with a range of dormancy states (Springthorpe and Penfield 2015). Late flowering would not only disrupt this alignment of reproduction with a specific temperature range but would also increase risks from herbivory and interspecific competition (Rathcke & Lacey 1985; Molau 1996).

The central aim of this thesis was to explore vernalization responses in *A. thaliana* to determine whether climate change might impair vernalization and delay flowering by the end of the century.

6.2 The potential ecological significance of effective vernalizing temperatures

This thesis proposes that an effective vernalization temperature range of (0^{o}C,14^{o}C), combined with an optimal response at 8^{o}C, represents adaptation specifically to

recurrent climate variables at the northerly limit of the *Arabidopsis* range. Field experiments also established that this 8^{o}C optimal response was not necessary for other accession to vernalize during autumn in northern Sweden.

The effective vernalizing temperature range of (0^{o}C, 14oC) is shared by *A. thalinana* accessions with varied vernalization requirements (see Chapter 1 and Wollenburg and Amasino 2012). But contrary to the common perception that vernalization provides plants with memory of winter (Amasino 2004; Song et al., 2013) this range essentially precludes winter vernalization from occurring in many northerly locations where annual snow cover and freezing temperatures are commonplace. This effective temperature range suggests that vernalization is permitted during both winter and spring in many locations across Europe, however for the majority of winter annual accessions that germinate in autumn, average daily temperatures across Europe are likely to remove any *FLC*/*FRI* block to flowering by the end of this season. This is contrary to the view that vernalization has evolved to delay flowering *per se*, instead it suggests that the primary function of this cold requirement is to delay flowering until the temperature and photoperiod have reduced sufficiently to inhibit floral transition until spring. Consistent with this theory, 99.5% reduction in *FLC* mRNA is reported to occur between September and November in natural populations of the semi-perennial species *A. halleri* (Aikawa et al., 2010). The similarity observed between the seasonal timing of vernalization in *A. thaliana* and *A. halleri*, together with the conservation of the effective temperature range, merits experiments in other crop and wild species to explore autumn responses outside the *Arabidopsis* genus. (Chouard et al., 1960; also see Chapter 1, Figure 1.5).

If three out of the four seasons are conducive for vernalization in temperate areas, this suggests that seed dormancy is a key determinant of life history strategy. Indeed, a predominant impact of germination date, rather than vernalization was observed for flowering recorded during a comprehensive *A. thaliana* field experiment. Wilczek and colleagues showed that establishment during autumn was required to reveal the late flowering phenotype associated with a functional *FRI* allele (Wilzcek et al., 2009). Consideration of these results in the context of this thesis suggests that saturated vernalization requirements could account for the small difference observed between Col-0 and Col*FRI*Sf2 flowering dates in spring cohorts. Although this range does not fully explain the responses observed for the plants germinated in summer, it

is possible that any remaining *FRI*/*FLC* block to flowering may have been overridden by an SOS type response triggered by a combination of high fluctuating temperatures and long photoperiods. This theory is consistent with accelerated flowering responses observed for plants grown under high temperature, long day conditions (Seaton et al., 2015; Pose et al., 2013; Lee et al 2013; Kumar et al 2012).

Several field experiments have not observed associations between flowering time and natural genetic variation in well-studied flowering genes (Agren et al., 2013; Brachi et al., 2010; Weinig et al., 2002; Wilzcek et al., 2009). This has led some researchers to question the ecological significance of results from laboratory experiments that are conducted under wholly artificial conditions (Weigel et al., 2012; Shindo et al., 2007; Hoffman et al., 2002). Whilst large-scale field studies will remain the gold standard for determining the genetic basis of adaptive traits, this thesis argues that consideration of laboratory derived data, in the context of climate and life histories, can contribute to understanding of how genetic variation might contribute to fitness at specific locales. Although the analysis of phenotypes in a wide range of accessions enables conclusions to be drawn about the species as a whole, this thesis and other recent work (Springthorpe and Penfield 2015) demonstrate that a pared-down approach in the laboratory can successfully detect small phenotypic differences that have significant fitness and life-cycle implications.

6.3 Exploring the molecular basis of vernalizing temperature effectiveness

This thesis has demonstrated that vernalization responses elicited by naturally fluctuating conditions are equal to those generated by constant temperatures matching the field mean. Furthermore, the optimal vernalizing temperature for one accession was found to match the autumn average. The notion that a long-term averaging mechanism drives the vernalization process under natural conditions is further corroborated by a report by Aikawa and colleagues that showed 6-weeks of preceding temperatures to be required to accurately predict *FLC* levels in *A. halleri* (Aikawa et al., 2010). This type of long-term averaging is likely to have evolved to provide plants with a robust filtering mechanism that prevents short-term temperature fluctuations from triggering precocious flowering.

High-throughput methodologies have recently helped to bridge the gap between molecular biology and ecology in recent years by enabling time-series experiments to be carried out in natural environments (Nagano et al., 2012; Izawa 2012; Richards et al., 2012; Aikawa et al., 2010). This type of *in natura* approach would be ideal to dissect how plants are able to integrate complex temperatures cues in the wild (Kudoh and Nagano 2013). In addition to *FLC* expression, chromatin modifications also could be monitored for accessions throughout different seasons in different locations to help establish differences or similarities between field and laboratory responses. Also it would be informative to grow more established vernalization mutants and *FLC* NILs in the field, as complex environmental cues might expose novel phenotypes. Assessment of these data would help identify genetic components required specifically for this averaging process and help to identify how natural alleles have been modulated by evolution.

Work by Camblong and colleagues showed that antisense RNA stabilization can induce transcriptional gene silencing in *S. cerevisae* under 4^{o}C growth conditions (Camblong et al., 2007). This raises the intriguing possibility that non-coding *FLC* RNA may act as a key thermo-sensor during vernalization. Determining natural variation in *COOLAIR* induction and turnover rates at different temperatures would be a starting point for testing this hypothesis. Although a traditional RT-qPCR approach could be used to provide these data, the novel smFISH method presented in this thesis, could also reveal whether temperature-dependent changes in subcellular localisation occur. Also *COOLAIR* has previously been shown to bind to the *FLC* locus during cold exposure and this physical association may help to mediate the switching of chromatin states (Csorba et al., 2014). Further analyses to determine the thermo-dynamic impact of temperature on *COOLAIR* structure using SHAPE (Selective 2'-hydroxyl acylation analyzed by primer extension) analysis might reveal changes that could impede its ability to bind with the *FLC* locus and mediate this switch.

6.4 The predicted impact of climate change on *A. thaliana* vernalization

The ultimate aim of this thesis was to predict whether increasing temperatures over the coming century would be likely to contribute toward delayed phenology for this species. To achieve this, an effective temperature range suggested by laboratory studies was initially validated using data collected during field studies. A chilling unit

model that incorporated this range was then used to predict effective vernalization periods in three locations that span the latitudinal range inhabited by winter annual accessions.

Assessments of present and future climates predicted a ~12% reduction in effective vernalizing days for Spanish accessions by the end of the century. This prediction was made using the extended (0^{o}C, 18^{o}C) range suggested by data presented in Chapter 4 and Wollenburg and Amasino findings for several Spanish accessions. Greater reductions were predicted for accessions with lower threshold temperatures. A similar ~12% reduction in effective vernalizing days was predicted for central England by the end of the century, however a ~10% increase in effective vernalizing days was predicted for northern Sweden.

The most striking predictions were made for plants with low maximum threshold temperatures that grow in southern Europe. Almost no average daily temperatures are predicted to be lower than 5^{o}C by the end of the century in Barcelona. Therefore plants with low maximum temperature threshold requirements might need to rely on phenotypic plasticity for short-term survival and a combination of adaptive evolution and pole-ward range shifts to persist over the coming century (Parmesan and Yohe, 2003, Nicotra 2010).

In central and northern Europe, vernalization requires are likely to be met or exceeded for *A. thaliana* and other plant species with a similar (0^{o}C,15^{o}C) effective temperature range, however the ability to advance phenology may also be required for future survival (Willis et al., 2008). Results reported by Li and colleagues suggest that this advance is possible. They grew over a thousand accessions in sophisticated growth cabinets under climate regimes programmed to simulate present and future climates in Spain and Sweden and found that almost all advanced their flowering dates in response to climate warming (Li et. al., 2014).

The epigenetic basis of vernalization is well understood in *A. thaliana*, but these findings prompt more studies to be carried out to improve our limited understanding of the molecular mechanisms that control ambient temperature flowering responses. Work that aims to understand how temporal and thermal aspects of vernalization

interact to impact seed yield may prove valuable for optimizing crop production in the future.

6.5 Concluding Remarks

Rises in global temperature have already reduced vernalization periods to an extent that has impacted the phenology of a range of plant species (Fitter and Fitter, 2002, Cook et al. 2012). Although *A. thaliana* accessions are unlikely to be subject to phenological delay over the coming century, this thesis highlights the susceptibility of species with low maximum threshold vernalizing temperatures that grow in southern Europe. Existing vernalization temperature plasticity, in addition to the timescale over which this adaptive evolution can occur, will determine whether these populations will survive under future climate scenarios.

Appendices

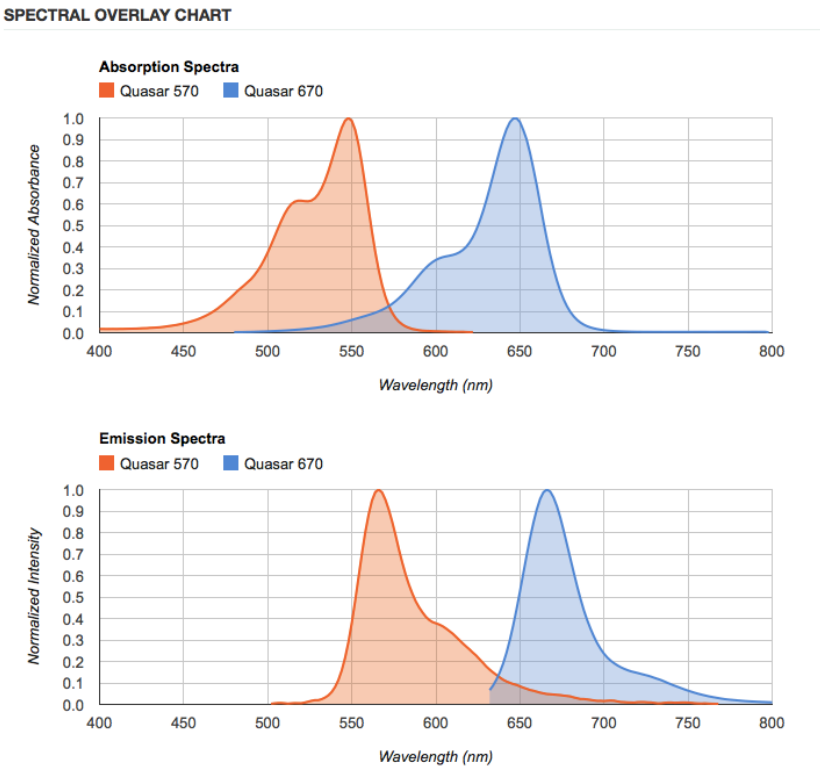

Appendix Figure 1

Overlays of Quasar 570© and Quasar 670© probe dye absorption and emission spectra. Downloaded from: http://www.qpcrdesign.com/spectral-overlay.

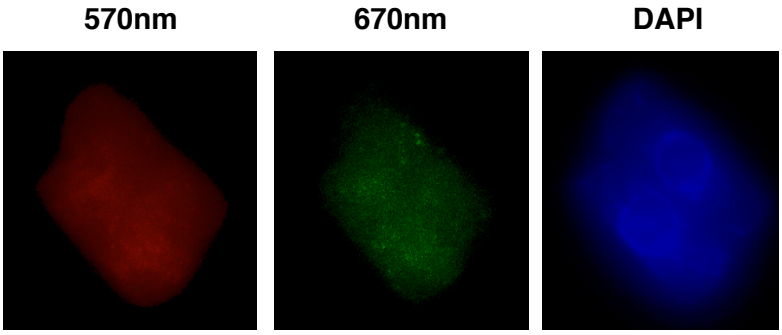

Appendix Figure 2

Representative maximum projection images taken of samples with *PP2A* mRNA labeled with a Quasar 570© probe set and nascent *PP2A* RNA labeled with a Quasar 670© probe set, following 20 minute incubation with RNase.

Appendix Table 1 - Markers used to map the introgressed regions on Chromosome 5

The positions correspond to AGI coordinates. Where the marker is a simple sequence length polymorphism (SSLP), the product size is shown for Col-0/Lov-1. Where the marker is a Cleaved Amplified Polymorphic sequence (CAPS), the enzyme required to digest the PCR product of the specified accession is given.

Type	Position (bp)	Enzyme	Product (bp)	Digest	Forward (5'-3')	Reverse (5'-3')
SSLP	3175482	-	472/442	-	TATATGCACGTC CGGGAGAT	GAGGCACCAAAG AAACAAGG
CAPS	3199916	SacII	625	Col	GACACCCGCGAT TCATCAGTC	GGGATCATCAGG TAATCCGATA
SSLP	4254762	-	249/<249	-	CCCAGTCTAACC ACGACCAC	AATCCCAGTAAC CAAACACACA
SSLP	4618913	-	164/212	-	TCACAAAGGCCT AAGAACCAA	TTTAGGACATGA GTAATGTGCATC
CAPS	5171185	AluI	310	Lov-1	AAACCTTGTGGA TTACAACTCGAG T	TATGATGAAAGA ATTCACCCTGCA GC
SSLP	5344505	-	100/<100	-	AGGGGAAAAAGC GGACTAGA	TGCTCAGGCATA AGAAGAGC

Appendix Table 2 – Primers used for ChIP analysis

Primers	Sequence (5'-3')
-2429_F -2376_R	ATCCAGAAAAGGGCAAGGAG CGAATCGATTGGGTGAATG
-1708_F -1639_R	TGGAGGGAACAACCTAATGC TCATTGGACCAAACCAAACC
-501_F -381_R	ACTATGTAGGCACGACTTTGGTAAC TGCAGAAAGAACCTCCACTCTAC
-158_F -56_R	GCCCGACGAAGAAAAAGTAG TCCTCAGGTTTGGGTTCAAG
307_F 393_R	GGCGGATCTCTTGTTGTTTC CTTCTTCACGACATTGTTCTTCC
543_F 700_R	CGTGCTCGATGTTGTTGAGT TCCCGTAAGTGCATTGCATA
1424_F 1561_R	TTGACAATCCACAACCTCAATC TCAATTTCCTAGAGGCACCAA
2356_F 2451_R	AGTTTGGCTTCCTCATACTTATGG CAATGAACCTTGAGGACAAGG
3088_F 3224_R	GGGGCTGCGTTTACATTTTA GTGATAGCGCTGGCTTTGAT
4213_F 4360_R	AGAACAACCGTGCTGCTTTT TGTGTGCAAGCTCGTTAAGC
5030_F 5135_R	CCGGTTGTTGGACATAACTAGG CCAAACCCAGACTTAACCAGAC
6768_F 6838_R	TTGTAAAGTCCGATGGAGACG ACTCGGCGAGAAAGTTTGTG
STM exon F STM exon R	GCCCATCATGACATCACATC GGGAACTACTTTGTTGGTGGTG

Appendix Table 3 – smFISH probe set used to detect *PP2A* mRNA

***PP2A* Exon Probes**	**Sequences (5'-3')**
1	ccgagcgatctatcaatcag
2	gacatcctcaccaaaactca
3	tcgggtataaaggctcatca
4	tagctcgtcgataagcacag
5	ccaagagcacgagcaatgat
6	atcaactcttttcttgtcct
7	catcgtcattgttctcacta
8	atagccaaaagcacctcatc
9	atacagaataaaacccccca
10	caagtttcctcaacagtgga
11	tcatctgagcaccaattcta
12	tagccagaggagtgaaatgc
13	cattcaccagctgaaagtcg
14	ggaaaatcccacatgctgat
15	atattgatcttagctccgtc
16	attggcatgtcatcttgaca
17	aaattagttgctgcagctct
18	gctgattcaattgtagcagc
19	ccgaatcttgatcatcttgc
20	caaccctcaacagccaataa
21	ctccaacaatttcccaagag
22	caaccatataacgcacacgc
23	agtagacgagcatatgcagg
24	gaacttctgcctcattatca
25	cacagggaagaatgtgctgg
26	tgacgtgctgagaagagtct
27	cccattataactgatgccaa
28	tggttcacttggtcaagttt
29	tctacaatggctggcagtaa
30	cgattatagccagacgtact
31	gactggccaacaagggaata
32	catcaaagaagcctacacct
33	ttgcatgcaaagagcaccaa
34	acggattgagtgaaccttgt
35	cttcagattgtttgcagcag
36	ggaccaaactcttcagcaag
37	ggaactatatgctgcattgc
38	gtgggttgttaatcatctct
39	tgcacgaagaatcgtcatcc
40	ttactggagcgagaagcga
41	ctctgtctttagatgcagtt
42	gaacatgtgatctcggatcc
43	catcattttggccacgttaa
44	cgtatcatgttctccacaac
45	atcaacatctgggtcttcac
46	ttggagagcttgatttgcga
47	acacaattcgttgctgtctt
48	cgcccaacgaacaaatcaca

Appendix Table 4 – smFISH probes used to detect nascent *PP2A* RNA

***PP2A* Intron Probes**	**Sequences (5'-3')**
1	actattaccattcttagact
2	gaactgaaactttgtgccgt
3	tgacccattagcctctaaaa
4	ctttaaactcaattccgcct
5	tgcatacatagacaccatca
6	gtaaaccagccttatctaac
7	ttgacagagcatggaaagga
8	tcttctgttttagtggctta
9	acaattgacaaaggacccca
10	gcatatttccaaactttggg
11	acacctataaggggaacact
12	acttcaacctaccaatttcc
13	atgttctcttagatcaacca
14	aaagagcgctaaagccagag
15	tcacatacacaaccacaacc
16	acctataccgaggtatgtat
17	gcttaagtcggtttcacatt
18	acacaatgacagtgttcagt
19	cccataactaggcttgatga
20	acttgcctattacacatcag
21	tgttcaatgcagtaacccta
22	gcttaacttcagctaatggt
23	agctgagatgtagacaaccg
24	ctttcccataaagctcatca
25	agcagctcatacatatctgc
26	aacttcaaccatcactgctt
27	acctctgaagtcagtaatct
28	catggacttccaagtaccaa
29	cacactcttcttaagtgtgt
30	tggtcctttgcataatatga
31	cttagcaaacaccgacagta
32	ctacgtgtagatttataggt
33	atcggtttttaattctgctt
34	gtattcatgatatgagaggc
35	cactccaaactatagagcca
36	atctttatctctaagatgct
37	gatgacagtgactaggacga
38	ccttccaggcacagttaaaa
39	acatagtgaggttttcttat
40	atgccaagttaaaagctgca
41	gagtaacttggtcaatagca
42	acccaatgtcgtacaaagag
43	acagctcctttgaacatgtg
44	tagtcattgacttgaccaaa
45	ggacaaagaatttgctgtca
46	ctggatgattcaatgaaggt
47	ttcaagcagtagagacgaca
48	actccaataaccaatagcta

Appendix Table 6 – smFISH probes used to detect nascent *FLC* RNA

Sense *FLC* Intron Probes	Sequences (5'-3')
1	gatccgccggaaaaaaacca
2	catgtatctatcatggtcgc
3	cacgacattgttcttcctta
4	caacaacatcgagcacgcat
5	ctctatagatctcccgtaag
6	acattgttcagcattaaccc
7	caatagctgcacaatgtggt
8	aggtccacagcaaagatagg
9	aggctgagtttttgaagct
10	tgaagtagcatatgtgcggt
11	gcacacgacgattgtgattc
12	agaccagtttatgtacagca
13	tttataaatctcccggacgt
14	tccttttaccattaacctc
15	tttcccaattaatgtggctt
16	gtgtaactgcaagagtggga
17	attgaggttgtggattgtca
18	ggttgtgtgattgtcgattt
19	atttcctagaggcaccaaag
20	tagatccgtaccaaagaggt
21	tggagggttgtagtagacac
22	gaccaacatggccaaactac
23	atcaagtgagaatcggccag
24	gacctaactaggggtgaaca
25	tagtcaggtgtctcgacaat
26	tccacgttctaaaaggcttc
27	gctctttgcatcaacctaag
28	gcccttgaagttacactaac
29	cggtcttccattttgttatt
30	tacatggaccgagtcttaga
31	gtatgaggaagccaaactcc
32	tgtggcggtaaccagataac
33	gctagtattgatgacccata
34	caaggtttttccagcgata
35	ggtaacatcagctctttgtt
36	aaacgcctctttcatgagtt
37	cttttcttttgtatcccag
38	acctatttaccctctatttt
39	ccataccacaacttttagca
40	agagattcagagcttccatt
41	tagtggaagactgcttccaa
42	ccaagtacacagactgagtc
43	gccacaatgtgatgacatgg
44	agccccaatcttaaatgcaa
45	tccagattgtttctatgcat
46	ccctaaacataagcctctac
47	tagcgctggctttgattaac
48	agcacatctgaatttccact

Appendix Table 5 – smFISH probe set used to detect *FLC* mRNA

Sense *FLC* Exon Probes	Sequences (5'-3')
1	ttttttttttccttttctcg
2	actaagcgttttctctttct
3	tcaggtttgggttcaagtcg
4	gctttgtgccctaatttgat
5	ctagtttttttcttcccatg
6	ttgttctcaattcgcttgat
7	gaaggtgacttgtcggctac
8	tgagaccgttgcgacgtttg
9	gaaagctgacgagctttctc
10	gacggatgcgtcacagagaa
11	gaggcggagacgacgagaag
12	gaggagaagctgtagagctt
13	aggatcttgaccaggttatc
14	atgctgtttcccatatcgat
15	ccaaggctttaagatcatca
16	agttcagagcttttgactga
17	agtagctcatagtgtgaacc
18	aagcttgctatccacaagtt
19	catttttgacatttgatccc
20	ccagttgaacaagagcatcg
21	agggcagtctcaaggtgttc
22	tcttcttggctctagtcacg
23	acaagcttcaacatgagttc
24	gcattttctccttttcttta
25	caaaacctggttctcttctt
26	atccaaggaatatctggcta
27	tcactttctctttttgtctt
28	ctccatctgtacgataatca
29	ctgctcccacatgatgatta
30	aggtgacatctccatctcag
31	agattgtcggagatttgtcc
32	taagtagtgggagagtcacc
33	tttcaaccgccgatttaagg
34	cccttatcagcggaataatt
35	ggccaaagagagagtattaa
36	agtatcacacacaaagtctc
37	agtattgacttagttccgtc
38	gttcatcaacctttgtctt

Appendix Table 7 – smFISH probe set: nascent antisense *FLC* RNA

Antisense *FLC* Intron Probes	Sequences (5'-3')
1	gtagtgctacttttacatgc
2	ttccaactccaagtgtctag
3	ttatggttaggtttggatcc
4	gtttatggaccgattagttt
5	agttaatcacctttaacca
6	ggttgtgtaaacgttgtcta
7	gttcaatattggtttccttg
8	tggtctggttcagtctagtt
9	ttcttgattctctttcaggt
10	tctgggtttggtagagattc
11	gaacctttatagtctggtt
12	ggttttggttcatttggaga
13	taggttttggttcttcttct
14	aattccggttgttggacata
15	acggctggttagagttaagg
16	gggttagtgagattattact
17	gttgttggtagtttggttta
18	ttcttctcaagattagggca
19	gtcttgtatagttgtattct
20	cattcactagttagcacttt
21	tatatagtcagtgcatttca
22	acactcttatgcttgcagat
23	atgtccatgtacatggacat
24	aataagcactgcgtgttgtg
25	acgaaagctacatttcctaa
26	acgaaagctacatttcctaa
27	attctgaagttgttaggttt
28	cttcatatgttttggattcc
29	gcttgcacacatatttgcaa
30	ctctgttactttaagtctgc
31	gatatatcctcttctgtgtt
32	gctaccaattttattgtaca
33	cgtgctgcttttgtttgttg
34	ctgaattttgtttgctgaga
35	atttcgtaatgtctactcct
36	ctctccacctttgattacaa
37	tcttctgtccctttttcatg
38	ttcatagcccttgtctttta
39	atgcattatgcataccgcaa
40	taaaatgaggtggtggctcc
41	actattagtttgccgagtga
42	atggagttttataaggcgta
43	aacattttgaatcttttccc
44	attttttttgtcatctctcc
45	agctagtagttttgatccta
46	tttccagtggccttttcaag
47	ggtgttctctcaatgtttca
48	gttacgaatactagcgtgtt

Appendix Table 8 – smFISH probe set: spliced antisense *FLC* RNA

Antisense *FLC* Exon Probes	Sequences (5'-3')
1	attttgcaacagggacgtgg
2	acagtgaagaagcctacggc
3	gtcaaaaacttgtgtttgct
4	gagtgtatgtgttcttcact
5	tcgtgtgagaattgcatcga
6	ggttgatgaactttgtacct
7	gagactttgtgtgtgatact
8	ttaatactctctctttggcc
9	taagggcgagcgtttgtata
10	agatatgtaattattccgct
11	accttaaatcggcggttgaa
12	gactctcccactacttaatt
13	aaatctccgacaatcttccg
14	tgagatggagatgtcacctg
15	atcatcatgtgggagcagaa
16	gattatcgtacagatggaga
17	gtgaatagtgattttgacct
18	tattccttggatagaagaca
19	gttgttatttggtggtgtga
20	accttctgtagtgtttttta
21	tttacttttactgcttcca
22	ccttttatcttctgttttgt
23	acctgggttttcatttgttc
24	gcgataagtacgccttttcc
25	aagctctacagcttctcctc
26	ttctgttctctgtgacgcat
27	tcatcgagaaagctcgtcag
28	ttctccaaacgtcgcaacgg
29	caaaagtagccgacaagtca
30	ggagagaagccatgggaaga
31	caaattagggcacaaagccc
32	acttgaacccaaacctgagg
33	aaaacgcttagtatctccgg
34	aaatatctggcccgacgaag
35	ctcgtttacccccaaaaaaa
36	tatttggtttttttgcatca
37	cgtggcaatcttgtcttcaa

Appendix Table 9 – smFISH probe set used to detect *VIN3* RNA

***VIN3* mRNA Probes**	**Sequences (5'-3')**
1	tctaaggaggaaaccctctg
2	tttctgtgatggatggttct
3	cttcgtgttcttcgtttttt
4	cgaagcagcttgcatttttt
5	ttaccatcgaaacgccagat
6	agaatccatgttctctggac
7	tctcctttcacttacattca
8	ggttagacaatgcgtggatc
9	tcaaaagctccgaagcttct
10	ccatctcagcacatatgatc
11	taagaccagtgtacttcctt
12	gattctctatgagctttggt
13	cggtcagaacaagaggtctc
14	gtaaccgatcatcttcttct
15	agcaagaacaccttctgcaa
16	agccataaactaggatcctt
17	agacgatccacaagcatcac
18	tgcttcaaaccacattccaa
19	cctaccatcaagatcatcac
20	tatctttaccgcaatacgcg
21	gttccaacagattccgatac
22	aagtctattgacgatgcctc
23	gagaacacagcttctggaca
24	agattctgatggtgagacca
25	gcttgaatctcttctactct
26	tctactctcacagtgactga
27	acctgtgatcttgttttgtg
28	gtccttcgactttcgacaaa
29	tgagacagaactcggtgtcg
30	aagtcaccttcctcgttaaa
31	atcatccttcaacgttgtga
32	cttgagtttgtcaaagggct
33	ttgctgcagcttttattgac
34	actacagtgttcagtgttgt
35	tctcttcttcaagctcagat
36	gtttgctttcctctttacaa
37	aagcaagtctcttccatcta
38	aatatctctcttgcagggtg
39	ttgaatcttttattccctcc
40	ggcattattgatctcaggtt
41	atgacccaagtctttatctc
42	cttgtctatatgtccttctt
43	tgtcaagaacctttccctaa
44	caactcttacttctcggtga
45	tcctccataaacgtctcaac
46	caagctgttgtcccaaagaa
47	caccatttgtcgatgatctc
48	taatgccaaagcttgaggca

References

AGREN, J., OAKLEY, C. G., MCKAY, J. K., LOVELL, J. T. & SCHEMSKE, D. W. 2013. Genetic mapping of adaptation reveals fitness tradeoffs in Arabidopsis thaliana. *Proc Natl Acad Sci U S A,* 110**,** 21077-82.

AIKAWA, S., KOBAYASHI, M. J., SATAKE, A., SHIMIZU, K. K. & KUDOH, H. 2010. Robust control of the seasonal expression of the Arabidopsis FLC gene in a fluctuating environment. *Proc Natl Acad Sci U S A,* 107**,** 11632-7.

AKIYAMA, R. & AGREN, J. 2012. Magnitude and timing of leaf damage affect seed production in a natural population of Arabidopsis thaliana (Brassicaceae). *PLoS One,* 7**,** e30015.

AL-SHEHBAZ, I. & O'KANE, S. 2002. Taxonomy and phylogeny of Arabidopsis (Brassicaceae). *In:* SOMERVILLE, C. & MEYEROWITZ, E. (eds.) *The Arabidopsis Book. American Society of Plant Biologists.* Rockville, Maryland.

ALBANI, M. C., CASTAINGS, L., WOTZEL, S., MATEOS, J. L., WUNDER, J., WANG, R., REYMOND, M. & COUPLAND, G. 2012. PEP1 of Arabis alpina is encoded by two overlapping genes that contribute to natural genetic variation in perennial flowering. *PLoS Genet,* 8**,** e1003130.

ALEXANDRE, C. M. & HENNIG, L. 2008. FLC or not FLC: the other side of vernalization. *J Exp Bot,* 59**,** 1127-35.

AMASINO, R. 2004. Vernalization, competence, and the epigenetic memory of winter. *Plant Cell,* 16**,** 2553-9.

AMASINO, R. 2009. Floral induction and monocarpic versus polycarpic life histories. *Genome Biol,* 10**,** 228.

AMI, E., J, ISLAM, M., T & FAROOQUE, A., M 2013. Effect of vernalization on seed production of onion. *Agriculture, Forestry and Fisheries,* 2**,** 212-217.

ANDERSSON, C. R., HELLIWELL, C. A., BAGNALL, D. J., HUGHES, T. P., FINNEGAN, E. J., PEACOCK, W. J. & DENNIS, E. S. 2008. The FLX gene of Arabidopsis is required for FRI-dependent activation of FLC expression. *Plant Cell Physiol,* 49**,** 191-200.

ANGEL, A., SONG, J., DEAN, C. & HOWARD, M. 2011. A Polycomb-based switch underlying quantitative epigenetic memory. *Nature,* 476**,** 105-8.

ANGEL, A., SONG, J., YANG, H., QUESTA, J. I., DEAN, C. & HOWARD, M. 2015. Vernalizing cold is registered digitally at FLC. *Proc Natl Acad Sci U S A,* 112**,** 4146-51.

ANGILLETTA, M. J., JR., SEARS, M. W. & PRINGLE, R. M. 2009. Spatial dynamics of nesting behavior: lizards shift microhabitats to construct nests with beneficial thermal properties. *Ecology,* 90**,** 2933-9.

ARANZANA, M. J., KIM, S., ZHAO, K., BAKKER, E., HORTON, M., JAKOB, K., LISTER, C., MOLITOR, J., SHINDO, C., TANG, C., TOOMAJIAN, C., TRAW, B., ZHENG, H., BERGELSON, J., DEAN, C., MARJORAM, P. & NORDBORG, M. 2005. Genome-wide association mapping in Arabidopsis identifies previously known flowering time and pathogen resistance genes. *PLoS Genet,* 1**,** e60.

ATHERTON, J., CRAIGON, J. & BASHER, E. 1998. Flowering and bolting in carrot. *Journal of Horticultural Science,* 65**,** 423-429.

ATWELL, S., HUANG, Y. S., VILHJALMSSON, B. J., WILLEMS, G., HORTON, M., LI, Y., MENG, D., PLATT, A., TARONE, A. M., HU, T. T., JIANG, R., MULIYATI, N. W., ZHANG, X., AMER, M. A., BAXTER, I., BRACHI, B., CHORY, J., DEAN, C., DEBIEU, M., DE MEAUX, J., ECKER, J. R., FAURE, N., KNISKERN, J. M., JONES, J. D., MICHAEL, T., NEMRI, A., ROUX, F., SALT, D. E., TANG, C., TODESCO, M., TRAW, M. B., WEIGEL, D., MARJORAM, P., BOREVITZ, J. O., BERGELSON, J. & NORDBORG, M. 2010. Genome-wide association study of 107 phenotypes in Arabidopsis thaliana inbred lines. *Nature,* 465**,** 627-31.

AUKERMAN, M. J. & SAKAI, H. 2003. Regulation of flowering time and floral organ identity by a MicroRNA and its APETALA2-like target genes. *Plant Cell,* 15**,** 2730-41.

BASTOW, R., MYLNE, J. S., LISTER, C., LIPPMAN, Z., MARTIENSSEN, R. A. & DEAN, C. 2004. Vernalization requires epigenetic silencing of FLC by histone methylation. *Nature,* 427**,** 164-7.

BAUMBUSCH, L. O., THORSTENSEN, T., KRAUSS, V., FISCHER, A., NAUMANN, K.,

ASSALKHOU, R., SCHULZ, I., REUTER, G. & AALEN, R. B. 2001. The Arabidopsis thaliana genome contains at least 29 active genes encoding SET domain proteins that can be assigned to four evolutionarily conserved classes. *Nucleic Acids Res,* 29**,** 4319-33.

BAXTER, I., BRAZELTON, J. N., YU, D., HUANG, Y. S., LAHNER, B., YAKUBOVA, E., LI, Y., BERGELSON, J., BOREVITZ, J. O., NORDBORG, M., VITEK, O. & SALT, D. E. 2010. A coastal cline in sodium accumulation in Arabidopsis thaliana is driven by natural variation of the sodium transporter AtHKT1;1. *PLoS Genet,* 6**,** e1001193.

BELLE, C., KULCZYNSKI, S., M, BASSO, C., J, KASPARY, T., E, LAMEGO, F., P & PINTO, M., A, B 2014. Yield and quality of wheat seeds as a function of dessication stages and herbicides. *Journal of Seed Science,* 36**,** 63-70.

BERR, A., SHAFIQ, S. & SHEN, W. H. 2011. Histone modifications in transcriptional activation during plant development. *Biochim Biophys Acta,* 1809**,** 567-76.

BERRY, S., HARTLEY, M., OLSSON, T. S., DEAN, C. & HOWARD, M. 2015. Local chromatin environment of a Polycomb target gene instructs its own epigenetic inheritance. *Elife,* 4.

BERTIN, R., I 2008. Plant phenology and distribution in relation to recent climate change. *Journal of the Torrey Botanical Society,* 135**,** 126-146.

BETZ, J. L., CHANG, M., WASHBURN, T. M., PORTER, S. E., MUELLER, C. L. & JAEHNING, J. A. 2002. Phenotypic analysis of Paf1/RNA polymerase II complex mutations reveals connections to cell cycle regulation, protein synthesis, and lipid and nucleic acid metabolism. *Mol Genet Genomics,* 268**,** 272-85.

BLANCHARD, M. G. & RUNKLE, E. S. 2006. Temperature during the day, but not during the night, controls flowering of Phalaenopsis orchids. *J Exp Bot,* 57**,** 4043-9.

BOND, D. M., WILSON, I. W., DENNIS, E. S., POGSON, B. J. & JEAN FINNEGAN, E. 2009. VERNALIZATION INSENSITIVE 3 (VIN3) is required for the response of Arabidopsis thaliana seedlings exposed to low oxygen conditions. *Plant J,* 59**,** 576-87.

BOSS, P. K., BASTOW, R. M., MYLNE, J. S. & DEAN, C. 2004. Multiple pathways in the decision to flower: enabling, promoting, and resetting. *Plant Cell,* 16 Suppl**,** S18-31.

BOX, M. S., COUSTHAM, V., DEAN, C. & MYLNE, J. S. 2011. Protocol: A simple phenol-based method for 96-well extraction of high quality RNA from Arabidopsis. *Plant Methods,* 7**,** 7.

BRACHI, B., FAURE, N., BERGELSON, J., CUGUEN, J. & ROUX, F. 2013. Genome-wide association mapping of flowering time in in nature: genetics for underlying components and reaction norms across two successive years. *Acta Bot Gallica,* 160**,** 205-219.

BRACHI, B., FAURE, N., HORTON, M., FLAHAUW, E., VAZQUEZ, A., NORDBORG, M., BERGELSON, J., CUGUEN, J. & ROUX, F. 2010. Linkage and association mapping of Arabidopsis thaliana flowering time in nature. *PLoS Genet,* 6**,** e1000940.

BRADLEY, D., RATCLIFFE, O., VINCENT, C., CARPENTER, R. & COEN, E. 1997. Inflorescence commitment and architecture in Arabidopsis. *Science,* 275**,** 80-3.

BRADLEY, N. L., LEOPOLD, A. C., ROSS, J. & HUFFAKER, W. 1999. Phenological changes reflect climate change in Wisconsin. *Proc Natl Acad Sci U S A,* 96**,** 9701-4.

BRENGUES, M., TEIXEIRA, D. & PARKER, R. 2005. Movement of eukaryotic mRNAs between polysomes and cytoplasmic processing bodies. *Science,* 310**,** 486-9.

BRENNAN, A. C., MENDEZ-VIGO, B., HADDIOUI, A., MARTINEZ-ZAPATER, J. M., PICO, F. X. & ALONSO-BLANCO, C. 2014. The genetic structure of Arabidopsis thaliana in the south-western Mediterranean range reveals a shared history between North Africa and southern Europe. *BMC Plant Biol,* 14**,** 17.

BREWER, S., CHEDDADI, R., DE BEAULIEU, J. L. & REILLE, M. 2002. The spread of deciduous Quercus throughout Europe since the last glacial period. *Forest Ecology and Management,* 156**,** 27-48.

BURROWS, M. T., SCHOEMAN, D. S., BUCKLEY, L. B., MOORE, P., POLOCZANSKA, E. S., BRANDER, K. M., BROWN, C., BRUNO, J. F., DUARTE, C. M., HALPERN, B. S., HOLDING, J., KAPPEL, C. V., KIESSLING, W., O'CONNOR, M. I., PANDOLFI, J. M., PARMESAN, C., SCHWING, F. B., SYDEMAN, W. J. & RICHARDSON, A. J. 2011. The pace of shifting climate in marine and terrestrial ecosystems. *Science,* 334**,** 652-5.

BURROWS, M. T., SCHOEMAN, D. S., RICHARDSON, A. J., MOLINOS, J. G., HOFFMANN, A., BUCKLEY, L. B., MOORE, P. J., BROWN, C. J., BRUNO, J. F., DUARTE, C. M.,

HALPERN, B. S., HOEGH-GULDBERG, O., KAPPEL, C. V., KIESSLING, W., O'CONNOR, M. I., PANDOLFI, J. M., PARMESAN, C., SYDEMAN, W. J., FERRIER, S., WILLIAMS, K. J. & POLOCZANSKA, E. S. 2014. Geographical limits to species-range shifts are suggested by climate velocity. *Nature,* 507**,** 492-5.

BYRNE, D. & BACON, T. 1992. Chilling estimation: its importance and estimation. *The Texas Horticulturist,* 18**,** 8-9.

CAICEDO, A. L., RICHARDS, C., EHRENREICH, I. M. & PURUGGANAN, M. D. 2009. Complex rearrangements lead to novel chimeric gene fusion polymorphisms at the Arabidopsis thaliana MAF2-5 flowering time gene cluster. *Mol Biol Evol,* 26**,** 699-711.

CAICEDO, A. L., STINCHCOMBE, J. R., OLSEN, K. M., SCHMITT, J. & PURUGGANAN, M. D. 2004. Epistatic interaction between Arabidopsis FRI and FLC flowering time genes generates a latitudinal cline in a life history trait. *Proc Natl Acad Sci U S A,* 101**,** 15670-5.

CAMBLONG, J., IGLESIAS, N., FICKENTSCHER, C., DIEPPOIS, G. & STUTZ, F. 2007. Antisense RNA stabilization induces transcriptional gene silencing via histone deacetylation in S. cerevisiae. *Cell,* 131**,** 706-17.

CAMPOLI, C. & VON KORFF, M. 2014. Genetic Control of Reproductive Development in Temperate Cereals. *Advances in Botanical Research,* 72**,** 131-158.

CAO, J., SCHNEEBERGER, K., OSSOWSKI, S., GUNTHER, T., BENDER, S., FITZ, J., KOENIG, D., LANZ, C., STEGLE, O., LIPPERT, C., WANG, X., OTT, F., MULLER, J., ALONSO-BLANCO, C., BORGWARDT, K., SCHMID, K. J. & WEIGEL, D. 2011. Whole-genome sequencing of multiple Arabidopsis thaliana populations. *Nat Genet,* 43**,** 956-63.

CAO, Y., DAI, Y., CUI, S. & MA, L. 2008. Histone H2B monoubiquitination in the chromatin of FLOWERING LOCUS C regulates flowering time in Arabidopsis. *Plant Cell,* 20**,** 2586-602.

CAPOVILLA, G., SCHMID, M. & POSE, D. 2015. Control of flowering by ambient temperature. *J Exp Bot,* 66**,** 59-69.

CASTAINGS, L., BERGONZI, S., ALBANI, M. C., KEMI, U., SAVOLAINEN, O. & COUPLAND, G. 2014. Evolutionary conservation of cold-induced antisense RNAs of FLOWERING LOCUS C in Arabidopsis thaliana perennial relatives. *Nat Commun,* 5**,** 4457.

CASTELNUOVO, M., RAHMAN, S., GUFFANTI, E., INFANTINO, V., STUTZ, F. & ZENKLUSEN, D. 2013. Bimodal expression of PHO84 is modulated by early termination of antisense transcription. *Nat Struct Mol Biol,* 20**,** 851-8.

CHAUDHARY, K., DEB, S., MONIAUX, N., PONNUSAMY, M. P. & BATRA, S. K. 2007. Human RNA polymerase II-associated factor complex: dysregulation in cancer. *Oncogene,* 26**,** 7499-507.

CHEW, Y. H., WENDEN, B., FLIS, A., MENGIN, V., TAYLOR, J., DAVEY, C. L., TINDAL, C., THOMAS, H., OUGHAM, H. J., DE REFFYE, P., STITT, M., WILLIAMS, M., MUETZELFELDT, R., HALLIDAY, K. J. & MILLAR, A. J. 2014. Multiscale digital Arabidopsis predicts individual organ and whole-organism growth. *Proc Natl Acad Sci U S A,* 111**,** E4127-36.

CHEW, Y. H., WILCZEK, A. M., WILLIAMS, M., WELCH, S. M., SCHMITT, J. & HALLIDAY, K. J. 2012. An augmented Arabidopsis phenology model reveals seasonal temperature control of flowering time. *New Phytol,* 194**,** 654-65.

CHIANG, G. C., BARUA, D., KRAMER, E. M., AMASINO, R. M. & DONOHUE, K. 2009. Major flowering time gene, flowering locus C, regulates seed germination in Arabidopsis thaliana. *Proc Natl Acad Sci U S A,* 106**,** 11661-6.

CHOI, J., HYUN, Y., KANG, M. J., IN YUN, H., YUN, J. Y., LISTER, C., DEAN, C., AMASINO, R. M., NOH, B., NOH, Y. S. & CHOI, Y. 2009. Resetting and regulation of Flowering Locus C expression during Arabidopsis reproductive development. *Plant J,* 57**,** 918-31.

CHOI, K., KIM, S., KIM, S. Y., KIM, M., HYUN, Y., LEE, H., CHOE, S., KIM, S. G., MICHAELS, S. & LEE, I. 2005. SUPPRESSOR OF FRIGIDA3 encodes a nuclear ACTIN-RELATED PROTEIN6 required for floral repression in Arabidopsis. *Plant Cell,* 17**,** 2647-60.

CHOI, K., PARK, C., LEE, J., OH, M., NOH, B. & LEE, I. 2007. Arabidopsis homologs of components of the SWR1 complex regulate flowering and plant development. *Development,* 134**,** 1931-41.

CHOUARD, P. 1960. Vernalization and its relations to dormancy. *Annual Review of Plant Physiology,* 11**,** 191-238.

CHUBB, J. R., TRCEK, T., SHENOY, S. M. & SINGER, R. H. 2006. Transcriptional pulsing of a

developmental gene. *Curr Biol,* 16**,** 1018-25.
CHUINE, I., MORIN, X. & BUGMANN, H. 2010. Warming, photoperiods, and tree phenology. *Science,* 329**,** 277-8; author reply 278.
CLELAND, E. E., CHUINE, I., MENZEL, A., MOONEY, H. A. & SCHWARTZ, M. D. 2007. Shifting plant phenology in response to global change. *Trends Ecol Evol,* 22**,** 357-65.
COOK, B. I., WOLKOVICH, E. M. & PARMESAN, C. 2012. Divergent responses to spring and winter warming drive community level flowering trends. *Proc Natl Acad Sci U S A,* 109**,** 9000-5.
COUSTHAM, V., LI, P., STRANGE, A., LISTER, C., SONG, J. & DEAN, C. 2012. Quantitative modulation of polycomb silencing underlies natural variation in vernalization. *Science,* 337**,** 584-7.
CRAIGON, J., ATHERTON, J. & BASHER, E. 1990. Flowering and bolting in carrot. *Journal of Horticultural Science,* 65**,** 423-429.
CREVILLEN, P. & DEAN, C. 2011. Regulation of the floral repressor gene FLC: the complexity of transcription in a chromatin context. *Curr Opin Plant Biol,* 14**,** 38-44.
CREVILLEN, P., SONMEZ, C., WU, Z. & DEAN, C. 2013. A gene loop containing the floral repressor FLC is disrupted in the early phase of vernalization. *EMBO J,* 32**,** 140-8.
CSORBA, T., QUESTA, J. I., SUN, Q. & DEAN, C. 2014. Antisense COOLAIR mediates the coordinated switching of chromatin states at FLC during vernalization. *Proc Natl Acad Sci U S A,* 111**,** 16160-5.
CZECHOWSKI, T., STITT, M., ALTMANN, T., UDVARDI, M. K. & SCHEIBLE, W. R. 2005. Genome-wide identification and testing of superior reference genes for transcript normalization in Arabidopsis. *Plant Physiol,* 139**,** 5-17.
DAVIS, M. B. & SHAW, R. G. 2001. Range shifts and adaptive responses to Quaternary climate change. *Science,* 292**,** 673-9.
DE BODT, S., RAES, J., VAN DE PEER, Y. & THEISSEN, G. 2003. And then there were many: MADS goes genomic. *Trends Plant Sci,* 8**,** 475-83.
DE LUCIA, F., CREVILLEN, P., JONES, A. M., GREB, T. & DEAN, C. 2008. A PHD-polycomb repressive complex 2 triggers the epigenetic silencing of FLC during vernalization. *Proc Natl Acad Sci U S A,* 105**,** 16831-6.
DEAL, R. B., KANDASAMY, M. K., MCKINNEY, E. C. & MEAGHER, R. B. 2005. The nuclear actin-related protein ARP6 is a pleiotropic developmental regulator required for the maintenance of FLOWERING LOCUS C expression and repression of flowering in Arabidopsis. *Plant Cell,* 17**,** 2633-46.
DEAL, R. B., TOPP, C. N., MCKINNEY, E. C. & MEAGHER, R. B. 2007. Repression of flowering in Arabidopsis requires activation of FLOWERING LOCUS C expression by the histone variant H2A.Z. *Plant Cell,* 19**,** 74-83.
DEBIEU, M., TANG, C., STICH, B., SIKOSEK, T., EFFGEN, S., JOSEPHS, E., SCHMITT, J., NORDBORG, M., KOORNNEEF, M. & DE MEAUX, J. 2013. Co-variation between seed dormancy, growth rate and flowering time changes with latitude in Arabidopsis thaliana. *PLoS One,* 8**,** e61075.
DECH, J. P. & NOSKO, P. 2004. Rapid growth and early flowering in an invasive plant, purple loosestrife (Lythrum salicaria L.) during an El Nino spring. *Int J Biometeorol,* 49**,** 26-31.
DELL, A. I., PAWAR, S. & SAVAGE, V. M. 2011. Systematic variation in the temperature dependence of physiological and ecological traits. *Proc Natl Acad Sci U S A,* 108**,** 10591-6.
DENG, W., YING, H., HELLIWELL, C. A., TAYLOR, J. M., PEACOCK, W. J. & DENNIS, E. S. 2011. FLOWERING LOCUS C (FLC) regulates development pathways throughout the life cycle of Arabidopsis. *Proc Natl Acad Sci U S A,* 108**,** 6680-5.
DING, L., KIM, S. Y. & MICHAELS, S. D. 2013. FLOWERING LOCUS C EXPRESSOR family proteins regulate FLOWERING LOCUS C expression in both winter-annual and rapid-cycling Arabidopsis. *Plant Physiol,* 163**,** 243-52.
DING, L., PASZKOWSKI-ROGACZ, M., NITZSCHE, A., SLABICKI, M. M., HENINGER, A. K., DE VRIES, I., KITTLER, R., JUNQUEIRA, M., SHEVCHENKO, A., SCHULZ, H., HUBNER, N., DOSS, M. X., SACHINIDIS, A., HESCHELER, J., IACONE, R., ANASTASSIADIS, K., STEWART, A. F., PISABARRO, M. T., CALDARELLI, A., POSER, I., THEIS, M. & BUCHHOLZ, F. 2009. A genome-scale RNAi screen for Oct4 modulators defines a role of

the Paf1 complex for embryonic stem cell identity. *Cell Stem Cell,* 4**,** 403-15.
DODD, I. B., MICHEELSEN, M. A., SNEPPEN, K. & THON, G. 2007. Theoretical analysis of epigenetic cell memory by nucleosome modification. *Cell,* 129**,** 813-22.
DREA, S., DERBYSHIRE, P., KOUMPROGLOU, R., DOLAN, L., DOONAN, J. H. & SHAW, P. 2009. In situ analysis of gene expression in plants. *Methods Mol Biol,* 513**,** 229-42.
FAUSEY, B. & CAMERON, A. 2007. Differing vernalization responses of Veronica spicata Red Fox and Laurentia axillaries *J. Amer. Soc. Hort. Sci.,* 132.
FINNEGAN, E. J. & DENNIS, E. S. 2007. Vernalization-induced trimethylation of histone H3 lysine 27 at FLC is not maintained in mitotically quiescent cells. *Curr Biol,* 17**,** 1978-83.
FITTER, A. H. & FITTER, R. S. 2002. Rapid changes in flowering time in British plants. *Science,* 296**,** 1689-91.
FOURNIER-LEVEL, A., KORTE, A., COOPER, M. D., NORDBORG, M., SCHMITT, J. & WILCZEK, A. M. 2011. A map of local adaptation in Arabidopsis thaliana. *Science,* 334**,** 86-9.
FOURNIER-LEVEL, A., WILCZEK, A. M., COOPER, M. D., ROE, J. L., ANDERSON, J., EATON, D., MOYERS, B. T., PETIPAS, R. H., SCHAEFFER, R. N., PIEPER, B., REYMOND, M., KOORNNEEF, M., WELCH, S. M., REMINGTON, D. L. & SCHMITT, J. 2013. Paths to selection on life history loci in different natural environments across the native range of Arabidopsis thaliana. *Mol Ecol*.
FOWLER, S. G., COOK, D. & THOMASHOW, M. F. 2005. Low temperature induction of Arabidopsis CBF1, 2, and 3 is gated by the circadian clock. *Plant Physiol,* 137**,** 961-8.
FRANCOIS, O., BLUM, M. G., JAKOBSSON, M. & ROSENBERG, N. A. 2008. Demographic history of european populations of Arabidopsis thaliana. *PLoS Genet,* 4**,** e1000075.
FRANKS, S. J. & WEIS, A. E. 2008. A change in climate causes rapid evolution of multiple life-history traits and their interactions in an annual plant. *J Evol Biol,* 21**,** 1321-34.
FROST, F. 1995. Fluorescent Microscopy *Autofluorescence: plants, fungi, bacteria.* Cambridge, UK: Cambridge University Press.
FU, D., DUNBAR, M. & DUBCOVSKY, J. 2007. Wheat VIN3-like PHD finger genes are up-regulated by vernalization. *Mol Genet Genomics,* 277**,** 301-13.
GAUDIN, V., LIBAULT, M., POUTEAU, S., JUUL, T., ZHAO, G., LEFEBVRE, D. & GRANDJEAN, O. 2001. Mutations in LIKE HETEROCHROMATIN PROTEIN 1 affect flowering time and plant architecture in Arabidopsis. *Development,* 128**,** 4847-58.
GENDALL, A. R., LEVY, Y. Y., WILSON, A. & DEAN, C. 2001. The VERNALIZATION 2 gene mediates the epigenetic regulation of vernalization in Arabidopsis. *Cell,* 107**,** 525-35.
GERALDO, N., BAURLE, I., KIDOU, S., HU, X. & DEAN, C. 2009. FRIGIDA delays flowering in Arabidopsis via a cotranscriptional mechanism involving direct interaction with the nuclear cap-binding complex. *Plant Physiol,* 150**,** 1611-8.
GOLDING, I., PAULSSON, J., ZAWILSKI, S. M. & COX, E. C. 2005. Real-time kinetics of gene activity in individual bacteria. *Cell,* 123**,** 1025-36.
GORDO, O. & SANZ, J., J 2009. Impact of climate change on plant phenology in Mediterranean ecosystems. *Global Change Biology,* 16**,** 1082-1106.
GREB, T., MYLNE, J. S., CREVILLEN, P., GERALDO, N., AN, H., GENDALL, A. R. & DEAN, C. 2007. The PHD finger protein VRN5 functions in the epigenetic silencing of Arabidopsis FLC. *Curr Biol,* 17**,** 73-8.
GREENUP, A. G., SASANI, S., OLIVER, S. N., TALBOT, M. J., DENNIS, E. S., HEMMING, M. N. & TREVASKIS, B. 2010. ODDSOC2 is a MADS box floral repressor that is down-regulated by vernalization in temperate cereals. *Plant Physiol,* 153**,** 1062-73.
GU, P., LE MENUET, D., CHUNG, A. C. & COONEY, A. J. 2009. Differential recruitment of methylated CpG binding domains by the orphan receptor GCNF initiates the repression and silencing of Oct4 expression. *Mol Cell Biol,* 29**,** 1987.
GU, X., JIANG, D., WANG, Y., BACHMAIR, A. & HE, Y. 2009. Repression of the floral transition via histone H2B monoubiquitination. *Plant J,* 57**,** 522-33.
GU, X., LE, C., WANG, Y., LI, Z., JIANG, D., WANG, Y. & HE, Y. 2013. Arabidopsis FLC clade members form flowering-repressor complexes coordinating responses to endogenous and environmental cues. *Nat Commun,* 4**,** 1947.
HAGENBLAD, J., TANG, C., MOLITOR, J., WERNER, J., ZHAO, K., ZHENG, H., MARJORAM, P., WEIGEL, D. & NORDBORG, M. 2004. Haplotype structure and phenotypic

associations in the chromosomal regions surrounding two Arabidopsis thaliana flowering time loci. *Genetics,* 168**,** 1627-38.
HANCOCK, A. M., BRACHI, B., FAURE, N., HORTON, M. W., JARYMOWYCZ, L. B., SPERONE, F. G., TOOMAJIAN, C., ROUX, F. & BERGELSON, J. 2011. Adaptation to climate across the Arabidopsis thaliana genome. *Science,* 334**,** 83-6.
HANSEN, C. & VAN OUDENAARDEN, A. 2013. Allele-specific detection of single mRNA molecules in situ. *Nature Methods* 10**,** 869.
HARTMANN, U., HOHMANN, S., NETTESHEIM, K., WISMAN, E., SAEDLER, H. & HUIJSER, P. 2000. Molecular cloning of SVP: a negative regulator of the floral transition in Arabidopsis. *Plant J,* 21**,** 351-60.
HE, F., ZHANG, X., HU, J., TURCK, F., DONG, X., GOEBEL, U., BOREVITZ, J. & DE MEAUX, J. 2012. Genome-wide analysis of cis-regulatory divergence between species in the Arabidopsis genus. *Mol Biol Evol,* 29**,** 3385-95.
HE, Y., DOYLE, M. R. & AMASINO, R. M. 2004. PAF1-complex-mediated histone methylation of FLOWERING LOCUS C chromatin is required for the vernalization-responsive, winter-annual habit in Arabidopsis. *Genes Dev,* 18**,** 2774-84.
HELLIWELL, C. A., ANDERSSEN, R. S., ROBERTSON, M. & FINNEGAN, E. J. 2015. How is FLC repression initiated by cold? *Trends Plant Sci,* 20**,** 76-82.
HELLIWELL, C. A., WOOD, C. C., ROBERTSON, M., JAMES PEACOCK, W. & DENNIS, E. S. 2006. The Arabidopsis FLC protein interacts directly in vivo with SOC1 and FT chromatin and is part of a high-molecular-weight protein complex. *Plant J,* 46**,** 183-92.
HENDERSON, I. R. & DEAN, C. 2004. Control of Arabidopsis flowering: the chill before the bloom. *Development,* 131**,** 3829-38.
HENDERSON, I. R., SHINDO, C. & DEAN, C. 2003. The need for winter in the switch to flowering. *Annu Rev Genet,* 37**,** 371-92.
HIROSE, T., VIRNICCHI, G., TANIGAWA, A., NAGANUMA, T., LI, R., KIMURA, H., YOKOI, T., NAKAGAWA, S., BENARD, M., FOX, A. H. & PIERRON, G. 2014. NEAT1 long noncoding RNA regulates transcription via protein sequestration within subnuclear bodies. *Mol Biol Cell,* 25**,** 169-83.
HOFFMANN, H. 2002. Biogeography of Arabidopsis thaliana (L.) Heynh. (Brassicaceae). *Journal of Biogeography,* 29**,** 125-134.
HONG, E. H., JEONG, Y. M., RYU, J. Y., AMASINO, R. M., NOH, B. & NOH, Y. S. 2009. Temporal and spatial expression patterns of nine Arabidopsis genes encoding Jumonji C-domain proteins. *Mol Cells,* 27**,** 481-90.
HORNYIK, C., TERZI, L. C. & SIMPSON, G. G. 2010. The spen family protein FPA controls alternative cleavage and polyadenylation of RNA. *Dev Cell,* 18**,** 203-13.
HORTON, M. W., HANCOCK, A. M., HUANG, Y. S., TOOMAJIAN, C., ATWELL, S., AUTON, A., MULIYATI, N. W., PLATT, A., SPERONE, F. G., VILHJALMSSON, B. J., NORDBORG, M., BOREVITZ, J. O. & BERGELSON, J. 2012. Genome-wide patterns of genetic variation in worldwide Arabidopsis thaliana accessions from the RegMap panel. *Nat Genet,* 44**,** 212-6.
HUANG, X., PAULO, M. J., BOER, M., EFFGEN, S., KEIZER, P., KOORNNEEF, M. & VAN EEUWIJK, F. A. 2011. Analysis of natural allelic variation in Arabidopsis using a multiparent recombinant inbred line population. *Proc Natl Acad Sci U S A,* 108**,** 4488-93.
HUEY, R. B. & KINGSOLVER, J. G. 2011. Variation in universal temperature dependence of biological rates. *Proc Natl Acad Sci U S A,* 108**,** 10377-8.
IETSWAART, R., WU, Z. & DEAN, C. 2012. Flowering time control: another window to the connection between antisense RNA and chromatin. *Trends Genet,* 28**,** 445-53.
IMAMURA, K., IMAMACHI, N., AKIZUKI, G., KUMAKURA, M., KAWAGUCHI, A., NAGATA, K., KATO, A., KAWAGUCHI, Y., SATO, H., YONEDA, M., KAI, C., YADA, T., SUZUKI, Y., YAMADA, T., OZAWA, T., KANEKI, K., INOUE, T., KOBAYASHI, M., KODAMA, T., WADA, Y., SEKIMIZU, K. & AKIMITSU, N. 2014. Long noncoding RNA NEAT1-dependent SFPQ relocation from promoter region to paraspeckle mediates IL8 expression upon immune stimuli. *Mol Cell,* 53**,** 393-406.
IPCC CORE WRITING TEAM: R.K. PACHAURI and MEYER, L. A. (eds.) 2014. Climate Change 2014: Synthesis Report. Contribution of Working Groups I, II and III to the Fifth Assessment Report of the Intergovernmental Panel on Climate Change, IPCC, Geneva,

Switzerland, 151 pp
IZAWA, T. 2012. Physiological significance of the plant circadian clock in natural field conditions. *Plant Cell Environ,* 35**,** 1729-41.
JEGU, T., LATRASSE, D., DELARUE, M., HIRT, H., DOMENICHINI, S., ARIEL, F., CRESPI, M., BERGOUNIOUX, C., RAYNAUD, C. & BENHAMED, M. 2014. The BAF60 subunit of the SWI/SNF chromatin-remodeling complex directly controls the formation of a gene loop at FLOWERING LOCUS C in Arabidopsis. *Plant Cell,* 26**,** 538-51.
JEONG, J. H., SONG, H. R., KO, J. H., JEONG, Y. M., KWON, Y. E., SEOL, J. H., AMASINO, R. M., NOH, B. & NOH, Y. S. 2009. Repression of FLOWERING LOCUS T chromatin by functionally redundant histone H3 lysine 4 demethylases in Arabidopsis. *PLoS One,* 4**,** e8033.
JI, N., MIDDELKOOP, T. C., MENTINK, R. A., BETIST, M. C., TONEGAWA, S., MOOIJMAN, D., KORSWAGEN, H. C. & VAN OUDENAARDEN, A. 2013. Feedback control of gene expression variability in the Caenorhabditis elegans Wnt pathway. *Cell,* 155**,** 869-80.
JIANG, D., KONG, N. C., GU, X., LI, Z. & HE, Y. 2011. Arabidopsis COMPASS-like complexes mediate histone H3 lysine-4 trimethylation to control floral transition and plant development. *PLoS Genet,* 7**,** e1001330.
JIANG, D., YANG, W., HE, Y. & AMASINO, R. M. 2007. Arabidopsis relatives of the human lysine-specific Demethylase1 repress the expression of FWA and FLOWERING LOCUS C and thus promote the floral transition. *Plant Cell,* 19**,** 2975-87.
JOHANSON, U., WEST, J., LISTER, C., MICHAELS, S., AMASINO, R. & DEAN, C. 2000. Molecular analysis of FRIGIDA, a major determinant of natural variation in Arabidopsis flowering time. *Science,* 290**,** 344-7.
JONES, H. G., GORDON, S. L. & BRENNAN, R. M. 2014. Chilling requirement of Ribes cultivars. *Front Plant Sci,* 5**,** 767.
KAWAGOE, T. & KUDOH, H. 2010. Escape from floral herbivory by early flowering in Arabidopsis halleri subsp. gemmifera. *Oecologia,* 164**,** 713-20.
KAWAGUCHI, T., TANIGAWA, A., NAGANUMA, T., OHKAWA, Y., SOUQUERE, S., PIERRON, G. & HIROSE, T. 2015. SWI/SNF chromatin-remodeling complexes function in noncoding RNA-dependent assembly of nuclear bodies. *Proc Natl Acad Sci U S A,* 112**,** 4304-9.
KIM, D. H. & SUNG, S. 2013. Coordination of the vernalization response through a VIN3 and FLC gene family regulatory network in Arabidopsis. *Plant Cell,* 25**,** 454-69.
KIM, D. H. & SUNG, S. 2014. Genetic and epigenetic mechanisms underlying vernalization. *Arabidopsis Book,* 12**,** e0171.
KIM, D. H., ZOGRAFOS, B. R. & SUNG, S. 2010. Vernalization-mediated VIN3 Induction Overcomes the LIKE-HETEROCHROMATIN PROTEIN1/POLYCOMB REPRESSION COMPLEX2-mediated epigenetic repression. *Plant Physiol,* 154**,** 949-57.
KIM, S. Y. & MICHAELS, S. D. 2006. SUPPRESSOR OF FRI 4 encodes a nuclear-localized protein that is required for delayed flowering in winter-annual Arabidopsis. *Development,* 133**,** 4699-707.
KOORNNEEF, M., HANHART, C. J. & VAN DER VEEN, J. H. 1991. A genetic and physiological analysis of late flowering mutants in Arabidopsis thaliana. *Mol Gen Genet,* 229**,** 57-66.
KOTAKE, T., TAKADA, S., NAKAHIGASHI, K., OHTO, M. & GOTO, K. 2003. Arabidopsis TERMINAL FLOWER 2 gene encodes a heterochromatin protein 1 homolog and represses both FLOWERING LOCUS T to regulate flowering time and several floral homeotic genes. *Plant Cell Physiol,* 44**,** 555-64.
KOVER, P. X., VALDAR, W., TRAKALO, J., SCARCELLI, N., EHRENREICH, I. M., PURUGGANAN, M. D., DURRANT, C. & MOTT, R. 2009. A Multiparent Advanced Generation Inter-Cross to fine-map quantitative traits in Arabidopsis thaliana. *PLoS Genet,* 5**,** e1000551.
KROGAN, N. J., DOVER, J., WOOD, A., SCHNEIDER, J., HEIDT, J., BOATENG, M. A., DEAN, K., RYAN, O. W., GOLSHANI, A., JOHNSTON, M., GREENBLATT, J. F. & SHILATIFARD, A. 2003. The Paf1 complex is required for histone H3 methylation by COMPASS and Dot1p: linking transcriptional elongation to histone methylation. *Mol Cell,* 11**,** 721-9.
KUDOH, H. & NAGANO, A. 2013. Memory of Temperature in the Seasonal Control of Flowering Time: An Unexplored Link Between Meteorology and Molecular Biology. *In:*

PONTEROTTI, P. (ed.) *Evolutionary Biology: Exobiology and Evolutionary Mechanisms.* Springer.
KUMAR, S. V., LUCYSHYN, D., JAEGER, K. E., ALOS, E., ALVEY, E., HARBERD, N. P. & WIGGE, P. A. 2012. Transcription factor PIF4 controls the thermosensory activation of flowering. *Nature,* 484**,** 242-5.
LAUBE, J., SPARKS, T., ESTRELLA, N., HOFLER, J., ANKERST, D. & MENZEL, A. 2013. Chilling outweighs photoperiod in preventing precocious spring development. *Global Change Biology,* 20**,** 170-182.
LAZARO, A., GOMEZ-ZAMBRANO, A., LOPEZ-GONZALEZ, L., PINEIRO, M. & JARILLO, J. A. 2008. Mutations in the Arabidopsis SWC6 gene, encoding a component of the SWR1 chromatin remodelling complex, accelerate flowering time and alter leaf and flower development. *J Exp Bot,* 59**,** 653-66.
LEE, H., SUH, S. S., PARK, E., CHO, E., AHN, J. H., KIM, S. G., LEE, J. S., KWON, Y. M. & LEE, I. 2000. The AGAMOUS-LIKE 20 MADS domain protein integrates floral inductive pathways in Arabidopsis. *Genes Dev,* 14**,** 2366-76.
LEE, J. & AMASINO, R. M. 2013. Two FLX family members are non-redundantly required to establish the vernalization requirement in Arabidopsis. *Nat Commun,* 4**,** 2186.
LEE, J. H., RYU, H. S., CHUNG, K. S., POSE, D., KIM, S., SCHMID, M. & AHN, J. H. 2013. Regulation of temperature-responsive flowering by MADS-box transcription factor repressors. *Science,* 342**,** 628-32.
LEMPE, J., BALASUBRAMANIAN, S., SURESHKUMAR, S., SINGH, A., SCHMID, M. & WEIGEL, D. 2005. Diversity of flowering responses in wild Arabidopsis thaliana strains. *PLoS Genet,* 1**,** 109-18.
LEVESQUE, M. J., GINART, P., WEI, Y. & RAJ, A. 2013. Visualizing SNVs to quantify allele-specific expression in single cells. *Nat Methods,* 10**,** 865-7.
LEVESQUE, M. J. & RAJ, A. 2013. Single-chromosome transcriptional profiling reveals chromosomal gene expression regulation. *Nat Methods,* 10**,** 246-8.
LI, P., FILIAULT, D., BOX, M. S., KERDAFFREC, E., VAN OOSTERHOUT, C., WILCZEK, A. M., SCHMITT, J., MCMULLAN, M., BERGELSON, J., NORDBORG, M. & DEAN, C. 2014. Multiple FLC haplotypes defined by independent cis-regulatory variation underpin life history diversity in Arabidopsis thaliana. *Genes Dev,* 28**,** 1635-40.
LI, P., TAO, Z. & DEAN, C. 2015. Phenotypic evolution through variation in splicing of the noncoding RNA COOLAIR. *Genes Dev,* 29**,** 696-701.
LI, Y., CHENG, R., SPOKAS, K. A., PALMER, A. A. & BOREVITZ, J. O. 2014. Genetic variation for life history sensitivity to seasonal warming in Arabidopsis thaliana. *Genetics,* 196**,** 569-77.
LI, Y., HUANG, Y., BERGELSON, J., NORDBORG, M. & BOREVITZ, J. O. 2010. Association mapping of local climate-sensitive quantitative trait loci in Arabidopsis thaliana. *Proc Natl Acad Sci U S A,* 107**,** 21199-204.
LI, Y., ROYCEWICZ, P., SMITH, E. & BOREVITZ, J. 2006. Genetics of local adaptation in the laboratory: flowering time quantitative trait loci under geographic and seasonal conditions in Arabidopsis. *PloS one,* 1.
LILLO, C., KATAYA, A. R., HEIDARI, B., CREIGHTON, M. T., NEMIE-FEYISSA, D., GINBOT, Z. & JONASSEN, E. M. 2014. Protein phosphatases PP2A, PP4 and PP6: mediators and regulators in development and responses to environmental cues. *Plant Cell Environ,* 37**,** 2631-48.
LIM, M. H., KIM, J., KIM, Y. S., CHUNG, K. S., SEO, Y. H., LEE, I., KIM, J., HONG, C. B., KIM, H. J. & PARK, C. M. 2004. A new Arabidopsis gene, FLK, encodes an RNA binding protein with K homology motifs and regulates flowering time via FLOWERING LOCUS C. *Plant Cell,* 16**,** 731-40.
LINKERT, M., RUEDEN, C. T., ALLAN, C., BUREL, J. M., MOORE, W., PATTERSON, A., LORANGER, B., MOORE, J., NEVES, C., MACDONALD, D., TARKOWSKA, A., STICCO, C., HILL, E., ROSSNER, M., ELICEIRI, K. W. & SWEDLOW, J. R. 2010. Metadata matters: access to image data in the real world. *J Cell Biol,* 189**,** 777-82.
LIU, F., BAKHT, S. & DEAN, C. 2012. Cotranscriptional role for Arabidopsis DICER-LIKE 4 in transcription termination. *Science,* 335**,** 1621-3.
LIU, F., MARQUARDT, S., LISTER, C., SWIEZEWSKI, S. & DEAN, C. 2010. Targeted 3'

processing of antisense transcripts triggers Arabidopsis FLC chromatin silencing. *Science,* 327**,** 94-7.
LIU, F., QUESADA, V., CREVILLEN, P., BAURLE, I., SWIEZEWSKI, S. & DEAN, C. 2007. The Arabidopsis RNA-binding protein FCA requires a lysine-specific demethylase 1 homolog to downregulate FLC. *Mol Cell,* 28**,** 398-407.
LOLAS, I. B., HIMANEN, K., GRONLUND, J. T., LYNGGAARD, C., HOUBEN, A., MELZER, M., VAN LIJSEBETTENS, M. & GRASSER, K. D. 2010. The transcript elongation factor FACT affects Arabidopsis vegetative and reproductive development and genetically interacts with HUB1/2. *Plant J,* 61**,** 686-97.
MAAMAR, H., CABILI, M. N., RINN, J. & RAJ, A. 2013. linc-HOXA1 is a noncoding RNA that represses Hoxa1 transcription in cis. *Genes Dev,* 27**,** 1260-71.
MACKNIGHT, R., BANCROFT, I., PAGE, T., LISTER, C., SCHMIDT, R., LOVE, K., WESTPHAL, L., MURPHY, G., SHERSON, S., COBBETT, C. & DEAN, C. 1997. FCA, a gene controlling flowering time in Arabidopsis, encodes a protein containing RNA-binding domains. *Cell,* 89**,** 737-45.
MAGRI, D., VENDRAMIN, G. G., COMPS, B., DUPANLOUP, I., GEBUREK, T., GOMORY, D., LATALOWA, M., LITT, T., PAULE, L., ROURE, J. M., TANTAU, I., VAN DER KNAAP, W. O., PETIT, R. J. & DE BEAULIEU, J. L. 2006. A new scenario for the quaternary history of European beech populations: palaeobotanical evidence and genetic consequences. *New Phytol,* 171**,** 199-221.
MANZANO-PIEDRAS, E., MARCER, A., ALONSO-BLANCO, C. & PICO, F. X. 2014. Deciphering the adjustment between environment and life history in annuals: lessons from a geographically-explicit approach in Arabidopsis thaliana. *PLoS One,* 9**,** e87836.
MARCH-DIAZ, R., GARCIA-DOMINGUEZ, M., FLORENCIO, F. J. & REYES, J. C. 2007. SEF, a new protein required for flowering repression in Arabidopsis, interacts with PIE1 and ARP6. *Plant Physiol,* 143**,** 893-901.
MARQUARDT, S., RAITSKIN, O., WU, Z., LIU, F., SUN, Q. & DEAN, C. 2014. Functional consequences of splicing of the antisense transcript COOLAIR on FLC transcription. *Mol Cell,* 54**,** 156-65.
MARTIN-TRILLO, M., LAZARO, A., POETHIG, R. S., GOMEZ-MENA, C., PINEIRO, M. A., MARTINEZ-ZAPATER, J. M. & JARILLO, J. A. 2006. EARLY IN SHORT DAYS 1 (ESD1) encodes ACTIN-RELATED PROTEIN 6 (AtARP6), a putative component of chromatin remodelling complexes that positively regulates FLC accumulation in Arabidopsis. *Development,* 133**,** 1241-52.
MENDEZ-VIGO, B., GOMAA, N. H., ALONSO-BLANCO, C. & PICO, F. X. 2013. Among- and within-population variation in flowering time of Iberian Arabidopsis thaliana estimated in field and glasshouse conditions. *New Phytol,* 197**,** 1332-43.
MENDEZ-VIGO, B., PICO, F. X., RAMIRO, M., MARTINEZ-ZAPATER, J. M. & ALONSO-BLANCO, C. 2011. Altitudinal and climatic adaptation is mediated by flowering traits and FRI, FLC, and PHYC genes in Arabidopsis. *Plant Physiol,* 157**,** 1942-55.
MENZEL, A., SPARKS, T. H., ESTRELLA, N., KOCH, E., AASA, A., AHAS, R., ALM-KUBLER, K., BISSOLLI, P., BRASLAVSKA, O., BRIEDE, A., CHMIELEWSKI, F. M., CREPINSEK, Z., CURNEL, Y., DAHL, A., DEFILA, C., DONNELLY, A., FILELLA, Y., JATCZA, K., MAGE, F., MESTRE, A., NORDLI, O., PENUELAS, J., PIRINEN, P., REMISOVA, V., SCHEIFINGER, H., STRIZ, M., SUSNIK, A., VAN VLIET, A. J. H., WIELGOLASKI, F. E., ZACH, S. & ZUST, A. 2006. European phenological response to climate change matches the warming pattern. *Global Change Biology,* 12**,** 1969-1976.
MENZEL, A., SPARKS, T. H., ESTRELLA, N. & ROY, D. B. 2006. Altered geographic and temporal variability in phenology in response to climate change. *Global Ecology and Biogeography,* 15**,** 498-504.
MICHAELS, S. D. & AMASINO, R. M. 1999. FLOWERING LOCUS C encodes a novel MADS domain protein that acts as a repressor of flowering. *Plant Cell,* 11**,** 949-56.
MICHAELS, S. D. & AMASINO, R. M. 2001. Loss of FLOWERING LOCUS C activity eliminates the late-flowering phenotype of FRIGIDA and autonomous pathway mutations but not responsiveness to vernalization. *Plant Cell,* 13**,** 935-41.
MICHAELS, S. D., BEZERRA, I. C. & AMASINO, R. M. 2004. FRIGIDA-related genes are required for the winter-annual habit in Arabidopsis. *Proc Natl Acad Sci U S A,* 101**,** 3281-

5.
MICHAELS, S. D., DITTA, G., GUSTAFSON-BROWN, C., PELAZ, S., YANOFSKY, M. & AMASINO, R. M. 2003. AGL24 acts as a promoter of flowering in Arabidopsis and is positively regulated by vernalization. *Plant J,* 33**,** 867-74.
MICHAELS, S. D., HE, Y., SCORTECCI, K. C. & AMASINO, R. M. 2003. Attenuation of FLOWERING LOCUS C activity as a mechanism for the evolution of summer-annual flowering behavior in Arabidopsis. *Proc Natl Acad Sci U S A,* 100**,** 10102-7.
MILLER-RUSHING, A. J. & PRIMACK, R. B. 2008. Global warming and flowering times in Thoreau's Concord: a community perspective. *Ecology,* 89**,** 332-41.
MOLAU, U. 1996. Climatic impacts on flowering, growth and vigour in an arctic-alpine cushion plant, Diapensia lapponic, under different snow cover regimes. *Ecological Bulletins,* 45**,** 210-219.
MONTESINOS, A., TONSOR, S. J., ALONSO-BLANCO, C. & PICO, F. X. 2009. Demographic and genetic patterns of variation among populations of Arabidopsis thaliana from contrasting native environments. *PLoS One,* 4**,** e7213.
MOON, J., LEE, H., KIM, M. & LEE, I. 2005. Analysis of flowering pathway integrators in Arabidopsis. *Plant Cell Physiol,* 46**,** 292-9.
MYLNE, J. S., BARRETT, L., TESSADORI, F., MESNAGE, S., JOHNSON, L., BERNATAVICHUTE, Y. V., JACOBSEN, S. E., FRANSZ, P. & DEAN, C. 2006. LHP1, the Arabidopsis homologue of HETEROCHROMATIN PROTEIN1, is required for epigenetic silencing of FLC. *Proc Natl Acad Sci U S A,* 103**,** 5012-7.
NAGANO, A. J., SATO, Y., MIHARA, M., ANTONIO, B. A., MOTOYAMA, R., ITOH, H., NAGAMURA, Y. & IZAWA, T. 2012. Deciphering and prediction of transcriptome dynamics under fluctuating field conditions. *Cell,* 151**,** 1358-69.
NAPP-ZINN, K. 1957. Untersuchungen über das Vernalisationsverhalten einer winterannuellen Rasse von Arabidopsis thaliana. *Planta,* 50**,** 177-210.
NEKRASOV, M., KLYMENKO, T., FRATERMAN, S., PAPP, B., OKTABA, K., KOCHER, T., COHEN, A., STUNNENBERG, H. G., WILM, M. & MULLER, J. 2007. Pcl-PRC2 is needed to generate high levels of H3-K27 trimethylation at Polycomb target genes. *EMBO J,* 26**,** 4078-88.
NEUERT, G., MUNSKY, B., TAN, R. Z., TEYTELMAN, L., KHAMMASH, M. & VAN OUDENAARDEN, A. 2013. Systematic identification of signal-activated stochastic gene regulation. *Science,* 339**,** 584-7.
NICOTRA, A. B., ATKIN, O. K., BONSER, S. P., DAVIDSON, A. M., FINNEGAN, E. J., MATHESIUS, U., POOT, P., PURUGGANAN, M. D., RICHARDS, C. L., VALLADARES, F. & VAN KLEUNEN, M. 2010. Plant phenotypic plasticity in a changing climate. *Trends Plant Sci,* 15**,** 684-92.
NOH, B., LEE, S. H., KIM, H. J., YI, G., SHIN, E. A., LEE, M., JUNG, K. J., DOYLE, M. R., AMASINO, R. M. & NOH, Y. S. 2004. Divergent roles of a pair of homologous jumonji/zinc-finger-class transcription factor proteins in the regulation of Arabidopsis flowering time. *Plant Cell,* 16**,** 2601-13.
NOH, Y. S. & AMASINO, R. M. 2003. PIE1, an ISWI family gene, is required for FLC activation and floral repression in Arabidopsis. *Plant Cell,* 15**,** 1671-82.
NORDBORG, M., HU, T. T., ISHINO, Y., JHAVERI, J., TOOMAJIAN, C., ZHENG, H., BAKKER, E., CALABRESE, P., GLADSTONE, J., GOYAL, R., JAKOBSSON, M., KIM, S., MOROZOV, Y., PADHUKASAHASRAM, B., PLAGNOL, V., ROSENBERG, N. A., SHAH, C., WALL, J. D., WANG, J., ZHAO, K., KALBFLEISCH, T., SCHULZ, V., KREITMAN, M. & BERGELSON, J. 2005. The pattern of polymorphism in Arabidopsis thaliana. *PLoS Biol,* 3**,** e196.
OH, S., PARK, S. & VAN NOCKER, S. 2008. Genic and global functions for Paf1C in chromatin modification and gene expression in Arabidopsis. *PLoS Genet,* 4**,** e1000077.
OH, S., ZHANG, H., LUDWIG, P. & VAN NOCKER, S. 2004. A mechanism related to the yeast transcriptional regulator Paf1c is required for expression of the Arabidopsis FLC/MAF MADS box gene family. *Plant Cell,* 16**,** 2940-53.
PADHYE, S. & CAMERON, A. 2008. Dianthus gratianopolitanus Vill. 'Bath's Pink' has a Near-obligate Vernalization Requirement. *Horticultural Science,* 43**,** 346-349.
PADHYE, S. & CAMERON, A. 2009. Vernalization Responses of Campanula 'Birch Hybrid'. *J.*

Amer. Soc. Sci, 134**,** 497-504.
PARK, S., OH, S., EK-RAMOS, J. & VAN NOCKER, S. 2010. PLANT HOMOLOGOUS TO PARAFIBROMIN is a component of the PAF1 complex and assists in regulating expression of genes within H3K27ME3-enriched chromatin. *Plant Physiol,* 153**,** 821-31.
PARMESAN, C., BURROWS, M. T., DUARTE, C. M., POLOCZANSKA, E. S., RICHARDSON, A. J., SCHOEMAN, D. S. & SINGER, M. C. 2013. Beyond climate change attribution in conservation and ecological research. *Ecol Lett,* 16 Suppl 1**,** 58-71.
PARMESAN, C. & YOHE, G. 2003. A globally coherent fingerprint of climate change impacts across natural systems. *Nature,* 421**,** 37-42.
PETIT, R., AGUINAGALDE, I., DE BEAULIEU, J. L., BITTKAU, C., BREWER, S., CHEDDADI, R., ENNOS, R., FINESCHI, S., GRIVET, D., LASCOUX, M., MOHANTY, A., MULLER-STARCK, G., DEMESURE-MUSCH, B., PALME, A., MARTIN, J. P., RENDELL, S. & VENDRAMIN, G. G. 2003. Glacial refugia: hotspots but not melting pots of genetic diversity. *Science,* 300**,** 1563-5.
PICO, F. X., MENDEZ-VIGO, B., MARTINEZ-ZAPATER, J. M. & ALONSO-BLANCO, C. 2008. Natural genetic variation of Arabidopsis thaliana is geographically structured in the Iberian peninsula. *Genetics,* 180**,** 1009-21.
PIEN, S., FLEURY, D., MYLNE, J. S., CREVILLEN, P., INZE, D., AVRAMOVA, Z., DEAN, C. & GROSSNIKLAUS, U. 2008. ARABIDOPSIS TRITHORAX1 dynamically regulates FLOWERING LOCUS C activation via histone 3 lysine 4 trimethylation. *Plant Cell,* 20**,** 580-8.
PIZER, S., AMBURN, E. & AUSTIN, J. 1987. Adaptive Histogram Equalization and its variations. *Computer Vision, Graphic, and Image Processing,* 39**,** 355-368.
PONTIER, D., GAN, S., AMASINO, R. M., ROBY, D. & LAM, E. 1999. Markers for hypersensitive response and senescence show distinct patterns of expression. *Plant Mol Biol,* 39**,** 1243-55.
PORTER, J. & GAWITH, M. 1999. Temperatures and the growth and development of wheat: a review. *European Journal of Agronomy,* 10**,** 23-36.
POSE, D., VERHAGE, L., OTT, F., YANT, L., MATHIEU, J., ANGENENT, G. C., IMMINK, R. G. & SCHMID, M. 2013. Temperature-dependent regulation of flowering by antagonistic FLM variants. *Nature,* 503**,** 414-7.
PRASANTH, K. V., PRASANTH, S. G., XUAN, Z., HEARN, S., FREIER, S. M., BENNETT, C. F., ZHANG, M. Q. & SPECTOR, D. L. 2005. Regulating gene expression through RNA nuclear retention. *Cell,* 123**,** 249-63.
PRENTICE, I. 1992. A global biome model based on plant physiology and dominance, soil properties and climate. *Journal of Biogeography,* 19**,** 117-134.
PROMISLOW, D. E. L. & HARVEY, P. H. 1990. Living Fast and Dying Young - a Comparative-Analysis of Life-History Variation among Mammals. *Journal of Zoology,* 220**,** 417-437.
QUIRINO, B. F., NORMANLY, J. & AMASINO, R. M. 1999. Diverse range of gene activity during Arabidopsis thaliana leaf senescence includes pathogen-independent induction of defense-related genes. *Plant Mol Biol,* 40**,** 267-78.
RAJ, A. & TYAGI, S. 2010. Detection of individual endogenous RNA transcripts in situ using multiple singly labeled probes. *Methods Enzymol,* 472**,** 365-86.
RAJ, A., VAN DEN BOGAARD, P., RIFKIN, S. A., VAN OUDENAARDEN, A. & TYAGI, S. 2008. Imaging individual mRNA molecules using multiple singly labeled probes. *Nat Methods,* 5**,** 877-9.
RATCLIFFE, O. J., KUMIMOTO, R. W., WONG, B. J. & RIECHMANN, J. L. 2003. Analysis of the Arabidopsis MADS AFFECTING FLOWERING gene family: MAF2 prevents vernalization by short periods of cold. *Plant Cell,* 15**,** 1159-69.
RATCLIFFE, O. J., NADZAN, G. C., REUBER, T. L. & RIECHMANN, J. L. 2001. Regulation of flowering in Arabidopsis by an FLC homologue. *Plant Physiol,* 126**,** 122-32.
RATHCKE, B. & LACEY, E. 1985. Phenological patterns of terrestrial plants. *Annula Review of Ecology, Evolution and Systematics,* 16**,** 179-214.
REEVES, P. A., HE, Y., SCHMITZ, R. J., AMASINO, R. M., PANELLA, L. W. & RICHARDS, C. M. 2007. Evolutionary conservation of the FLOWERING LOCUS C-mediated vernalization response: evidence from the sugar beet (Beta vulgaris). *Genetics,* 176**,** 295-307.
RICHARDS, C. L., ROSAS, U., BANTA, J., BHAMBHRA, N. & PURUGGANAN, M. D. 2012.

Genome-wide patterns of Arabidopsis gene expression in nature. *PLoS Genet,* 8**,** e1002662.
ROLLINS, J. A., DROSSE, B., MULKI, M. A., GRANDO, S., BAUM, M., SINGH, M., CECCARELLI, S. & VON KORFF, M. 2013. Variation at the vernalisation genes Vrn-H1 and Vrn-H2 determines growth and yield stability in barley (Hordeum vulgare) grown under dryland conditions in Syria. *Theor Appl Genet,* 126**,** 2803-24.
ROSA, S., DE LUCIA, F., MYLNE, J. S., ZHU, D., OHMIDO, N., PENDLE, A., KATO, N., SHAW, P. & DEAN, C. 2013. Physical clustering of FLC alleles during Polycomb-mediated epigenetic silencing in vernalization. *Genes Dev,* 27**,** 1845-50.
ROSENZWEIG, C., G. CASASSA, D.J. KAROLY, A. IMESON, C. LIU, A. MENZEL, S. RAWLINS, T.L ROOT, B. SEGUIN, P. TRYJANOWSKI 2007. Assessment of observed changes and responses in natural and managed systems. *Climate Change 2007: Impacts, Adaptation and Vulnerability. Contribution of Working Group II to the Fourth Assessment Report of the Intergovernmental Panel on Climate Change.*
ROSLOSKI, S. M., JALI, S. S., BALASUBRAMANIAN, S., WEIGEL, D. & GRBIC, V. 2010. Natural diversity in flowering responses of Arabidopsis thaliana caused by variation in a tandem gene array. *Genetics,* 186**,** 263-76.
SALATHIA, N., DAVIS, S. J., LYNN, J. R., MICHAELS, S. D., AMASINO, R. M. & MILLAR, A. J. 2006. FLOWERING LOCUS C-dependent and -independent regulation of the circadian clock by the autonomous and vernalization pathways. *BMC Plant Biol,* 6**,** 10.
SALEH, A., ALVAREZ-VENEGAS, R., YILMAZ, M., LE, O., HOU, G., SADDER, M., AL-ABDALLAT, A., XIA, Y., LU, G., LADUNGA, I. & AVRAMOVA, Z. 2008. The highly similar Arabidopsis homologs of trithorax ATX1 and ATX2 encode proteins with divergent biochemical functions. *Plant Cell,* 20**,** 568-79.
SALOME, P. A., BOMBLIES, K., LAITINEN, R. A., YANT, L., MOTT, R. & WEIGEL, D. 2011. Genetic architecture of flowering-time variation in Arabidopsis thaliana. *Genetics,* 188**,** 421-33.
SAMACH, A., ONOUCHI, H., GOLD, S. E., DITTA, G. S., SCHWARZ-SOMMER, Z., YANOFSKY, M. F. & COUPLAND, G. 2000. Distinct roles of CONSTANS target genes in reproductive development of Arabidopsis. *Science,* 288**,** 1613-6.
SANCHEZ-BERMEJO, E., MENDEZ-VIGO, B., PICO, F. X., MARTINEZ-ZAPATER, J. M. & ALONSO-BLANCO, C. 2012. Novel natural alleles at FLC and LVR loci account for enhanced vernalization responses in Arabidopsis thaliana. *Plant Cell Environ,* 35**,** 1672-84.
SARMA, K., MARGUERON, R., IVANOV, A., PIRROTTA, V. & REINBERG, D. 2008. Ezh2 requires PHF1 to efficiently catalyze H3 lysine 27 trimethylation in vivo. *Mol Cell Biol,* 28**,** 2718-31.
SATAKE, A. & IWASA, Y. 2012. A stochastic model of chromatin modification: cell population coding of winter memory in plants. *J Theor Biol,* 302**,** 6-17.
SATAKE, A., KAWAGOE, T., SABURI, Y., CHIBA, Y., SAKURAI, G. & KUDOH, H. 2013. Forecasting flowering phenology under climate warming by modelling the regulatory dynamics of flowering-time genes. *Nat Commun,* 4**,** 2303.
SCHLAPPI, M. R. 2006. FRIGIDA LIKE 2 is a functional allele in Landsberg erecta and compensates for a nonsense allele of FRIGIDA LIKE 1. *Plant Physiol,* 142**,** 1728-38.
SCHMID, K. J., TORJEK, O., MEYER, R., SCHMUTHS, H., HOFFMANN, M. H. & ALTMANN, T. 2006. Evidence for a large-scale population structure of Arabidopsis thaliana from genome-wide single nucleotide polymorphism markers. *Theor Appl Genet,* 112**,** 1104-14.
SCHMID, M., UHLENHAUT, N. H., GODARD, F., DEMAR, M., BRESSAN, R., WEIGEL, D. & LOHMANN, J. U. 2003. Dissection of floral induction pathways using global expression analysis. *Development,* 130**,** 6001-12.
SCHMITTGEN, T. D. & LIVAK, K. J. 2008. Analyzing real-time PCR data by the comparative C(T) method. *Nat Protoc,* 3**,** 1101-8.
SCHMITZ, R. J., TAMADA, Y., DOYLE, M. R., ZHANG, X. & AMASINO, R. M. 2009. Histone H2B deubiquitination is required for transcriptional activation of FLOWERING LOCUS C and for proper control of flowering in Arabidopsis. *Plant Physiol,* 149**,** 1196-204.
SCHNEIDER, R., BANNISTER, A. J., MYERS, F. A., THORNE, A. W., CRANE-ROBINSON, C. & KOUZARIDES, T. 2004. Histone H3 lysine 4 methylation patterns in higher eukaryotic

genes. *Nat Cell Biol,* 6**,** 73-7.
SCHOMBURG, F. M., PATTON, D. A., MEINKE, D. W. & AMASINO, R. M. 2001. FPA, a gene involved in floral induction in Arabidopsis, encodes a protein containing RNA-recognition motifs. *Plant Cell,* 13**,** 1427-36.
SCHONROCK, N., BOUVERET, R., LEROY, O., BORGHI, L., KOHLER, C., GRUISSEM, W. & HENNIG, L. 2006. Polycomb-group proteins repress the floral activator AGL19 in the FLC-independent vernalization pathway. *Genes Dev,* 20**,** 1667-78.
SCHUETTENGRUBER, B., CHOURROUT, D., VERVOORT, M., LEBLANC, B. & CAVALLI, G. 2007. Genome regulation by polycomb and trithorax proteins. *Cell,* 128**,** 735-45.
SCHWARTZ, C., BALASUBRAMANIAN, S., WARTHMANN, N., MICHAEL, T. P., LEMPE, J., SURESHKUMAR, S., KOBAYASHI, Y., MALOOF, J. N., BOREVITZ, J. O., CHORY, J. & WEIGEL, D. 2009. Cis-regulatory changes at FLOWERING LOCUS T mediate natural variation in flowering responses of Arabidopsis thaliana. *Genetics,* 183**,** 723-32, 1SI-7SI.
SCHWARTZ, Y. B. & PIRROTTA, V. 2008. Polycomb complexes and epigenetic states. *Curr Opin Cell Biol,* 20**,** 266-73.
SCORTECCI, K., MICHAELS, S. D. & AMASINO, R. M. 2003. Genetic interactions between FLM and other flowering-time genes in Arabidopsis thaliana. *Plant Mol Biol,* 52**,** 915-22.
SCORTECCI, K. C., MICHAELS, S. D. & AMASINO, R. M. 2001. Identification of a MADS-box gene, FLOWERING LOCUS M, that represses flowering. *Plant J,* 26**,** 229-36.
SEARLE, I., HE, Y., TURCK, F., VINCENT, C., FORNARA, F., KROBER, S., AMASINO, R. A. & COUPLAND, G. 2006. The transcription factor FLC confers a flowering response to vernalization by repressing meristem competence and systemic signaling in Arabidopsis. *Genes Dev,* 20**,** 898-912.
SEATON, D. D., SMITH, R. W., SONG, Y. H., MACGREGOR, D. R., STEWART, K., STEEL, G., FOREMAN, J., PENFIELD, S., IMAIZUMI, T., MILLAR, A. J. & HALLIDAY, K. J. 2015. Linked circadian outputs control elongation growth and flowering in response to photoperiod and temperature. *Mol Syst Biol,* 11**,** 776.
SELTH, L. A., SIGURDSSON, S. & SVEJSTRUP, J. Q. 2010. Transcript Elongation by RNA Polymerase II. *Annu Rev Biochem,* 79**,** 271-93.
SHAFFER, S. M., WU, M. T., LEVESQUE, M. J. & RAJ, A. 2013. Turbo FISH: a method for rapid single molecule RNA FISH. *PLoS One,* 8**,** e75120.
SHARBEL, T. F., HAUBOLD, B. & MITCHELL-OLDS, T. 2000. Genetic isolation by distance in Arabidopsis thaliana: biogeography and postglacial colonization of Europe. *Mol Ecol,* 9**,** 2109-18.
SHELDON, C. C., BURN, J. E., PEREZ, P. P., METZGER, J., EDWARDS, J. A., PEACOCK, W. J. & DENNIS, E. S. 1999. The FLF MADS box gene: a repressor of flowering in Arabidopsis regulated by vernalization and methylation. *Plant Cell,* 11**,** 445-58.
SHIMIZU, K., KUDOH, H. & KOBAYASHI, M. 2011. Plant sexual reproduction during climate change: gene function in natura studied by ecological and evolutionary systems biology. *Annals of botany,* 108**,** 777-864.
SHINDO, C., ARANZANA, M. J., LISTER, C., BAXTER, C., NICHOLLS, C., NORDBORG, M. & DEAN, C. 2005. Role of FRIGIDA and FLOWERING LOCUS C in determining variation in flowering time of Arabidopsis. *Plant Physiol,* 138**,** 1163-73.
SHINDO, C., BERNASCONI, G. & HARDTKE, C. 2007. Natural genetic variation in Arabidopsis: tools, traits and prospects for evolutionary ecology. *Annals of botany,* 99**,** 1043-1097.
SHINDO, C., BERNASCONI, G. & HARDTKE, C. S. 2008. Intraspecific competition reveals conditional fitness effects of single gene polymorphism at the Arabidopsis root growth regulator BRX. *New Phytol,* 180**,** 71-80.
SHINDO, C., LISTER, C., CREVILLEN, P., NORDBORG, M. & DEAN, C. 2006. Variation in the epigenetic silencing of FLC contributes to natural variation in Arabidopsis vernalization response. *Genes Dev,* 20**,** 3079-83.
SIDAWAY-LEE, K., JOSSE, E. M., BROWN, A., GAN, Y., HALLIDAY, K. J., GRAHAM, I. A. & PENFIELD, S. 2010. SPATULA links daytime temperature and plant growth rate. *Curr Biol,* 20**,** 1493-7.
SIMPSON, G. G. & DEAN, C. 2002. Arabidopsis, the Rosetta stone of flowering time? *Science,* 296**,** 285-9.
SIMPSON, G. G., DIJKWEL, P. P., QUESADA, V., HENDERSON, I. & DEAN, C. 2003. FY is an

RNA 3' end-processing factor that interacts with FCA to control the Arabidopsis floral transition. *Cell,* 113**,** 777-87.
SONG, J., ANGEL, A., HOWARD, M. & DEAN, C. 2012. Vernalization - a cold-induced epigenetic switch. *J Cell Sci,* 125**,** 3723-31.
SONG, J., IRWIN, J. & DEAN, C. 2013. Remembering the prolonged cold of winter. *Curr Biol,* 23**,** R807-11.
SPRINGTHORPE, V. & PENFIELD, S. 2015. Flowering time and seed dormancy control use external coincidence to generate life history strategy. *Elife,* 4.
SRIKANTH, A. & SCHMID, M. 2011. Regulation of flowering time: all roads lead to Rome. *Cell Mol Life Sci,* 68**,** 2013-37.
STINCHCOMBE, J. R., WEINIG, C., UNGERER, M., OLSEN, K. M., MAYS, C., HALLDORSDOTTIR, S. S., PURUGGANAN, M. D. & SCHMITT, J. 2004. A latitudinal cline in flowering time in Arabidopsis thaliana modulated by the flowering time gene FRIGIDA. *Proc Natl Acad Sci U S A,* 101**,** 4712-7.
STRANGE, A., LI, P., LISTER, C., ANDERSON, J., WARTHMANN, N., SHINDO, C., IRWIN, J., NORDBORG, M. & DEAN, C. 2011. Major-effect alleles at relatively few loci underlie distinct vernalization and flowering variation in Arabidopsis accessions. *PLoS One,* 6**,** e19949.
STRECK, N. & SCHUH, M. 2005. Simulating the vernalization response of the "Snow Quees" lilly (Lilium longiflorum Thnb.). *Scientia Agricola,* 62**,** 117-121.
SUN, Q., CSORBA, T., SKOURTI-STATHAKI, K., PROUDFOOT, N. J. & DEAN, C. 2013. R-loop stabilization represses antisense transcription at the Arabidopsis FLC locus. *Science,* 340**,** 619-21.
SUNG, S. & AMASINO, R. M. 2004. Vernalization in Arabidopsis thaliana is mediated by the PHD finger protein VIN3. *Nature,* 427**,** 159-64.
SUNG, S. & AMASINO, R. M. 2006. Molecular genetic studies of the memory of winter. *J Exp Bot,* 57**,** 3369-77.
SUNG, S., HE, Y., ESHOO, T. W., TAMADA, Y., JOHNSON, L., NAKAHIGASHI, K., GOTO, K., JACOBSEN, S. E. & AMASINO, R. M. 2006. Epigenetic maintenance of the vernalized state in Arabidopsis thaliana requires LIKE HETEROCHROMATIN PROTEIN 1. *Nat Genet,* 38**,** 706-10.
SUNG, S., SCHMITZ, R. J. & AMASINO, R. M. 2006. A PHD finger protein involved in both the vernalization and photoperiod pathways in Arabidopsis. *Genes Dev,* 20**,** 3244-8.
SWARUP, K., ALONSO-BLANCO, C., LYNN, J. R., MICHAELS, S. D., AMASINO, R. M., KOORNNEEF, M. & MILLAR, A. J. 1999. Natural allelic variation identifies new genes in the Arabidopsis circadian system. *Plant J,* 20**,** 67-77.
SWIEZEWSKI, S., CREVILLEN, P., LIU, F., ECKER, J. R., JERZMANOWSKI, A. & DEAN, C. 2007. Small RNA-mediated chromatin silencing directed to the 3' region of the Arabidopsis gene encoding the developmental regulator, FLC. *Proc Natl Acad Sci U S A,* 104**,** 3633-8.
SWIEZEWSKI, S., LIU, F., MAGUSIN, A. & DEAN, C. 2009. Cold-induced silencing by long antisense transcripts of an Arabidopsis Polycomb target. *Nature,* 462**,** 799-802.
TAMADA, Y., YUN, J. Y., WOO, S. C. & AMASINO, R. M. 2009. ARABIDOPSIS TRITHORAX-RELATED7 is required for methylation of lysine 4 of histone H3 and for transcriptional activation of FLOWERING LOCUS C. *Plant Cell,* 21**,** 3257-69.
THINGNAES, E., TORRE, S., ERNSTSEN, A. & MOE, R. 2003. Day and night temperature responses in Arabidopsis: effects on gibberellin and auxin content, cell size, morphology and flowering time. *Ann Bot,* 92**,** 601-12.
THOMASHOW, M. F. 1999. PLANT COLD ACCLIMATION: Freezing Tolerance Genes and Regulatory Mechanisms. *Annu Rev Plant Physiol Plant Mol Biol,* 50**,** 571-599.
THUILLER, W., LAVOREL, S., ARAUJO, M. B., SYKES, M. T. & PRENTICE, I. C. 2005. Climate change threats to plant diversity in Europe. *Proc Natl Acad Sci U S A,* 102**,** 8245-50.
TODESCO, M., BALASUBRAMANIAN, S., HU, T. T., TRAW, M. B., HORTON, M., EPPLE, P., KUHNS, C., SURESHKUMAR, S., SCHWARTZ, C., LANZ, C., LAITINEN, R. A., HUANG, Y., CHORY, J., LIPKA, V., BOREVITZ, J. O., DANGL, J. L., BERGELSON, J., NORDBORG, M. & WEIGEL, D. 2010. Natural allelic variation underlying a major fitness trade-off in Arabidopsis thaliana. *Nature,* 465**,** 632-6.

VAN DER WALT, S., COLBERT, S. & VAROQUAUX, G. 2011. The NumPy Array: A Structure for Efficient Numerical Compuatation. *Computing in Science and Engineering,* 30**,** 22-30.
VAN DER WALT, S., SCHONBERGER, L., NUNEZ-INGLASIAS, J., BOULOGUE, F., WARNER, J., YAGER, N., GOUILLART, E. & YU, T. 2014. Scikit-Image: Image Processing in Python. *PeerJ 2*.
VERBELEN, J. P., DE CNODDER, T., LE, J., VISSENBERG, K. & BALUSKA, F. 2006. The Root Apex of Arabidopsis thaliana Consists of Four Distinct Zones of Growth Activities: Meristematic Zone, Transition Zone, Fast Elongation Zone and Growth Terminating Zone. *Plant Signal Behav,* 1**,** 296-304.
VISSER, M. E. 2008. Keeping up with a warming world; assessing the rate of adaptation to climate change. *Proc Biol Sci,* 275**,** 649-59.
VITASSE, Y., BRESSON, C., C, KREMER, A., MICHALET, R. & DELZON, S. 2010. Qunatifying phenological plasticity to temperature in two temperate tree species. *Functional Ecology,* 24**,** 1211-1218.
WALTHER, G. R., POST, E., CONVEY, P., MENZEL, A., PARMESAN, C., BEEBEE, T. J., FROMENTIN, J. M., HOEGH-GULDBERG, O. & BAIRLEIN, F. 2002. Ecological responses to recent climate change. *Nature,* 416**,** 389-95.
WANG, P., BOWL, M. R., BENDER, S., PENG, J., FARBER, L., CHEN, J., ALI, A., ZHANG, Z., ALBERTS, A. S., THAKKER, R. V., SHILATIFARD, A., WILLIAMS, B. O. & TEH, B. T. 2008. Parafibromin, a component of the human PAF complex, regulates growth factors and is required for embryonic development and survival in adult mice. *Mol Cell Biol,* 28**,** 2930-40.
WANG, R., FARRONA, S., VINCENT, C., JOECKER, A., SCHOOF, H., TURCK, F., ALONSO-BLANCO, C., COUPLAND, G. & ALBANI, M. C. 2009. PEP1 regulates perennial flowering in Arabis alpina. *Nature,* 459**,** 423-7.
WANG, Z. W., WU, Z., RAITSKIN, O., SUN, Q. & DEAN, C. 2014. Antisense-mediated FLC transcriptional repression requires the P-TEFb transcription elongation factor. *Proc Natl Acad Sci U S A,* 111**,** 7468-73.
WEIGEL, D. 2012. Natural variation in Arabidopsis: from molecular genetics to ecological genomics. *Plant Physiol,* 158**,** 2-22.
WEIGEL, D. & MOTT, R. 2009. The 1001 genomes project for Arabidopsis thaliana. *Genome Biol,* 10**,** 107.
WEINIG, C., UNGERER, M. C., DORN, L. A., KANE, N. C., TOYONAGA, Y., HALLDORSDOTTIR, S. S., MACKAY, T. F., PURUGGANAN, M. D. & SCHMITT, J. 2002. Novel loci control variation in reproductive timing in Arabidopsis thaliana in natural environments. *Genetics,* 162**,** 1875-84.
WERNER, J. D., BOREVITZ, J. O., WARTHMANN, N., TRAINER, G. T., ECKER, J. R., CHORY, J. & WEIGEL, D. 2005. Quantitative trait locus mapping and DNA array hybridization identify an FLM deletion as a cause for natural flowering-time variation. *Proc Natl Acad Sci U S A,* 102**,** 2460-5.
WIGGE, P. A. 2013. Ambient temperature signalling in plants. *Curr Opin Plant Biol,* 16**,** 661-6.
WILCZEK, A. M., BURGHARDT, L. T., COBB, A. R., COOPER, M. D., WELCH, S. M. & SCHMITT, J. 2010. Genetic and physiological bases for phenological responses to current and predicted climates. *Philos Trans R Soc Lond B Biol Sci,* 365**,** 3129-47.
WILCZEK, A. M., COOPER, M. D., KORVES, T. M. & SCHMITT, J. 2014. Lagging adaptation to warming climate in Arabidopsis thaliana. *Proc Natl Acad Sci U S A,* 111**,** 7906-13.
WILCZEK, A. M., ROE, J. L., KNAPP, M. C., COOPER, M. D., LOPEZ-GALLEGO, C., MARTIN, L. J., MUIR, C. D., SIM, S., WALKER, A., ANDERSON, J., EGAN, J. F., MOYERS, B. T., PETIPAS, R., GIAKOUNTIS, A., CHARBIT, E., COUPLAND, G., WELCH, S. M. & SCHMITT, J. 2009. Effects of genetic perturbation on seasonal life history plasticity. *Science,* 323**,** 930-4.
WILKINSON, K. A., MERINO, E. J. & WEEKS, K. M. 2006. Selective 2'-hydroxyl acylation analyzed by primer extension (SHAPE): quantitative RNA structure analysis at single nucleotide resolution. *Nat Protoc,* 1**,** 1610-6.
WILLIS, C. G., RUHFEL, B., PRIMACK, R. B., MILLER-RUSHING, A. J. & DAVIS, C. C. 2008. Phylogenetic patterns of species loss in Thoreau's woods are driven by climate change. *Proc Natl Acad Sci U S A,* 105**,** 17029-33.

WOLKOVICH, E. M., COOK, B. I., ALLEN, J. M., CRIMMINS, T. M., BETANCOURT, J. L., TRAVERS, S. E., PAU, S., REGETZ, J., DAVIES, T. J., KRAFT, N. J., AULT, T. R., BOLMGREN, K., MAZER, S. J., MCCABE, G. J., MCGILL, B. J., PARMESAN, C., SALAMIN, N., SCHWARTZ, M. D. & CLELAND, E. E. 2012. Warming experiments underpredict plant phenological responses to climate change. *Nature,* 485**,** 494-7.

WOLLENBERG, A. C. & AMASINO, R. M. 2012. Natural variation in the temperature range permissive for vernalization in accessions of Arabidopsis thaliana. *Plant Cell Environ,* 35**,** 2181-91.

WOZNIAK, G. G. & STRAHL, B. D. 2014. Catalysis-dependent stabilization of Bre1 fine-tunes histone H2B ubiquitylation to regulate gene transcription. *Genes Dev,* 28**,** 1647-52.

WURR, D., FELLOWS, J., PHELPS, K. & READER, R. 1995. Vernalization in calabrese (Brassica oleracea var. italica) - a model for apex development. *Journal of Experimental Botany,* 46**,** 1487-1496.

XU, L., MENARD, R., BERR, A., FUCHS, J., COGNAT, V., MEYER, D. & SHEN, W. H. 2009. The E2 ubiquitin-conjugating enzymes, AtUBC1 and AtUBC2, play redundant roles and are involved in activation of FLC expression and repression of flowering in Arabidopsis thaliana. *Plant J,* 57**,** 279-88.

IWASA, Y and Levin, S., 1995. The timing of life history events. *Journal of Theoretical Biology,* **172,** 33-42.

YANG, B., TREWEEK, J. B., KULKARNI, R. P., DEVERMAN, B. E., CHEN, C. K., LUBECK, E., SHAH, S., CAI, L. & GRADINARU, V. 2014. Single-cell phenotyping within transparent intact tissue through whole-body clearing. *Cell,* 158**,** 945-58.

YANG, H., HOWARD, M. & DEAN, C. 2014. Antagonistic roles for H3K36me3 and H3K27me3 in the cold-induced epigenetic switch at Arabidopsis FLC. *Curr Biol,* 24**,** 1793-7.

YOSHIDA, N., YANAI, Y., CHEN, L., KATO, Y., HIRATSUKA, J., MIWA, T., SUNG, Z. R. & TAKAHASHI, S. 2001. EMBRYONIC FLOWER2, a novel polycomb group protein homolog, mediates shoot development and flowering in Arabidopsis. *Plant Cell,* 13**,** 2471-81.

YU, H., XU, Y., TAN, E. L. & KUMAR, P. P. 2002. AGAMOUS-LIKE 24, a dosage-dependent mediator of the flowering signals. *Proc Natl Acad Sci U S A,* 99**,** 16336-41.

YU, X. & MICHAELS, S. D. 2010. The Arabidopsis Paf1c complex component CDC73 participates in the modification of FLOWERING LOCUS C chromatin. *Plant Physiol,* 153**,** 1074-84.

ZHANG, H., RANSOM, C., LUDWIG, P. & VAN NOCKER, S. 2003. Genetic analysis of early flowering mutants in Arabidopsis defines a class of pleiotropic developmental regulator required for expression of the flowering-time switch flowering locus C. *Genetics,* 164**,** 347-58.

ZHANG, H. & VAN NOCKER, S. 2002. The VERNALIZATION INDEPENDENCE 4 gene encodes a novel regulator of FLOWERING LOCUS C. *Plant J,* 31**,** 663-73.

ZHANG, X., HAUSE, R. J., JR. & BOREVITZ, J. O. 2012. Natural Genetic Variation for Growth and Development Revealed by High-Throughput Phenotyping in Arabidopsis thaliana. *G3 (Bethesda),* 2**,** 29-34.

ZHAO, K., ARANZANA, M. J., KIM, S., LISTER, C., SHINDO, C., TANG, C., TOOMAJIAN, C., ZHENG, H., DEAN, C., MARJORAM, P. & NORDBORG, M. 2007. An Arabidopsis example of association mapping in structured samples. *PLoS Genet,* 3**,** e4.

ZHAO, Z., YU, Y., MEYER, D., WU, C. & SHEN, W. H. 2005. Prevention of early flowering by expression of FLOWERING LOCUS C requires methylation of histone H3 K36. *Nat Cell Biol,* 7**,** 1256-60.

ZHU, D., ROSA, S. & DEAN, C. 2015. Nuclear Organization Changes and the Epigenetic Silencing of FLC during Vernalization. *J Mol Biol,* 427**,** 659-669.